Can Plant Plastid Produce a Candidate Influenza Vaccine?

A thesis submitted by

Aisling Dunne BSc.

To the National University of Ireland, Maynooth
In fulfilment of the requirement for the degree of

Doctor of Philosophy

Supervisor: Dr. Jackie Nugent
Head of Department: Prof. Kay Ohlendieck

Department of Biology,
National University of Ireland,
Maynooth,
Co. Kildare
Ireland
July, 2011

Table of contents

Abbreviations

2,4-D	2,4-dichlorophenoxyacetic acid
2L21	canine parvovirus 21 mer peptide
A	absorbance
aadA	aminoglycoside 3'-adenylyltransferase
atpB	tobacco chloroplast gene encoding the β subunit of ATP synthase
badh	betaine aldehyde dehydrogenase
BAP	6-benzylaminopurine
bp	base pair
BSA	bovine serum albumin
Bt	*Bacillus thuringiensis*
^{0}C	degrees centigrade
$CaCl_2$	calcium chloride
CDP-star	1,2-dioxetane chemiluminescent substrate
CTB	Cholera toxin B subunit
dH_2O	distilled water
DIG	digoxigenin
DNA	deoxyribonuxleic acid
DNase	deoxyribonuclase
dATP	deoxyadenosine triphosphate
dCTP	deoxycytosine triphosphate
dGTP	deoxyguanosine triphosphate
dNTP	deoxynucleotide triphosphate
dTTP	deoxythymidine triphosphate
EDTA	ethylenediaminetetraacetic acid (disodium salt)
EPSPS	enzyme 5-enol-pyruvl-shikimate-3-phosphate synthase
EtOH	ethanol
g	gram
g	relative centrifugal force
GFP	green fluorescent protein
GOI	gene of interest
gus	β-glucoronidase
HA	Hemaglutinin
HCL	hydrochloric acid

His	histidine
IR	inverted repeat
ISF	insoluble fraction
k	kilo
kb	kilobase
kDa	kilodalton
L	litre
LB	Luria-Bertani
LSC	large single copy
LTB	*E.coli* heat-labile toxin, B subunit
M	molar
MCS	multiple cloning site
mg	milligram
mM	millimolar
mm	millimetre
mRNA	messenger RNA
MS	Murashige and Skoog
NAA	α-naphtaleneacetic acid
NaCl	sodium chloride
NaOH	sodium hydroxide
NEB	New England Biolabs
NPTII	neomycin phosphotransferase
PAGE	polyacrylamide gel electrophoresis
PAT	phosphinothricin acetyltransferase
PBS	phosphate buffered saline
PBST	phosphate buffered saline tween
PCR	polymerase chain reaction
PEG	polyethylene glycol
pMol	pica mole
PPT	phosphinothricin
Prrn	16S ribosomal RNA promoter
psi	pound per square inch
rbcL	gene encoding large subunit of Rubisco
RBS	ribosome binding site

RNA	ribonucleic acid
RNase	ribonuclease
R.T.	room temperature
Rubisco	Rubulose-1,5-biphosphate carboxylase/oxygenase
SDS	sodium dodecyl sulphate
SF	soluble fraction
SSC	small single copy region of the chloroplast genome
TBE	Tris-borate-EDTA buffer
TE	Tris-EDTA buffer
TEMED	N,N,N',N'-tetramethylethylenediamine
TetC	Tetanus toxin, fragment C
Tm	melting point
TpsbA	3' terminator from subunit A of photosystem II
tRNA	transfer RNA
trnA	chloroplast transfer RNA gene containing anticodon for alanine
trnfM	chloroplast transfer RNA gene containing anticodon for methionine
trnG	chloroplast transfer RNA gene containing anticodon for glycine
trnH	chloroplast transfer RNA gene containing anticodon for histidine
trnI	chloroplast transfer RNA gene containing anticodon for isoleucine
trnV	chloroplast transfer RNA gene containing anticodon for valine
TSP	total soluble protein
μg	microgram
μl	microlitre
μM	micromolar
U	unit
UTR	untranslated region
UV	ultraviolet
V	volts
v/v	volume per volume
w/v	weight per volume

Abstract

Recent global flu pandemic highlights the obvious need for a vaccine against the influenza virus that is both inexpensive to produce and can be produced fast enough for development on a large scale. The influenza virus coat protein hemagglutinin (HA) is a major surface antigen and has emerged as a good candidate antigen for subunit vaccine development. Previous attempts to express HA from the A/Sichuan/2/87 H3N2 influenza subtype in plastids achieved HA gene transcription but no protein accumulation, suggesting that the HA protein may be unstable in the plastid. The aim of this work is to investigate alternative strategies that might achieve HA antigen accumulation in plastids. Two series of gene constructs were made. The first series of constructs coded for the first 14 amino acids of GFP and RBCL N-terminally fused to the full length HA, a full length GFP N-terminally fused to HA and a full length GFP N-terminally fused to HA1. The second series of gene constructs coded for two candidate influenza virus hemagglutinin epitopes, HA91-108 and HA 307-319 fused singly as N and C terminal fusions and as double terminal fusions to full length GFP. A total of ten gene constructs were introduced into the chloroplast genome by biolistic bombardment. Transformants were generated and confirmed through molecular analyses. Transplastomic lines generated with the 14aaRBCL/HA and 14aaGFP/HA constructs accumulated a recombinant protein that was smaller than expected. Further analysis is required to confirm that these proteins are indeed truncated HA fusion proteins. No transformed plant lines were generated with the full length GFP/HA and GFP/HA1 constructs suggesting that the tobacco plastid is not a useful system for producing full-length flu virus HA and HA1 proteins suitable for vaccine development. Expression and stability of

recombinant HA91-108/GFP and GFP/HA307-319 fusion proteins was clearly demonstrated showing that conserved influenza virus HA epitopes can be expressed in plant chloroplasts. No transgene transcripts could be detected in transplastomic lines generated with the GFP/HA91-108, HA307-319/GFP or HA307-319/GFP/HA91-108 gene constructs. No transformed lines were generated with the HA91-108/GFP/HA307-319 construct. Conditions for shoot regeneration and the parameters required for biolistic-mediated chloroplast transformation of lettuce were also assessed. However, despite numerous attempts, no plastid transformed lettuce shoots were obtained.

Acknowledgements

I would like to thank my supervisor Jackie Nugent for her advice and encouragement throughout the last few years. I would also like to thank all the members of the Plant Molecular Biology Lab especially Hong, the Plant Cell Biology Lab and the Biology Department, both past and present, who have made my time here so enjoyable.

I would like to thank Orlaith for all those days when we literally ended up on the floor because we were laughing so hard (especially at the eppendorf rack incident!!!) and Team CAKE for making my time in "the cell" bearable!!!!

Finally, I'd like to thank my Mam and Dad, John and Liam for their incredible support in every respect, without which I would never have come this far, I'm eternally grateful.

Declaration of Originality

This thesis has not been submitted in whole or in any part, to this, or any other university for any degree, and is, except where stated otherwise the original work of the author.

Signed:_____

Aisling Dunne

Chapter 1
General Introduction

1 General Introduction

1.1 Introduction to plastids

Plant cells have three genomes: a large one in the nucleus and two smaller ones in the mitochondria and the plastids (Bock & Warzecha, 2010). Plastids are an important group of plant organelles and are thought to have originated by endosymbiosis from ancestral cyanbacteria (Lopez-Juez & Pyke, 2005). All plastid types are derived from small, undifferentiated plastids called proplastids that are mainly found in the dividing cells in meristems. During cell differentiation proplastids differentiate into particular plastid types according to the cell types and/or plant organs in which they reside. These include:

(1) Chromoplasts are plastids enriched with large concentrations of red, yellow or orange carotenoids (Juneau *et al.*, 2002). Chromoplasts are found in fruits, flowers and leaves where their main function is thought to serve primarily as visual attractors for pollinators and fruit dispersing animals (Wise, 2007) however, they are also present in some roots e.g. carrots and tubers e.g. sweet potatoes (Egea *et al.*, 2010). Chromoplast formation can arise directly from proplastids (e.g. carrots) (Benshaul & Klein, 1965), indirectly from chloroplasts (e.g. in ripening fruit) (Bathgate *et al.*, 1985), or from amyloplasts (e.g. tobacco floral nectaries) (Horner *et al.*, 2007).

(2) Leucoplasts are non-pigmented plastids. The three recognized types are the starch storing amyloplasts, oil and lipid storing elaioplast and the protein storing proteoplast. Amyloplasts can be characterised by the presence of one to many large starch granules. They are found in fruits, seeds, tubers and stems and are responsible for the synthesis and storage of starch. Elaioplasts are small, round

oil containing leucoplasts and can be characterised by the presence of numerous oil droplets within the organelle. These oil droplets are composed of prokaryotic-like triacylglycerol and sterol esters (Hernandez-Pinzon *et al.*, 1999). Proteoplasts are plastids containing a large protein inclusion with a granular matrix which is bound by a single membrane (Hurkman & Kennedy, 1976). They are found mainly in seeds and it is thought that they are a site of protein storage within the cell however, it is uncertain as to whether or not they are specialised protein storage organelles (Wise, 2007).

(3) Etioplasts are plastids found in shoot tissues which form when the conversion of proplastids to chloroplasts stops due to extremely low, or the absence, of light conditions (Harsanyi *et al.*, 2005). They are mainly located in white light deprived stem and leaf tissue but do not form in dark-grown root cells (Newcomb, 1967).

(4) Chloroplasts are highly specialised types of plastids (Figure 1.1) (Schwenkert *et al.*, 2010). Chloroplasts are lens-shaped plastids. Each chloroplast consists of two envelope membranes which control the transport of metabolites, lipids and proteins into and out of the chloroplast. Contained within these envelope membranes is an aqueous matrix, the stroma, which contains enzymes involved in carbon fixation, circular DNA anchored to the thylakoids, ribosomes, starch granules and plastoglobuli (Staehelin, 2003). Also present in the stroma are the internal photosynthetic membranes, the thylakoids. It is within the thylakoid membranes that the four main protein complexes involved in the light cycle of photosynthesis reside: photosystems (PS) I and II, the cytochrome b_6/f complex and the ATP synthase complex. Chloroplasts are central to a plants overall metabolism. Their primary role is the photosynthesis

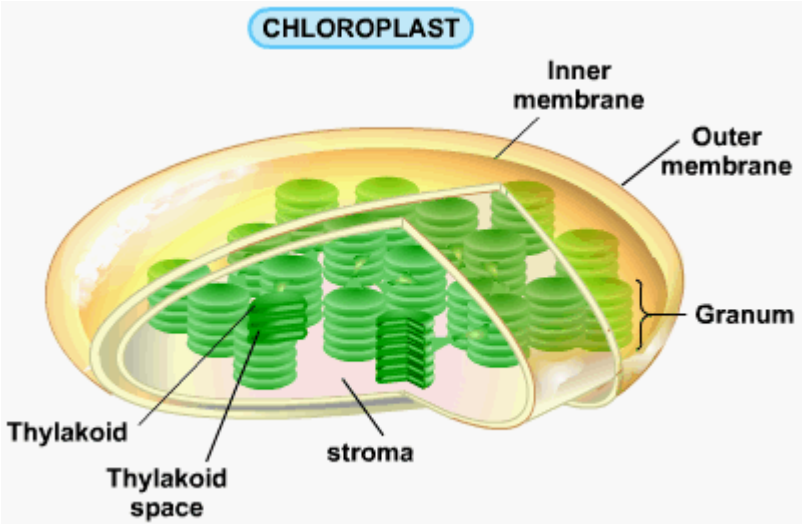

Figure 1.1: Internal structure of a chloroplast. The chloroplast is composed of a double membrane containing the stroma, a liquid matrix surrounding the thylakoids. Thylakoids appear as either individual stromal thylakoids or are organised into stacks or grana containing an internal space or lumen.

of carbohydrates which is the main source of the world's food productivity. In addition to this, chloroplasts are also involved in the evolution of oxygen, sequestration of carbon, production of starch, synthesis of amino acids, fatty acids and pigments, and key aspects of sulfur and nitrogen metabolism (Verma & Daniell, 2007). As all plastids differentiate from proplastids, all plastids of a given plant share an identical genetic complement, therefore any modifications made to the plastome in cells of any one tissue type will ultimately be present in the chloroplasts, chromoplasts, amyloplasts and leucoplasts (Heifetz, 2000).

Chloroplasts are thought to have evolved following an endosymbiotic event in which a non-photosynthetic eukaryotic cell engulfed and retained a photosynthetic bacterium (Wise, 2007). Although most of the polypeptides present in chloroplasts are encoded by the nucleus, chloroplasts have retained a complete protein synthesising machinery and can code for about 100 of their approximately 2,500 proteins. All other plastid proteins are coded for by the nuclear genome and imported from the cytoplasm (Wise, 2007). The organisation of the plant chloroplast genome is generally highly conserved (Raubeson & Jansen, 2005). The circular molecule (Figure 1.2) can be divided into three distinct domains: a large single copy (LSC) region, a small single copy region (SSC) and the inverted repeat region (IR) which is present in exact duplicate and separated by the two single copy regions (Verma & Daniell, 2007). Restriction site analysis indicates that the molecule exists in two orientations present in equimolar proportions within the plastid (Palmer, 1983). Despite the relatively small size of plastid genomes, plastid DNA makes up as much as 10-20% of the total cellular DNA content (Bendich, 1987). This is

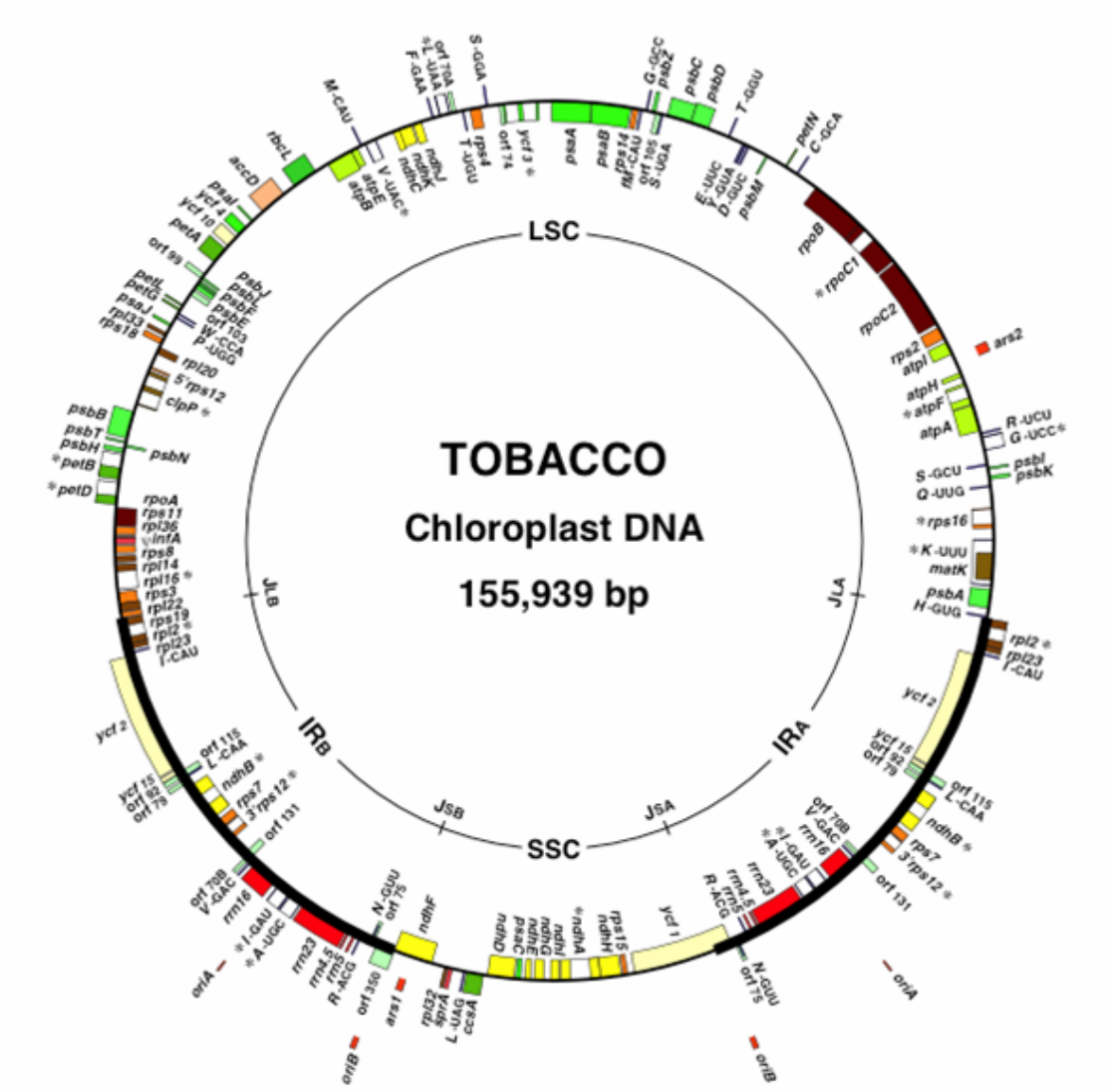

Figure 1.2: Map of the tobacco chloroplast genome (Wakasugi *et al.*, 2001). The genome is 155, 939 bp in size and consists of a 86, 686 bp large single copy region (LSC), a 18,571 bp small single copy region (SSC) and two 25, 341 bp inverted repeats (IR_A and IR_B). Genes shown on the inside of the genome are transcribed in a clockwise fashion and genes on the outside of the genome are transcribed in a counter clockwise fashion.

because the plastid genome is highly polyploid containing thousands of copies of its plastid genome compared to only two copies of its nuclear genome (Bock, 2001). On average, the plastome contains approximately 100 genes, of which approximately 40 code for components of the photosynthetic electron transport machinery while the remainder encode elements of the transcriptional and translational apparatus (Toyoshima *et al.,* 2005). Many genes of the plastid genome are organised in operons and are expressed as polycistronic units resembling bacterial operons (Stern *et al.*, 1997). These transcription units are co-transcribed as polycistronic pre-mRNAs and then processed into shorter RNA species (Hirose & Sugiura, 1997).

1.2 Chloroplast transformation

The main objective of plastid genome genetic engineering is to either alter or delete the DNA sequence of the native plastid genomes or to incorporate new functions (Lutz *et al.*, 2007). Chloroplast transformation involves three steps:

1. The introduction of transforming DNA into the plastid in the form of transformation vectors which include a selectable marker gene by biolistic bombardment or polyethylene glycol (PEG) treatment.
2. The integration of the transforming DNA into the plastid genome following two homologous recombination events.
3. The regeneration of transplastomic shoots and the gradual elimination of wild type genome copies following repeated cell division on a selective medium.

1.3 Vector design

1.3.1 Insertion sites

Chloroplast transformation vectors possess left and right flanking sequences each approximately 1–2 kb in size from the host plastid genome, which are used for targeted foreign gene insertion into plastid DNA via homologous recombination (Wang *et al.*, 2009). To achieve efficient homologous recombination and integration of the transgenes into the chloroplast genome, the use of identical sequences between the target genome and the flanking sequences is essential (Clarke & Daniell, 2011). A recent study has shown that the use of lettuce flanking sequences used for the transformation of the tobacco chloroplast genome significantly reduced the transformation efficiency (Ruhlman *et al.*, 2010). The use of chloroplast transformation vectors with tobacco flanking sequences generated up to 15 independent tobacco transplastomic lines from 10 bombardments whereas, only two independent tobacco transplastomic lines were obtained from 30 bombardments with chloroplast transformation vectors containing lettuce flanking sequence (Ruhlman *et al.*, 2010).

Insertion of foreign DNA into intergenic regions of the plastid genome has been accomplished at 16 sites (Maliga, 2004). The most commonly used site for integration is the intergenic region between the *trnI / trnA* genes located within the *rrn* operon in the inverted repeat regions of the chloroplast genome (Verma & Daniell, 2007). The site of integration may also play an important part in transgene expression. A recent study has shown that transgene integration into the *trnI / trnA* site increased the expression of the lux operon (driven by the

same regulatory sequences) 25-fold more than the transcriptionally silent spacer region, *rps12-trnV* (Krichevsky *et al.,* 2010). While this targeting region has its advantages e.g. location within the inverted repeat region resulting in double the copy number of transgenes (Verma & Daniell, 2007), integration of transgenes into regions within the inverted repeat is not necessary for high levels of protein accumulation. The *trnfM-trnG* region is located within the large single copy region of the plastid DNA. Transgene insertion between *trnfM* and *trnG* (which should have only one copy per plastid DNA in comparison to transgenes targeted to intergenic regions contained within the inverted repeat) has resulted in enormously high levels of a phage lytic protein, >70% of the plant's total soluble protein following transgene integration into this intergenic region (Oey *et al.*, 2009a).

1.3.2 Regulatory sequences

Expression cassettes generally include a strong promoter to ensure high levels of transcription of the transgene (Nugent & Joyce, 2005). The most commonly used promoter is the strong rRNA operon promoter (P*rrn*) (Maliga & Bock, 2011). However, other promoters have also been tested for use in expression cassette design. Valkov *et al.,* (2011) tested five promoters (a full length and shortened *Prrn*, P*psbA, trc* and the *clpP* promoter region from potato) in addition to five terminators (T*rrnB*, T*rbcL*, T*psbA*, T*petD* and T*rpoA*), and four 5' UTRs (*trc, psbA, clpP* and a synthetic *rbcL* derived 5'UTR), to increase the expression of the *gfp* transgene in potato leaves and tubers. Analysis of transgene expression in the different plastid types showed that the differences in *gfp* transcript accumulation in leaf chloroplasts were mainly due to the promoter

used. In potato leaves, accumulation of GFP (about 4% of TSP) was obtained with the strong promoter of the *rrn* operon, the synthetic rbcL-derived 5'UTR and the bacterial *rrnB* terminator. The highest level of GFP (up to approximately 0.02% TSP) was obtained in tubers of plants using two gene constructs; (1) the P*rrn*, the rbcL-derived 5'UTR and *TrrnB* and (2) the promoter and 5' UTR from the plastid *clpP* gene from potato and the T*rrnB* (Valkov *et al.*, 2011).

Although protein levels in chloroplasts depend on mRNA abundance / stability, high levels of mRNA do not necessarily result in high levels of protein accumulation as post transcriptional processes significantly impact levels of protein accumulation within transgenic chloroplasts (Verma *et al.*, 2008). The function of the 5' untranslated region (5'UTR) is to stabilise the mRNA and to allow loading of mRNAs onto the prokaryotic-type 70s ribosomes. Loading of the mRNAs is facilitated by mRNA-16s rRNA interactions by a variant of the prokaryotic Shine-Dalgarno (SD) sequence located upstream of the AUG translation initiation codon (Maliga & Bock, 2011). In plants, many 5' UTRs of plastid genes have been shown to enhance the translation of downstream open-reading frames (Zerges, 2000). The most commonly used 5' regulatory sequences are derived from the *psbA* and *rbcL* genes (Verma *et al.*, 2008) with the tobacco *psbA* 5'UTR being one of the most effective 5' UTRs (Ruhlman *et al.*, 2010). Non-plant sequences have also been used to engineer translational enhancing elements (Daniell *et al.*, 2002). Such non-plant sequences include the bacteriophage T7 gene 10 leader sequence (T7G10L) which promotes high level translation in chloroplasts (Staub *et al.*, 2000).

Most chloroplast genes contain an inverted repeat sequence in their 3' UTR which typically harbour a stem loop type RNA secondary structure (Maliga & Bock, 2011). These inverted repeat sequences do not function as very efficient transcription terminators however, they do stabilise upstream sequences, mediate correct 3' end processing and are involved in translation initiation (Tangphatsornruang *et al.*, 2010). Tangphatsornruang *et al.* (2010) examined the effects of different 3' UTRs (*rbcL, psbA, petD, rpoA* and *rrnB*) on the accumulation and stability of transcripts of a *gfp* transgene in transplastomic tobacco. Levels of *gfp* transcripts were four times higher in plants expressing *gfp* with the *rrnB* terminator compared to plants expressing *gfp* with the *rbcL* and *rpoA* 3'UTRs as *gfp* transcript levels were enhanced because of enhanced mRNA stability. However, when the amount of accumulated GFP was assessed, all plant lines contained the same amount of protein (~0.2% total soluble protein), suggesting either that translation was limited by something other than the amount of transcript or that the 3'UTR was affecting translation (Tangphatsornruang *et al.*, 2010).

Levels of recombinant protein produced in plastids is very much dependant on expression cassette design. The use of endogenous regulatory sequences may be required for optimal expression of foreign gene within the chloroplast as was observed when the use of the lettuce *psbA* promoter and 5' and 3' UTRs in tobacco chloroplast transformation vectors and the tobacco *psbA* regulatory sequences in lettuce chloroplast transformation vectors resulted in a > 90% reduction in the level of transgene expression compared to the transformation vectors containing endogenous regulatory elements (Ruhlman *et al.*, 2010).

1.4 Genetic markers

1.4.1 Selectable marker genes

The choice of selective marker gene and selective agent is vital for successful plastid transformation. Initial tobacco plastid transformation vectors used transformation of a mutagenised plastid 16S rRNA (*rrn16*) gene as a selectable marker. This gene was engineered to contain point mutations which prevented the antibiotics spectinomycin or streptomycin binding to the 16S rRNA, allowing selection of transgenomes (Svab *et al.*, 1990). However, the mutagenised 16S rRNA gene was not an efficient selectable marker as it produced on average only one or two tobacco chloroplast transformants per 100 bombarded leaves (Svab *et al.*, 1990). This relatively low transformation frequency was attributed to the recessive mode of action of the rRNA marker during the selection phase, conferring antibiotic resistance to only the few chloroplast ribosomes which had received their 16S rRNA molecule from the very few initially transformed plastid DNA copies (Bock, 2001).

In 1991, the stable integration and expression of an alternative selectable marker gene, aminoglycoside 3'-adenylyltransferase (*aadA*) was first used for plastid transformation in *Chlamydomonas* (Goldschmidt-Clermont, 1991). Since then, the *aadA* gene has become the most commonly used selectable marker gene for chloroplast transformation. Originally identified in *E. coli*, the *aadA* gene encodes the enzyme aminoglycoside 3’ adenylyltransferase which inactivates spectinomycin and streptomycin by adenylation and hence prevents the antibiotic from binding to the plastid ribosomes. The antibiotic routinely used for chloroplast transformation is spectinomycin due to its high specificity and its

low side effects on plant cells (Li *et al.*, 2010). Putative transformants are identified as green shoots on spectinomycin containing medium which suppresses greening and shoot formation of wild type plants (Maliga, 2003). Spectinomycin selection yields on average one transplastomic line per bombarded tobacco leaf sample, an increase of 100-fold over the mutant 16S rRNA gene used in the initial experiments (Svab & Maliga, 1993). However, transformation efficiency can vary between 0.5 and 5 transplastomic lines per bombarded sample (Maliga, 2003).

The neomycin phosphotransferase gene, *nptII,* is an alternative selective marker gene for chloroplast transformation which confers kanamycin resistance. The *nptII* gene has been used with some success in tobacco plastids however it appears to be less efficient with a higher frequency of nuclear escapes being reported than for spectinomycin/streptomycin selection (Heifetz, 2000). Carrer *et al.*,(1993) were only able to obtain one transformant per 25 bombardments with vectors containing the *nptII* gene following selection on kanamycin (Carrer *et al.*, 1993). However, a dramatic improvement in efficiency was obtained following transformation with a vector containing the highly expressed *neo* gene. This resulted in 34 kanamycin resistant clones from 25 bombarded leaves (Kuroda & Maliga, 2001).

The aminoglycoside phosphotransferase gene *aphA-6* from *Acinetobacter baumannii* is an alternative kanamycin resistance gene (Huang *et al.*, 2002). It is related to the *nptII* gene; both encode aminoglycoside phosphotransferases but originate from different organisms. Vectors containing the *aphA-6* gene were

used to transform tobacco plants and although the overall transformation efficiency was lower than that obtainable with the *aadA* gene, the use of the *aphA-6* gene as a selectable marker resulted in higher transformation efficiency than that obtained with the *nptII* gene (Huang *et al.*, 2002). Furthermore, transformation of the cotton plastid genome using a vector containing the two different genes (*aphA-6* and *nptII*) resulted in a 8-fold increase in the transformation efficiency when compared to a single gene (*aphA-6*) vector (Verma & Daniell, 2007).

The possibility of using chloramphenicol acetyltransferase (CAT) as a selectable marker for chloroplast transformation has also been explored (Li *et al.*, 2010). Chloramphenicol is a widely used antibiotic that blocks prokaryotic translation by inhibiting the peptidyl transferase activity of the 70S ribosome. *CAT*, a bacterial enzyme, detoxifies the antibiotic chloramphenicol hence conferring chloramphenicol resistance. Chloramphenicol and the standard *aadA*-based spectinomycin selection of transplastomic cells were compared by introducing transformation vectors containing the two selectable marker genes into tobacco. The transformation efficiency was found to be less with *cat* (5 transformants from 500 bombarded leaf pieces) than with the *aadA* gene (10 transformants from 297 bombarded leaf pieces). However, selection of putative transformants with the *cat* gene offers one big advantage over *aadA*-based selection. The *cat* gene prevents the production of spontaneous antibiotic resistant mutants which is widely associated with both spectinomycin and kanamycin selection (Li *et al.*, 2010).

To overcome the disadvantages associated with antibiotic resistance genes, several studies have explored strategies for engineering the chloroplast with plant derived selectable marker genes. An example is the spinach betaine aldehyde dehydrogenase (*badh*) gene which was developed as a plant derived selectable marker gene to transform chloroplast genomes (Daniell *et al.*, 2001c). BADH converts toxic betaine aldehyde to non toxic glycine betaine. Transformation of tobacco using betaine aldehyde selection resulted in rapid regeneration of transgenic shoots within 2 weeks and a 25-fold increase in transformation efficiency when compared to spectinomycin selection (Daniell *et al.*, 2001c). However, these results have not been repeated by other groups (Maliga, 2004; Whitney & Sharwood, 2008).

The bacterial *bar* gene has also been evaluated as a plastid selectable marker. It encodes phosphinothricin acetyltransferase (PAT) and confers resistance to the herbicide phosphinothricin (PPT). The *bar* gene has been used as an excellent selectable marker in nuclear transformation, conferring resistance to the herbicide phosphinothricin. However, this has not transferred to chloroplast transformation. Following its introduction into tobacco as an *aadA* linked gene, direct selection of transplastomic tobacco clones on PPT containing media was not possible. Expression of the *bar* gene in the chloroplast and hence phosphinothricin resistance was only detected after transplastomic lines had been selected using the *aadA* gene on media containing spectinomycin (Lutz *et al.*, 2001).

Another alternative selectable marker gene which has been explored for use in chloroplast transformation is the naturally occurring feedback-insensitive anthranilate synthase α-subunit gene of tobacco (ASA2) (Barone *et al.*, 2009). Anthranilate synthase (AS) is a feedback regulated gene and is controlled by its end-product, tryptophan (Trp) (Bohlmann *et al.*, 1996). Trp analogues are toxic to tobacco plants as they cause Trp deficiency by mimicking the feedback effect of Trp on AS, thus affecting protein synthesis. Feedback sensitive AS enzymes are unable to completely discriminate between the normal feedback inhibitor Trp and an analogue. Therefore a feedback insensitive ASA2 gene has the potential to be used as a selectable marker gene for tobacco transformation, selecting on media containing the toxic analogue 4-methylindole (4MI) or 7-methyl-DL-tryptophan (7MT). The transformation efficiency using the ASA2 / 4MI or 7MT selection system is less efficient than the *aad*A selection system with just 5 shoots reported from 130 bombarded leaves (Barone *et al.*, 2009). However, the ASA2 gene has the potential as a selectable marker system for use in many economically important crops such as cereals which are naturally resistant to spectinomycin and for which a specific selection system has yet to be established. A summary of selectable marker genes used for the selection of plastid transformed plants is outlined in Table 1.1.

1.4.2 Reporter Genes

Reporter genes are important tools in biology. Both the *E. coli* β-glucuronidase (*uidA*) and the *Aequorea victoria* green fluorescent protein (*gfp*) genes have been used as plastid reporter genes. These reporter enzymes allow tracking of

Table 1.1: Selectable marker genes used for selection of plastid transformed plants.

Selection agent	Genes	Enzymes	Sources	Reference
Neomycin, kanamycin	*neo*, *nptII*	Neomycin	*Escherichia coli* Tn5	Kuroda & Maliga, (2001) Heifetz, (2000)
Kanamycin	*aphA-6*	Aminoglycoside phosphotransferase	*Acinetobacter baumannii*	Huang *et al.,* (2002)
Spectinomycin	*aadA*	Aminoglycoside-3'-adenylyltransferase	*Shigella* sp.	Svab and Maliga (1993)
Chloramphenicol	*cat*	Chloramphenicol acetyltransferase	*Escherichia coli* Tn5, Phage p1cm	Li *et al.,* (2010)
Phosphinothricin	*pat, bar*	Phosphinothricin acetyltransferase	*Streptomyces hygroscopicus*	Lutz *et al.,* (2001)
5-Methyltryptophan	*ASA2*	Anthranilate synthase	Tobacco	Barone *et al.,* (2009)
Betaine aldehyde	*badh*	Betaine aldehyde dehyrogenase	*Spinacia aleracea*	Daniell *et al.,* (2001b)

gene expression but do not confer a selective advantage or disadvantage to plastids (Maliga, 2004). The enzymatic activity of GUS in chloroplasts can be visualised using histochemical staining (Jefferson *et al.*, 1987), whereas GFP is a visual marker and allows direct imaging of the fluorescent gene product in living cells (Maliga, 2002). The GFP chromophore forms autocatalytically in the presence of oxygen and fluoresces green when absorbing blue or UV light (Maliga, 2004). Its non invasive nature and its ability to emit fluorescence without the requirement of a co-factor makes GFP a very appealing reporter gene (Peckham *et al.*, 2006).

GFP has been used to detect transient plastid-based transgene expression in tobacco, *Arabidopsis thaliana*, marigold petals, potato tubers, carrot roots and pepper fruits (Hibberd *et al.*, 1998). GFP has previously been used in numerous transplastomic studies to establish plastid transformation for a range of plant species including lettuce (Kanamoto *et al.*, 2006; Lelivelt *et al.*, 2005), *Nicotiana benthamiana* (Davarpanah *et al.*, 2009) and sugar beet (De Marchis *et al.*, 2009) as the protein stably accumulates and is visible in the range of a few per cent TSP (Reed *et al.*, 2001). Ruf *et al.*, (2007) used GFP to determine the level of transgene containment in tobacco seeds following chloroplast transformation. Oey *et al.*, (2009b) used GFP as a reporter gene to assess a strategy which allowed antimicrobial genes to be cloned into *E. coli* before being transformed into plants. Furthermore, GFP has been used to test the idea of receptor mediated oral delivery of foreign proteins. A cholera toxin B-subunit (CTB) – GFP fusion protein was used to visualise the path of CTB and GFP in the circulatory system (Limaye *et al.*, 2006).

1.5 Marker gene excision

Marker genes are essential for the selection of initially transformed plastid DNA copies. However, the integration of antibiotic resistance genes in transformed plants raises environmental as well as health concerns towards the commercialisation of transgenic plants (Lossl & Waheed, 2011). A number of approaches have been developed to eliminate antibiotic resistance genes following transformation.

One approach is based on the deletion of marker genes by homologous recombination using direct repeats flanking the selectable marker gene (Iamtham & Day, 2000). Following the confirmation of homoplasmy in transplastomic plant lines, the selective pressure, in the form of the specific antibiotic, is removed allowing the accumulation of *aadA*- free plastid genomes which have resulted from spontaneous excision. Early experiments using *Chlamydomonas reinhardtii* showed that homologous recombination between two 483 bp direct repeats allowed for excision of the *aadA* genes under non-selective growth conditions (Fischer *et al.*, 1996). In contrast, direct repeats of 100 and 230 bp were inefficient in the removal of the *aadA* gene suggesting that the length of the direct repeats may play a large role in the efficiency of this excision. However, in addition to the length of the direct repeats, the number of direct repeats also influences the efficiency of recombination. This was observed when two 418 bp direct repeats failed to excise the *aadA* from transplastomic tobacco plants. However, the use of two 174 bp direct repeats placed within the two 418 bp direct repeats subsequently resulted in the excision of the *aadA* gene from the plastid genomes by the outmost 418 bp repeats

(Iamtham & Day, 2000). Kode *et al.,* (2006) reported the use of duplicated DNA corresponding to the *atpB* promoter region to efficiently delete the intervening *aadA, gusA* and the native *rbcL* genes following a single transformation event (Kode *et al.,* 2006). Yellow pigment deficient sectors were observed on transgenic tobacco leaves resulting from the loss of the photosynthetic *rbcL* gene. Another strategy using a split *bar* gene has also resulted in the excision of selectable marker gene through direct repeat homologous recombination. The split *bar* gene flanking the *aad*A and *gfp* genes resulted in PPT resistant transplastomic soybean plants following the reconstitution of the *bar* gene following homologous recombination (Lestrade *et al.,* 2009). However, homology-based marker excision relies on spontaneous secondary recombination and segregation of plastid DNA (Lossl & Waheed, 2011). Thus, if the selection gene is removed before all the wild-type plastomes are eliminated, there is no way to select for homoplastomic marker free lines (Klaus *et al.,* 2004).

A second approach involves the use of an antibiotic/phenotype selection system in which mutants lacking photosynthetic genes providing chlorophyll are used. The marker gene is excised using mutant plastid transformed tobacco lines already containing the *aadA* gene (Klaus *et al.,* 2004). Vectors are constructed which contain the gene sequences for pigment restoration, the gene of interest and a kanamycin resistance gene, *aphA-6,* which is cloned outside the homologous flanking regions on the vector backbone. Incorporation of the transforming DNA results in the restoration of the wild type pigmentation while at the same time removing the *aadA* gene. The antibiotic resistance gene *aphA-6*

is then eliminated due to its position on the vector backbone. This system allows for the generation of marker-free chloroplast transformants without the need for re-transformation or crossing. However, use of this system is dependant upon the use of mutant donor plants rather than wild type plants (Klaus *et al.*, 2004).

The third approach involves the excision of the selectable marker gene using the *Cre-loxP* site specific recombination system. Two recombinases (Cre and ΦC31 phage integrase; Int) have been tested for plastid marker excision. The Cre-lox site specific recombination system of the bacteriophage P1 involves the removal of the selectable marker gene flanked by directly repeated 34 bp *loxP* sites following the introduction of Cre recombinase into the plastids (Corneille *et al.*, 2001). The introduction of the Cre gene into transplastomic plants either stably or transiently using *Agrobacterium tumefaciens* or fertilisation using pollen from plants expressing the nuclear Cre gene is efficient. However, use of Cre recombinase has resulted in a number of unexpected recombination events. These events have resulted from recombination between *loxP* sites present in the gene constructs and loxP-like hotspots within the plastid genome itself e.g. the promoter region of the *rps7/3'rps12* operon contains a pseudo *loxP* site (Corneille *et al.*, 2003) and another pseudo *loxP* site is present in the *psbA* promoter The second site specific recombinase which has been tested for marker gene excision is the ΦC31 phage integrase (Int) (Kittiwongwattana *et al.*, 2007). To facilitate excision, selectable marker genes are flanked with directly orientated non-identical 39 bp phage *attP* and 34 bp bacterial *attB* attachments sites. As the pseudo *attP* and *attB* sites are not present in plastid

DNA, the Int recombinase may be a better choice for *aadA* excision as unintended recombination events are minimized (Lutz *et al.*, 2007).

1.6 Delivery of DNA into the chloroplast

Biotechnologists have a range of methods at their disposal for introducing foreign DNA into plant cells. Three main methods exist for the introduction of DNA into the chloroplast genome: polyethylene glycol (PEG)-mediated DNA uptake, microinjection and biolistics, all of which are direct gene transfer technologies which have been successfully used to produce transgenic tissues and plants (Taylor & Fauquet, 2002).

1.6.1 Polyethylene glycol (PEG) mediated transformation

Polyethylene glycol (PEG)-mediated transformation of plastids involves the enzymatical removal of the cell wall to obtain protoplasts followed by exposure of these protoplasts to purified DNA in the presence of PEG. The introduction of PEG causes the protoplasts to shrink first and then lyse due to disintegration of the cell membrane. However, for transformation the PEG is removed before the membrane is irreversibly damaged and reversing the process (Maliga, 2004). PEG treatment was first used to test transient expression of GUS in chloroplasts (Sporlein *et al.*, 1991) and then for stable transformation of the chloroplast genome (Golds *et al.*, 1993; O' Neill *et al.*, 1993). PEG-mediated transformation was also used for the transformation of lettuce (Lelivelt *et al.*, 2005) and cauliflower (Nugent *et al.*, 2006). Although PEG is an effective method for plastid transformation, it is no longer a favoured system for recovering

transgenic plants. Producing sufficient amounts of high-quality protoplasts is laborious, technically demanding and expensive, while recovery of large numbers of fertile phenotypically normal plants from these single cells is not practical for many agronomically important crop species (Taylor & Fauquet, 2002).

1.6.2 Microinjection

Transformation of chloroplasts using microinjection involves the direct injection of DNA into the chloroplast using a very small syringe. The expansion of gallistan, a gallium-indium-tin alloy, within the glass syringe following heating, forces the DNA through a capillary tip and into the chloroplast (Knoblauch *et al.*, 1999). This technique has been successfully used for transient expression of GFP in *Vicia faba* and tobacco chloroplasts. However, it has failed to produce transgenic plants to date (Knoblauch *et al.*, 1999).

1.6.3 Biolistics

It was initially thought that plastid transformation was almost impossible to achieve due to the physical barrier imposed by the double membrane of the chloroplast envelope. In addition, there are no viruses or bacteria known to infect the chloroplast which could potentially be used as vectors for gene transfer. However, the development of the gene gun has allowed the delivery of foreign DNA directly into living cells and into chloroplasts (Verma *et al.*, 2008).

The first gene gun was developed by Sanford and co-workers in 1987 (Sanford *et al.*, 1987; Sanford, 1988). It used small plastic bullets coated in a mixture of transforming DNA and tungsten particles which were launched at plant tissue situated below using a 0.22- gun powder cartridge. Although this method was effective, it was soon replaced with an extensively modified version of the gene gun by BioRad which reduced the amount of damage to the plant tissue (Figure 1.3). This new generation gene gun uses pulses of helium gas under high pressure to propel DNA coated microcarriers (gold or tungsten) at target tissue eliminating the need for gun powder (Taylor & Fauquet, 2002).

Particle bombardment has become a preferred system for chloroplast transformation due to its higher transformation efficiency and ease of use (Wang *et al.*, 2009). The first successful plastid transformation using particle bombardment was carried out using the unicellular algae, *Chlamydomonas reinhardttii* (Boynton *et al.*, 1988). Soon after this, the first stable transformation of higher plants was obtained for *Nicotiana tabacum* (Svab *et al.*, 1990). To date, chloroplast transformation has been extended to many other higher plants including *Arabidopsis* (Sikdar *et al.*, 1998), oilseed rape (Hou *et al.*, 2003), *Lesquerella* (Skarjinskaia *et al.*, 2003), rice (Lee *et al.*, 2006b), potato (Sidorov *et al.*, 1999), lettuce (Kanamoto *et al.*, 2006), soybean (Dufourmantel *et al.*, 2004), cotton (Kumar *et al.*, 2004b), carrot (Kumar *et al.*, 2004a), tomato (Ruf *et al.*, 2001), petunia (Zubkot *et al.*, 2004), poplar (Okumura *et al.*, 2006), *Nicotiana benthamiana* (Davarpanah *et al.*, 2009), eggplant (Singh *et al.*, 2010), *Brassica napus* (Cheng *et al*., 2010) and

Biolistic® -PDS-1000/He Particle Delivery System

Figure 1.3: The BioRAD PDS-1000/HE particle delivery system (gene gun). The gene gun uses a high pressure pulse of helium gas to propel DNA coated gold/tungsten particles at target plant tissue.

sugarbeet (De Marchis *et al.*, 2009). Although plastid transformation has been achieved in several species, it is routine only in tobacco as the transformation efficiency is much higher than in other species (Wang *et al.*, 2009).

1.7 Attractions of chloroplast transformation

Transformation of the chloroplast genome has a number of distinct advantages for the engineering of gene expression in plants. These advantages include:

1. Transgene expression is more stable and uniform among transgenic lines following plastid transformation compared to nuclear transformation. Plant nuclear transformation occurs through non-homologous recombination with the random integration of transgenes into unpredictable genomic locations. This results in transgenic lines with varying expression levels (position effects) and usually requires the screening of a large numbers of transgenic plants in order to identify a line displaying reasonably high levels of transgene expression (Bock, 2001). In contrast, integration of transgenes into the chloroplast genome occurs at a precise location in the genome *via* homologous recombination facilitated by a RecA-type system between the plastid targeting sequences on the transformation vector and the targeted region of the plastid genome (Cerutti *et al.*, 1992). In addition, all transplastomic lines obtained from chloroplast transformation experiments with a given vector are usually genetically and phenotypically identical (Bock, 2001).
2. Plastids are predominantly maternally inherited in most crops. Maternal inheritance stops the escape of plastid genes and transgenes by pollen

transmission. This is achieved either by the exclusion of plastids by unequal cell divisions upon pollen grain mitosis or degradation of plastids and plastid DNA during male gametophyte development (Hagemann, 1992). Consequently, the sperm cell fertilising the egg is free of plastids and plastid DNA and hence the zygote receives its plastids exclusively from the egg cell without any contribution from the pollen (Bock, 2001). This mode of plastid inheritance minimises the risk of cross pollination with non-genetically modified plants or their relatives in the wild (Ruiz & Daniell, 2005). Furthermore, the plastid-chromosome-encoded protein is not produced in the pollen and hence does not affect insects that feed on pollen or pollen-coated plant tissues (Bogorad, 2000). Although a recent study by Ruf *et al.*, (2007) has shown that plastid-encoded transgenes can be transmitted by pollen at low frequencies in the *N. tabacum* cultivar Petit Havana, the frequency of occasional paternal transmission of transgenic plastids is so low (at most, in the range of 10^{-8}) that plastid transformation is still an excellent tool for the prevention of unwanted transgene dispersal *via* pollen.

3. Plastid transformed lines can accumulate large amounts of foreign protein, the current record stands at more than 70% of the plants total soluble protein (Oey *et al.*, 2009a). This is mostly due to the polyploid nature of the plastid genetic system with up to 10,000 copies of the chloroplast genome in each plant cell, resulting in the ability to sustain a very high number of functional gene copies compared to the typically diploid nucleus (Verma & Daniell, 2007).

4. Chloroplasts have the ability to fold complex proteins in the stroma and form disulfide bonds or other post-translational modifications required for protein function (Cardi *et al.*, 2010). The redox environment of the plastid stroma is sufficiently oxidizing for disulfide bond formation in proteins and this can be seen following transformation with a number of genes including the human growth hormone (Staub *et al.*, 2000), cholera toxin B (Daniell *et al.*, 2001a) and human serum albumin (Fernandez-San Millan *et al.*, 2003).
5. Chloroplast genetic engineering also allows the unique advantage of transgene stacking, i.e. simultaneous expression of multiple transgenes (Verma & Daniell, 2007). Transgene stacking allows the introduction of multiple genes through a single transformation event avoiding the problems associated with introducing one gene at a time into random locations in the nuclear genome (Bogorad, 2000) and opens up the possibility of expressing whole metabolic pathways or pharmaceutical proteins involving multiple genes (De Cosa *et al.*, 2001).

1.8 Applications of chloroplast transformation

1.8.1 Engineering plants with improved agronomic traits

Many transgenes have been used to engineer valuable agronomic traits *via* the chloroplast genome. These include insect and pathogen resistance, drought and salt tolerance (Verma *et al.*, 2008). The expression of the *B. thuringiensis* (*Bt*) *cry1A*(c) insecticidal protein was achieved in transplastomic tobacco chloroplasts (McBride *et al.*, 1995). Expression of the unmodified bacterial

coding region in chloroplasts resulted in mRNA stability and *cry1A*(c) protein accumulation levels of between 3-5% total soluble cellular protein. Even higher protein accumulation levels have been achieved following the expression of several other Bt proteins in the chloroplast. The cry9Aa2 Bt protein accumulated to approximately 10% of total soluble cellular protein in tobacco (Chakrabarti *et al.*, 2006). The cry1Ab Bt protein was detected in the range of 4.8-11.1% of TSP in transgenic mature leaves of two species of cabbage (Liu *et al.*, 2008). In addition, when two open reading frames were included upstream of the *cry2Aa2* operon, protein accumulated to up to 45% TSP (De Cosa *et al.*, 2001).

Herbicide resistance is another common commercial transgenic trait that has been achieved following the expression of transgenes in plastids. Resistance to glyphosate was achieved following the expression of 5-enolpyruvylshikimate-3-phosphate synthase (EPSPS) in transplastomic tobacco plants (Ye *et al.*, 2001). Plastid-expressed EPSPS protein accumulated to >10% total soluble protein in leaves and provided very high levels of glyphosate resistance. Resistance to phosphinothricin (PPT) was achieved following the expression of a bacterial bar gene (b-bar1) in tobacco plastids and was found to confer field-level tolerance to Liberty, an herbicide containing PPT (Lutz *et al.*, 2001). A sensitive bacterial 4-hydroxyphenylpyruvate dioxygenase (HPPD) gene from *Pseudomonas fluorescens* which was expressed in plastid transformed tobacco and soybean plants (Dufourmantel *et al.*, 2007) accumulated to approximately 5% of total soluble protein in transgenic chloroplasts of both species and resulted in the transformants acquiring a strong herbicide tolerance. The introduction of

Arabidopsis (*Arabidopsis thaliana*) mutated *ALS* (*mALS*) genes into the tobacco chloroplast genome resulted in transplastomic plant lines, G121A, A122V, and P197S, which were specifically tolerant to pyrimidinylcarboxylate, imidazolinon, and sulfonylurea / pyrimidinylcarboxylate herbicides, respectively (Shimizu *et al.*, 2008).

Environmental stress factors such as drought and salinity can be very detrimental to plants because of their sessile existence. Transplastomic plants have also been engineered to improve tolerance to these environmental stresses. Expression of the yeast trehalose phosphate synthase (TPS1) protein in tobacco chloroplasts was shown to result in the survival of chloroplast transgenic seedlings (T_1, T_3) following 7 hours of drying while control non-transformed seedlings died (Lee *et al.*, 2003). High-level expression of betaine aldehyde dehydrogenase (BADH) in cultured cells, roots, and leaves of carrot (*Daucus carota*) was achieved *via* chloroplast transformation (Kumar *et al.*, 2004a). Transgenic carrot plants expressing BADH grew in the presence of high concentrations of NaCl (up to 400 mM).

1.8.2 Plastids as vaccine bioreactors

Vaccine development for emerging infectious diseases and pathogens with quickly changing antigenic properties requires the quick production of specific antigens. Although first generation recombinant protein production systems such as bacteria, yeasts and mammalian cell cultures are being improved, novel expression systems such as transplastomic plants have attractive qualities giving them great potential as second generation expression systems (Bock &

Warzecha, 2010). These include high levels of antigen yields, low production costs once stable lines have been established and the potential to produce oral vaccines. During recent years, several vaccine candidates have been successfully produced *via* plastid transformation. The L1 gene from the human papillomavirus (HPV16) was expressed in tobacco chloroplasts, with protein accumulation levels of 3 mg / g fresh weight or 24% of TSP. More importantly, the L1 protein was shown to self-assemble into capsomers (pentameric structures of L1) and virus like particles (VLPs) (Fernandez-San Millan *et al.*, 2008; Lenzi *et al.*, 2008). Furthermore, as the oral immunogenicity of plant-made HPV11 VLPs already has been observed with the relatively low protein accumulation levels achieved *via* nuclear transformation of potato plants (Warzecha *et al.*, 2003), the higher amounts of recombinant protein obtained *via* plastid transformation should provide a much more potent oral HPV vaccine candidate. More recently, a modified HPV-16 L1 gene, which was shown to retain the assembly of L1 protein to capsomeres was expressed in tobacco chloroplasts and exhibited the conformational epitopes necessary for immunogenicity (Waheed *et al.*, 2011). A number of different antigens (p24, p24-Nef and $Pr55^{gag}$) against the human immunodeficiency virus (HIV), which causes human acquired immunodeficiency syndrome (AIDS), have been expressed in transplastomic plants (McCabe *et al.*, 2008; Scotti *et al.*, 2009; Zhou *et al.*, 2008). The immunogenicity of p24 and p24-NEF was investigated in mice using CTB as an adjuvant (Gonzalez-Rabade *et al.*, 2011). Subcutaneous immunization with purified chloroplast-derived p24 elicited a strong antigen-specific serum IgG response, which was comparable to that produced by *Escherichia coli*-derived p24. Oral administration of a partially

purified preparation of chloroplast-derived p24-Nef fusion protein, which was used as a booster after subcutaneous injection with either p24 or Nef, also elicited strong antigen-specific serum IgG responses. Furthermore both IgG1 and IgG2a subtypes, associated with cell-mediated Th1 and humoral Th2 responses, respectively, were found in sera after both subcutaneous and oral administration (Gonzalez-Rabade *et al.*, 2011). Zhou *et al.*, (2006) expressed the E2 fragment of hepatitis E virus (HEV) open reading frame 2 in transplastomic plants, and showed that this subunit vaccine was immunogenic in mice when injected subcutaneously (Zhou *et al.*, 2006). More recently, the hepatitis C virus core protein was also expressed in transplastomic tobacco plants (Madesis *et al.*, 2010). The existing vaccine against smallpox, which contains live attenuated vaccinia virus, is very effective although due to a high incidence of adverse side effects in certain groups of people (e.g. pregnant women, patients with immune disorders and patients with eczema and atopic dermatitis) its use has been hindered. Rigano *et al.,* (2009) expressed the vaccinia virus envelope protein (A27L) in tobacco chloroplasts (up to 18% of TSP) and demonstrated that it was correctly folded and recognized by serum obtained from a human infected with zoonotic orthopoxvirus (OPV) (Rigano *et al.*, 2009).

In addition to numerous other viral antigens, several bacterial antigens have also been successfully produced *via* plastid transformation demonstrating exceptionally high levels of recombinant protein accumulation. The expression of the native TetC fragment of the tetanus toxin from *Clostridium tetani* in tobacco chloroplasts resulted in recombinant protein accumulation levels of 25% of TSP (Tregoning *et al.,* 2003) showing that not only can plastids

synthesize high levels of recombinant proteins from non-optimized foreign genes but the assembly of functional oligomers of bacterial subunit toxins is also possible in plastids (Bock & Warzecha, 2010). The expression of the cholera toxin B subunit (CTB) in transgenic chloroplasts was shown to be functional by its ability to bind to the intestinal membrane GM1-ganglioside receptor (Daniell *et al.*, 2001a). More recently, a cholera toxin B subunit–human proinsulin (CTB-Pins) fusion protein was expressed in both tobacco and lettuce chloroplasts (Ruhlman *et al.*, 2007). Mice immunized both orally and subcutaneously with the chloroplast-derived CTB-Pins fusion protein were protected against cholera toxin challenge. A more recent study showed that mice immunised with a fusion protein containing CTB and the antigens AMA1 and MSP1 of malaria also conferred dual immunity following a cholera toxin and malaria challenge (Davoodi-Semiromi *et al.*, 2010). A fusion of the heat-labile enterotoxin subunit B (LTB) from *E. coli*, a close homologue of CTB and a heat-stable toxin (ST) has been expressed in tobacco chloroplasts (Rosales-Mendoza *et al.*, 2009). Mice immunised with the chloroplast-derived LTB-ST fusion protein induced both serum and mucosal LTB-ST specific antibodies and partly protected mice against cholera toxin challenge. Other bacterial antigens expressed in transplastomic plants include the plague F1-V antigen which generated a higher survival rate in orally immunised mice (88%) compared to subcutaneously immunised mice (33%) after challenge with a high dose of aerosolised *Yersinia pestis* (Arlen *et al.*, 2008). A multi-epitope diphtheria, pertussis and tetanus (DPT) fusion protein elicited both an IgG and IgA antibody response to each toxin in serum and mucosal tissue in mice after oral

immunisation with freeze dried transplastomic tobacco leaves (Soria-Guerra *et al.*, 2009).

1.8.3 Synthesis of protein antibiotics in plastids

The increased spread of antibiotic resistance in pathogenic bacteria is a major problem in clinical medicine (Bock & Warzecha, 2010). As bacteriophages have evolved to kill their bacterial hosts efficiently, they have become potential targets as antibacterial agents that could be used to control infectious diseases caused by bacterial pathogens: an idea commonly known as phage therapy (Fischetti *et al.*, 2006). Many bacteriophages have highly efficient hydrolytic enzymes (endolysins) which lyse the bacterial host cell towards the end of their life cycle to facilitate the release of newly assemble phage particles into the environment (Bock & Warzecha, 2010). As these endolysins have been successfully used in experimental animals to control the antibiotic resistant pathogenic bacteria (Cheng *et al.*, 2005; Fischetti *et al.*, 2006), they have been targeted as candidates for next generation antibiotics. Three phage endolysins, PlyGBS, Pal and Cpl-1, have been expressed in transplastomic tobacco (Oey *et al.*, 2009a; Oey *et al.*, 2009b). Accumulation of PlyGBS (which acts against group A and group B streptococci) protein reached levels of >70% TSP in transgenic plants, the highest expression level obtained in stably transplastomic plants (Oey *et al.*, 2009a). Both Pal and Cpl-1 (which act against *Streptococcus pneumonia*) recombinant proteins accumulated to approximately 30% and 10% TSP respectively. More importantly, all chloroplast-produced endolysins were highly active and efficiently killed their target pathogens (Oey *et al.*, 2009b).

1.8.4 Plastid engineering of biosynthetic pathways

Plastid engineering has become an important tool for metabolic engineering of pathways and offers great potential for improving the yield and nutritional quality of foodstuffs and animal feed (Maliga & Bock, 2011). The manipulation of the carotenoid biochemical pathway using plastid transformation in tomato has been successful. Carotenoids are important antioxidants in particular the carotenoid β-carotene (also know as provitamin A) which provides the precursor for vitamin A, a lipid soluble vitamin essential to all vertebrates (Maliga & Bock, 2011). The lycopene β – cyclase genes from *Erwinia herbicola* and daffodil (*Narcissus pseudonarcissus*) were introduced into the tomato genome. The most efficient synthesis of β-carotene was observed with a cyclase gene from daffodil with provitamin A levels reaching as much as 1 mg per g dry weight of the fruit (Apel & Bock, 2009). In addition, not only did the expression of the daffodil lycopene β-cyclase result in efficient conversion of lycopene to β-carotene, a 50% increase in total carotenoid content was observed providing additional improvement in the nutritional quality of the tomato fruit (Apel & Bock, 2009). In another study, Craig *et al.*, (2008) showed the feasibility of using plastid transformation to engineer lipid metabolic pathways. Expression of a fatty acid D^9 desaturase gene in tobacco chloroplasts from either a wild relative of potato (*Solanum commersonii*) or the cyanbacterium *Anacystis nidulans*, resulted in altered fatty acid profiles and improved cold tolerance in transgenic plants compared to control plants (Craig *et al.*, 2008).

1.9 Influenza virus

The influenza virus belongs to the *Orthomyxoviridae* family (Saitoh *et al.*, 2008). Influenza is a highly contagious and acute respiratory disease with a high level of morbidity and mortality. Symptoms of the infectious disease include chills, high fever, sore throat, muscle pains, severe headache, coughing, weakness and general discomfort (Chen & Deng, 2009). However, life-threatening complications such as pneumonia can lead to hospitalization and death particularly in young children, adults over 65 and individuals with certain underlying health conditions (Mett *et al.*, 2008).

Influenza can be classified into three types: A, B and C. The most common of the three types is Influenza A. It is highly diverse with subtypes ranging from H1 to H16 and evolves quite rapidly infecting birds, humans and a variety of other mammals (Fouchier *et al.*, 2005). In contrast, Influenza B viruses do not contain any distinct subtypes and are known to infect only humans and seals (Osterhaus *et al.*, 2000). Influenza C is known to infect pigs and humans however it is not associated with severe illness in humans (Katagiri *et al.*, 1983). Currently, vaccination of susceptible individuals is the preferred strategy for the prevention and control of influenza infections.

1.9.1 Morphology of the virus

Influenza virus particles are spherical or filamentous in shape (Figure 1.4) (Cox *et al.*, 2007). Each influenza virus consists of eight negative single-stranded RNA- segments encoding eight structural proteins and four additional proteins (Calder *et al.*, 2010)**.** Each RNA segment is encapsulated by the nucleoprotein

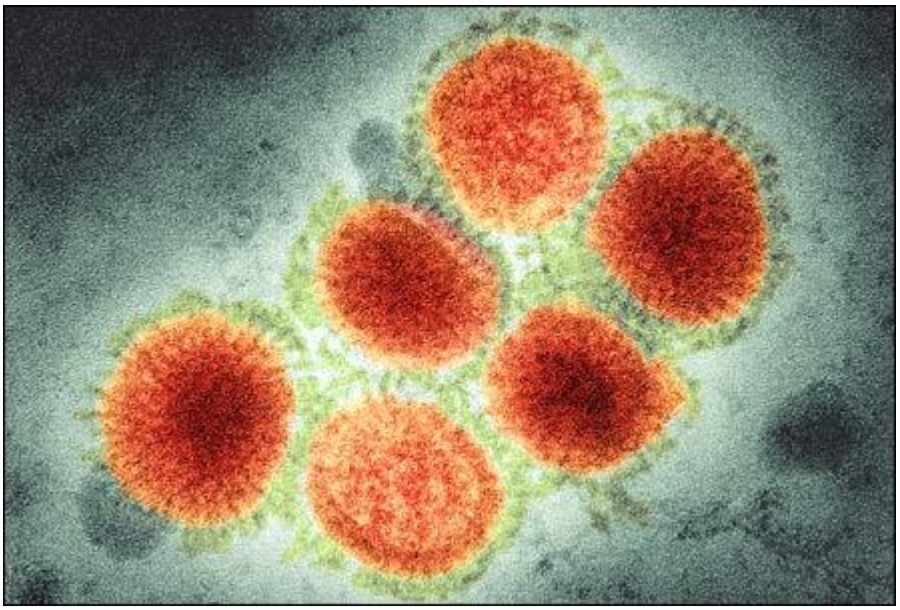

Figure 1.4: Influenza virus particles. Hemagglutinin and neuraminidase spikes can be seen protrusions on the surface of the viral particle.

to form a ribonucleotide nucleoprotein (RNP) complex (Coloma *et al.*, 2009). The RNPs are also associated with the viral polymerase which is composed of the PA, PB1 and PB2 subunits. This viral polymerase is necessary for viral replication (Calder *et al.*, 2010). The virus is surrounded by a lipid bilayer derived from the host cell upon budding through the host plasma membrane (Ghedin *et al.*, 2005). Protruding from the viral surface are the two main membrane glycoproteins: the rod-shaped hemagglutinin (HA) and the mushroom shaped neuraminidase (NA) (Cox *et al.*, 2004). A third membrane protein, the matrix protein, forms a layer associated with the inside of the envelope (Calder *et al.*, 2010). An ion channel formed by the matrix protein is also present on the virus envelope (Cox *et al.*, 2007).

1.9.2 Antigenic variation

Newly emerging influenza viruses that contain antigenic variations that arise by antigenic drift or shift require the production of new vaccines (Ping *et al.*, 2008). Antigenic drift is observed when changes within the HA or NA of an influenza subtype (e.g. H3) allows the virus to evade immune responses which were raised to a previous infection or vaccination while still maintaining antigenic classification within that subtype (Huber & McCullers, 2008a). These changes can be as minor as an amino acid substitution within the HA or NA resulting in an antigenic site change (Chen & Deng, 2009). It is antigenic drift which necessitate the almost annual revision of vaccine composition (Ghedin *et al.*, 2005).

Antigenic shift is observed when changes in the surface HA expression results in the formation of a new HA subtype which is not currently circulating within the human population. In addition, if this newly circulating virus satisfies three criteria (antigenic shift to a new HA, severe disease and good transmissibility), the virus is classified as a pandemic strain (Huber & McCullers, 2008b). In the 20th century, three influenza viruses have emerged in humans to cause major pandemics: The 1918 H1N1 virus, the 1957 H2N2 virus and the 1968 H3N2 virus, all of which resulted from the successful introduction and adaptation of a novel hemagglutinin subtype to humans from an animal source resulting in an antigenic shift (Smith *et al.*, 2009). In March 2009, a novel H1N1 virus emerged in Mexico and the United States and swept across the world developing into the first influenza pandemic of the 21st century (Guan *et al.*, 2010).

1.9.3 Hemagglutinin

The influenza virus has two surface glycoproteins, hemagglutinin (HA) and neuraminidase. HA forms trimeric spikes on the viral surface and has two major functional sites: (1) the stem domain which is relatively well conserved between strains of virus within the HA subtype and (2) a more variable globular domain which contains the majority of antigenic sites and epitopes which generate virus neutralization (Wiley *et al.*, 1981). HA is responsible for the attachment and entry of the virus into cells during the initial stages of infection. HA mediates entry by binding to receptors on the cell surface. The virus is then taken into the endosomes where the virus membrane fuses with the endosomal membrane, releasing the genome transcriptase complex into the cell. For this fusion to occur, HA requires activation by cleavage of a biosynthetic precursor and a

change in pH of the endosomes of between pH 5 and pH 6 (Skehel & Wiley, 2002).

HA is synthesised as a precursor, HA0. It consists of two disulphide-bonded glycopeptides, HA1 and HA2 which are produced during infection following cleavage of HA0 (Skehel & Wiley, 2000). HA1 primarily forms a globular head at the top of HA. It undergoes multiple mutations during a season (antigenic drift), which results in amino acid substitution (Saitoh *et al.*, 2008). Antibodies recognising HA1 inhibit the viral hemagglutinin, neutralise infectivity and provide adequate protection against infection (Gocnik *et al.*, 2008).

HA2 forms the central helix rich stem of HA (Skehel & Wiley, 2000). HA2 represents a relatively conserved region of the HA molecule (Gerhard *et al.*, 2006). Unlike HA1-specific antibodies, anti-HA2 antibodies do not prevent viral infection or neutralise infectivity. However, an increase in mice survival and faster elimination of the virus from the lungs was reported following immunization of mice with HA2 expressed by recombinant vaccinia virus (Gocnik *et al.*, 2008).

1.10 Anti-viral drugs

Two classes of antiviral drugs have been approved for both prevention of and therapeutic treatment of infection by the influenza virus: M2-ion channel inhibitors (amantadine and rimantadine) and neuraminidase inhibitors (zanamivir and oseltamivir) (Boltz *et al.*, 2010). Amantadine and rimantadine work by inhibiting viral replication by blocking the ion channel during the viral

entry stage into cells (Wang *et al.*, 1993). They also prevent the release of the virus by altering the conformation of the hemagglutinin protein (Betakova *et al.*, 2005; Grambas & Hay, 1992). The neuraminidase inhibitors zanamivir and oseltamivir block the activity of the neuraminidase enzyme by interrupting the establishment of the infection at a later stage of virus replication by inhibiting the release of virions from infected cells (Gubareva *et al.*, 2000). Neuraminidase inhibitors also cause the released virions to aggregate thus inhibiting viral penetration into mucous secretions and the spread of the virus to neighbouring cells. However, there is a major concern regarding the use of antiviral drugs to control influenza following the emergence of drug-resistant variants. The use of amantadine or rimantadine has resulted in the rapid emergence of viruses which are resistant to M2 inhibitors yet maintain full transmissibility (Boltz *et al.*, 2010).

1.11 Current influenza vaccines

The most decisive factor in determining the effectiveness of an influenza vaccine is its ability to stimulate the production of what are considered to be the most important virus-neutralizing antibodies in defence against the influenza virus infection (Gocnik *et al.*, 2008). HA, the dominant surface glycoprotein on the influenza virus is the recognised major antigen in the host response to influenza virus in both natural infection and vaccination. This makes it a logical candidate for recombinant vaccine technology (Huber & McCullers, 2008a).

Current influenza vaccines are produced by culturing live viruses in embryonated hen's eggs. Split-influenza vaccines are obtained after chemical

inactivation with formalin and disruption of purified virions with a detergent (D'Aoust *et al.*, 2010). In recent years, trivalent inactivated influenza vaccines have been standardised to contain 15 micrograms of each of three HAs, two derived from the influenza A subtype H1N1, H3N2 and one from an influenza B strain which is currently circulating in the community (Cox & Hollister, 2009). However, live attenuated influenza vaccines have also been used in the form of Fluenz (EU) / FluMist (US), a nasal spray influenza vaccine. In Ireland, the recommended virus strains for use in the 2011-2012 influenza season are: an A/California/7/2009 (H1N1)-like virus, an A/Perth/16/2009 (H3N2)-like virus and a B/Brisbane/60/2008-like virus (The World Health Organisation (WHO); Recommendations for influenza vaccines; www.who.int).

1.11.1 Subunit vaccines

With an emphasis on safety, there has been an increasing shift towards the development of subunit vaccines (Daniell *et al.*, 2009). Instead of propagating whole pathogens, genes which encode single antigens can now be expressed in various host organisms. Once purified and administered to vaccinees, these subunit antigens are capable of eliciting an immune response while eliminating the potential infection by the vaccination (Bock & Warzecha, 2010). One example is the recombinant HA subunit (H3N2) vaccine which was expressed in the yeast expression system *Pichia pastoris* (Saelens *et al.*, 1999). A full length HA0 protein was produced and administered to mice in combination with an adjuvant, *Samonella typhimurium* monophosphoryl lipid A. Vaccinated mice not only showed a strong virus specific antibody response, the mice were also protected when challenged with live virus (Saelens *et al.*, 1999).

1.11.2 Virus-like particles and DNA vaccines

Virus-like particles (VLPs) are produced following expression of specific viral proteins and present an external surface resembling that of the virus. But unlike true virus particles, VLPs do not incorporate genetic material (D'Aoust *et al.*, 2010). Influenza VLPs for several HAs (H1, H2, H3, H5, H6 and H9) from type A influenza, and from type B influenza (HAB) have been shown to form and accumulate following transient expression by agroinfiltration in *Nicotiana benthamiana* leaves (D'Aoust *et al.,* 2009). Furthermore, the parenteral administration of purified H5-VLPs (A/Indonesia/5/05 strain) in the presence or absence of an adjuvant was shown to induce a strong and protective immune response in mice and ferrets (D'Aoust *et al.,* 2009).

Vaccination with plasmid DNA (pDNA) – based vaccines encoding at least one influenza virus protein is an alternative influenza vaccine strategy. Previous studies testing a HA DNA vaccine using the *HA* gene from influenza A/Sichuan/2/87 (H3N2) strain in a mouse model showed that although the HA DNA did not induce an antibody response, a strong Th_1 response was sufficient to protect mice against intranasal challenge with live influenza virus (Johnson *et al.*, 2000). More recently, several pDNA vaccines have been tested for protective efficacy in mice and ferrets against the highly pathogenic A/Vietnam/1203/04 (H5N1) virus. The vaccines encoded influenza A virus hemagglutinin (HA), and / or nucleoprotein (NP), and M2 protein. Complete protection was conferred to mice following 2 doses of a vaccine containing H5 HA, NP, and M2 plasmids and in ferrets with only 1 dose (Lalor *et al.*, 2008).

1.11.3 Epitopes as vaccines

Influenza is a highly infectious and acute respiratory disease with a high level of morbidity and mortality (Shoji *et al.,* 2008). One major limitation of the currently available vaccines against the influenza virus is their restriction to the specific strains that are included in the vaccine. The failure to induce a broad level of protection to the different influenza strains is mainly due to the frequent and unpredictable changes of the two surface glycoproteins: hemagglutinin and neuraminidase. These changes / antigenic variations allow the virus to evade the immune system and reduces the effectiveness of the vaccines (Ben-Yedidia, 1998) as the efficiency of the vaccine depends on a close antigenic match between the vaccine composition and the circulating viral strains (Arnon & Van Regenmortel, 1992; Disis *et al.*, 1996). These antigenic variations limit current vaccines promoting the need to consider new approaches to influenza vaccine production. In view of this limitation, a novel approach for the development of influenza vaccines has been considered based on identifying the critical epitope(s) responsible for protection (Disis *et al.,* 1996). Jacob *et al.* were the first to report that a single synthetic epitope could be expressed in an appropriate vector and used for priming against cholera toxin and *E. coli* heat labile toxin (Jacob *et al.,* 1985). The toxin was neutralised by the recombinant products *in vivo* in both rats and mice (Arnon *et al.*, 2001). Many studies have showed the immunological efficiency of peptide based vaccines against diseases in animals (Adar *et al.,* 2009). In addition, clinical studies have also demonstrated the responses to peptide vaccine candidates against various diseases including malaria (Kashala *et al.,* 2002; Nardin *et al.*, 2000), hepatitis B (Engler *et al.*, 2001) and HIV (Gahery *et al.*, 2006; Pinto *et al.*, 1999). The

use of synthetic peptides in vaccines offers practical advantages such as the relative ease of construction and production, chemical stability, the avoidance of any infectious potential hazard and the ability to immunise with a minimal structure, consisting of a well-defined antigen that can be thoroughly characterised with respect to its antigenicity and immunogenicity (Adar *et al.*, 2009).

1.12 Alternative influenza production systems

Alternative production systems have been used to produce influenza vaccines. Optaflu is a European Medicines Agency approved influenza vaccine produced in canine kidney cell cultures (Doroshenko & Halperin, 2009). FluBlok is a trivalent vaccine composed of recombinant influenza HA produced in insect cell cultures using the baculovirus expression system. However, FluBlok has not yet been approved for use (Cox & Hollister, 2009). Although this method of recombinant influenza antigens production has advantages over that of egg-derived vaccines in terms of speed and safety, the product appears to be less efficacious than inactivated split-influenza vaccines as higher antigen content is required to generate a potent immune response (Treanor *et al.*, 2007).

1.12.1 Plants as alternative vaccine production systems

Most influenza vaccines that are currently in use are generated in embryonated hen's eggs (Shoji *et al.*, 2008). Although these vaccines are very effective, they are limited by the scale of production (Mett *et al.*, 2008). In addition, at least 6 months are required from the identification of a new viral strain to the

manufacture of bulk quantities (Gerdil, 2003). Furthermore, uncertainties over the robustness of egg-based vaccine production systems have intensified following the emergence of H5N1 strains which have proved highly virulent to both chickens and eggs (Martin *et al.*, 2006). Thus, there is a need to develop alternative production systems that allow rapid engineering and production of the vaccine in time to confront the influenza pandemic (Shoji *et al.*, 2009).

Plant cells are ideal bioreactors for the production of vaccines and biopharmaceuticals. Plants are the largest and most economical biomass generators eliminating the need for expensive fermenters and bioreactors and hence reduce manufacturing costs (Daniell *et al.*, 2009). Reactions to vaccines due to egg-based allergies can also be avoided through plant-based production systems. Antigens or therapeutic proteins can either be purified or the plant tissue can be processed into a form which can be applied either topically or more uniquely orally (Daniell *et al.*, 2009). Plant-based vaccines that can be administered orally or topically avoid the use of injections thus eliminating discomfort and more importantly the risk of disease transmission *via* re-use of contaminated syringes and needles (Lal *et al.*, 2007). In addition, the requirement for cold storage and transportation costs are also eliminated making plants a very appealing production system.

The hemagglutinin (HA) genes from several viruses have successfully been expressed in transgenic plants *via* nuclear transformation (Hahn *et al.*, 2007; Huang *et al.*, 2001; Kalthoff *et al.*, 2010; Khandelwal *et al.*, 2003; Marquet-Blouin *et al.*, 2003; Prasad *et al.*, 2004). Mice inoculated intraperitoneally with transgenic plant-derived recombinant HA protein from measles virus produced

serum anti-HA antibodies that neutralized the measles virus *in vitro*. Mice gavaged with transgenic tobacco leaf extracts also developed serum HA-specific antibodies with neutralizing activity against measles virus *in vitro* (Huang *et al.*, 2001). Mice immunised with transgenic carrot leaf or root extracts containing recombinant HA protein from the measles virus also induced high titres of IgG1 and IgG2a antibodies that cross-reacted strongly with the measles virus and neutralized the virus *in vitro* (Marquet-Blouin *et al.*, 2003). The hemagglutinin-neuraminidase (*HN*) gene of *Peste des petits ruminants virus* (PPRV) was expressed in pigeonpea plants for the development of an edible vaccine for *Peste des Petits ruminant* (PPR), a disease which results in a high mortality rate in sheep and goats. The expression of HN protein in transgenic lines was confirmed by Western blot and the plant-derived hemagglutinin-neuraminidase protein was shown to be biologically active as demonstrated by neuraminidase activity (Prasad *et al.*, 2004). The hemagglutinin-neuraminidase (HN) of Newcastle disease virus was introduced into tobacco plants *via* nuclear transformation. The highest level of expression of the recombinant HN proteins detected by Western blot analysis was approximately 0.069% of the total soluble protein. Chickens immunized with transgenic tobacco expressing HN developed slightly higher titers of anti-HN serum IgG compared with those immunized with wild type protein suggesting that oral immunization with *HN*-transgenic tobacco provides a potential means of protecting chickens from NDV (Hahn *et al.*, 2007). Intraperitoneal immunization of mice with transgenic peanut extracts expressing the HA protein of rinderpest virus elicited antibody response specific to HA (Khandelwal *et al.*, 2003). These antibodies neutralized the virus infectivity *in vitro.* Oral immunization of mice with transgenic peanut

induced HA-specific serum IgG and IgA antibodies (Khandelwal *et al.*, 2004). Most recently, the immunogenic capacity of plant-expressed full-length HA (rHA0) from the highly pathogenic avian influenza virus (HPAIV) H5N1 was analysed. Plant-expressed rHA0 accumulated to high levels, was highly immunogenic and could fully protect chickens against lethal challenge infection (Kalthoff *et al.*, 2010). These studies indicate that plant-derived hemagglutinin protein has the potential to become a viable approach to viral vaccine development.

Accumulation levels and yields of recombinant proteins in plants are the most important factors that limit their commercial exploitation. In order to compete with other production methods, it is necessary to develop transgenic plants accumulating recombinant protein to levels of at least 1% total soluble protein (TSP) (Rybicki, 2009). One of the main problems associated with the production of recombinant protein in nuclear transgenic plants is the relatively low accumulation levels that are generally achieved (<1% TSP; Daniell *et al.*, 2009) although some exceptions have been reported. The nuclear expression of the β-glucosidase protein from both *Aspergillus niger* and *Thermotoga martitima* resulted in accumulation levels of 2.3% TSP (Wei *et al.*, 2004) and 5.8% TSP (Jung *et al.*, 2010) respectively. However, chloroplast transformation has the potential to express recombinant protein to extraordinary high levels, with several studies reporting recombinant protein accumulation levels of well over 20% TSP. For example, the TetC protein from *Clostridium tetani* accumulated to approximately 25% TSP (Tregoning *et al.*, 2003), the cry2Aa2 protein accumulated to up to 45% TSP (De Cosa *et al.*, 2001) while more

recently, the phage endolysin protein (PlyGBS) from a *Streptococcus agalactiae* phage accumulated to more than 70% TSP in tobacco plastids (Oey *et al.*, 2009a).

1.13 Aims and objectives

Previous attempts to express HA from the A/Sichuan/2/87 H3N2 influenza subtype in plastids achieved HA gene transcription but no protein accumulation (Karen Shiel, unpublished data; Lelivelt *et al.*, 2005), suggesting that the HA protein may be unstable in the plastid. The aim of this work was to investigate alternative strategies that might achieve HA antigen accumulation in plastids. The first approach was to use a gene fusion strategy to try to stabilise HA or HA1 in plastids. In this case a full-length *gfp* gene or the coding region for the first 14 amino acids of GFP and RBCL were N-terminally fused to HA and HA1 coding regions. In the second approach, a series of *gfp* gene and HA epitope constructs were made to see if stable accumulation of HA epitope fusion proteins in tobacco chloroplasts could be achieved. All gene constructs were introduced into tobacco chloroplasts by biolistics-mediated transformation and transplastomic plant lines were assessed for either HA, HA1 or HA epitope fusion protein accumulation and stability. Finally, in an effort to develop a platform for the production of potentially edible plant-based vaccines various parameters required for biolistic-mediated lettuce plastid transformation were investigated and trial transformation experiments were carried out.

Chapter 2
Materials and Methods

2 Materials and Methods

2.1 Chemicals and reagents

All chemicals and reagents were purchased from Sigma-Aldrich, Ireland Ltd., or Duchefa Biochemie B.V., unless otherwise stated.

2.2 Enzymes

All enzymes were purchased from Promega, UK or New England Biolabs unless otherwise stated.

2.3 PCR primers

PCR primers were obtained from Eurofins MWG Operon (Anzingerstr. 7a, 85560 Ebersberg, Germany). Stock primers were diluted with sterile water to a working concentration of 10 pMol. A list of all primers used in cloning, identification of transformed plants and probe preparations are outlined in Table 2.1.

2.4 Plant material and culture conditions

2.4.1 Plant material

Nicotiana tabacum cv. Petit Havana was used in all tobacco chloroplast transformation experiments. *Lactuca sativa* cv. Flora and Evola were used in all lettuce chloroplast transformation optimisation experiments. *Lactuca sativa* cv. Simpson Elite and Cisco were used in all trial lettuce chloroplast transformation experiments. *Lactuca sativa* cv. Flora, Evola and Cisco seeds were supplied by

Table 2.1: Oligonucleotide primers used for PCR-mediated gene cloning and screening of transgenic plants. Restriction sites are in italics and underlined. Letters shown in red are base changes which were used during PCR mutagenesis of the *HA* and *gfp* genes.

Primer name:	Primer sequence (5' – 3')
HA-NdeIF	5'-GTAC*CATATG*CAAAAACTTCCCGGAAATG-3'
HA-XbaIR	5'GTAC*TCTAGA*TTAGTATCCTGACTTCAGCTCAACACC-3'
HA-SphIF	5'-ATT*GCATGC*CCCAGGTATGTTAAGC-3'
HA-SphIR	5'-GTAC*GCATGC*CCCATAAGTGATCTTG-3'
14aarbcL-F1	5'-GCAAAGCATCTGTAGGATTTAAACAAAAACTTCCCG-3'
14aarbcL-F2	5'-GA*CATATG*TCTCCTCAAACTGAAACTAAAGCATCTG-3'
14aaGFP-F1	5'-CGTTTACTGGAGTAGTTCCTATTCAAAAACTTCCCGG-3'
14aaGFP-F2	5'-CAG*CATATG*TCTAAAGGAGAAGAATTATTTACTGGA-3'
HA-HindIII-R	5'-GAAGTTGCTGT*AAGCTT*TGCTGCGTTC-3'
HA1-XbaIR	5'-GCC*TCTAGA*TTAAGTTTGTTTCTCTGG-3'
HA-LinkF	5'-GTATTAGGACCCGGGCCTATGCAAAAA CTTCCCGGAAATG-3'
GFP-NdeIF	5'-GATAC*CATATG*AGTAAAGGAGAAGAAC-3'
GFP-XbaIR	5'-GTATC*TCTAGA*TTATTTGTATAGTTCATC-3'
GFP-MutF	5'-CAAGATACCCAGATCACATGAAGCGG-3'
GFP-MutR	5'-CCGCTTCATGTGATCTGGGTATCTTG-3'
GFP-Link-XbaIR	5'-ATGC*TCTAGA*AGGCCCGGGTCCTTTGTATAGTTCATC-3'
HA91-108-F1	5'-TATCCTTATGATGTTCCTGATTATGCTTCTTTAAT CAGTAAAGGAGAAGAACTTTTC-3'
HA91-108-F2	5'-GCATGG*CATATG*TCTAAGGCTTATTCTAATTGTTAT CCTTATGATGTT-3'
HA91-108-R1	5'-ATAACAATTAGAATAAGCCTTAGATTTGTATAGTT CATCCATGCC-3'
HA91-108-R2	5'-CCAGGC*TCTAGA*TTATAAAGAAGCATAATCAGGAA CATCATAAGGATAACAATTAGAATA-3'
HA307-319-F1	5'-CAAAATACTTTAAAATTAGCTACTGGAATGAGTAA AGGAGAAGAACTTTTC-3'
HA307-319-F2	5'-GCCTGG*CATATG*AGATATGTTAAACAAAATACTTT AAAATTAG-3'
HA307-319-R1	5'-AGTATTTTGTTTAACATATCTTTTGTATAGTTCATCC ATGCC-3'
HA307-319-R2	5'-CCAGGC*TCTAGA*TTATCCAGTAGCTAATTTTAAAGT ATTTTGTTTAAC-3'
Ext-For	5'-ATGACTCTTGCTTTCCAATT-3'
Ext-Rev	5'-ATAAGGGTCTTTATGACACA-3'
aadA-For	5'-CTAGGATCCATGGCAGAAGCG-3'
aadA-Rev	5'-TATCTAGATTATTTGCCGA-3'

psaB-probe-For	5’-CCGAAATTGGTTCTATACATATGACC-3’
psaB-probe-Rev	5'-GCCCAGTGAATATCGCTTATTCTGG-3'
Prrn-Fw	5’-CTTATAGGCCGGCCGCTCCCCCGCCGTCGTTCAATGAG-3’
TrbcL-Rv	5'-TAATCATCCTGAATCTGCTCAATG-3'
aadA-3’For	5’-GATCAGTTGGAAGAATTTG-3’
rps14-Rev	5’-CATTATGGCAAGGAAAAGTT-3’
p24-For	5’-CATATGGCTAGCGGATCCCCTATT-3’
p24-Rev	5’-TCTAGAGGAATTCTACTCAGCTTTATGTC-3’
Let-Ex-For	5’-ACTGGAAGGTGCGGCTGGAT-3’
Let-Ex-Rev	5’-CTCGCCCTTAATTTTAAGGC-3’
psbC-probe-Fw	5'-GGGCAGTGCAAGAGAAATCATAC-3’
psbC-probe-Rv	5'-CAGAAACAAAAACAGCAATTGG-3’
trnH-Rv	5’-AGTCTATGTAAGTAAAAT-3’
accD-Rv	5’-CAAACTAACTACTTTTTTGCTACAAACAC-3’
trnV-Fw	5’-CAGTTCGAGCCTGATTAT-3’
trnH-probe-Fw	5’-CGATTTATGGATGGAATCAAATATGC-3’
trnH-probe-Rv	5’-CAAGGCAGTGGATTGTGAATC-3’

Cilia Lelivelt, Rijk Zwaan Breeding Bv, Eerste Kruisweg 9, 4793 RS Fijnaart. *Lactuca sativa* cv. Simpson Elite seeds were purchased from Seeds-By-Size, 45 Crouchfield, Heinel, Hempstead, Herts, HP1 1PA, England.

2.4.2 Plant growth regulators

Plant growth regulator stock solutions were made to a final concentration of 1 mg/ml except for myo-insitol which was made to a final concentration of 100 mg/ml. BA, NAA, thiamine HCL and myo-insitol were dissolved in 500 µl of 1 M NaOH and then made to a final volume of 1 ml in sterile distilled water. All solutions were filter sterilised using a 0.2 µm acrodisc and stored at -20 °C until required.

2.4.3 Plant tissue culture media

Tobacco/lettuce germination medium: 2.3 g/L MS salts + vitamins, 10 g/L sucrose, 8 g/L microagar, pH 5.8 with 1 M NaOH, sterilised by autoclaving at 121 °C for 20 minutes.

MS medium (Murashige & Skoog, 1962): 4.6 g/L MS salts + vitamins, 30 g/L sucrose, 8 g/L microagar, pH 5.8 with 1 M NaOH, sterilised by autoclaving at 121 °C for 20 minutes.

RMOP medium (Svab *et al.*, 1990): 4.6 g/L MS salts + vitamins, 30 g/L sucrose, 0.1 g/L myo-insitol, 1 mg/L thiamine HCL, 1 mg/L BA, 0.1 mg/L NAA, 8 g/L microagar, pH 5.8 with 1 M NaOH, sterilised by autoclaving at 121 °C for 20 minutes.

Lettuce Regeneration (LR) medium (Kanamoto *et al.*, 2006): 4.6 g/L MS salts + vitamins, 30 g/L sucrose, 0.1 mg/L NAA, 0.1 mg/L BA, 500 mg/L PVP, 2 g/L Phytagel, pH 5.8 with 1 M NaOH, sterilised by autoclaving at 121 °C for 20 minutes.

Lettuce Regeneration (SLR) medium (Ruhlman *et al.*, 2010): 4.6 g/L MS salts + vitamins, 30 g/L sucrose, 0.1 mg/L NAA, 0.2 mg/L BA, 500 mg/L PVP, 6 g/L Phyta agar, pH 5.8 with 1 M NaOH, sterilised by autoclaving at 121 °C for 20 minutes.

2.5 Tobacco growth conditions

2.5.1 Seed sterilisation

Tobacco seeds were immersed in 1 ml 70% ethanol in a 1.5 ml microcentrifuge tube and vortexed for 30 seconds. The ethanol was removed and the seeds were washed three times with 1ml of sterile distilled water. The seeds were washed in 1 ml of 10% (v/v) bleach solution (Domestos) for 20 minutes with constant agitation using a tube rotator. The bleach solution was removed and the seeds were washed four times in 1 ml of sterile distilled water. Seeds were sown on sterile plates containing germination medium (Section 2.4.3) and placed at 25 °C under a 16/8 hour light/dark photoperiod (48 μmol m^{-2} s^{-1}) for one week. Seedlings that germinated after one week were transferred to individual MS tubs (Section 2.4.3; Tubs supplied by Russell Will, C/O Boyne Valley Group, Platin Rd, Drogheda, Co Louth).

2.5.2 *In vitro* growth conditions

Tobacco plants were grown *in vitro,* in a culture room at 25 °C, under a 16/8 hour light/dark photoperiod cycle (48 μmol m^{-2} s^{-1}). Plants were sub-cultured every four to six weeks by nodal cuttings placed in fresh MS medium.

2.5.3 Potted plants

Tobacco plants were potted in multi-purpose potting compost (Westland Garden Health). Plants were grown in a growth chamber at 25 °C under 16/8 hour light/dark photoperiod (48 μmol m^{-2} s^{-1}).for approximately three months until they set seed.

2.5.4 Reciprocal genetic crosses

Reciprocal genetic crosses were performed between wild type tobacco and transformed spectinomycin-resistant plants. Prior to anthesis, flowers from some plastid transformed and wild type plants were emasculated by removing the stamens with a sterile forceps (female recipient flowers). Once the flowers had opened, pollen from either plastid transformed or wild type plants (male donor plants) was applied to the stigma of the emasculated female recipient flowers. Pollinated flowers were covered with clingfilm to prevent further pollination. Seeds obtained were sterilised as described in Section 2.5.1 and germinated on plates containing suitable selective media.

2.6 Bacterial material

2.6.1 Bacterial strains

Top10 *Escherichia coli* (Invitrogen) were used for all cloning experiments.

2.6.2 Antibiotic stock solutions

Spectinomycin and ampicillin were dissolved in distilled water to a final concentration of 100 mg/ml. Solutions were filter sterilised using a 0.2 μm acrodisc and stored at -20 °C until required.

2.6.3 Bacterial culture media

Luria-Bertani (LB) medium (Sambrook *et al.*, 1989): 10 g/L tryptone (Difco), 5 g/L yeast extract (Difco) and 10 g/L NaCl, pH 7, sterilised by autoclaving at 121 °C for 20 minutes.

LB Amp agar plates were prepared as above with the addition of 15 g/L Bactoagar (Difco). The media was sterilised by autoclaving at 121 °C for 20 minutes before being allowed to cool to 55 °C. Ampicillin (100 μg/ml) was added to the cooled media that was poured into sterile 9 cm Petri dishes and allowed to solidify. LB AMP agar plates were stored at 4 °C until required.

LB Amp X-gal agar plates were prepared as described above with the addition of 5-bromo-4-chloro-3-indolyl β-D-galactopyranoside (X-gal) (40 mg/ml) just prior to pouring.

SOC media from Invitrogen was used in all *E.coli* transformation experiments.

2.7 Molecular analysis

2.7.1 Polymerase chain reaction (PCR)

PCR reactions were set up in a 50 µl reaction volume as follows: 5 µl of 10X PfuUltra HF reaction buffer, 1 µl of 10 mM dNTPs [25 µl of dCTP, dGTP, dATP and dTTP (100 mM stocks from Promega) made up to a final volume of 1 ml], 2 µl each of the forward and reverse primers (10 pMol), 2.5 units of PfuUltra HF DNA polymerase (Stratagene), 50 ng of template DNA and made up to a final volume of 50 µl with sterile distilled water. Suitable PCR cycling conditions were determined for individual primer pairs based on primer Tm and expected amplicon size. A standard PCR cycle consisted of an initial denaturing step at 95 °C for one minute followed by 30 cycles of denaturation at 95 °C for 30 seconds, annealing for one minute at a temperature determined by the Tm of the specific primer pair (generally 5 °C below the lowest Tm) extension at 72 °C for one minute / kb of the expected amplicon size, a final extension step of 72 °C for ten minutes and a 4 °C hold. 5 µl of each PCR reaction was analysed by agarose gel electrophoresis.

2.7.2 Agarose gel electrophoresis

DNA samples were electrophoresed on a 0.7% agarose gel. 0.7 g of agarose was dissolved in 100 mls 0.5 X TBE buffer (45 mM Tris-borate, 1 mM EDTA, pH 8.0) by boiling in a microwave. The solution was allowed to cool to approximately 50 °C and then poured into a casting tray and allowed to set. Prior to loading, the samples were mixed with 6 X loading dye (0.25% bromophenol blue, 0.25% xylene cyanol FF and 15% ficoll in water) and then

run in 0.5 X TBE buffer at 100 V for 60 minutes. Following electrophoresis, the gel was stained with ethidium bromide (0.5 μg/ml), visualised under UV light and photographed using the Syngene gel viewing system.

2.7.3 DNA purification from agarose gels

DNA was extracted from agarose gels using a QIAquick® spin kit (Qiagen) following the manufacturers' instructions. All buffers (QG, PE and EB) and columns were supplied with the kit and details of buffer constituents are outlined in the QIAquick® spin kit handbook.

The required DNA fragment was visualized under low UV light intensity, excised from the agarose gel using a clean scalpel blade and placed in a sterile microcentrifuge tube. The gel slice was weighed and three volumes of QG buffer was added to one volume of the gel slice. The sample was incubated at 50 °C for 10 minutes and mixed by inversion every two to three minutes to help the gel to dissolve. One volume of isopropanol was added to the sample and mixed. The sample was applied to a QIAquick spin column in a 2 ml collection tube and centrifuged at 8504 X *g* for one minute. The flow-through was discarded and the spin column was placed back into the collection tube. QG buffer (500 μl) was added to the column, centrifuged at 8504 X *g* for one minute and the flow-through discarded. PE buffer (750 μl) was added to the spin column, centrifuged at 8504 X *g* for one minute and the flow-through discarded. The spin column was centrifuged at 8504 X *g* for one additional minute to remove any residual PE buffer. The spin column was placed in a new microcentrifuge tube. EB buffer (30 μl) was added to the centre of the QIAquick spin column

membrane to elute the DNA. The column was left to stand at room temperature for 20 minutes and then centrifuged at 8504 X *g* for one minute. The column was discarded and the eluted DNA was stored at -20 °C until required.

2.7.4 QIAquick PCR product purification

PCR products were purified using a QIAquick® PCR purification kit (Qiagen) following the manufacturers' instructions. All buffers (PB, PE and EB) and columns were supplied with the kit and details of the buffer constituents are outlined in the QIAquick® purification kit handbook.

Five volumes of buffer PB was added to one volume of the PCR sample and mixed. The sample was applied to a QIAquick spin column, centrifuged at 8504 X *g* for one minute and the flow-through discarded. The column was washed with 750 µl of buffer PE, centrifuged at 8504 X *g* for one minute and the flow-through discarded. The column was centrifuged at 8504 X *g* for one additional minute and subsequently placed into a fresh microcentrifuge tube. Buffer EB (30 µl) was applied directly to the QIAquick membrane and left at room temperature for 20 minutes. The DNA was eluted by centrifuging at 8504 X *g* for one minute. The DNA was stored at -20 °C until required.

2.7.5 Restriction digestion

Restriction digests were carried out using either New England Biolabs or Promega restriction enzymes with the corresponding buffer. Restriction digest reactions consisted of: 0.5 µg of DNA sample, 3 µl of the appropriate 10 X restriction enzyme buffer, 0.3 µl of BSA (100 mg/ml), two units of the

restriction enzyme made up to a final volume of 30 µl with sterile distilled water. The reaction was gently mixed and incubated at 37 °C for approximately four hours after which the restriction digests were analysed by agarose gel electrophoresis.

2.7.6 Ligation reactions

Ligation reactions were set up with a 1:3 and 1:7 molar ratio of vector to insert DNA. A typical reaction consisted of 100 ng of vector DNA, 300-700 ng of insert DNA, 1.5 µl ligase 10 X buffer, one unit of T4 DNA ligase and sterile distilled water to a final volume of 15 µl. The reaction was incubated at 16 °C overnight and stored at -20 °C until transformation into *E.coli* cells.

2.7.7 Transformation of E.coli

One vial of One shot ® Chemically Competent *E. coli* cells (Invitrogen) was thawed on ice. 3 µl of the ligation reaction was added to the cells and gently mixed by tapping. The cells were incubated on ice for 30 minutes, heat shocked at 42 °C for 30 seconds and then returned to the ice for two minutes. SOC medium (250 µl) was added to the cells which were then incubated at 37 °C for one hour with shaking at 200 rpm. 50 µl and 200 µl of the transformed cells were spread directly onto LB Amp (for pCR4-TOPO) or LB Amp X-gal (for pCR2.1-TOPO) agar plates containing 50 µg/ml ampicillin (40 mg/ml X-gal). The plates were incubated at 37 °C overnight. Plasmid DNA was isolated from selected antibiotic-resistant colonies and restriction digests were performed with the appropriate enzymes to confirm cloning of recombinant plasmids.

2.7.8 Minipreparation of bacterial plasmid DNA

Plasmid DNA was prepared using two methods:

1. Alkaline lysis method (Sambrook *et al.,* 1989)
2. QIAprep® spin miniprep kit (Qiagen)

2.7.8.1 Alkaline lysis plasmid miniprep

Top 10 *E.coli* cells containing plasmid DNA were streaked onto LB agar plates (Section 2.6.3) containing 50 μg/ml ampicillin and grown overnight at 37 °C. The following day, a single colony was inoculated into 5 ml of liquid LB medium containing 50 μg/ml ampicillin. The culture was grown overnight at 37 °C with shaking at 300 rpm. 1 ml of the overnight culture was centrifuged at room temperature for two minutes at 8504 X *g* and the supernatant discarded. The pellet was resuspended in 200 μl resuspension buffer (50 mM glucose, 25 mM Tris, 100 mM EDTA) containing 1 mg/ml RNase A and the sample incubated at room temperature for 10 minutes. 200 μl lysis buffer (0.2 M NaOH, 1% SDS) was added, gently mixed by inversion and the sample was incubated on ice for 10 minutes. 200 μl of 3 M sodium acetate pH 5.2 was added and the sample was incubated on ice for 20 minutes. The sample was centrifuged at 8504 X *g* for five minutes and the supernatant was transferred to a fresh 1.5 ml microcentrifuge tube. The sample was centrifuged at 8504 X *g* for a further five minutes and the supernatant was again transferred to a fresh 1.5 ml microcentrifuge tube. Two volumes of ice cold 100% ethanol was added, mixed gently by inversion and incubated at -20 °C for one hour. The precipitated DNA was pelleted by centrifugation for 10 minutes at 8504 X *g*. The pellet was

washed with 500 μl of 70% ethanol (room temperature). The sample was centrifuged at 8504 X *g* for five minutes, the 70% ethanol was discarded, the pellet was air dried and then resuspended in 50 μl of TE buffer (10 mM Tris-HCL, 1 mM EDTA, pH 8.0). DNA was stored at -20°C until required.

2.7.8.2 QIAprep spin minipreparation

The QIAprep spin miniprep kit (Qiagen) was used following the manufacturers' instructions. All buffers (P1, P2, N3, PB, PE and EB) and columns were supplied with the kit and details of buffer constituents are outlined in the QIAprep spin miniprep kit handbook

Top 10 *E.coli* cells containing the plasmid DNA were streaked onto an LB agar plate containing 50 μg/ml ampicillin and grown overnight at 37 °C. A single colony was inoculated into 5 ml of liquid LB medium containing 50 μg/ml ampicillin and grown at 37 °C overnight with shaking at 300 rpm. 1 ml of the overnight culture was centrifuged at 8504 X *g* for two minutes at room temperature. The supernatant was discarded and the pellet was resuspended in 250 μl buffer P1 containing 100 μg/ml RNase A. Buffer P2 (250 μl) was added to the sample and mixed by inversion four to six times. Buffer N3 (350 μl) was added to the sample, mixed by inversion four to six times and centrifuged at 8504 X *g* for 10 minutes. The supernatant was applied to a Qiagen spin column. The column was centrifuged for one minute at 8504 X *g* and the flow through discarded. The column was washed with 500 μl of PB buffer and centrifuged at 8504 X *g* for one minute and the flow through was discarded. The column was washed with 750 μl of PE buffer, centrifuged for one minute at 8504 X *g* and

the flow through was discarded. The column was centrifuged at 8504 X *g* for an additional minute to remove any residual PE buffer. The QIAprep column was placed in a fresh 1.5 ml microcentrifuge tube and 50 µl EB buffer was applied to the column. The column was left to stand for one minute and centrifuged at 8504 X *g* for one minute to elute the DNA. DNA was stored at -20 °C until required.

2.8 Construct preparation

2.8.1 Gene sources

2.8.1.1 Hemagglutinin

The hemagglutinin (*HA*) gene was amplified from the plasmid pZS-HA (supplied by Dr. Karen Shiel, Plant Molecular Biology Laboratory, NUI Maynooth, Co. Kildare). It consists of the full length *HA* gene, encoding the influenza virus A/Sichan/2/87 (H3N2) hemagglutinin protein (Johnson *et al.*, 2000).

2.8.1.2 Green fluorescent protein

The *gfp* gene coding for green fluorescent protein (GFP) was amplified from the plasmid pLCV2-GFP/aadA (Lelivelt *et al*., 2005). This gene is a modified *gfp* gene containing three solubility mutations F99S, M153T and V163A (sm*GFP*; Davis & Vierstra, 1998; GenBank accession number U70495).

2.8.2 Ligating PCR products into pCR TOPO

To ensure efficient ligation of the PCR product into the cloning vectors, 3' adenine (A) overhangs were added to the products. Following PCR clean up (Section 2.7.4) or gel purification (Section 2.7.3) of the PCR products, 10 µl 5 X *Taq* Flexi buffer, 12 µl of 6 mM $MgCl_2$, 5 µl of 10 mM dATPs, 22.8 µl of the cleaned up PCR product and one unit of *Taq* polymerase (Promega) were added to a sterile microcentrifuge tube, mixed by vortexing and incubated at 72 °C for 10 minutes. 4 µl of A-tailed PCR product, 1 µl of salt solution (1.2 M NaCl, 0.6 M $MgCl_2$) and 1 µl of either pCR2.1-TOPO or pCR4-TOPO vector (200 ng) was added to a sterile 0.2ml PCR tube. The mixture was gently mixed by tapping and was incubated at room temperature for 10 minutes. The reaction was kept on ice or at -20 °C until transformation into *E. coli* cells (Section 2.7.7).

2.8.3 Sequencing

DNA was sequenced commercially by either Agowa (LGC Genomics GmbH, P.O. Box 940327, D-12443, Berlin Germany) or MWG (Eurofins MWG Operon, Westway Estate, 28-32 Brunel Road, Acton, London W3 7XR).

2.8.4 Cloning genes into a chloroplast transformation vector

The pMO16 vector was kindly supplied by Prof. Ralph Bock, Max-Planck-Institut für Molekulare Pflanzenphysiologie, Am Mühlenberg 1, D-14476 Potsdam-Golm, Germany. The vector was originally engineered to include the phage lysin gene, *PlyGBS* (Oey *et al.*, 2009a).

2.8.4.1 pMO16 transformation vector

The pMO16 chloroplast transformation vector contains two expression cassettes. The first cassette contains the strong constitutive 16s ribosomal RNA operon promoter *Prrn*, the aminoglycoside 3'-adenyltransferase (*aadA*) gene which allows for selection of putative transformants by conferring spectinomycin and streptomycin resistance and the *psbA* 3'terminator. *LoxP* sites flank the *aadA* expression cassette to allow for eventual Cre-mediated excision of the cassette if required. The second expression cassette also contains the strong constitutive 16s ribosomal RNA operon promoter *Prrn*, followed by the gene 10 leader from phage T7 (T7g10L), the *plyGBS* gene flanked by *NdeI* and *XbaI* restriction sites, and the 3'untranslated region of the plastid rubisco large subunit gene (T*rbcL*). These two expression cassettes are flanked by chloroplast DNA sequences including the glycine tRNA gene (*trnG)* and the methionine tRNA gene (*trnfM).*

2.8.5 Generation of constructs

The *HA*-gene constructs could not be cloned directly into pMO16 by gene replacement using *NdeI* and *XbaI* restriction sites because these two restriction sites are not unique to the vector. Therefore, the *plyGBS* expression cassette was removed into an intermediate cloning vector, pBluescript SK (+), which allowed cloning of the HA-gene constructs. Newly generated expression cassettes were then cloned back into the pMO16 vector.

2.8.5.1 Generation of the GFP-HA epitope fusion constructs

To clone the GFP- HA epitope fusion constructs, both pBluescript SK (+) and the pMO16 vector were digested with *HindIII* and *SacI* restriction enzymes (Section 2.7.5). The pBluescript SK (+) vector backbone and the *plyGBS* expression cassette were gel purified (Section 2.7.3), ligated together (Section 2.7.6) and transformed into chemically competent TOP10 cells (Section 2.7.7). Positive colonies were identified and the pCas-HindIII construct was used in subsequent cloning experiments.

The pCR2.1-TOPO containing the GFP-HA epitope fusion genes and the pCas-HindIII construct were digested with *NdeI* and *XbaI* restriction enzymes according to section 2.7.5. Both the pBS-Cass1 vector backbone and the epitope fusion genes were gel purified and ligated as described above. Positive clones were identified. One of the clones was digested with *HindIII* and *SacI*, to release the GFP-HA epitope expression cassette which was ligated back into pMO16 at the *HindIII* and *SacI* sites to give the final GFP-HA epitope fusion plastid transformation vector.

2.8.5.2 Generation of pMO14rHA and pMO14gHA constructs

To clone the 14aaRBCL-HA (14rHA) and 14aaGFP-HA (14gHA) constructs, both the pMO16 vector and pBluescript SK (+) were digested with *ApaI* and *SacI* restriction enzymes (Section 2.7.5). The pBluescript SK (+) vector backbone and the *plyGBS* expression cassette were gel purified and ligated as described above. Positive colonies were identified and pCass-ApaI was used in subsequent cloning experiments.

The pCass-ApaI vector and the pCR4-14R-HA gene or the pCR4-14G-HA gene was digested with *NdeI* and *XbaI* restriction enzymes according to section 2.7.5. The pCass-ApaI vector backbone and the 14R-HA or the 14G-HA genes were gel purified, ligated as described in section 2.8.5.1 and recombinant clones were identified.

One recombinant clone and the pMO16 vector were re-digested with *ApaI* and *SacI*, and ligated as described above to give the final pMO14rHA and pMO14gHA transformation vectors.

2.8.5.3 Generation of pMOGFP/HA and pMOGFP/HA1 constructs

The pMOGFP/HA and pMOGFP/HA1 transformation vectors were constructed using the same method as described in section 2.8.5.2.

2.9 Chloroplast transformation of tobacco

2.9.1 Particle bombardment systems

2.9.1.1 Stock solutions for particle bombardment experiments

Stock solutions were prepared as follows:

2.5M Calcium chloride stock solution: 3.68 g $CaCl_2.2H_2O$ was dissolved in 10 ml of sterile distilled water. The solution was vortexed until the $CaCl_2.2H_2O$ had dissolved, filter sterilised through a 0.2 μM acrodisc and stored at -20 °C until required.

0.1M Spermidine stock solution: A 1 g ampoule of spermidine (Sigma) was heated at 37 °C for approximately five minutes until completely liquefied. The spermidine was divided into 15.8 µl aliquots, immediately frozen in liquid nitrogen and stored at -70 °C until required. Prior to transformation, one 15.8 µl aliquot was thawed on ice, made up to 1 ml with 984.2 µl of sterile distilled water, vortexed, divided into 50 µl aliquots and immediately flash frozen in liquid nitrogen. Aliquots were stored at -70 °C until required.

Gold Microparticle Stocks (60 mg/ml): 30 mg of gold microparticles (BioRad Laboratories, Molecular Bioscience Group, 2000 Alfred Nobel Drive, Hercules, California 94547) were weighed into a 1.5 ml eppendorf. 100% ethanol (1 ml) was added to the gold, vortexed for two minutes and centrifuged for five seconds, at room temperature, at 8504 X *g*. The ethanol was discarded and the pellet was resuspended in 1 ml sterile water. The mixture was vortexed for two minutes and centrifuged for five seconds at room temperature at 8504 X *g*. The water was removed and the last three steps were repeated twice. The pellet was resuspended in 500 µl of 50% sterile glycerol by vortexing and was divided into 50 µl aliquots (vortexing between each aliquot) and stored at room temperature until required.

2.9.2 Tobacco leaf preparation for bombardment

Tobacco leaves for plastid transformation were harvested from four to six week old *Nicotiana tabacum*, cv. Petit Havana grown *in vitro*. The day prior to bombardment, the leaves were placed adaxial side down on 9 cm Petri dishes

containing RMOP medium and incubated at 25 °C under a 16/8 hour light/dark photoperiod (48 μmol m^{-2} s^{-1}) for 24 hours.

2.9.3 Coating of gold microparticles

One 50 μl aliquot of gold particle stock (60 mg/ml) was vortexed for one minute. 15 μl of plasmid DNA (1 μg/μl) was added directly to the gold particles, followed by 20 μl of 0.1 M spermidine and 50 μl of 2.5 M $CaCl_2$. The sample was vortexed and incubated on ice for 10 minutes. The sample was vortexed for a further five seconds and centrifuged at 8504 X *g* for five seconds. The supernatant was removed and the pellet was washed in 100 μl of 100% ethanol, vortexed for 10 seconds and centrifuged at room temperature for five seconds at 8504 X *g*. The supernatant was removed and the particles were resuspended in 60 μl of 100% ethanol and kept on ice until bombardment.

2.9.4 Sterilisation of gene gun equipment

The bombardment chamber was sterilised with 70% ethanol and allowed to dry. Mesh stopping screens and macrocarrier holders were sterilised by autoclaving (121 °C for 20 minutes). Macrocarriers were sterilised by dipping in 100% ethanol and allowed to air dry on a sterile paper plate. The rupture discs were sterilised in 70% isopropanol immediately prior to each shot.

2.9.5 Particle bombardment

Particle bombardment was carried out using a biolistic PDS-1000/He gun

(Biorad). Sterile macrocarriers were placed into the macrocarrier holders. 8 μl of vortexed gold/DNA mixture was pipetted onto the centre of each sterile macrocarrier and left at room temperature for 10 minutes. A sterile rupture disc (1,100 psi) was inserted into the recess of the retaining cap, which was tightly screwed onto the gas acceleration tube. A sterile stopping screen was placed on the support and the macrocarrier holder was installed on the rim of the fixed nest. The macrocarrier lid was then screwed onto the assembly. The macrocarrier launch assembly was placed in the top slot inside the bombardment chamber. The target shelf was placed at the desired distance, 6 cm from the macro-projectile stopping screen and the Petri dish containing the target tissue was placed on it. The helium tank was opened to 1,300 psi (200 psi greater than the capacity of the rupture disc). The door of the gene gun was closed and the chamber was evacuated to 28 Hg (inches of mercury) and held at this vacuum. The fire button was pressed and then released once the rupture disc had burst. The chamber was vented, the Petri dish removed and the procedure was repeated for subsequent shots. When the shooting was finished, the Petri dishes were sealed with clingfilm and placed at 25 °C under a 16/8 hour light/dark photoperiod regime for 2 days (48 μmol m^{-2} s^{-1}).

2.9.6 Tissue culture of bombarded tobacco leaves

Two days after bombardment, the leaves were cut into 10 mm^2 pieces and placed abaxial side down onto RMOP regenerating medium, containing 500 mg/L spectinomycin for tobacco. After three weeks, leaf pieces were transferred to fresh regeneration medium containing spectinomycin. The first spectinomycin resistant tobacco shoots were visible after three to four weeks

and were transferred to MS medium containing 500 mg/L spectinomycin for root formation. Spectinomycin resistant shoots were screened for the presence of the transforming DNA by PCR using various primer combinations (Section 2.7.1).

2.9.7 Rounds of regeneration

Once shoots had been confirmed as transformed, they were subjected to three rounds of regeneration to achieve homoplasmy. Leaves from transformed shoots were cut into 10 mm^2 pieces, placed on RMOP plates containing 500 mg/L spectinomycin for shoot formation and then transferred to MS media containing 500 mg/L spectinomycin for rooting.

2.10 Confirmation of chloroplast transformation

2.10.1 Plant DNA extraction (Used for PCR analyses of putative transformed plants)

Total plant DNA was extracted from putatively transformed plants using a DNeasy plant mini kit (Qiagen). All buffers (QG, PE and EB) and columns were supplied with the kit and details of the buffer constituents are outlined in the DNeasy plant mini kit handbook.

Plant tissue (100 mg) was flash frozen in liquid nitrogen and ground using a micro-pestle. Buffer AP1 (400 µl) and 4 µl RNase A stock solution (100 mg/ml) were added to the sample and vortexed until no tissue clumps were visible. The sample was incubated at 65 °C for 10 minutes and mixed two to three times during the incubation by inversion. Buffer AP2 (130 µl) was added to the lysate,

vortexed and left on ice for five minutes. The lysate was centrifuged at 8504 X *g* for five minutes and the supernatant was pipetted into a QIAshredder Mini spin column placed in a 2 ml collection tube. The column was centrifuged at 8504 X *g* for two minutes and the flow-through fraction was transferred to a new microcentrifuge tube without disturbing the pellet. 1.5 volumes of AP3/E buffer was added to the cleared lysate and mixed by pipetting. 650 µl of the mixture was pipetted into a DNeasy Mini spin column placed in a 2 ml collection tube, centrifuged for one minute at 8504 X *g* and the flow-through was discarded. This step was repeated with the remaining sample and the flow-through and collection tube were then discarded. The DNeasy Mini spin column was placed into a new 2 ml collection tube. Buffer AW (500 µl) was added to the column, centrifuged for one minute at 8504 X *g* and the flow-through was discarded. Buffer AW (500 µl) was added to the column and centrifuged for two minutes at 8504 X *g* to dry the membrane. The column was transferred to a fresh microcentrifuge tube. Buffer AE (50 µl) was pipetted directly onto the membrane, incubated at room temperature for five minutes and centrifuged at 8504 X *g* for one minute to elute the DNA. The column was placed into a new microcentrifuge tube and the last step was repeated. DNA was stored at 4 °C until required.

2.10.2 Plant DNA extraction (Used for Southern blot analysis)

A modified version of a protocol by Frey *et al.*, 1999 was used to extract genomic DNA from putatively transformed plants. Leaf tissue (100 mg) was flash frozen in liquid nitrogen and ground up in 500 µl of lysis buffer (20 mM Tris, pH 8.0; 20 mM EDTA; 2 M NaCl) in a microcentrifuge tube using a micro

pestle. The sample was incubated at 85 °C for five minutes and then placed on ice for five minutes. This step was repeated twice. The sample was vortexed and centrifuged at 8504 X *g* for 10 minutes. The supernatant was transferred to a fresh tube and 10 µl of 10 mg/ml RNase A was added. The sample was incubated at 37 °C for 30 minutes. 0.1 volume of 3 M sodium acetate, pH 5.2 and one volume of isopropanol were added to the sample, mixed by inversion and incubated at -20 °C for one hour. The sample was centrifuged at 8504 X *g* for 10 minutes and the supernatant was carefully removed. The pellet was washed with 500 µl of 70% ethanol, centrifuged at 8504 X *g* for five minutes and the supernatant was removed. The pellet was air dried and then resuspended in 50 µl AE buffer.

2.10.3 PCR confirmation of plastid transformation

PCR was carried out on DNA extracted from wild type and putatively transformed plants using different primer combinations depending on the gene of interest used for transformation. Primer sequences are listed in Table 2.1. A standard PCR was used as described in section 2.7.1.

2.10.4 Southern blot analyses

2.10.4.1 PCR-based Digoxigenin (DIG)-probe labelling

Probes were synthesized using a PCR DIG-labelling kit (Roche). 5 µl of 10 X PCR buffer with $MgCl_2$, 2.5 µl of PCR DIG-labelled dNTPS, 2.5 µl of unlabelled PCR dNTPS, 1 µl of 10 pMol forward primer, 1 µl of 10 pMol

reverse primer, 0.75 µl of enzyme and 10 ng of template DNA were added to a 0.2 ml PCR tube and brought to a final volume of 50 µl with sterile distilled water. An unlabelled probe synthesising reaction was set up to assess the efficiency of the labelling reaction (the same reaction but with unlabelled dNTP's). The reaction reagents were mixed briefly by vortexing. PCR was as described previously in section 2.7.1. 5 µl of each reaction was analysed on a 0.7% agarose gel (Section 2.7.2). The unlabelled control reaction generated a PCR product of the expected size, the labelled probe reaction generated a PCR product larger than the expected size because of the incorporation of DIG-labelled dUTP's. DIG-labelled probes were stored at -20 °C until required.

2.10.4.2 Restriction digestion

Total plant DNA (4 µg) was digested with *BamHI* (NEB) in a total volume of 50 µl, including 5 µl of 10 X Buffer 2 (NEB), 0.5 µl of 100 X BSA (NEB), 1.5 µl of *BamHI* (20,000 units/ml; NEB) brought up to 50 µl with sterile distilled water. The reactions were incubated at 37 °C overnight. Samples were run out on a 0.7% agarose gel for five to six hours at 60 V and photographed using the SynGene gel viewing system.

2.10.4.3 Southern blotting

Agarose gels were blotted according to the protocol outlined in Sambrook *et al.*, 1989. The gel was submerged in denaturation solution (1.5 M NaCl, 0.5 M NaOH) twice for 15 minutes at room temperature with gentle shaking. The gel was then rinsed with sterile distilled water and submerged in neutralization

solution (0.5 M Tris-HCL, pH 7.5, 3 M NaCl) twice for 15 minutes at room temperature with gentle shaking. The gel was blotted onto Hybond N^+ nylon membrane (Amersham Biosciences), by capillary transfer overnight at room temperature using 20 X SSC buffer (3 M NaCl, 300 mM sodium citrate, pH 7). The following day, the capillary blot was dismantled and the membrane was rinsed in 2 X SSC for five minutes at room temperature with gentle shaking. The membrane was rinsed in sterile distilled water, baked at 120 °C for 30 minutes and stored at 4 °C until required.

2.10.4.4 Pre-hybridisation and hybridisation

The membrane was placed in a hybridisation roller tube and pre-hybridised in 20 ml of pre-warmed DIG Easy Hyb solution (Roche) for two to three hours at 42 °C in a hybaid oven. The DIG labelled probe was denatured by heating at 95 °C for 10 minutes and chilled on ice for five minutes. The pre-hybridisation solution was poured off and replaced with DIG Easy Hyb solution containing 10-20 ng/ml denatured probe. The roller tube was placed back in the hybaid oven at 42 °C for 16 hours. The hybridisation solution was stored at -20 °C for re-use.

2.10.4.5 Post-hybridisation washes

The membrane was washed twice with wash solution A (2 X SSC, 0.1% SDS) for five minutes. The first wash was carried out at room temperature and the second wash was carried out at 68 °C. The membrane was then washed with pre-warmed wash solution B (0.5 X SSC, 0.1% SDS) at 68 °C for 15 minutes

followed by a wash with pre-warmed wash solution C (0.1 X SSC, 0.1% SDS) at 68 °C for 15 minutes.

2.10.4.6 Chemiluminescence detection

All steps were performed at room temperature on a rotary shaker at 60 rpm. The membrane was rinsed in buffer 1A (0.1 M Maleic acid, 3 M NaCl, pH 8.0, autoclaved, 0.3% Tween-20) for one minute, followed by blocking in buffer 2 (1% blocking reagent (Roche) in buffer 1A) for two to three hours. The membrane was then incubated in anti-DIG-AP antibody, diluted 1:10,000 (v/v) in buffer 2 for 30 minutes. The unbound anti-DIG-AP was removed during four 10 minute washes in buffer 1A. The blot was equilibrated in buffer 3 (0.1 M Tris-base, 0.1 M NaCl, pH 9.5) for five minutes. The membrane was incubated in buffer 3 containing 0.24 mM CDP-star for 10 minutes. Any excess liquid was drained from the membrane before it was sealed between two acetate sheets. Hybridisation signals were detected using Kodak X-ray film using varying exposure times.

2.11 Protein analyses

2.11.1 Total protein extraction from plant tissue

Total soluble protein was isolated from transgenic plants using a two-step method. Plant tissue (100 mg) was flash frozen in liquid nitrogen and homogenised in 2 X (w/v) of a mild protein extraction buffer (2% Triton, 10% glycerol, 5% β-mercaptoethanol, 62.5 mM Tris-HCL) using a micro pestle. The sample was vortexed for five minutes and then centrifuged at 8504 X *g* for five

minutes. The supernatant was removed and placed in a fresh microcentrifuge tube (soluble fraction - SF). The pellet was resuspended in 2 X (w/v) of a more stringent 1% SDS protein extraction buffer (1% SDS, 10% glycerol, 5% β-mercaptoethanol, 62.5 mM Tris-HCL) vortexed for five minutes and then centrifuged at 8504 X *g* for 10 minutes. The supernatant was removed and transferred to a new microcentrifuge tube (insoluble fraction - ISF).

2.11.2 Protein extraction from *E. coli*

5 mls LB culture was inoculated with *E. coli* (strain Top10) containing a specific plasmid and were grown at 37 °C overnight with shaking (~280 rpm). 1 ml of the overnight culture was centrifuged for one minute at 8504 X *g* and the supernatant was discarded. The pellet was resuspended in 100 µl phosphate buffered saline (PBS) by vortexing and stored at -20 ° C until required.

2.11.3 Acetone precipitation of proteins

As the levels of SDS, triton X-100 and β-mercaptoethanol in both plant protein extraction buffers are not compatible with the Bradford reagent used for the determination of protein concentration, plant proteins were acetone precipitated and resuspended in a more compatible buffer. 4 X volumes of ice-cold acetone was added to the protein samples, mixed by inversion, placed at -20 °C for one hour and then centrifuged at 4 °C for 10 minutes at 8504 X *g*. The acetone was removed and the protein pellet was washed with 70% acetone. The sample was centrifuged at 4 °C for a further 10 minutes at 8504 X *g* and the 70% acetone

was removed. The pellets were air dried and resuspended in protein resuspension buffer (6 M urea, 50 mM Tris-Cl pH 6.8, 0.1% Triton X-100).

2.11.4 Protein concentration determination

Protein concentrations of leaf extracts were determined using a Bradford assay (Bradford, 1976). Protein samples were prepared as described in section 2.11.3. Samples were diluted 1:10 with distilled water. Standard protein solutions were prepared by diluting Bovine Serum Albumin (BSA) in distilled water to the following concentrations: 0.1 μg/μl, 0.15 μg/μl, 0.2 μg/μl, 0.25 μg/μl, 0.5 μg/μl, 0.75 μg/μl, 1 μg/μl, 1.5 μg/μl, 2 μg/μl and 4 μg/μl. 10 μl of the standards and plant samples were loaded in triplicate onto a 96-well microtiter plate (Sterilin). Bradford reagent (BioRad) was diluted 1:5 with distilled water and 200 μl was added to each well. The plate was left in the dark for five minutes after which the absorbance was measured at 595nm using a microplate reader. A standard curve was generated and used to calculate the unknown protein concentrations.

2.11.5 SDS-PAGE

SDS-PAGE was carried out according to Sambrook *et al.,* (1989). Mini protein gels (0.75-1 mm depth; BioRad) were cast using a 10% or 12% resolving gel depending on the size of the protein to be detected. Gels were prepared as follows (total volume 20 mls):

10% resolving gel: 7.9 ml distilled water, 6.7 ml of acrylamide/bis 30% stock, 5 ml of 1.5 M Tris-HCL pH 8.8, 200 μl of 10% SDS, 200 μl of 10% ammonium persulfate and 8 μl TEMED.

12% resolving gel: 6.6 ml distilled water, 8 ml of acrylamide/bis 30% stock, 5 ml of 1.5 M Tris-HCL pH 8.8, 200 µl of 10% SDS, 200 µl of 10% ammonium persulfate and 8 µl of TEMED.

5% stacking gel: 3.4 ml of distilled water, 0.83 ml of acrylamide/bis 30% stock, 0.63 ml of 1 M Tris-HCL pH 6.8, 50 µl of 10% SDS, 50 µl of 10% ammonium persulfate and 5 µl of TEMED.

Glass plates were assembled according to the manufacturer's instructions (BioRad). Resolving gel components were mixed in the order described above and poured between the glass plates leaving sufficient space for the stacking gel (about 2 cm). The resolving gel was overlaid with isobutanol to prevent oxygen diffusing into the gel and inhibiting polymerization. After polymerization was complete (30 minutes), the isobutanol was poured off and the top of the gel was washed with distilled water. The stacking gel was prepared by adding the components in the order described above, mixed and pipetted directly onto the surface of the polymerized resolving gel. A clean comb was inserted immediately into the stacking gel taking care to avoid trapping air bubbles. The stacking gel was left to polymerize for 30 minutes. Following polymerization, the gels were assembled in the electrophoresis rig (BioRad) according to the manufacturers instructions ready for use.

2.11.5.1 Preparation of protein samples for SDS-PAGE

Protein samples were prepared by adding 2 X laemmli loading buffer (Sigma). The samples were incubated at 37 °C for 10 minutes and cooled on ice for five minutes. Samples were then loaded onto the gel and run at 120 V for two hours.

2.11.5.2 Coomassie brilliant blue staining

SDS-PAGE resolved gels were stained in coomassie brilliant blue staining solution [0.5 g coomassie blue in 500 ml destain solution (400 ml methanol, 100 ml acetic acid, 500 ml water)] overnight with gentle shaking. The gels were destained in destaining solution (400 ml methanol, 100 ml acetic acid, 500 ml water) for two to three hours with gentle shaking. Stained gels were visualised using the Syngene gel viewing system.

2.11.5.3 Western blotting

Following SDS-PAGE, the gels were equilibrated in transfer buffer (20% methanol, 24 mM Tris base, 194 mM glycine, pH 8.5) for 15 minutes. Nitrocellulose membrane (Whatman) and eight pieces of filter paper (Whatman) were cut to the exact dimensions of the gel. Both the nitrocellulose membrane and the filter paper were immersed in transfer buffer. The blot was arranged by layering four pieces of buffer saturated filter paper on a Trans-Blot SD Semi-Dry Electrophoretic Transfer cell (BioRad), followed by the nitrocellulose membrane, the gel and the remaining four transfer buffer-saturated pieces of filter paper. Care was taken to remove any air bubbles. The cathode was placed onto the blot and the proteins were transferred to the membrane at 15 volts for 45 minutes. Following transfer, the nitrocellulose membrane was removed and placed in 5% PBSTM blocking solution [5% non-fat dried milk (Marvel) in PBST (phosphate buffered saline, pH 7.4, 0.1% Tween-20)] with gentle rocking overnight at room temperature. The membrane was incubated in diluted primary antibody (protein dependant) for two hours at room temperature with gentle rocking. The membrane was washed four times in 1% PBSTM, five minutes per

wash. The membrane was incubated in the secondary peroxidase conjugate antibody diluted 1:20,000 in 1% PBSTM for one hour at room temperature with gentle rocking. The membrane was washed four times in PBST, five minutes per wash. Blots were developed using the chemiluminescence detection system.

2.11.5.4 Chemiluminescence detection

The Immbilon Western Chemiluminescence HRP substrate kit (Millipore) was used for detection. Luminol reagent (3 ml) and peroxide reagent (3 ml) were mixed together in a 15 ml falcon tube (detection solution) and left to reach room temperature for 10 minutes. The blot was incubated in the detection solution for five minutes at room temperature. The blot was then sealed between two acetate sheets and signals were detected by exposure to Kodak X-ray film for 5-60 seconds. Following exposure, the film was developed in developing solution (Kodak) and fixed in fixing solution (Kodak).

2.12 Northern blot analysis

2.12.1 Isolation of RNA

The QIAGEN RNeasy plant mini kit was used according to the manufacturers' instructions. All buffers (RLT, RWI, and RPE) and columns were supplied with the kit and details of the buffer constituents are outlined in the Qiagen RNeasy plant mini kit handbook. Plant tissue (50 mg) was flash frozen in liquid nitrogen, ground immediately using a pestle and mortar and transferred to an RNase-free, liquid nitrogen cooled 2 ml microcentrifuge tube. 450 µl RLT buffer (containing 10 µl of 14.3 M ß-Mercaptoethanol) was added to the sample

and the sample was vortexed vigorously to disrupt the tissue. The lysate was added to a QIAshredder spin column placed in a 2 ml collection tube and the sample was centrifuged at 8504 X *g* for two minutes. The filtrate was then transferred to a fresh eppendorf tube for subsequent steps. 0.5 X volume of 100 % ethanol (v/v) was added to the filtrate and the sample was mixed immediately by pipetting. The sample was then transferred to an RNeasy spin column placed in a 2 ml collection tube and centrifuged at 8504 X *g* for 15 seconds. The flow-through was discarded. Buffer RWI (700 µl) was added to the RNeasy spin column and the sample was centrifuged at 8504 X *g* for two minutes to wash the spin column membrane. The flow-through was discarded. Buffer RPE (500 µl) was added to the RNeasy spin column and the sample was centrifuged at 8504 X *g* for 15 seconds to wash the spin column membrane. The flow-through was discarded. Buffer RPE (500 µl) was added to the RNeasy spin column, and the sample was centrifuged at 8504 X *g* for two minutes to wash the spin column membrane once again. To remove residual RPE buffer, the RNeasy spin column was placed in a new 2 ml collection tube, and the sample was centrifuged at 8504 X *g* for two minutes. Sterile water (50 µl) was placed on the centre of the column, and the column was allowed to stand for one minute. The column was centrifuged at 8504 X *g* for one minute to collect the eluted RNA. RNA was stored at -70 °C until required.

2.12.2 RNA gel electrophoresis

Agarose gels (1% w/v) were prepared by adding agarose (1 g) to double-autoclaved water (80 ml). The agarose was boiled in a microwave oven and allowed to cool to 65 °C. 10 ml of 10 X Formaldehyde Agarose (FA) gel buffer

(200 mM MOPS, 50 mM NaAcetate, 10 mM EDTA, pH 7 with NaOH, autoclaved at 121 °C for 20 minutes) was added in a fume hood, and the final volume was adjusted to 100 ml with double-autoclaved water. The gel was poured into a gel casting tray and allowed to set. The gel was then placed in an electrophoresis tank and submerged in 1 X Formaldehyde Agarose running buffer (100 ml 10 X FA Buffer, 20 ml 37% formaldehyde (12.3 M), 880 ml distilled water). The gel was allowed to equilibrate in this buffer for 10 minutes prior to loading. RNA samples (up to 3 µg) were added to the following components: 10 X FA Buffer (2.5 µl), 37% formaldehyde (4 µl), formamide (12 µl) and ethidium bromide (1 mg/ml; 1 µl). The RNA samples were denatured at 65 °C for 15 minutes and then left on ice. Samples were loaded onto the gel and electrophoresed at 70 V for 60 minutes. Formaldehyde agarose gels were visualised using the SynGene gel viewing system. The gels were blotted onto Hybond N^+ nylon membrane (Amersham Biosciences), by capillary transfer overnight at room temperature using 20 X SSC transfer buffer (3 M NaCl, 300 mM sodium citrate, pH 7). The capillary blot was dismantled and the membrane was washed in 2 X SSC for five minutes at room temperature with gentle shaking. The membrane was rinsed in sterile distilled water, baked at 120 °C for 30 minutes and stored at 4 °C until required. The membrane was prehybridised and hybridised (Section 2.10.4.4), washed (Section 2.10.4.5) and detected using a chemiluminescence kit (Section 2.10.4.6).

2.13 Chloroplast transformation of lettuce by particle bombardment

2.13.1 Optimisation of regeneration media for lettuce

2.13.1.1 Plant material

Lettuce (*Lactuca sativa* L. cv Flora and *Lactuca sativa* L. cv Evola) seeds were used for both the callus induction and shoot regeneration experiments.

2.13.1.2 Seed sterilisation

Seeds were immersed in 1ml 70% ethanol in a 1.5 ml microcentrifuge tube and vortexed for 30 seconds. The ethanol was removed and the seeds were washed three times with 1 ml of sterile distilled water. The water was removed and 1 ml of 100% (v/v) bleach solution (Domestos) was added to the seeds which were then agitated on a tube rotator for one hour. The bleach solution was removed and the seeds were washed four times in 1 ml of sterile distilled water. Seeds were sown on sterile plates containing germination medium (Section 2.4.3), placed at 23 °C and grown under a 16/8 hour light/dark photoperiod (48 μmol m^{-2} s^{-1}) for one week. Seedlings that germinated after one week were transferred to individual MS tubs (Section 2.4.3).

2.13.1.3 Lettuce *in vitro* growth conditions

Lettuce seedlings were grown *in vitro* on MS medium (Section 2.4.3) in a culture room at 23 °C and grown under a 16/8 hours light/ dark photoperiod cycle.

2.13.2 Assessing shoot regeneration from cotyledon derived callus

2.13.2.1 Callus formation from cotyledons

Cotyledons from four-day old seedlings were excised at the petioles and scored laterally across the midrib with the blunt side of a scalpel blade. The cotyledons were placed, wounded side down, into 9 cm Petri dishes containing a basic MS medium (Section 2.4.3) supplemented with various combinations and concentrations of the plant growth regulators 2,4-D, Kinetin, NAA and Zeatin. The plant growth regulators were added to the culture media prior to autoclaving with the exception of Zeatin, which was added afterwards. The Petri dishes were sealed with plastic wrap and placed in a growth room at 23 °C ± 2 °C in dim light (02 μmol m^{-1} s^{-1}) for four weeks. At the end of the four week incubation period, the calli were weighed and any shoot formation noted.

2.13.2.2 Assessing shoot regeneration from cotyledons

Cotyledons from four-day old seedlings were excised at the petioles and scored laterally across the midrib with the blunt side of a scalpel blade. The cotyledons were placed, wounded side down, into 9 cm Petri dishes containing a basic MS medium with varying combinations and concentrations of plant growth regulators kinetin and NAA (Section 2.4.2). The Petri dishes were sealed with plastic wrap and placed in a growth room at 23 °C ± 2 °C in light (48 μmol m^{-1} s^{-1}) with a 16h photoperiod, for eight weeks at which time the amount of shoot regeneration per explant was recorded.

2.13.2.3 Shoot regeneration from callus

Four week old calli were transferred to 9 cm Petri dishes containing a basic MS medium supplemented with varying concentrations, and combinations, of the plant growth regulators kinetin, NAA and BAP. Regenerating calli were maintained in a growth room at 23 °C ± 2 °C in the light (48 μmol m^{-1} s^{-1}) with a 16 hour light/ 8 hour dark photoperiod and were subcultured every 14 days. Four weeks after the initial transfer to shooting medium, the amount of shoot proliferation was recorded for each individual regenerating callus.

2.13.2.4 Rooting of shoots

Following a four-week incubation on shooting medium, regenerated shoots were excised and placed in tubs containing MS medium without hormones. The shoots were placed in a growth room at 23 °C ± 2 °C in light (26 μmol m^{-1} s^{-1}) with a 16 hour light/ 8 hour dark photoperiod, for three weeks in order for rooting to occur.

2.13.3 Optimisation of particle bombardment conditions for lettuce

2.13.3.1 Plant material

Lettuce (*Lactuca sativa* L. cv Flora) seeds were used for all particle bombardment optimisation experiments. Seeds were sterilised and germinated as described in section 2.13.1.2.

2.13.3.2 GFP construct

The LCV2-GFP/aadA lettuce chloroplast transformation vector (Lelivelt *et al*., 2005) contains two expression cassettes: the selectable marker gene *aadA* under the transcriptional control of the tobacco *rrn* promoter (P*rrn*) and containing the tobacco *psbA* 3' untranslated region (T*psbA*): the soluble modified *gfp* gene (sm*gfp*) engineered with the tobacco *rrn* promoter (P*rrn)* and *rbcL* 5'UTR and the *E.coli rrnB* terminator (T*rrnB*). The two cassettes are flanked by two lettuce chloroplast genes, *trnI* and *trnA,* to facilitate targeted integration.

2.13.3.3 Cotyledon preparation for bombardment

One day prior to bombardment, four-day old healthy lettuce cotyledons (cv Flora) were excised at the petioles. Approximately 40 cotyledons were placed abaxial side down within a 4 cm circle in the centre of a 9 cm Petri dish containing CIM2 medium (MS medium, section 2.4.3, supplemented with 0.1 mg/L 2, 4-D & 2 mg/L Kinetin). Sterile filter paper was placed on top of the cotyledons to prevent them from curling (the filter paper was removed from the cotyledons prior to bombardment). The plates were placed in a plant tissue culture room at 25 °C ± 2 °C under a 16 hour light/ 8 hour dark (48 μmol m^{-1} s^{-1}) photoperiod regime for 24 hours.

2.13.3.4 Preparation of gold particles

Gold microparticles of two different diameters, 0.6 μM and 1.0 μM, were used in these experiments (BioRad). Gold particles were sterilised and coated as previously described in section 2.9.3.

2.13.3.5 Particle bombardment of cotyledons

Bombardment of cotyledons was performed as described in section 2.9.5 with the following modifications:

Bombardments were carried out using three different pressures: 650 psi, 900 psi & 1,100 psi and with two different sizes of gold particles.

2.13.4 Analysis of plastid-based GFP expression

Chloroplast-localised transient GFP expression was assayed for in protoplasts prepared from bombarded cotyledons.

2.13.4.1 Stock solutions for protoplast isolation

CPW165 salts stock 100 X (100 ml): 1.01 g KNO_3, 2.46 g $MgSO_4.7H_20$, 272 mg KH_2PO_4, 1.6 mg KI and 0.16 mg $CuSO_4$ brought up to 100 ml with distilled water and stored at -20 °C.

B_5 macro 40 X (250 ml): 25 g KNO_3, 1.2156 g $MgSO_4$, 1.7 g $NaH_2PO_4.2H_2O$ and 1.34 g $(NH_4)_2SO_4$ brought up to 250 ml and stored at -20 °C.

B_5 micro 1000 X (100 ml): 25 mg $Na_2MoO_4.2H_2O$, 1 g $MnSO_4.H_2O$, 200 mg $ZnSO_4.7H_2O$, 300 mg H_3BO_3, 75 mg KI, 1.6 mg $CuSO_4$ and 2.5 mg $CoCl_2.6H_2O$ brought up to 100 ml with distilled water.

$CuSO_4$ stock: 160 mg $CuSO_4$ was added to 10 ml distilled water to give a final concentration of 16 mg/ml.

$CoCl_2.6H_2O$ stock: 250 mg $CoCl_2.6H_2O$ was added to 10 ml distilled water to give a final concentration of 25 mg/ml.

NaFeEDTA stock (1000 X): 367 mg NaFeEDTA was added to 10 ml distilled water to give a final concentration of 36.7 mg/ml.

B_5 vitamin stock (1000 X): 1.12 g of B_5 vitamins was added to 10 ml distilled water to give a final concentration of 0.112 g/ml.

Enzyme B solution (100 ml): 2.5 ml B_5 macro stock (40 X), 100 µl B_5 micro stock (1000 X), 150 mg $CaCl_2$, 100 µl NaFeEDTA stock (1000 X), 100 µl B_5 vitamin stock (1000 X), 13.7 g saccharose, 1 g cellulose R10 and 250 mg macerozyme R10 bought up to 100 ml with distilled water. The solution was centrifuged at 453 X *g* for 10 minutes, filter sterilised and stored at -20 °C.

CPW165 salt working solution (100 ml): 1 ml CPW salt stock, 16 g saccharose, 148 mg $CaCl_2$ brought up to 100 ml with distilled water. The pH of the solution was adjusted to 5.8, autoclaved and stored at 4 °C for no longer than one week.

PG solution (100 ml): 5.47 g sorbitol and 0.735 g $CaCl_2.H_2O$ was added to 100 ml distilled water.

W5 solution (100 ml): 900 mg NaCl, 1.84g $CaCl_2.H_2O$, 37 mg KCL, 99 mg glucose and 10 mg MES was added to 100 ml distilled water. The solution was adjusted to a pH of 5.8, autoclaved and stored at 4 °C for no longer than one week.

Lettuce B solution (100 ml): 1.25 ml B_5 macro 40 X (½Strength), 50 µl B_5 micro 1000 X (½Strength), 50 µl B_5 vitamins 1000 X (½Strength), 37.5 mg $CaCl_2.H_20$, 50 µl NaFeEDTA, 27 mg Na succinate, 10.3 g saccharose, 30 µl BAP stock (mg/ml), 10 µl 2,4-D stock (mg/ml), 10 mg MES were added to 100 ml distilled water, pH 5.8, filter sterilised and stored at 4 °C for no longer than one week.

2.13.4.2 Protoplast isolation

24 hours after bombardment, lettuce cotyledons with obvious puncture holes from the bombardment, as well as some surrounding cotyledon tissue, were removed from the CIM2 medium and weighed. On average, 0.08 g of cotyledon tissue was used per protoplast isolation. The cotyledons were placed into a Petri dish containing 7 ml of PG solution (Section 2.13.4.1) and were cut into 4 mm^2 pieces. The Petri dish was covered in tinfoil and was placed at 4 °C for one hour. The PG solution was then removed and replaced with 7 ml of enzyme B solution (Section 2.13.4.1). The Petri dish was sealed, covered with tinfoil and incubated at 25 °C for 16 hours. The Petri dish (still covered with tinfoil) was then placed on a shaker for two hours. CPW165 solution (3 ml; Section 2.13.4.1) was added and very gently swirled. The solution was filtered through sterile mesh (100 μM pore size) into a 10 ml tube. W5 solution (1 ml; Section 2.13.4.1) was very gently layered on top of the filtrate. The tube was spun at 100 X *g* for eight minutes after which a distinct band of protoplasts was seen. The protoplasts were removed very gently with a sterile glass pipette and were placed in a new tube. W5 solution (9 ml) was layered on top of the protoplasts and the tube was spun at 100 X *g* for five minutes causing the protoplasts to pellet at the bottom of the tube. The supernatant was poured off very gently in one smooth motion and the tube was placed on sterile filter paper for a few seconds to remove the last of the supernatant. The protoplasts were resuspended in 50 μl of lettuce B solution (Section 2.13.4.1) that was pre-warmed to room temperature. The resuspended protoplasts were transferred to a 1.5 ml eppendorf and were kept at room temperature until needed (no longer than one hour).

2.13.4.3 Visualisation of plastid localised GFP

Plastid-based GFP expression was assessed by examining protoplasts, prepared as described, using an Olympus BX-51/Genus FISH Imaging System. 10 μl of the protoplast solution was placed onto a glass slide and very gently covered with a cover slip so as not to burst the protoplasts. The slide was placed on the stage of the microscope and the protoplasts were initially viewed with the X 20 lens using the DAPI excitation filter for identification of potential fluorescing plastids within the protoplasts. When a putative GFP expressing plastid was located, the excitation filter was changed to the GFP excitation filter and the plastid was assessed for GFP fluorescence with the X 40 lens. Five slides containing 10 μl of the protoplast solution were analysed in this way for each bombardment and the number of GFP fluorescing plastids were counted.

2.13.5 Particle bombardment of lettuce

2.13.5.1 Vectors used for bombardment of lettuce

The following vectors were used for the bombardment of lettuce: pLCV2-LEC1 and pLCV2-GFP/aadA 231 (Lelivelt *et al*., 2005); pLCV5-p24, pLCV6-p24NC and pLCV7-p24Nef supplied by Dr. Bridget Hogg, Plant Molecular Biology, NUI Maynooth, Co Kildare. All five vectors with the exception of pLCV2-LEC1 are modified versions of the pLCV2-GFP/aadA (Lelivelt *et al.*, 2005).

2.13.5.1.1 pLCV2-LEC1 vector

The pLCV2-LEC1 lettuce transformation vector contains the *aadA* gene and the influenza virus hemagglutinin gene (*HA*) under the control of the lettuce *rrn*

operon promoter (PL*s-rrn*) and the lettuce *psbA* 3'UTR (3'L*s-psbA*). A chloroplast ribosome binding site (rbs) precedes both genes. This expression cassette is flanked by lettuce chloroplast DNA targeting sequences, the *trnI* and the *trnA* genes to facilitate targeted insertion.

2.13.5.1.2 pLCV5-p24 vector

The pLCV5-p24 contains two expression cassettes. The first cassette contains the selectable marker gene *aadA* with a 5' ribosome binding site and a 3' *psbA* UTR (T*psbA*) flanked by two loxP sites to facilitate marker gene removal by Cre-mediated site specific recombination if required. The second cassette includes the codon optimised HIV-1 p24 gene under the control of the lettuce *rrn* operon promoter (PL*s-rrn*) fused to the 5' leader from the gene 10 of phage T7 (g10L), and the lettuce *rbcL* 3'UTR (T*rbcL*). The transgene cassettes are flanked by lettuce chloroplast DNA *trnI* - *trnA* targeting sequences to facilitate targeted integration.

2.13.5.1.3 pLCV6-p24NC vector

The pLCV6-p24NC lettuce transformation vector is a modified version of the pLCV5-p24vector. The pLCV-6 vector contains the *aadA* expression cassette without the loxP sites. The codon optimised p24 gene is replaced with a native HIV-1 p24 gene.

2.13.5.1.4 pLCV7-p24Nef vector

The pLCV7-p24Nef lettuce transformation vector is identical to the pLCV5-p24 vector except that the HIV-1 *nef* gene is fused to the 3' end of the p24 gene to give a p24-nef fusion gene.

2.13.5.1.5 pLCV2-GFP/aadA 231 vector

The pLCV2-GFP/aadA 231 lettuce transformation vector contains: (1) the *aadA* gene under the control of the tobacco P*rrn* with an 18 bp synthetic leader and ribosome-binding site and T*psbA* and (2) sm*GFP* under the control of the lettuce *Prrn*/ *rbcL* 5' UTR and the *E.coli rrnB* terminator (*TrrnB*). The two expression cassettes are integrated into the vector in opposite orientations to avoid potential excision events mediated by recombination across directly repeated *Prrn* sequences.

2.13.5.2 Plant Material

Lettuce (*Lactuca sativa* L. cv Flora, Evola, Simpson Elite and Cisco) seeds were used for all trial-transformation experiments. Seeds were sterilised and germinated as described in section 2.13.1.2.

2.13.5.3 Lettuce *in vitro* growth conditions

Lettuce plants were grown *in vitro* on MS medium (Section 2.4.3) in a culture room at 25 °C and grown under a 16 hour light/ 8 hour dark light/ dark

photoperiod cycle (48 μmol m^{-1} s^{-1}). Plants were sub-cultured every four to six weeks by nodal cuttings placed in fresh MS medium.

2.13.5.4 Particle bombardment of lettuce

Lettuce plastid transformation was as described for tobacco (Section 2.9) with the following modifications:

Leaf preparation:

Two hours prior to bombardment, leaves were harvested from three to four week old wild-type lettuce plants grown *in vitro*. The leaves were placed adaxial side down on 9 cm Petri dishes containing either LR or SLR medium (Section 2.4.3) in preparation for bombardment.

Particle bombardment:

Bombardment of lettuce leaves was performed as described for tobacco (Section 2.9.5) with the following modifications: Rupture disks at 900 psi were used instead of the 1,100 psi disks used for tobacco transformation.

2.13.5.5 Tissue culture of bombarded lettuce leaves

Two days after the bombardment, the lettuce leaves were cut into 10 mm^2 pieces and placed onto LR / SLR plates (Section 2.4.3) containing 50 mg/L spectinomycin. Expanded leave pieces were transferred to fresh plates every two to three weeks.

Chapter 3
Transformation of tobacco with HA fusion gene constructs

3 Transformation of tobacco with HA fusion gene constructs

3.1 Introduction

Transplastomic plants are interesting candidates for the production of potential plant-based vaccines (Daniell *et al.*, 2009). The expression of antigens in plants offers several unique advantages over more conventional production systems including reduced manufacturing costs, the elimination of health risks arising from contamination with human pathogens or toxins, and the ease of production of multi-component combined vaccines (Molina *et al.*, 2004). The chloroplast expression system has been used to produce a number of viral antigens. These include the VP6 capsid protein from the rotavirus which accumulated to approximately 3% TSP (Birch-Machin *et al.*, 2004), the HIV antigen p24 (approximately 40% TSP; McCabe *et al.*, 2008; Zhou *et al.*, 2008), the major capsid L1 protein from the human papillomavirus (HPV- approximately 1.5% TSP; (Lenzi *et al.*, 2008) and the HIV-1 $Pr55^{gag}$ polyprotein, (approximately 7% TSP; Scotti *et al.*, 2009), all of which were expressed in tobacco plants. The *VP1* gene from the foot and mouth disease virus (FMDV) accumulated to approximately 3% TSP in *C. reinhardtii* (Sun *et al.*, 2003). However, other studies have reported difficulty in expressing viral antigens in plastids. For example, expression of the viral capsid antigen gene (*VCA*) from the Epstein-Barr virus in tobacco plastids only resulted in protein accumulation levels of between 0.002% - 0.004% TSP (Lee *et al.*, 2006a). This low level of protein accumulation was thought to be due to post-translational events affecting protein stability (Ye *et al.*, 2001). VP6 protein accumulation levels in transplastomic tobacco leaves was estimated to be approximately 3% TSP.

However, when protein accumulation levels were assessed in leaves of different ages, the protein was found to be unstable in mature leaves suggesting that the VP6 protein was subject to proteolytic degradation in plastids of older leaves (Birch-Machin *et al.*, 2004).

Hemagglutinin (HA) is an antigenic glycoprotein found on the surface of influenza viruses (Steinhauer, 2010). HA is a trimer of identical subunits. Each subunit contains two unique polypeptides, HA1 and HA2, which result from proteolytic cleavage of a single precursor HA0. Cleavage of HA0 is an absolute requirement for activation of the membrane fusion potential of the virus and hence infectivity (Steinhauer, 2010). Influenza infection has previously been shown to elicit antibodies against most influenza proteins (Potter, 1982), however, the most significant for their protective capacity are the anti-HA antibodies (Jeon *et al.,* 2002). The neutralising effect of anti-HA antibodies can be attributed to either the prevention of viral entry into susceptible host cells or to their actions in the later stages of viral replication (Ada & Jones, 1986). Resistance to influenza infection has also been shown to correlate with serum anti-HA antibody levels (Hobson *et al.,* 1972; Couch & Kasel, 1983) and passive transfer of immune serum provides protection against further challenge (Virelizier, 1979) making HA an obvious target for vaccine development. Anti-HA1 antibodies are also known to neutralise the infectivity of the influenza virus and provide protection against the infection (Gocnik *et al.,* 2008). Nwe *et al.,* (2006) showed that recombinant insoluble HA1 (H5N1) protein produced using an insect suspension cell system elicited a neutralising antibody response in guinea pigs against the H5N1 avian influenza virus (Nwe *et al.,* 2006). In

addition, the HA1 domain of HA contains almost all of the antigenic sites (Shih *et al.,* 2007) and so represents another obvious target for vaccine development.

Previous studies using flu virus (H3N2) hemagglutinin (HA) gene constructs yielded fertile, homoplasmic, plastid transformed tobacco lines (Karen Shiels, unpublished data) and lettuce lines (Lelivelt *et al.,* 2005). However, in both instances although the gene constructs were transcribed in the transgenic plants no HA protein accumulation was detected in any of the lines. The lack of detectable HA protein could be due to HA protein instability in the plant plastids. A number of strategies have been employed to increase recombinant protein stability in the plastid such as fusing the 5' region of certain genes (e.g. *atpB*, *rbcL* and *gfp*) to the gene of interest (Gray *et al.*, 2009a; Maliga, 2002). Lenzi *et al.,* (2008) reported that L1 (the major capsid L1 protein from the human papillomavirus) antigen accumulation could only be detected when the N-terminus of L1 protein was translationally fused with the first 14 amino acids of atpB (the β subunit of chloroplast ATP synthase) or RBCL (the large subunit of Rubisco). When recombinant protein accumulation levels were compared for both fusion tags, the 14aa RBCL tag yielded the highest level of L1 protein accumulation -1.5% TSP compared to 0.1% TSP with the 14aa atpB tag. A gene construct coding for the first 14 amino acids of RBCL N-terminally fused to the pr55 gag (the gag polyprotein precursor from HIV) protein achieved a 25-fold increase in plastid-based protein accumulation compared to the gene construct without the fusion tag sequence (Scotti *et al.*, 2009). Another fusion tag that has been used very successfully to stabilise plastid-based protein accumulation is the first 14 amino acids of GFP. Levels of CP4 (from *Agrobacterium* 5-

enolpyruvylshikimate-3-phosphate synthase (EPSPS)) protein accumulation in plastids increased by 50-fold (>10% TSP) when N-terminally fused to the 14aa GFP tag (Ye *et al.,* 2001). The increase in protein accumulation was found to be not only due to increased protein stability but also to an increased rate of translation for the fusion protein compared to the non-fusion version (Ye *et al.*, 2001). More recently, a gene construct coding for the first 14 amino acids of GFP N-terminally fused to LTB-L1 (the heat-labile enterotoxin B subunit (LTB) fused to L1 protein from human papillomavirus), also resulted in significantly higher levels of protein expression (approximately 2% TSP) compared to the levels of accumulation obtained by individual expression of the LTB and modified L1 proteins in tobacco plastids (Kang *et al.,* 2003; Waheed *et al.*, 2011).

Another strategy that has been used to improve the accumulation of difficult to express proteins in the plant plastid is to fuse them to proteins that typically express well in the plastid system. Fusion of viral antigens to full-length protein partners such as GFP has helped to achieve plastid-based viral protein accumulation. GFP is a popular fusion partner since it is very stable in plastids and can accumulate to levels of up to 38% TSP (Yabuta *et al.,* 2008). High levels of protein accumulation (22.6% TSP) were achieved for the canine parvovirus peptide 2L21 in tobacco plastids using C-terminal translational fusion with GFP (Molina *et al.*, 2004).

Although fusing proteins of low stability to stably expressed protein has been shown to result in increased levels of protein accumulation, the location of the

fusion partner can greatly affect accumulation levels. Zhou *et al.,* (2008) reported that fusion of the HIV antigens p24 and Nef with p24 at the N-terminus and Nef at the C-terminus (p24-Nef) resulted in protein accumulation levels of up to 40% TSP. In contrast, fusion of the two proteins in the opposite orientation (Nef-p24) resulted in a less stable protein (Zhou *et al.,* 2008). Gene constructs coding for GFP fused to the HIV-1 fusion inhibitor protein, cyanovirin-N (CV-N) as an N-terminal fusion or with *cv-n* embedded within the *gfp* coding region (thus producing a protein whose N and C termini are from GFP) resulted in protein accumulation levels up to 0.3% TSP. However, no protein was detected in plants transformed with C-terminal or non-fusion gene constructs (Elghabi *et al.,* 2011). This suggests that the nature of the N-terminal region has a greater impact on protein stability than the C-terminus. Indeed Apel *et al.,* (2010) showed that although different penultimate N-terminal amino acid residues resulted in strong differences in protein stability and influenced the protein half-life, it was in the most N-terminal part of the protein that the major determinants of plastid protein stability / instability resided. In contrast, they found that the C-terminus is relatively unimportant for affecting plastid protein stability (Apel *et al.,* 2010).

The aim of this work was to use gene fusion strategies to achieve HA or HA1 accumulation in tobacco plastids. Both HA and HA1 are known to neutralise the infectivity of the influenza virus and provide protection against infection (Hobson *et al.,* 1972; Couch & Kasel, 1983; Gocnik *et al.,* 2008). To explore the possibility of achieving HA and HA1 accumulation in tobacco chloroplasts, four gene constructs were designed (pMO14rHA, pMO14gHA, pMOGFP/HA1 and

pMOGFP/HA) for chloroplast transformation. The first two constructs were designed to code for a full length HA fused at the N-terminus to the first 14 amino acids of RBCL or GFP (pMO14rHA and pMO14gHA). The second set of constructs were designed to code for a full length GFP N-terminally fused to a full length HA (pMOGFP/HA) or a full length GFP N-terminally fused to the HA1 polypeptide (pMOGFP/HA1).

3.2 Results

The four gene constructs, 14aaRBCL/HA, 14aaGFP/HA, GFP/HA1 and GFP/HA, designed to assess if a protein fusion strategy can achieve stable HA or HA1 protein accumulation in tobacco plastids are illustrated in Figure 3.1. All four constructs were cloned into the transformation vector pMO16 (Oey *et al.*, 2009a) for insertion between the *trnG* and *trnfM* genes in the tobacco plastome.

3.2.1 Amplification and modification of HA gene

The *HA* gene from the influenza virus A/Sichuan/2/87 (H3N2) was amplified by PCR from the pZS-HA vector supplied by Dr. Karen Shiel (NUI Maynooth) in two separate reactions using the four primers HA-NdeIF, HA-XbaIR, HA-SphIF and HA-SphIR. Primers HA-NdeIF and HA-XbaIR were designed to add an *NdeI* restriction site immediately upstream of the start codon and an *XbaI* restriction site immediately after the stop codon of the *HA* gene (Figure 3.2). As all future cloning of this gene was to be performed using the restriction sites *NdeI* and *XbaI,* it was necessary to eliminate an internal *NdeI* site in the *HA* gene. This was achieved using the primers HA-SphIF and HA-SphIR which were designed to remove the internal *NdeI* restriction site by changing the nucleotide T, at position 1004 bp, to C (CATATG to CACATG) without changing the amino acid specification of the DNA sequence. The first PCR using the primer pair HA-NdeIF and HA-SphIR generated a 930 bp PCR fragment containing the *NdeI* restriction site at the 5' end of the fragment and a mutagenised *NdeI* restriction site at the 3' end of the fragment (HA-F1). The second PCR used the primer pair HA-SphIF and HA-XbaIR to produce a 633 bp

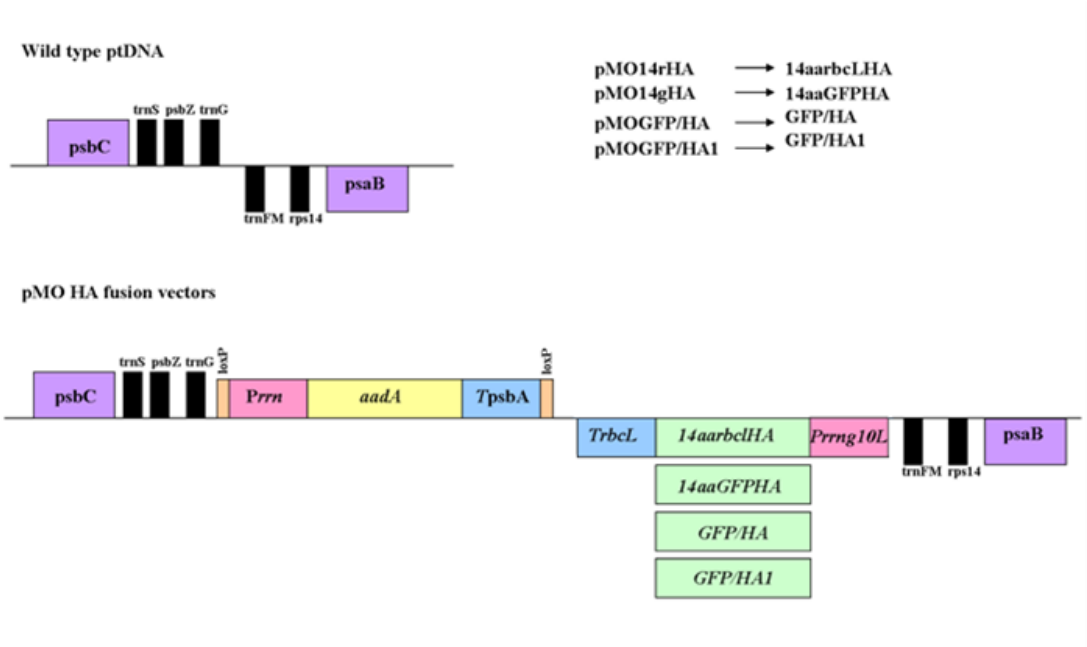

Figure 3.1: Physical map of the targeted region (not drawn to scale) in the tobacco plastid genome and the structure of plastid transformation vectors containing the various HA fusion gene constructs. The transgenes are targeted to the intergenic region between *trnG* and *trnfM*.

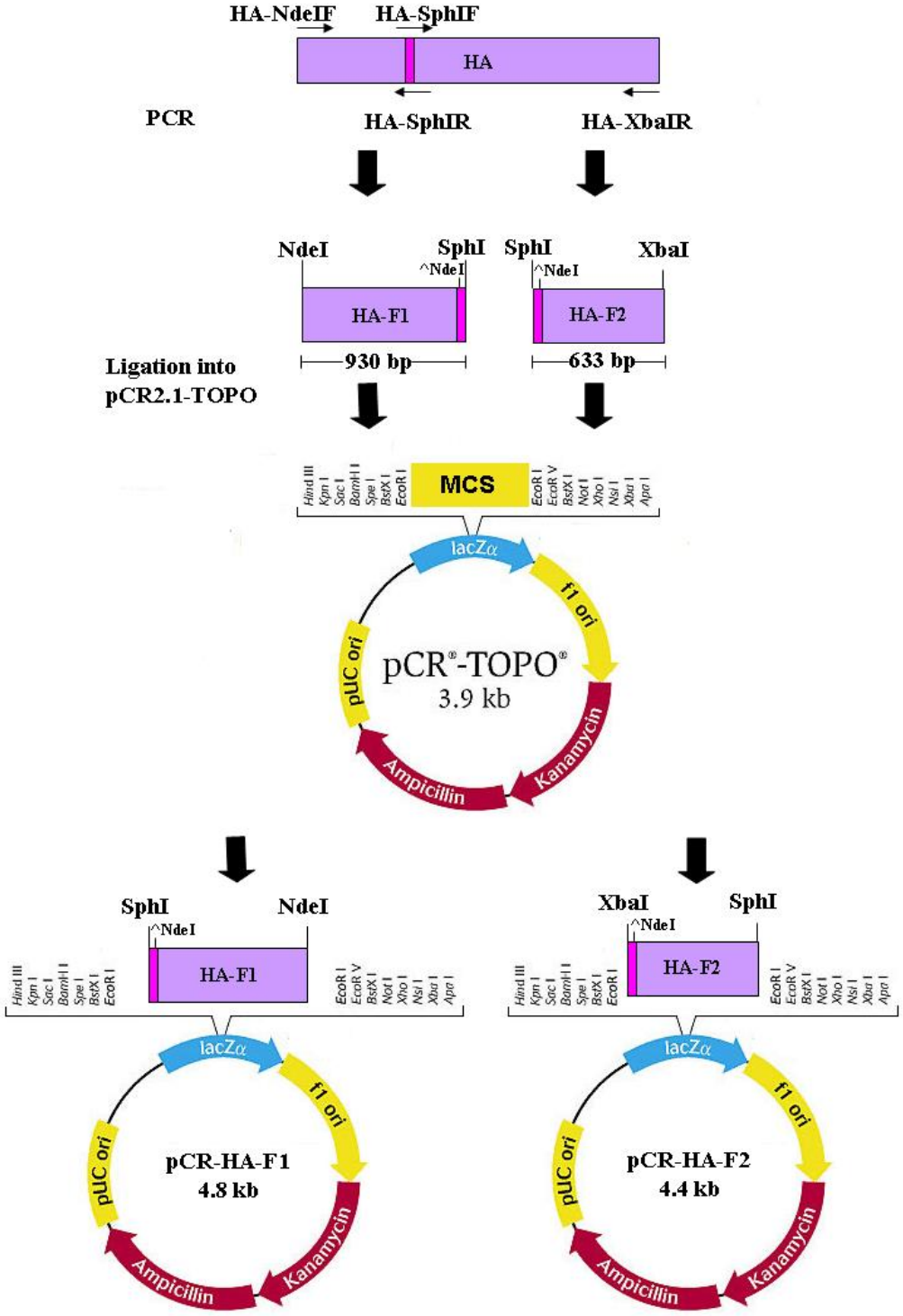

Figure 3.2: Schematic representation of the cloning strategy used to generate the modified *HA* gene. HA-NdeIF and HA-SphIR generated HA-fragment-1 (HA-F1) with a 5'*NdeI* restriction site and a mutagenised *NdeI* site at the 3' end. HA-fragment-2 (HA-F2) has a mutagenised *NdeI* restriction site at the 5' end and an *XbaI* site at the 3' end and was generated using the primer pair HA-SphIF and HA-XbaIR. Both fragments were separately cloned into pCR2.1-TOPO.

fragment containing the mutagenised *NdeI* restriction site at the 5' end and a *XbaI* restriction site at the 3' end (HA-F2). Both PCR products were gel purified, ligated separately into pCR2.1-TOPO and transformed into *E. coli* cells. Plasmid DNA was isolated from 12 HA-F1 colonies, digested with *EcoRI* and analysed by agarose gel electrophoresis on a 0.7% agarose gel to confirm fragment cloning. Successful ligation of the HA-F1 PCR product into pCR2.1-TOPO vector resulted in a 3.9 kb band representing the pCR2.1-TOPO vector backbone and a 930 bp HA-F1 band (pCR-HA-F1) (Figure 3.3 A). Plasmid DNA from 12 HA-F2 colonies were digested with *SpeI* and *XbaI* and analysed by agarose gel electrophoresis on a 0.7% agarose gel to confirm fragment cloning. Successful ligation of the HA-F2 PCR product into pCR2.1-TOPO vector resulted in a 3.9 kb band representing the pCR2.1-TOPO vector backbone and a 633 bp HA-F2 band (pCR-HA-F2) (Figure 3.3 B). Insert orientation in pCR-HA-F1 was checked by digesting plasmid DNA with *SpeI* and *NdeI* and selecting for plasmids releasing a 940 bp fragment (Figure 3.3 C) and in pCR-HA-F2 by digesting with *XbaI* and selecting for plasmids releasing a 633 bp fragment (Figure 3.3 D) pCR-HA-F1 plasmid 5 and pCR-HA-F2 plasmids 1 and 5 were sequenced completely to ensure that the internal *NdeI* restriction site had been removed and that no errors had been introduced into the gene sequence during PCR amplification. All three cloned inserts sequenced correctly.

3.2.1.1 Generation of full length modified HA

It was not possible to reassemble the *HA* gene in pCR2.1-TOPO using the *SphI*

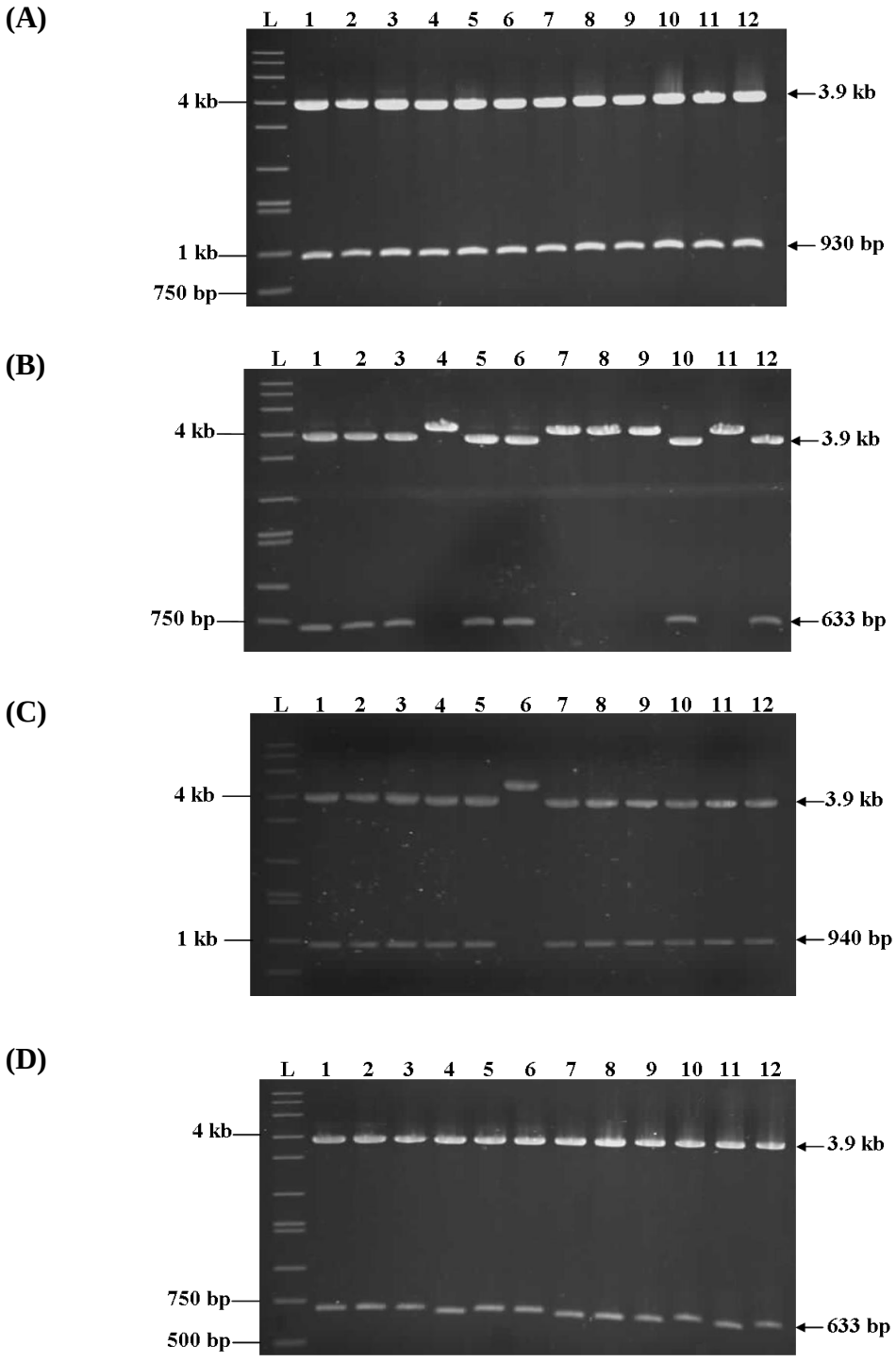

Figure 3.3: Restriction digest analysis of HA recombinant plasmids. (A) Recombinant HA-F1 plasmids digested with *EcoRI* produced the 3.9 kb pCR2.1-TOPO vector backbone and the excised HA-F1 insert at 930 bp. Lanes 1-12. (B) Recombinant HA-F2 plasmids digested with *SpeI* and *XbaI* produced the 3.9 kb pCR2.1-TOPO vector backbone and the excised HA-F2 insert at 633 bp. Lanes 1-12. (C) Recombinant HA-F1 plasmids digested with *SpeI* and *NdeI* to check insert orientation. Lanes 1-12. (D) Recombinant HA-F2 clones digested with *XbaI* to check insert orientation. Lanes 1-12. Lane L (A, B, C & D): 10 kb ladder (Sigma).

restriction sites due to the presence of two additional *SphI* restriction sites in the pCR2.1-TOPO vector. The two HA fragments, pCR-HA-F1 and pCR-HA- F2 were cloned individually into the cloning vector pBluescript SK (+) using the *SpeI* and *NotI* cloning sites to give pBS-HA-F1 and pBS-HA-F2.

To reassemble the modified *HA* gene, pBS-HA-F1 was digested with *SphI* and *SpeI* and the HA-F1 plus vector backbone fragment were gel purified. pBS-HA-F2 was digested with *SphI* and *SpeI* and the HA-F2 insert was gel purified and ligated into the cut pBS-HA-F1 vector (Figure 3.4). Ligation reactions were transformed into Top 10 chemically competent *E. coli* cells and selected on LB/Amp agar plates. Plasmid DNA was isolated from five recombinant clones, digested with *SphI* and *SpeI* and analysed on a 0.7% agarose gel. Correct recombinant plasmids produced a 3.9 kb band representing the vector backbone and a 651 bp band representing the HA-F2 fragment (Figure 3.5). These clones were subsequently referred to as pBS-HA.

3.2.2 14aaRBCL and 14aaGFP

The full length *HA* gene (Section 3.2.1.1) was cloned into pCR4-TOPO to facilitate easier assembly of the two 5' fusion constructs. This HA clone was subsequently referred to as pCR4-HA.

3.2.2.1 Cloning 14aaRBCL/HA into pCR4-TOPO

The first 42 nucleotides of the *rbcL* gene (coding for the first 14 aa of RBCL - 14aaRBCL) were fused to the 5' end of the modified *HA* gene (Section 3.2.1.1)

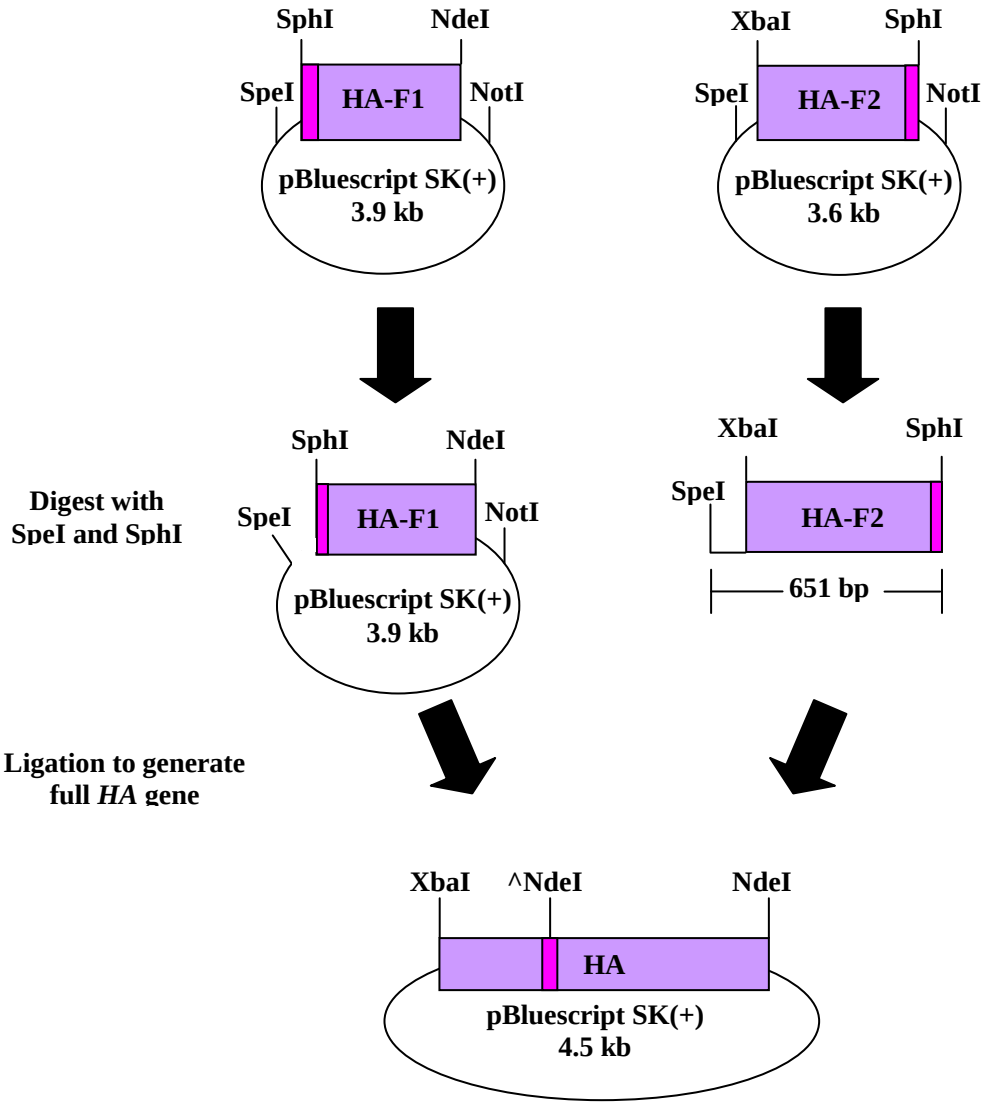

Figure 3.4: Schematic representation of the cloning strategy used to generate the modified full length *HA* gene. Both HA-F1 and HA-F2 fragments were digested with *SpeI / SphI* and the HA-F2 insert was ligated into the HA-F1 vector to give the full length *HA* gene.

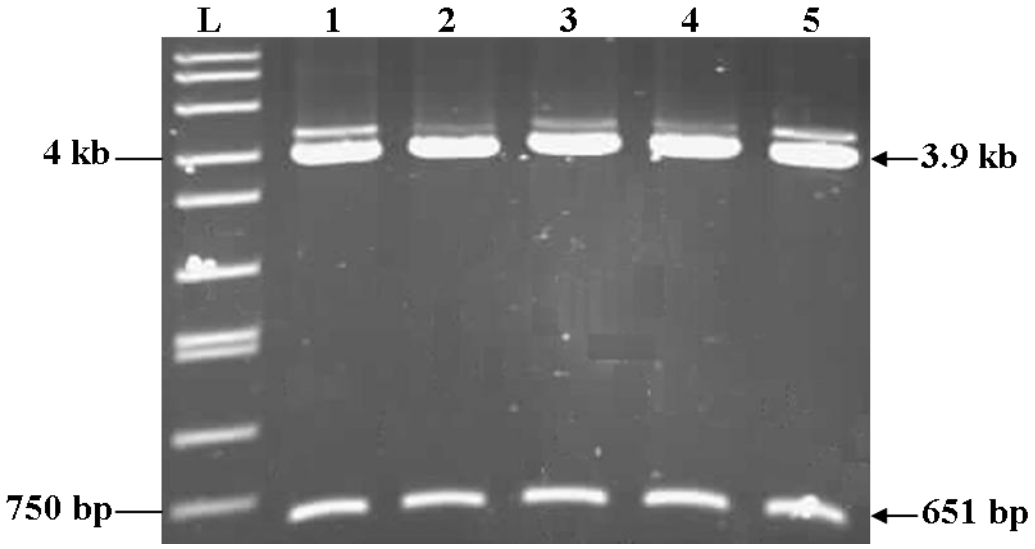

Figure 3.5: Restriction digest analysis of putative pBS-HA clones. Recombinant pBS-HA plasmids were digested with *SpeI* and *SphI*. All plasmids digested as expected, producing a 3.9 kb vector backbone band and a 651 bp HA-F2 product. Lane L: 10 kb ladder (Sigma). Lanes 1-5: pBS-HA plasmids 1-5.

using primer overlap extension. To minimise the possibility of introducing mutations or nucleotide changes caused by long-range PCR, the *rbcL* sequence was fused to the first 325 bp of the *HA* gene. This fusion PCR was performed across an internal *HindIII* restriction site that allowed replacement cloning of the *rbcL* fusion sequence within the original *HA* gene using *NdeI* and *HindIII* restriction sites (Figure 3.6).

Primer overlap extension was performed in two separate PCRs. The first reaction used the primer pair 14aarbcL-F1 and HA-HindIII-R. 14aarbcL-F1 was designed to fuse the first 18 nucleotides of the *rbcL* gene to the 5' end of the *HA*-HindIII fragment. A 303 bp PCR product was generated, cleaned using a Qiagen PCR clean-up kit and used as template DNA for second round PCR. Primers 14aarbcL-F2 and HA-HindIII-R were used to fuse the remaining 24 *rbcL* nucleotides to the *HA*-HindIII fragment while simultaneously adding an *NdeI* restriction site immediately upstream of the start codon. This reaction produced a 330 bp PCR product (Figure 3.7 A) that was gel extracted, ligated into pCR2.1-TOPO and transformed into *E. coli* cells. Plasmid DNA was isolated from nine recombinant clones, digested with *NdeI* and *HindIII* and analysed by agarose gel electrophoresis on a 0.7% gel. Eight out of nine recombinant plasmids produced the 3.9 kb vector backbone band and the 330 bp 14rHA-HindIII insert (14rHA-H) (Figure 3.7 B). Three recombinants were sequenced to ensure that no errors had been introduced into the sequence during PCR amplification. Two out of three cloned inserts sequenced correctly. Plasmid 14rHA-H1 was used for all subsequent cloning steps.

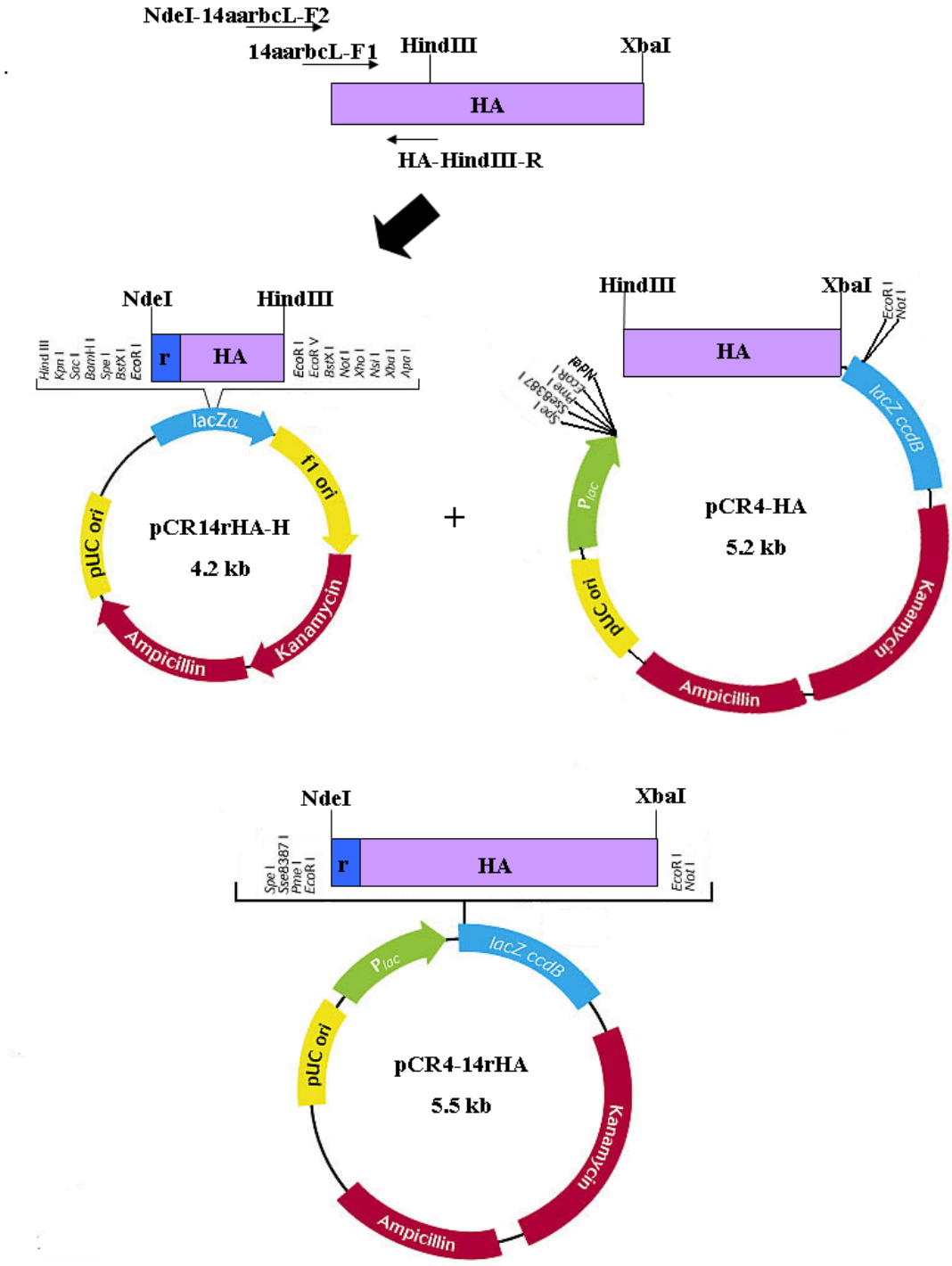

Figure 3.6: Schematic representation of the cloning strategy used to fuse the first 14 amino acids of RBCL to the N-terminus of HA. The first 42 nucleotides coding for the first 14 amino acids of RBCL were fused to the *HA* gene using primer overlap extension. The resulting PCR product was ligated into pCR2.1-TOPO. 14rHA-H and pCR4-HA were digested with *NdeI* / *HindIII* and the resulting fragments were ligated together to give pCR4-14rHA.

(A)

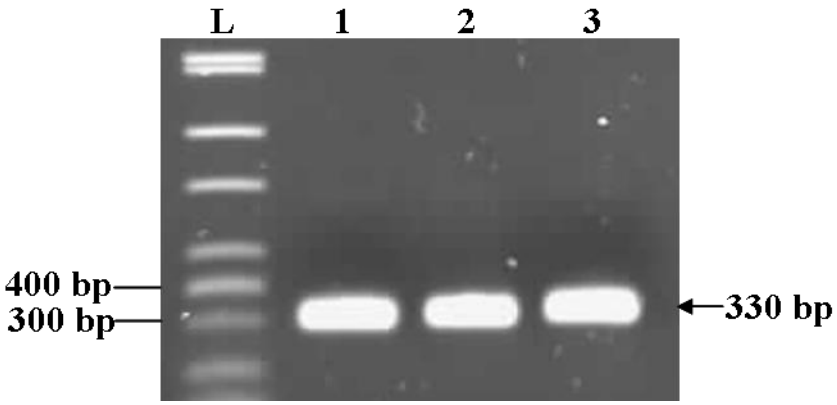

(B)

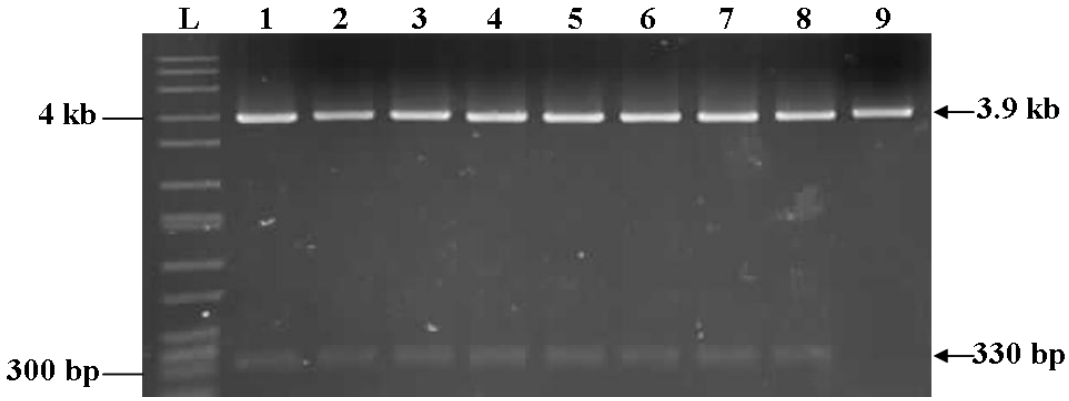

Figure 3.7: 14rHA-H amplification by PCR and restriction digest analysis of 14rHA-H clones. (A) Generation of the 14rHA-H fragment using PCR. Lane L: 10 kb Ladder (Sigma). Lanes 1-3: PCR products from 2nd round PCR which generated the 14rHA-H fragment (330 bp). (B) Nine independent recombinant plasmids were digested with *NdeI* / *HindIII*. Positive recombinant clones produced a 3.9 kb pCR2.1-TOPO backbone and the 330 bp 14rHA-H fragment. Lane L: 10 kb DNA ladder (Sigma). Lanes 1-9: 14rHA-H clones.

To generate the full length 14aaRBCL/HA gene, 14rHA-H1 and pCR4-HA were digested with *NdeI* and *HindIII* and the insert and vector backbone were gel extracted and ligated together. Plasmid DNA was isolated from five recombinant clones, digested with *NdeI* and *HindIII* and analysed on a 1% agarose gel. Correct recombinant plasmids produced a 5.2 kb pCR4-HA vector backbone and a 330 bp 14rHA-H fragment. These clones were subsequently referred to as pCR4-14rHA (Figure 3.8 C).

3.2.2.2 Cloning 14aaGFP/HA into pCR4-TOPO

The first 42 nucleotides of the *gfp* gene (14aaGFP) were fused to the 5' end of the first 325 bp of the modified *HA* gene (Section 3.2.1.1) using primer overlap extension and the primer combination 14aaGFP-F1 / HA-HindIII-R and 14aaGFP-F2 / HA-HindIII-R. Primer overlap extension was performed in two separate PCR reactions (Figure 3.8 A) using the same method as described for 14rHA gene (Section 3.2.2.1). The resulting 330 bp PCR product (Figure 3.8 B) was gel purified and ligated into pCR2.1-TOPO. Plasmid DNA was isolated from five recombinant clones and digested with *NdeI* / *HindIII*. Four of the five plasmid digests produced the 3.9 kb pCR2.1-TOPO vector backbone band and the 330 bp 14gHA-H fragment. Three recombinant plasmids were sequenced to ensure that no errors had been introduced into the gene sequence during PCR amplification. One of the plasmids sequenced correctly. Plasmid 14gHA-H2 was used for all subsequent cloning steps.

To generate the full length 14aaGFP/HA gene, 14gHA-H2 and pCR4-HA were digested with *NdeI / HindIII* and ligated together using the same method as

(A)

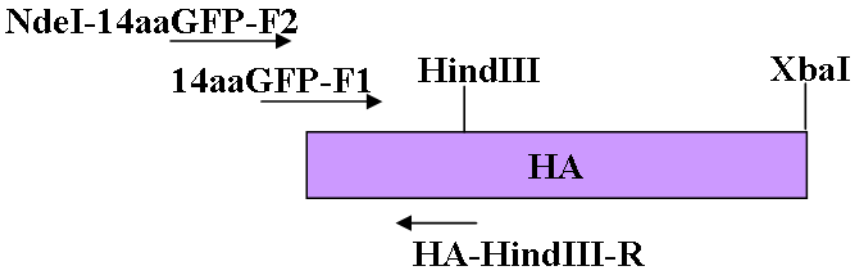

(B)

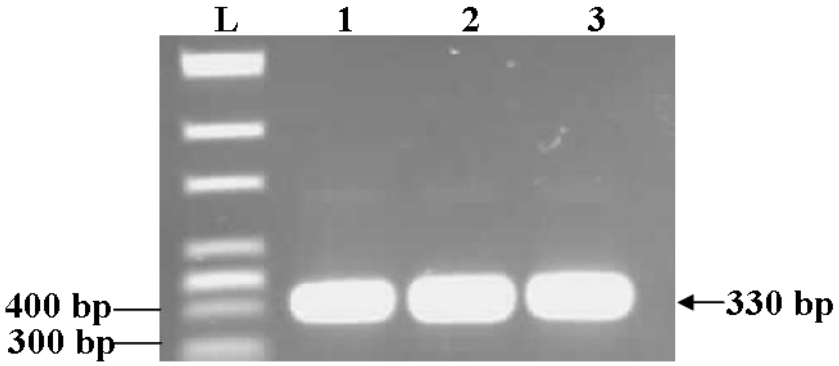

(C)

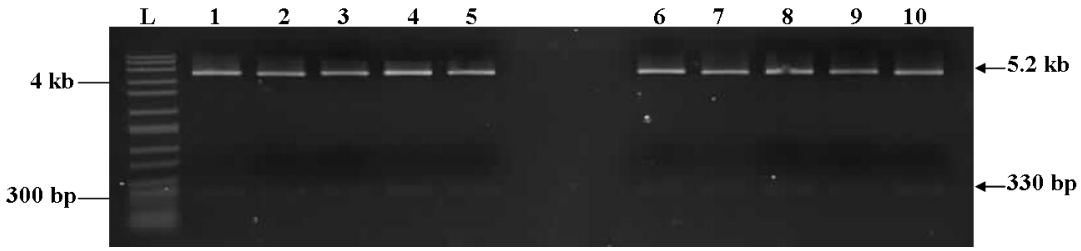

Figure 3.8: 14gHA-H amplification by PCR and restriction digest analysis of 14gHA-H clones. (A) Schematic representation of primer overlap extension (B) Generation of 14gHA-H fragment using primer overlap extension. Lane L: 10 kb Ladder (Sigma). Lanes 1-3: PCR products from 2nd round PCR which generated the 14gHA-H fragment (330 bp). (C) Restriction digest of pCR4-14rHA and pCR4-14gHA recombinant clones using *NdeI* / *HindIII*. Successful integration of the 14rHA-H and 14gHA-H inserts resulted in a 5.2 kb vector backbone and a 330 bp insert. Lane L: 10 kb Ladder (Sigma). Lanes 1-5: pCR4-14rHA clones 1-5. Lanes: 6-10: pCR4-14gHA clones 1-5.

described for the 14rHA gene (Section 3.2.2.1). Plasmid DNA was isolated from five recombinant clones, digested with *NdeI* and *HindIII* and analysed on a 1% agarose gel. Correct recombinant plasmids produced a 5.2 kb pCR4-HA vector backbone band and the 330 bp 14gHA-H insert (Figure 3.8 C). These plasmids were subsequently referred to as pCR4-14gHA.

3.2.3 Generation of the pMO14rHA and pMO14gHA vectors

The plastid transformation vector pMO16 was kindly provided by Prof. Ralph Bock (Figure 3.9). The 14aa *HA* fusion genes could not be cloned directly into the *NdeI* and *XbaI* restriction sites in the pMO16 vector as the two sites were not unique to the vector. Instead, the transgene cassette was cloned into an intermediate cloning vector, pBluescript SK (+), using the restriction sites *ApaI* and *SacI* (Figure 3.10).

To clone the *plyGBS* transgene expression cassette into pBluescript SK (+), both pBluescript SK (+) and the pMO16 plasmid were digested with *ApaI* and *SacI*. The pBluescript SK (+) vector and the transgene expression cassette were gel purified, ligated together and transformed into Top 10 chemically competent *E. coli* cells. Plasmid DNA was isolated from six colonies, digested with *ApaI* and *SacI* and analysed on a 0.7% agarose gel. Positive recombinant plasmids produced a 3 kb vector backbone band and a 1.7 kb transgene cassette band. These plasmids were subsequently referred to as pCas-ApaI.

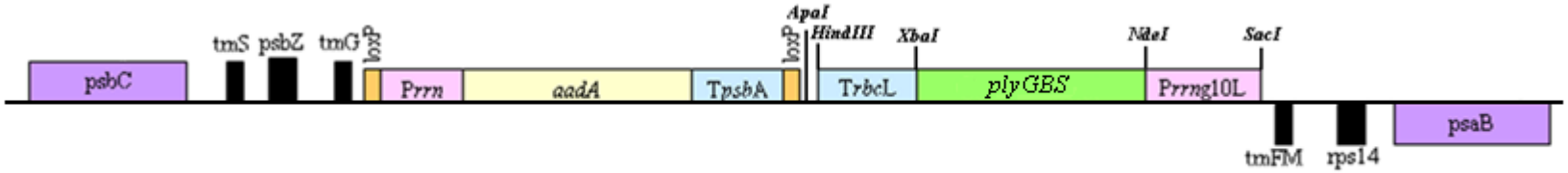

pMO16

Figure 3.9: Schematic representation of pMO16 plastid transformation vector (not drawn to scale). pMO16 contains two expression cassettes flanked by the *trnG* and *trnfM* genes to facilitate homologous recombination. The *aad*A cassette contains the 16s ribosomal RNA operon promoter *Prrn*, the *aadA* marker gene which provides both spectinomycin and streptomycin resistance and the *psbA* 3' terminator. *LoxP* sites flank the *aadA* expression cassette to allow for eventual Cre-mediated excision if required. The second cassette also contains the 16s ribosomal RNA operon promoter *Prrn*, followed by the gene 10 leader from phage T7 (T7g10L), cloning sites for genes of interest at *NdeI* and *XbaI* and the 3' untranslated region of the plastid rubisco large subunit gene T*rbcL*.

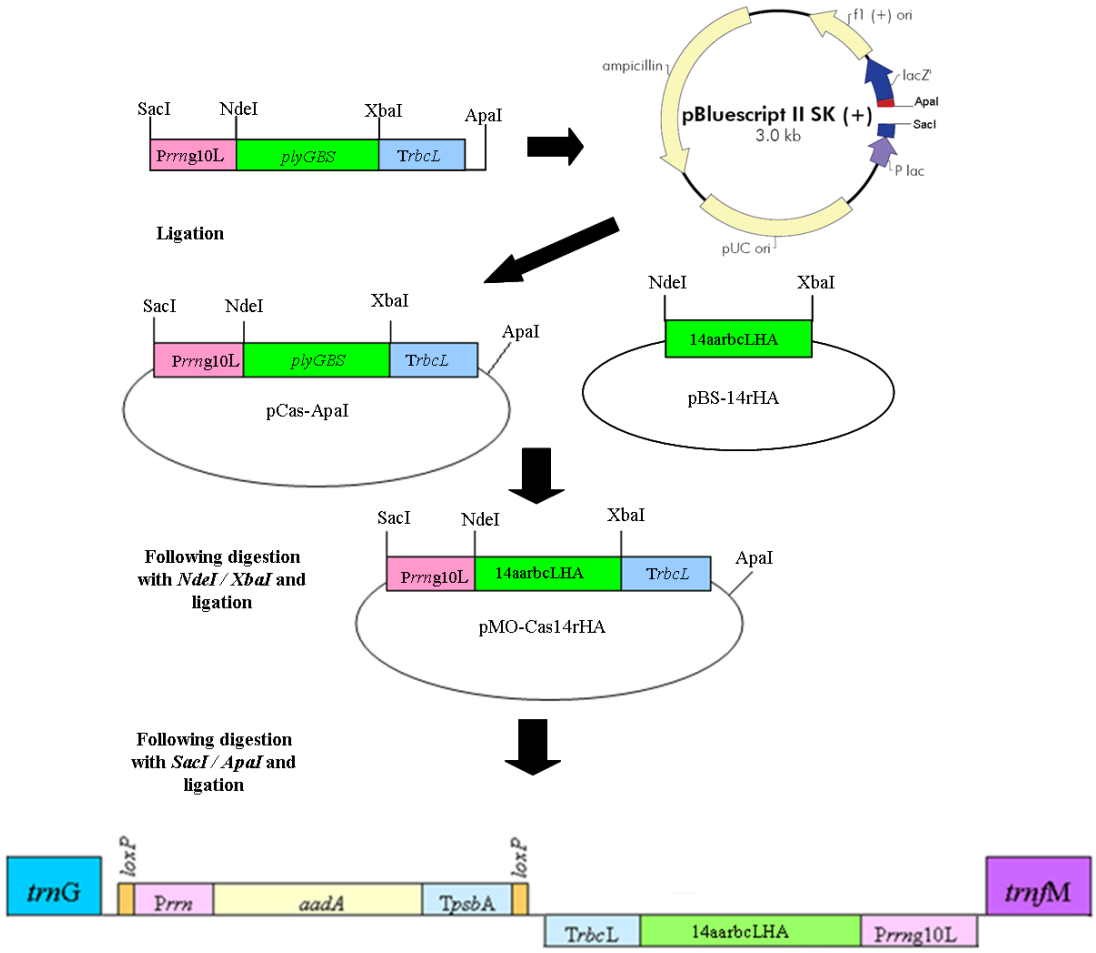

Figure 3.10: Schematic representation of the strategy used for cloning the 14aarbcLHA fusion gene into the pMO16 transformation vector. The transgene expression cassette from the pMO16 transformation vector was digested using *SacI* and *ApaI* and ligated into an intermediate vector, pBluescript SK (+) to produce pCas-ApaI. The *plyGBS* gene was replaced with the 14aarcLHA fusion gene following restriction digest of pCas-ApaI and pBS-14rHA with *NdeI* and *XbaI*. The transgene cassette was ligated back into the pMO16 vector to give the pMO14rHA transformation vector.

pCas-ApaI-1 was digested with *NdeI* and *XbaI* to remove the *plyGBS* gene and the vector backbone was gel purified. pCR-14rHA was also digested with *NdeI* and *XbaI*, excising the 14rHA gene which was gel purified and ligated into the pCas-ApaI-1 vector backbone. The ligation reaction was transformed into Top 10 chemically competent *E. coli* cells which were grown on LB amp agar plates. Plasmid DNA was isolated and digested with *NdeI* and *XbaI*. Recombinant plasmids produced a 3.4 kb vector backbone band and the 1.6 kb 14rHA insert. These were subsequently referred to as pMO-Cas14rHA.

pMO-Cas14rHA was re-digested with *ApaI* and *SacI*, gel purified and ligated back into the pMO16 vector. DNA was isolated from six colonies which grew on LB amp agar plates and was digested with *ApaI* and *SacI*. Recombinant plasmids produced a 7 kb vector backbone band and 1.9 kb 14rHA transgene cassette insert to give the pMO14rHA transformation vector.

The 14gHA was cloned into the pMO16 vector using the same strategy as described above to produce the pMO14gHA plastid transformation vector.

3.2.4 GFP/HA and GFP/HA1

Before the two constructs, GFP/HA and GFP/HA1 could be made, the HA1 coding region was amplified from the *HA* gene and an internal *NdeI* site was removed from the *gfp* gene. A twelve base pair sequence coding for a flexible glycine-proline-glycine-proline (gpgp) linker was also incorporated between the fusion genes to generate a protein hinge between GFP/HA and GFP/HA1. This

type of hinge has previously been used to improve the conformation of fusion proteins such as CTB / HIV-1 gp-41 fusion protein (Matoba *et al.*, 2004).

3.2.4.1 Amplification of the HA1 coding region

The pBS-HA gene construct (Section 3.2.1.1) was used as template DNA. Primers HA-NdeIF and HA1-XbaIR were used to amplify the HA1 coding region while simultaneously adding an *NdeI* restriction site immediately upstream of the start codon and a stop codon and an *XbaI* restriction site immediately downstream of the HA1 coding region (Figure 3.11). This PCR reaction produced a 990 bp PCR product (Figure 3.12 A) that was ligated into the pCR4-TOPO vector. Plasmid DNA was isolated from 13 recombinant colonies, digested with *NdeI* / *XbaI* and analysed by agarose gel electrophoresis on a 0.7% gel. Required recombinant plasmids produced the 3.9 kb pCR4-TOPO vector backbone and the 990 bp HA1 insert (Figure 3.12 B). Three plasmid preparations were sent for sequencing to ensure that no errors had been introduced into the gene sequence during PCR amplification. Two plasmids sequenced correctly. These plasmids were subsequently referred to as pCR4-HA1-2 and pCR4-HA1-3.

3.2.4.2 Amplification of *HA* with gpgp linker sequence

To minimise the possibility of introducing mutations or nucleotide changes caused by long-range PCR, the glycine proline (gpgp) linker was fused to the 5' end of the first 325 bp of the *HA* gene by PCR using the primer pair HA-LinkF / HA-HindIII-R (Figure 3.13). The resulting 325 bp PCR product (Figure 3.14 A) was gel purified and ligated into the cloning vector pNEB193 using the *XmaI*

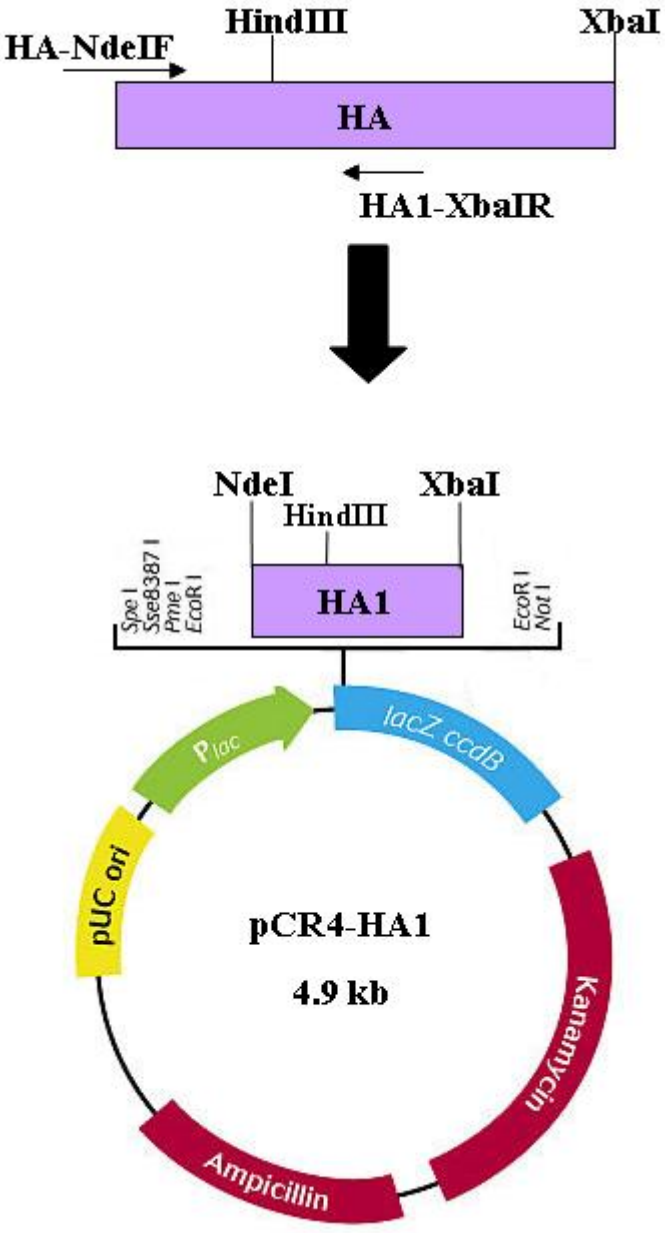

Figure 3.11: Schematic representation of the cloning strategy used to generate pCR4-HA1. The *HA1* coding region was amplified using the primer combination HA-NdeIF and HA1-XbaIR. The resulting PCR product was then cloned into pCR4-TOPO to give pCR4-HA1.

(A)

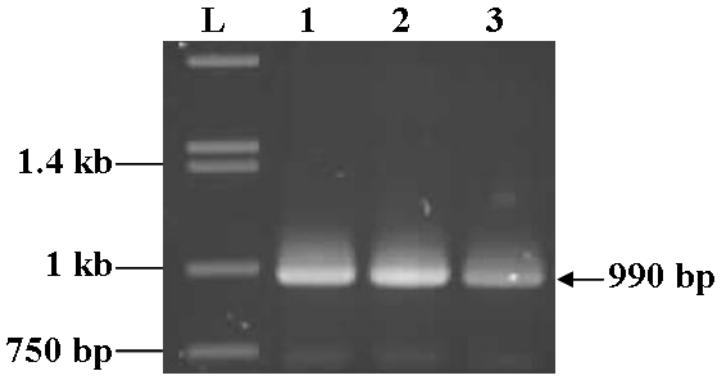

(B)

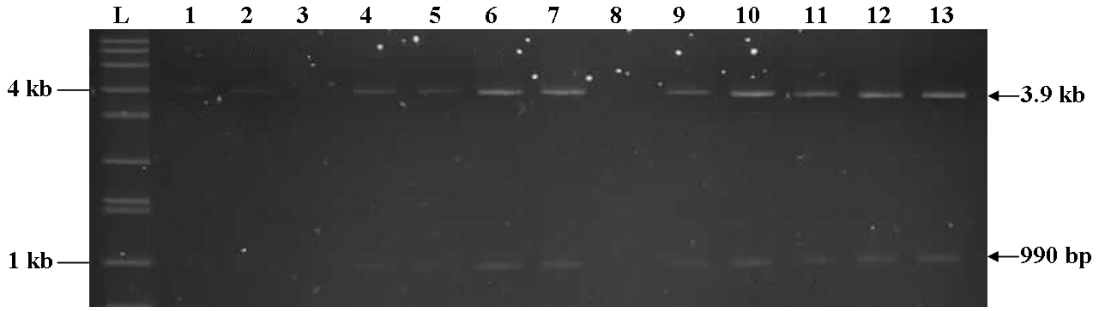

Figure 3.12: HA1 amplification by PCR and restriction digest analysis. (A) A 990 bp HA1 PCR product was amplified using the primers HA-NdeIF and HA-XbaIR. Lane L: 10 kb ladder (Sigma). Lanes 1-3: Independent HA1 PCR products 1-3. (B) Restriction digest of pCR4-HA1 recombinant plasmids with the restriction enzymes *NdeI / XbaI.* Digestion produced a 990 bp HA1 fragment and a 3.9 kb pCR4-TOPO vector backbone DNA fragment. Lane L: 10 kb ladder. Lanes 1-13: pCR4-HA1 clones 1-13.

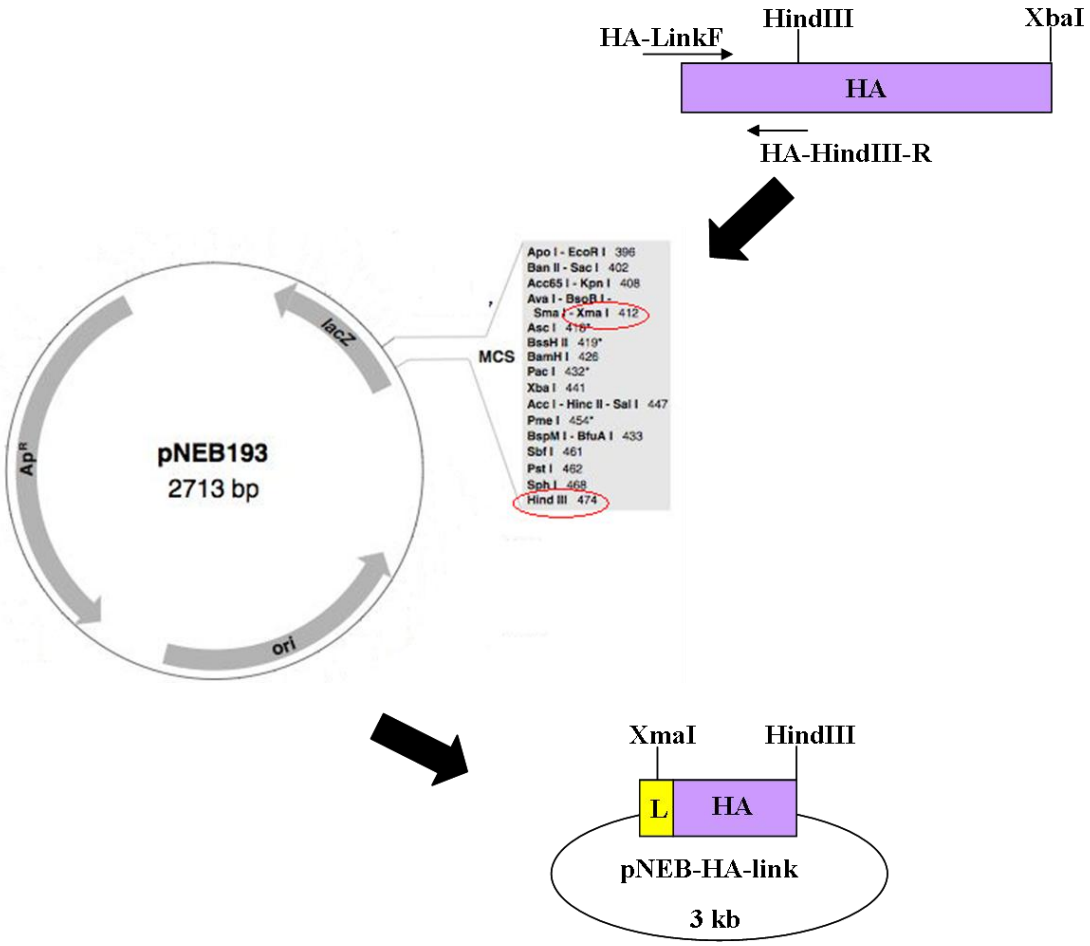

Figure 3.13: Schematic representation of the cloning strategy used to generate the *HA* gene with the 5' gpgp linker. The gpgp linker was fused to the first 325 bp of the *HA* gene using primer overlap extension. The resulting PCR product was then cloned into pNEB193 using the *XmaI* site present in the gpgp linker sequence and *HindIII* to give pNEB-HA-Link.

(A)

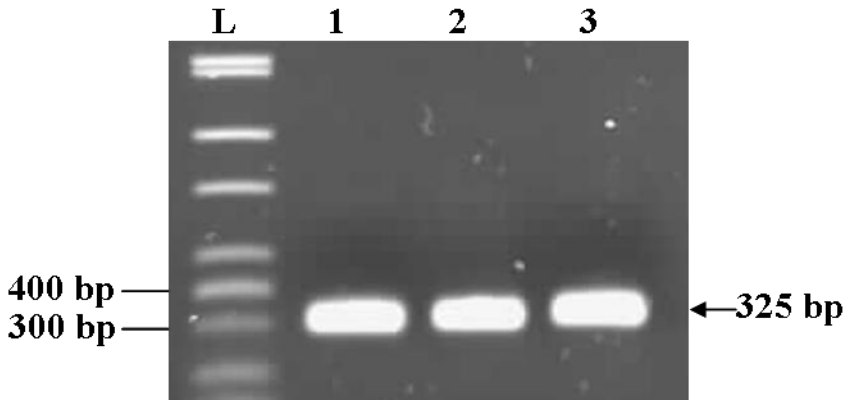

(B)

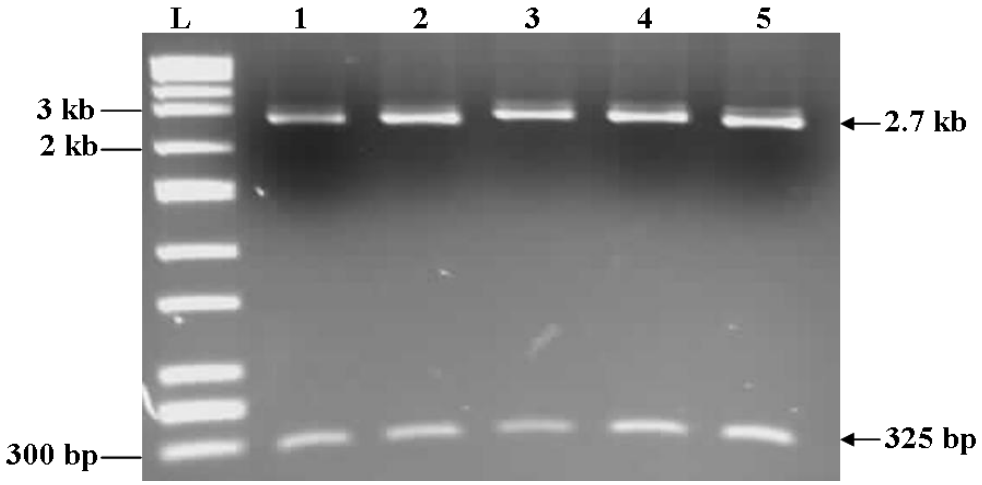

Figure 3.14: HA-link amplification by PCR and restriction digest analysis. (A) A 301 bp HA-link product was amplified using the primers HA-LinkF / HA-HindIII-R. Lane L: 10 kb ladder (Sigma). Lanes 1-3: Three independent HA-link PCR products. (B) Restriction digest of pNEB-HA-link recombinant plasmids with *XmaI / HindIII.* Correct clones produced the 2.7 kb pNEB193 vector backbone and the 301 bp HA-link insert. Lane L: 10 kb ladder. Lanes 1-5: pNEB-HA-link clones 1-5.

restriction site present in the linker sequence and the 3' *HindIII* restriction site. Plasmid DNA was isolated from five recombinant clones, digested with *XmaI* / *HindIII* and analysed by agarose gel electrophoresis. Correct recombinant plasmids produced the 2.7 kb pNEB193 vector backbone band and the 325 bp HA-linker insert (pNEB-HA-link) (Figure 3.14 B).

3.2.4.3 Generation of HA/link and HA1/link constructs

To assemble the HA/link construct, pCR4-HA and pBluescript SK (+) were first digested with *HindIII* / *XbaI* (Figure 3.15). The HA insert and pBluescript SK (+) vector backbone were gel purified and ligated together. Plasmid DNA was isolated from four colonies and digested with *HindIII* / *XbaI*. Correct recombinant plasmids produced a 3 kb vector backbone band and a 1.3 kb HA band and these were subsequently referred to as pBS-HA-HX.

pNEB-HA-link (Section 3.2.4.2) and pBS-HA-HX were then digested with *KpnI* / *HindIII*. The pBS-HA-HX vector and HA-link insert were gel purified and ligated together. Plasmid DNA was isolated from five colonies and digested with *KpnI* / *HindIII*. Correct recombinant plasmids produced a 4.3 kb vector backbone and the 325 bp HA-link insert and were subsequently referred to as pBS-HA-link (Figure 3.16 A).

To assemble the HA/link onto the 5' end of the HA1 gene construct, pCR4-HA1 (Section 3.2.4.1) was digested with *HindIII* / *XbaI* and ligated into pBluescript SK(+) as described above to produce pBS-HA1-HX. pNEB-HA- link and pBS-HA1-HX were digested with *KpnI* / *HindIII* and ligated together as described

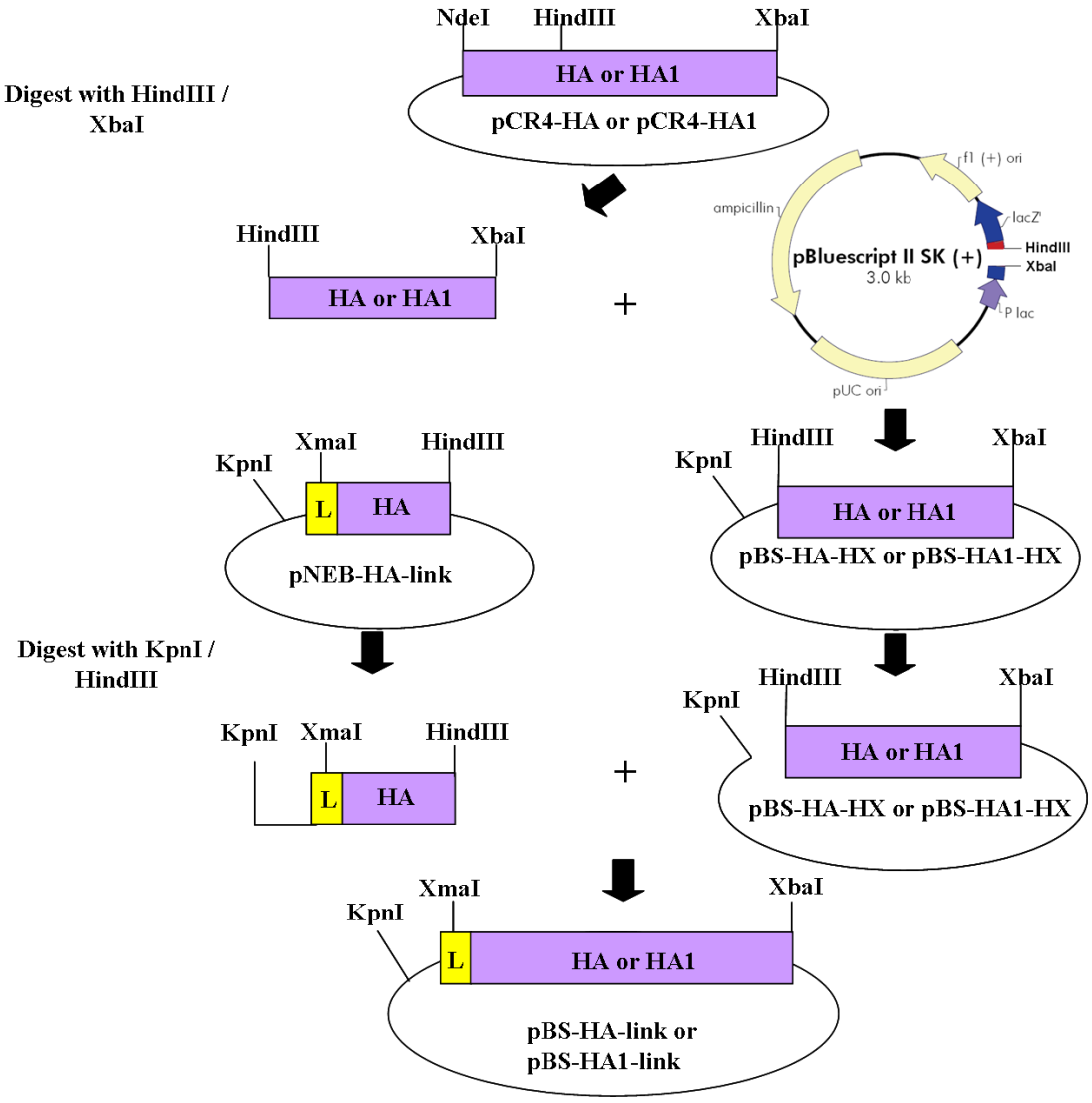

Figure 3.15: Schematic representation of the strategy used to add the 5' gpgp linker to *HA* and *HA1*. pCR4-HA and pCR4-HA1 were digested with *HindIII* / *XbaI* and cloned into the cloning vector pBluescript SK (+) to give pBS-HA-HX and pBS-HA1-HX. Both pBS-HA-HX and pBS-HA1-HX were digested with *KpnI* / *HindIII.* pNEB-HA-link was also digested with *KpnI* / *HindIII.* Both fragments were ligated together to give either pBS-HA-link or pBS-HA1-link.

(A)

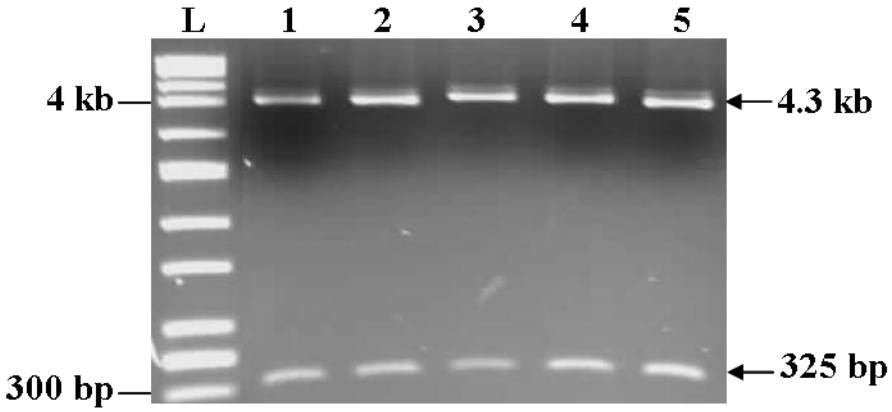

(B)

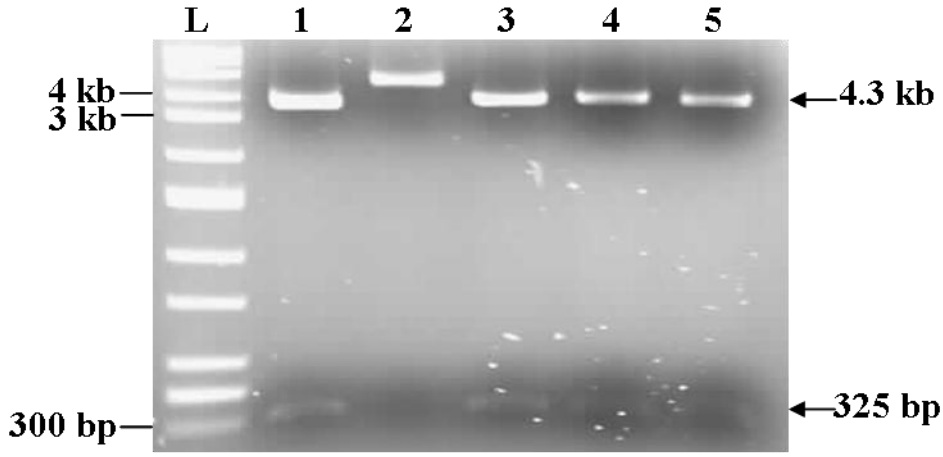

Figure 3.16: Recombinant clones containing the gpgp linker sequence fused to *HA* and *HA1*. (A) pBS-HA-link plasmids were digested with *KpnI* / *HindIII*. The excised HA-link fragment is seen at 301 bp. Lane L: 10 kb ladder (Sigma). Lanes 1-5: pBS-HA-link plasmids 1-5. (B) pBS-HA1-link plasmids were digested with *KpnI / HindIII*. Restriction digests produced a 4.3 kb pBluescript SK (+) vector backbone and a 325 bp HA-link insert. Lane L: 10 kb ladder (Sigma) Lanes 1-5: pBS-HA1-link plasmids 1-5.

above. Plasmid DNA was isolated from five colonies and digested with *KpnI* / *HindIII*. Correct recombinant plasmids produced a 4.3 kb vector backbone band and a 325 bp HA1-link band. These recombinant plasmids were subsequently referred to as pBS-HA1-link (Figure 3.16 B).

3.2.5 Generation of GFP/HA and GFP/HA1 fusion constructs

Before the GFP/HA and GFP/HA1 fusion constructs could be generated, it was necessary to eliminate an internal *NdeI* site in the *gfp* gene as all future cloning was performed using the 5' *NdeI* and 3' *XbaI* restriction sites.

3.2.5.1 Modification of *gfp* gene

The *gfp* gene was amplified by PCR from the plasmid pLCV2-GFP/aadA (Lelivelt *et al.*, 2005) and was modified for cloning into the *NdeI* / *XbaI* restriction sites of the tobacco chloroplast transformation vector pMO16 (Oey *et al.*, 2009a). The primer pair GFP-NdeIF and GFP-XbaIR were designed to introduce an *NdeI* and an *XbaI* restriction site at the 5' and 3' end of the gene respectively. A second complementary primer pair, GFP-MutF and GFP-MutR, were designed to eliminate the internal *NdeI* restriction site in the *gfp* gene (from CATATG to CACATG). This change eliminates the restriction site but does not change the deduced amino acid sequence of the gene. Modification of the *gfp* gene was achieved by PCR and site directed mutagenesis using two rounds of PCR (Figure 3.17). The first round of PCR used the primer pairs (1) GFP-NdeIF / GFP-MutR and (2) GFP-MutF / GFP-XbaIR. The primer pair GFP-NdeIF / GFP-MutR produced a 243 bp fragment containing an *NdeI*

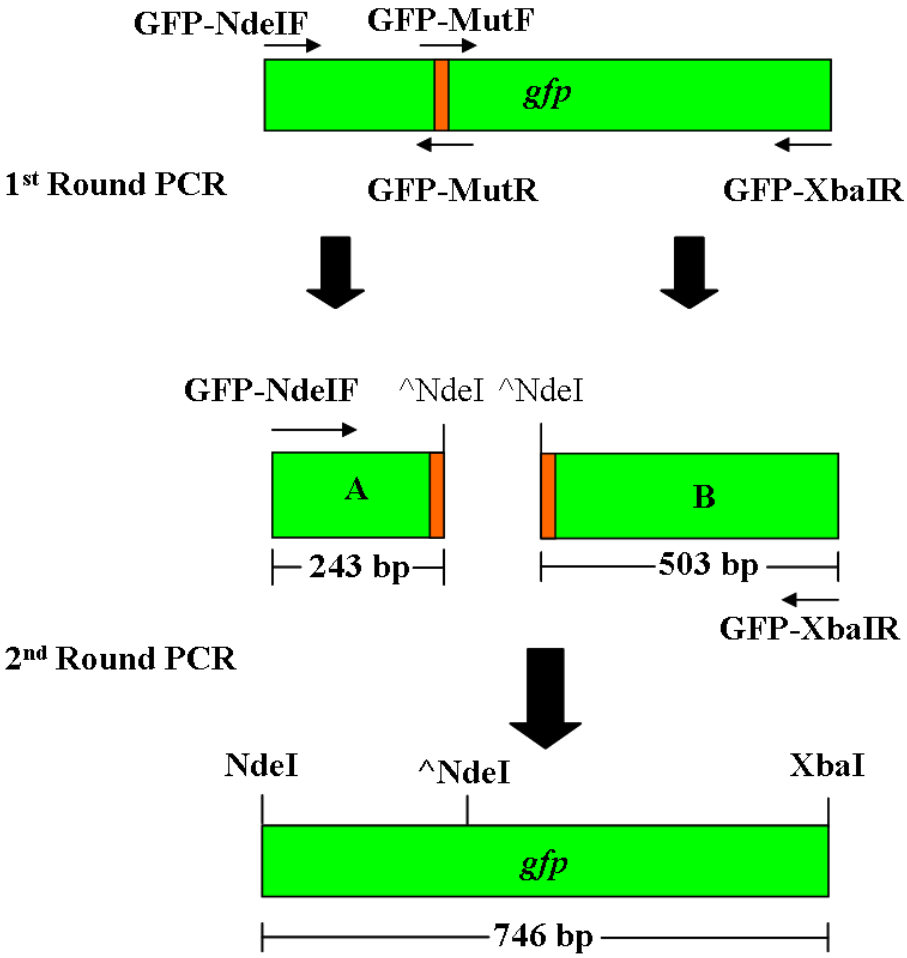

Figure 3.17: Schematic representation of the modified *gfp* gene generated by primer overlap extension. First round PCR, generated product A using the primer pair GFP-NdeIF / GFP-MutR and product B using the primer pair GFP-MutF / GFP-XbaIR. Both primers GFP-MutF and GFP-MutR were designed to eliminate an internal *NdeI* restriction site in the *gfp* gene. In the second round PCR, products A and B were used as template DNA to generate the full length *gfp* gene using the primer pair GFP-NdeIF / GFP-XbaIR by primer overlap extension.

restriction site at the 5’ end and a mutated *NdeI* restriction site at the 3’ end (Figure 3.18 A, lane 1). The primer pair GFP-MutF / GFP-XbaIR generated a 503 bp product containing the mutated *NdeI* restriction site at the 5’ end and an *XbaI* restriction site at the 3’ end of the gene. (Figure 3.18 A, lane 2). These two products were gel purified and used as template DNA in the second round PCR to generate the 746 bp full length *gfp* gene (Figure 3.18 A, lane 3) using the primer pair GFP-NdeIF / GFP-XbaIR. The modified *gfp* gene was gel purified and ligated into the pCR2.1-TOPO cloning vector (Invitrogen). Plasmid DNA was isolated from 15 ampicillin-resistant colonies and digested with *EcoRI*. All 15 plasmid DNA digests released the cloned fragment of the expected size (750 bp) (Figure 3.18 B). Plasmids 2, 6 and 9 were sequenced to ensure that the internal *NdeI* site had been completely removed and that no errors had been introduced into the gene sequence during PCR amplification. Sequence analysis showed that no errors had occurred and that the internal *NdeI* site had been correctly removed.

3.2.5.2 Amplification of the GFP/link gene construct

A glycine proline (gpgp) linker sequence was also added to the 3’ end of the modified *gfp* gene (Section 3.2.5.1) by PCR using the primer pair GFP-NdeIF / GFP-Link-XbaIR. The primer GFP-Link-XbaIR was designed to fuse the gpgp linker sequence to the 3’ end of the *gfp* gene as well as incorporating an *XbaI* site immediately downstream of the linker (Figure 3.19). A 750 bp PCR product was produced (Figure 3.20 A), gel purified and ligated into pCR4-TOPO. Plasmid DNA was isolated from three colonies and digested with *EcoRI*. All three recombinant plasmids produced the 3.9 kb vector backbone band and the

(A)

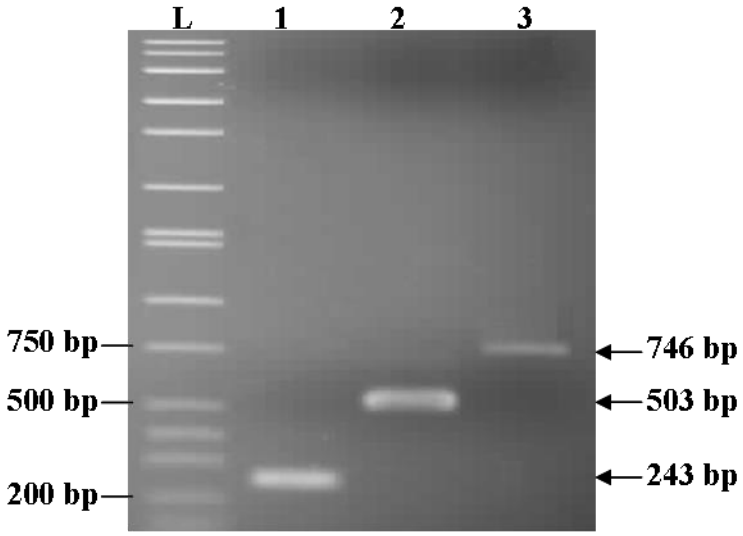

(B)

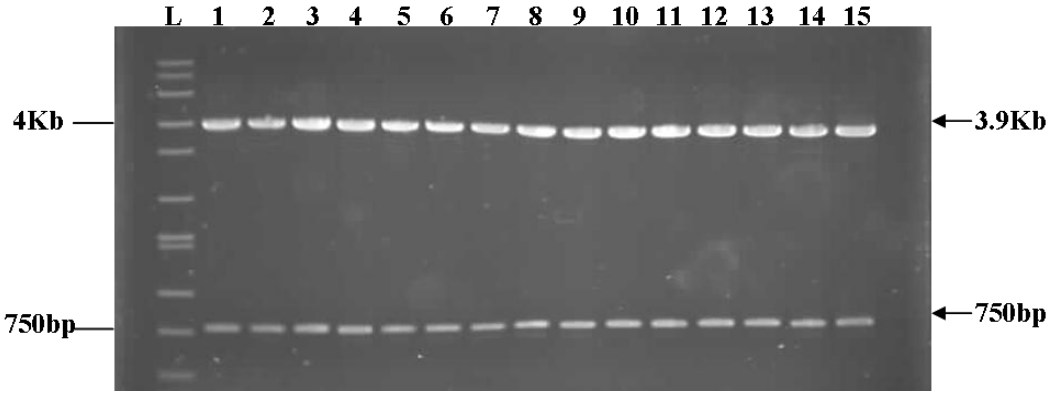

Figure 3.18: Amplification and restriction digest analysis of modified *gfp* PCR products. (A) A modified *gfp* gene was generated using four primer combinations. Lane 1: First round PCR product generated using GFP-NdeIF / GFP-MutR. Lane 2: First round PCR product generated using GFP-MutF / GFP-XbaIR. Lane 3: Full length modified *gfp* gene generated using first round PCR products as templates and the primer pair, GFP-NdeIF / GFP-XbaIR. Lane L: 10 kb Ladder (Sigma). (B) Recombinant plasmids containing the modified *gfp* gene in the sequencing vector pCR2.1-TOPO. Recombinant plasmids, Lanes: 1-15, were digested with *EcoRI*. Digests released a 750 bp *gfp* insert from the 3.9 kb pCR2.1-TOPO cloning vector backbone. Lane L: 10 kb ladder (Sigma).

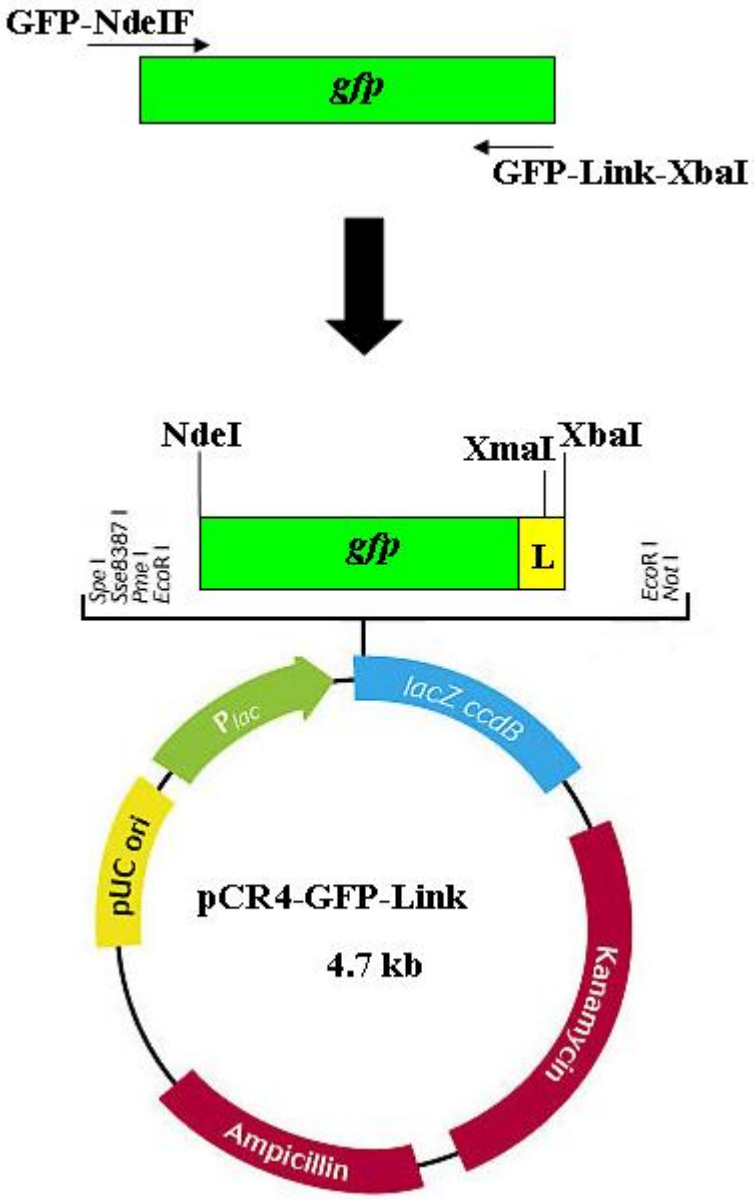

Figure 3.19: Schematic representation of the cloning strategy used to generate the *gfp* gene with the 3' gpgp linker. The gpgp linker was added to the 3' end of the *gfp* using the primers GFP-NdeIF and GFP-LinkR. The resulting PCR product was then cloned into pCR4-TOPO to give pCR4-GFP-Link.

(A)

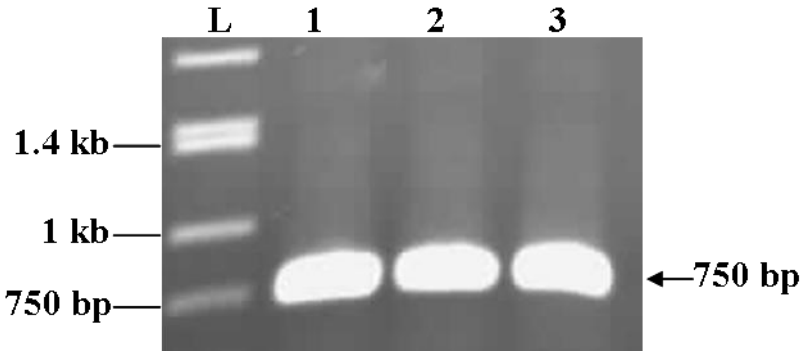

(B)

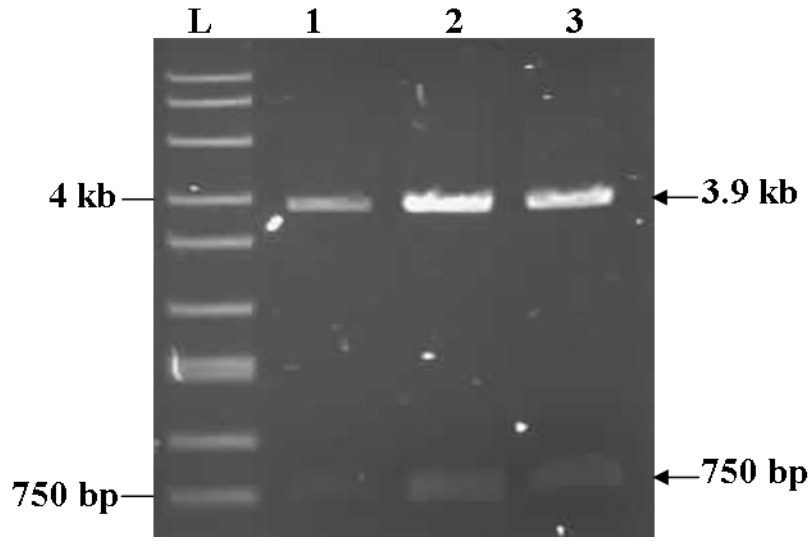

Figure 3.20: GFP-link amplification by PCR and restriction digest analysis. (A) A 750 bp GFP-link PCR product was amplified using the primers GFP-NdeIF / GFP-LinkR. Lane L: 10 kb ladder (Sigma). Lanes 1-3: GFP-Link PCR products 1-3 (B) Restriction digest of pCR4-GFP-link with *EcoRI.* Digest produced a 3.9 kb vector backbone and a 750 bp GFP-link insert. Lane L: 10 kb ladder. Lanes 1-3: pCR4-GFP-Link clones 1-3.

750 bp GFP-Link band (pCR4-GFP-link) (Figure 3.20 B).

3.2.5.3 Generation of GFP/HA and GFP/HA1 fusion constructs

To generate the GFP/HA fusion construct, both pCR4-GFP-link and pBS-HA-link were digested with *XmaI* / *XbaI* (Figure 3.21). The GFP-link vector and the HA-link insert were gel purified and ligated together. Plasmid DNA was isolated from four recombinant clones and digested with *XmaI* / *XbaI*. Correct recombinant plasmids produced a 4.6 kb vector backbone and a 1.6 kb HA-link insert (pCR4-GFP/HA) (Figure **3.22** A). To generate the GFP/HA1 fusion, both the pCR4-GFP-link and the pBS-HA1-link were digested with *XmaI* / *XbaI* and ligated together as described above. Plasmid DNA was isolated from seven recombinant clones and digested with *XmaI* / *XbaI*. Correct recombinant plasmids produced a 4.6 kb vector backbone band and a 1 kb HA-link insert (pCR4-GFP/HA1) (Figure **3.22** B).

3.2.6 Generation of pMOGFP/HA and pMOGFP/HA1 Vectors

The GFP/HA and GFP/HA1 fusion genes were cloned into the pMO16 vector using the same method as described in Section 3.2.3 to produce the pMOGFP/HA and pMOGFP/HA1 plastid transformation vectors.

3.2.7 Functional analysis of pMOGFP/HA and pMOGFP/HA1 in *E. coli*

E. coli cells containing the pMOGFP/HA and pMOGFP/HA1 recombinant plasmids were streaked onto plates containing spectinomycin (500 mg/L) and grown overnight at 37^0C. The bacteria grew in the presence of the antibiotic

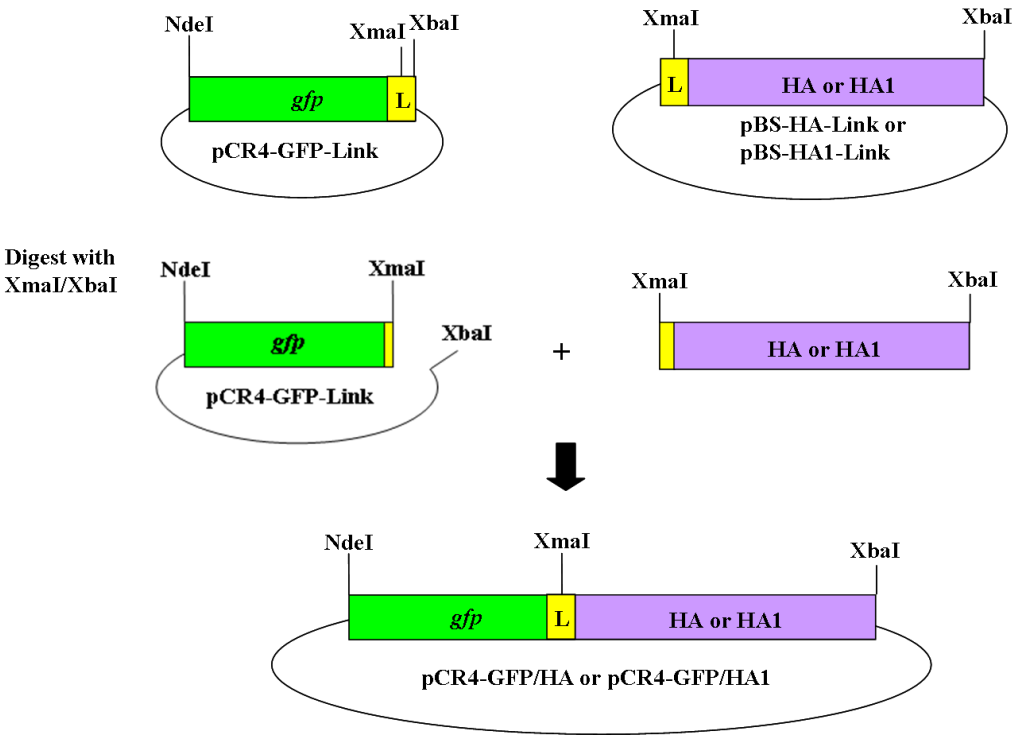

Figure 3.21: Schematic representation of the cloning strategy used to generate the *GFP*/HA and GFP/HA1 fragments. Both pCR4-GFP-Link and either pBS-HA-Link or pBS-HA1-Link were digested with *XmaI* / *XbaI*. The resulting fragments were then ligated together to give pCR4-GFP/HA or pCR4-GFP/HA1.

(A)

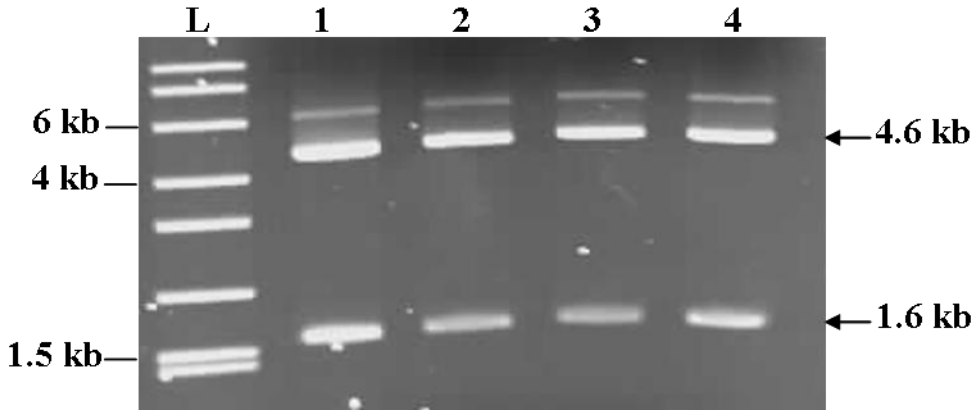

(B)

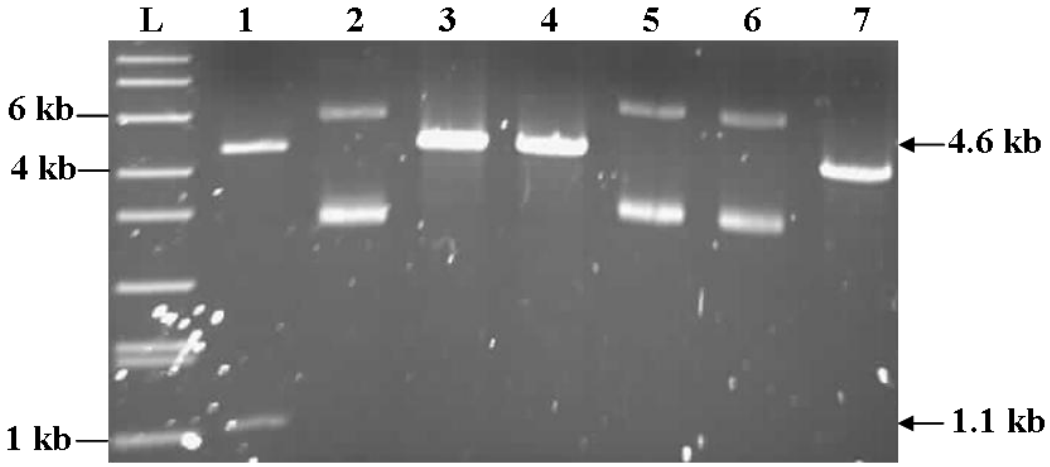

Figure 3.22: Recombinant pCR4-TOPO plasmids containing the GFP/HA and GFP/HA1 fragments. (A) pCR4-GFP-HA plasmids 1-4 digested with *XmaI / XbaI*. Digests produce a 4.6 kb vector backbone and the excised HA-Link band at 1.6 kb. Lane L: 10 kb Ladder (Sigma). Lanes 1-4: pCR4-GFP/HA plasmids 1-4. (B) pCR4-GFP-HA1 plasmids 1-7 digested with *XmaI / XbaI*. Digests produce a 4.6 kb vector backbone and the excised HA1-Link band at 1.1 kb. Lane L: 10 kb Ladder (Sigma). Lanes 1-7: pCR4-GFP/HA1 clones 1-7.

indicating that the *aadA* gene was being expressed. The plates were also placed under UV light to assess GFP expression. Bacteria transformed with both the transformation vectors fluoresced confirming GFP expression (Figure 3.23 A). Total protein was extracted from *E. coli* cells containing pMOGFP/HA, pMOGFP/HA1 and pProEx-HA plasmids. Protein extracts were run on a 10% SDS-PAGE gel, blotted onto nitrocellulose membrane and accumulation of HA and HA1 fusion proteins was assayed for using an anti-HA tag antibody. No protein was detected in cells transformed with the pMOGFP/HA vector (Figure 3.23 B, lane 1). The antibody detected a protein at the expected size, 60 kDa, in cells transformed with the pMOGFP/HA1 vector (Figure 3.23 B, lane 2) indicated that GFP/HA1 was expressed in *E. coli*. The HA positive control protein was detected in cells transformed with pProEx-HA at the expected size, 62 kDa (Figure 3.23 B, lane +ive). Although no HA protein accumulation was detected in *E.coli* cells transformed with the pMOGFP/HA vector, it was decided to go ahead and still use this vector for chloroplast transformation since GFP expression was detected in these cells.

3.2.8 Transformation of tobacco chloroplasts

Large-scale plasmid DNA preparations of pMO14rHA, pMO14gHA, pMOGFP/HA and pMOGFP/HA1 were prepared for tobacco chloroplast transformation. Transforming DNA was introduced into tobacco leaf chloroplasts on the surface of gold particles using the Bio-Rad PDS-1000 He gun (outlined in Section 2.9.5). Following bombardment, leaves were cut into 10 mm^2 pieces and placed on RMOP medium containing 500 mg/L spectinomycin. The first spectinomycin resistant shoots were

(A)

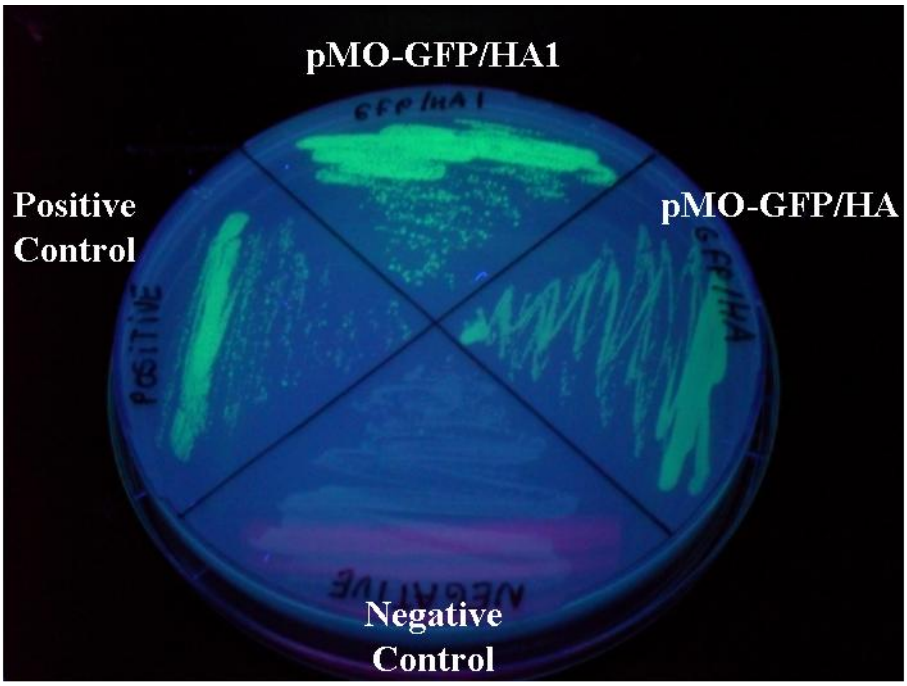

(B)

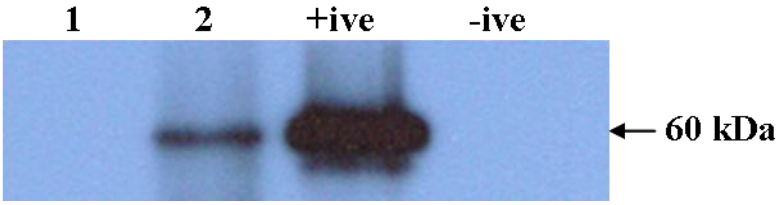

Figure 3.23: Expression analysis of the GFP/HA and GFP/HA1 gene constructs in *E.coli.* (A) *E. coli* transformed with both plasmids were plated on LB agar containing 500 mg/L spectinomycin. MSK18 and pZSUreB were used as positive and negative controls respectively. Cells were viewed under UV light to check for GFP expression. Bacteria containing both the GFP/HA and GFP/HA1 gene constructs grew in the presence of spectinomycin and fluoresced indicating that both the *aadA* and the *gfp* cassettes were expressing in the pMOGFP/HA and pMOGFP/HA1 plasmids. (B) Western blot showing that GFP/HA1 protein (60 kDa) is expressed in *E. coli* transformed with the plasmid pMOGFP/HA1 (lane 2). The full length HA protein was not detected in cells transformed with the pMOGFP/HA plasmid (lane 1). pProExHA, positive control (+ive), pZSUreB, negative control (–ive).

visible after 3-4 weeks. Spectinomycin resistant shoots were subjected to three rounds of regeneration on RMOP medium containing 500 mg/L spectinomycin and subsequently transferred to MS medium containing 500 mg/L spectinomycin for root formation.

3.2.9 Molecular characterisation of primary transformants

Total DNA was extracted from regenerated shoots and was subjected to PCR analysis using a combination of both gene specific primers (aadA-Rev, HA-XbaIR and HA1-XbaIR) and external primers (Ext-For and Ext-Rev) that flanked the vector integration site. These primer combinations allowed for the detection of chloroplast transformants only.

3.2.9.1 Characterisation of pMO14rHA regenerated lines

DNA was isolated from ten spectinomycin resistant shoots and analysed by PCR to determine if the 14rHA gene construct had integrated into the plastome at the expected vector integration site. The first PCR used the primers Ext-For / aadA-Rev which anneal upstream of the vector integration site and within the *aadA* gene respectively. This PCR amplified a 1.7 kb PCR product of the expected size in seven out of ten primary regenerated shoots (Figure 3.24 A). The second PCR used the primers HA-XbaIR / Ext-Rev which anneal to the 14rHA gene and downstream of the vector integration site respectively. This reaction produced a 3.8 kb PCR product of the expected size in four of the seven primary regenerated shoots tested indicating that targeted integration had been achieved in these lines (Figure 3.24 B). No PCR product was amplified from

(A)

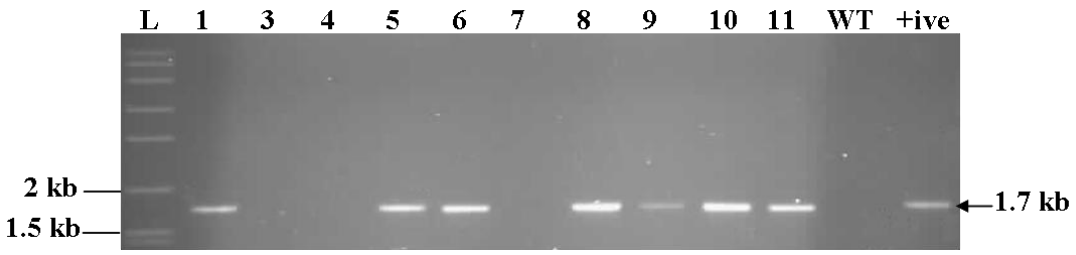

(B)

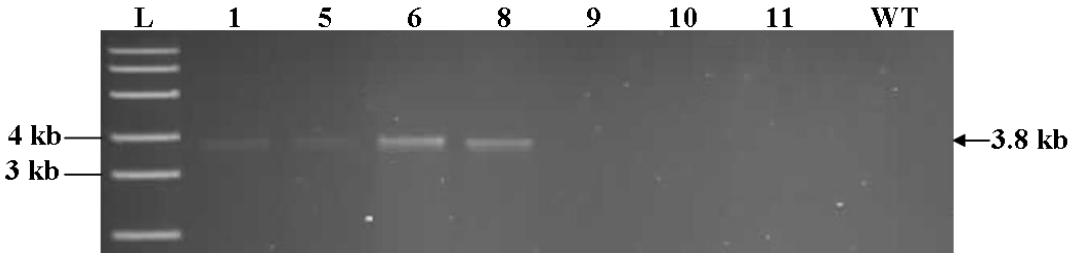

Figure 3.24: PCR analysis of putative 14rHA plants. (A) Primers Ext-For, specific to the chloroplast genome and aadA-Rev, specific to the *aadA* gene were used to confirm the integration of 14rHA gene construct into the tobacco chloroplast genome. The expected fragment size of 1.7 kb was amplified in seven out of ten plants. Lane L: 10 kb ladder (Sigma). Lane 1: 14rHA-1, Lanes 3-11: 14rHA-3, 14rHA-4, 14rHA-5, 14rHA-6, 14rHA-7, 14rHA-8, 14rHA-9, 14rHA-10 and 14rHA-11. Lane WT: Wild type Petite Havana (negative control) Lane +ive: Plant line 9G-1 (Section 4.2.5.1). (B) Primers HA-XbaIR, specific to the 14rHA gene and Ext-Rev, specific to the chloroplast genome were used to confirm the integration of 14rHA gene construct into the tobacco plastome. The expected fragment size of 3.8 kb was amplified in four out of seven plants. Lane L: 10 kb ladder (Sigma). Lane 1: 14rHA-1, Lanes 5-6: 14rHA-5, 14rHA-6. Lanes 8-11: 14rHA-8, 14rHA-9, 14rHA-10 and Lane 11: 14rHA-11. Lane WT: Wild type Petite Havana (negative control).

WT DNA. The four confirmed chloroplast transformed lines were subsequently referred to as 14rHA-1, 14rHA-5, 14rHA6 and 14rHA8.

3.2.9.2 Characterisation of pMO14gHA regenerated lines

DNA was isolated from nine spectinomycin resistant shoots and analysed by PCR to determine if the 14gHA gene construct had integrated as expected into the plastome. The same combination of primers as described in section 3.2.9.1 was used to test for targeted integration. Three out of nine putative transformants generated products of the expected size with both primer sets (Figure 3.25 A & B). These three confirmed plastid transformed lines were subsequently referred to as 14gHA-3, 14gHA-7 and 14gHA-8.

3.2.9.3 Characterisation of pMOGFP/HA1 regenerated lines

DNA was isolated from seven spectinomycin resistant shoots and analysed by PCR to determine if the GFP/HA1 gene construct had integrated at the expected site on the plastome. Primers aadA-For and aadA-Rev generated a 792 bp PCR product of the expected size and was amplified in two out of seven shoots (Figure 3.26 A). These same shoots also generated a product of the expected size (1.7 kb) using the primers Ext-For and aadA-Rev (Figure 3.26 B). However, none of these shoots generated a product of the expected size (3.3 kb) using the primers HA1-XbaIR and Ext-Rev (data not shown). A third PCR was carried out on the same two shoots using the primer combination GFP-NdeIF / HA1-XbaIR to see if the GFP/HA1 fusion gene was present. Again, neither of the two plants yielded a PCR product of the expected size (1.8 kb) suggesting

(A)

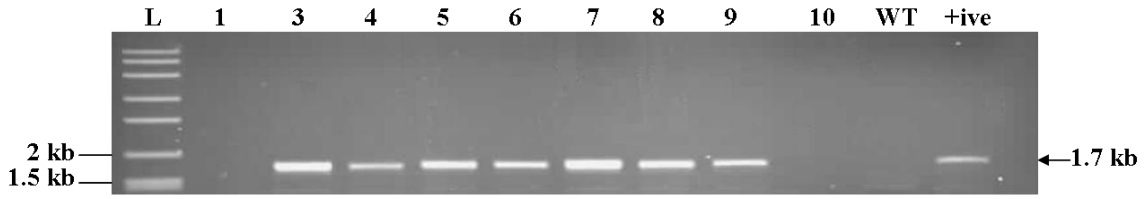

(B)

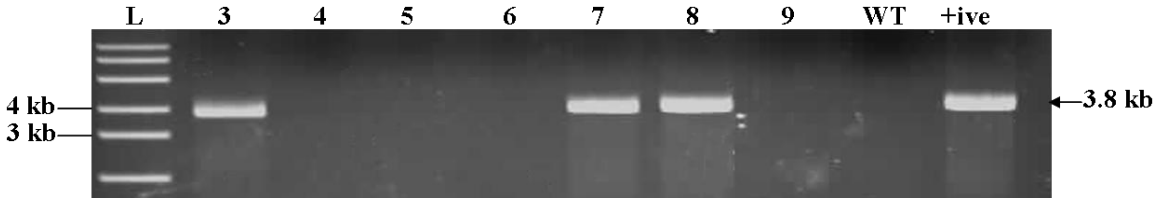

Figure 3.25: PCR analysis of putative 14gHA plants. (A) Primers Ext-For / aadA-Rev were used to confirm the integration of 14gHA into the tobacco chloroplast genome. The expected fragment size of 1.7 kb was amplified in seven out of nine plants. Lane L: 10 kb ladder (Sigma). Lane 1: 14gHA-1, Lanes 3-10: 14gHA-3, 14gHA-4, 14gHA-5, 14gHA-6, 14gHA-7, 14gHA-8, 14gHA-9 and 14gHA-10. Lane WT: Wild type Petite Havana (negative control). Lane +ive: 14rHA-1 (positive control) (B) Primers HA-XbaIR / Ext-Rev were used to confirm the integration of 14gHA into the tobacco plastome. The expected fragment size of 3.8 kb was amplified in three out of seven plants. Lane L: 10 kb ladder (Sigma). Lane 3-9: 14gHA-3, 14gHA-4, 14gHA-5, 14gHA-6, 14gHA-7, 14gHA-8 and 14gHA-9. Lane WT: Wild type Petite Havana (negative control). Lane +ive: 14rHA-1 (positive control).

(A)

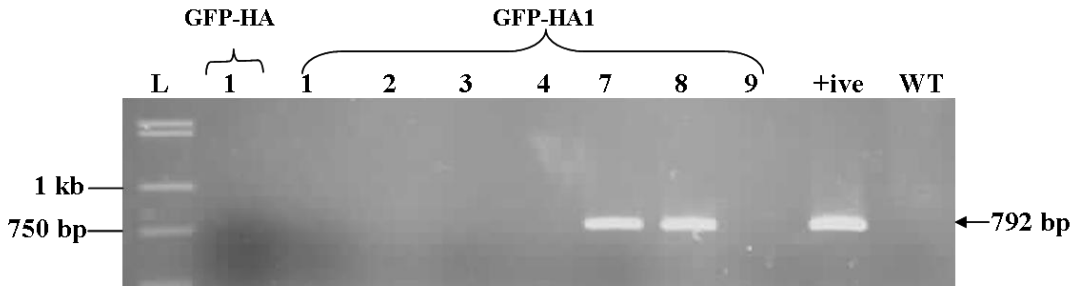

(B)

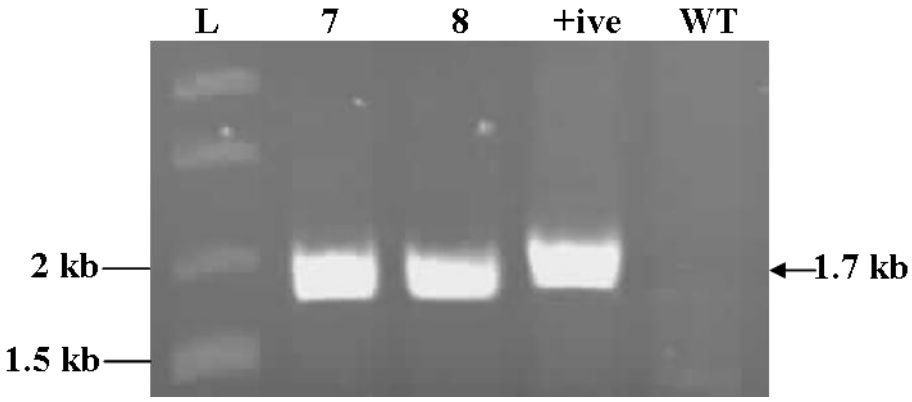

Figure 3.26: PCR analysis of putative pMOGFP/HA and pMOGFP/HA1 plants. (A) Primers aadA-For and aadA-Rev specific to the *aadA* gene were used to confirm the presence of the *aadA* gene in the pMOGFP/HA and pMOGFP/HA1 plants. The 792 bp PCR product was amplified in two out of seven pMOGFP/HA1 plants. No product was amplified for the pMOGFP/HA plant. Lane L: 10 kb ladder (Sigma) Lane 1 (GFP/HA): GFP/HA-1. Lanes 1-4 (GFP/HA1): GFP/HA1-1, GFP/HA1-2, GFP/HA1-3 and GFP/HA1-4. Lanes 7-9: GFP/HA1-7, GFP/HA1-8 and GFP/HA1-9. Lane +ive: pMOGFP/HA1 in *E. coli* (Positive control). Lane WT: Wild type Petite Havana (negative control) (B) Primers Ext-F / aadA-Rev were used to confirm the integration of GFP/HA1 gene into the tobacco chloroplast genome. The expected fragment size of 1.7 kb was amplified in both plants. Lane L: 10 kb ladder (Sigma). Lane 7-8: GFP/HA1-7 and GFP/HA1-8. Lane +ive: Line 14rHA-1 (Positive control). Lane WT: Wild type Petite Havana (negative control).

that only the *aadA* transgene had integrated into the plastid genome in these two lines (data not shown).

3.2.9.4 Characterisation of pMOGFP/HA regenerated lines

Only one spectinomycin resistant shoot regenerated after transformation with the pMOGFP/HA gene construct. PCR analysis was carried out on DNA isolated from this shoot. Primers, aadA-For / aadA-Rev, specific for the *aadA* gene did not generate a PCR product (Figure 3.26 A, lane 1 GFP/HA) suggesting that this shoot was a spontaneous mutant that conferred spectinomycin resistance.

3.2.10 Summary of biolistic transformation results

Table **3.1** provides a summary of biolistic experiments carried out and the resulting transformed lines obtained using the four transformation vectors.

3.2.11 Southern blot analysis of 14rHA and 14gHA transplastomic plants

Total DNA was isolated from wild type tobacco and confirmed third round T_0 14rHA and 14gHA transformed lines. DNA was digested with *BamHI*, Southern blotted and probed with a DIG labelled *psaB* probe to assess the level of homoplasmy. This probe was expected to hybridise to a 4.5 kb *BamHI* fragment in wild type tobacco DNA and to an 8 kb *BamHI* fragment in 14rHA and 14gHA transformed plants (Figure 3.27).

Table 3.1: Summary of biolistic results and transplastomic plants obtained

Constructs	**Number of shots**	**Number of shoots recovered**	**Number of shoots analysed by PCR**	**PCR confirmed *aadA* presence**	**PCR confirmed left border region[A]**	**PCR confirmed right border region[B]**	**Confirmed primary transformation events**
pMO14rHA	20	56	10	7	7	4	4
pMO14gHA	20	30	9	7	7	3	3
pMOGFP/HA	20	2	1	0	0	0	0
pMOGFP/HA1	20	10	7	2	2	0	0

[A] Primers Ext-For and aadA-Rev were designed to amplify *aadA*, *trnG* and part of the *psbZ* gene.
[B] A gene specific primer and Ext-Rev were designed to amplify the gene of interest, *trnfM*, *rps14* and part of the *psaB* gene.

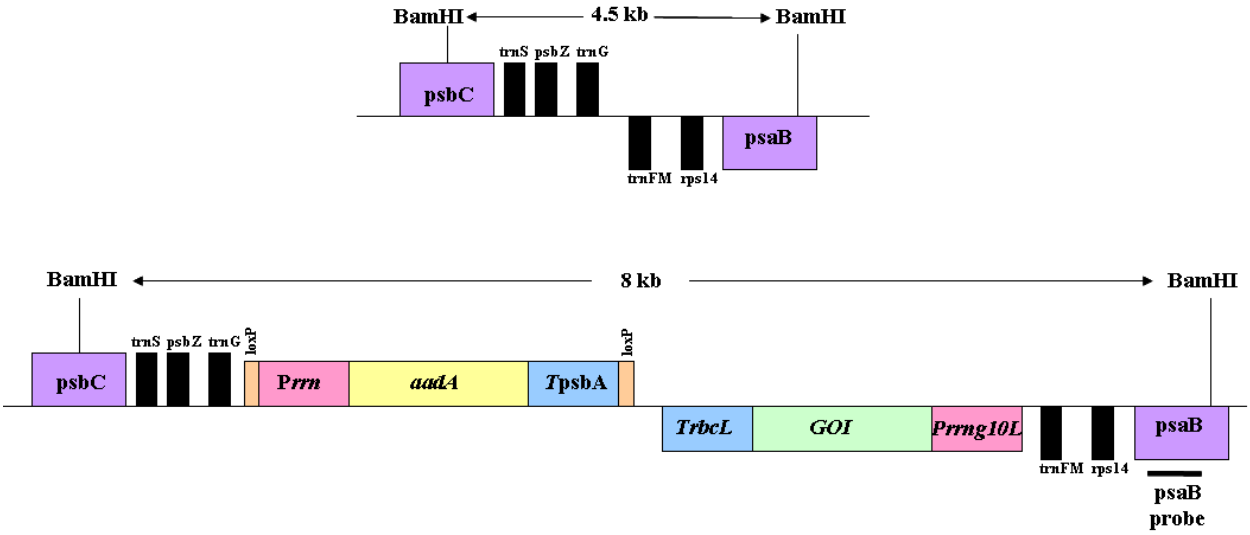

Figure 3.27: Map of the targeted region (not to scale) in the WT plastid genome and the transgenic plastid genome in transplastomic HA fusion lines generated. Relevant restriction sites used for southern blot analysis of transplastomic lines are indicated. The location of the *psaB* DIG probe is shown as a solid black bar. This probe hybridises to a 4.5 kb fragment in wild type plants and to an 8 kb fragment in 14rHA and 14gHA transplastomic lines.

The Southern blots confirmed that all four lines transformed with 14rHA (Figure 3.28) and all three lines transformed with 14gHA (Figure 3.29) had achieved homoplasmy. All homoplasmic transformed lines were transferred to soil for seed production.

3.2.12 Analysis of T1 generation plant lines

3.2.12.1 Seedling analysis

All homoplasmic 14rHA and 14gHA transformed lines were grown in soil to flowering. Plants were allowed to self pollinate and set seed which were then harvested. Seeds from the transgenic lines and from wild type plants were germinated on germination media containing 500 mg/L spectinomycin. All of the plated 14rHA and 14gHA seeds gave rise to green spectinomycin-resistant seedlings; all of the wild type seeds plated produced seedlings that bleached white (Figure 3.30). This 100% spectinomycin-resistance observed in the T_1 lines confirmed homoplasmy in these lines.

3.2.13 HA expression in 14rHA and 14gHA lines

3.2.13.1 Analysis of 14rHA expression in transformed plants

Western blot analysis of 14rHA protein accumulation was performed using protein extracted from leaves of the T_1 lines. Protein was extracted from the 1st leaf (oldest leaf) of four-week-old 14rHA transformed plants and WT plants. HA accumulation was assessed in the soluble (SF) and insoluble (ISF) protein fractions using an anti-HA antibody and an anti-HA307-319 antibody. A protein of approximately 48 kDa

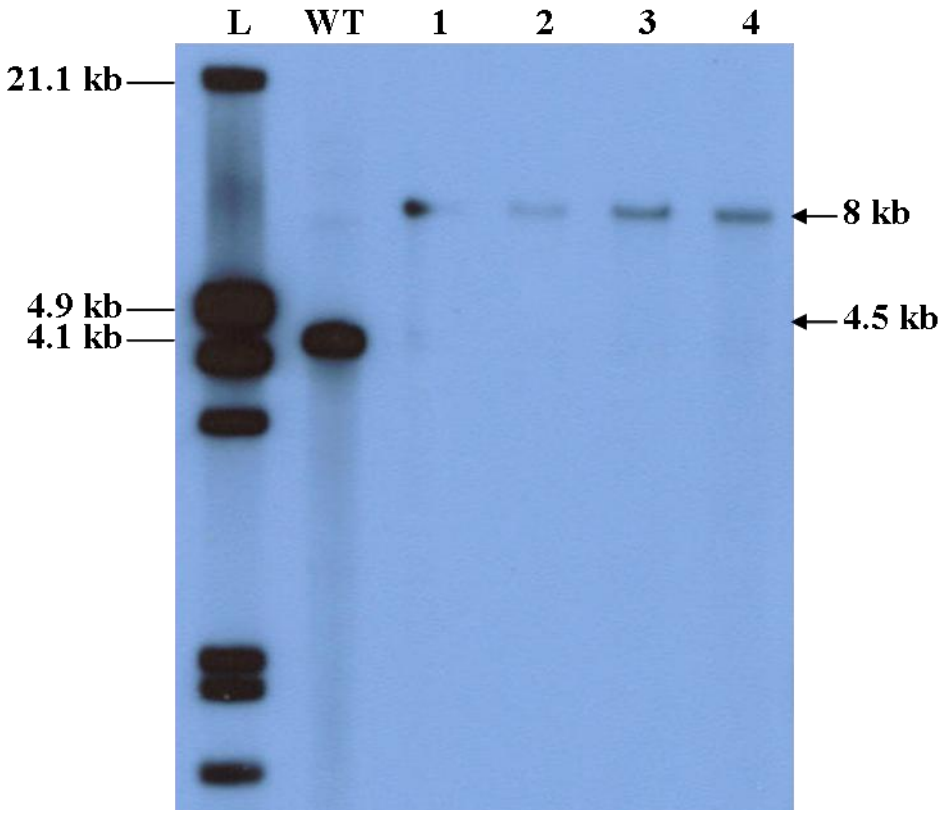

Figure 3.28: Southern blot analysis of T_0 generation of 14rHA transformed plants. Total DNA from 14rHA transformed plants was digested with *BamHI*. Digests were separated on a 0.7% agarose gel, blotted onto a nylon membrane and hybridised with *psaB* probe. Hybridisation of the *psaB* probe with WT Petit Havana produces a 4.5 kb fragment and an 8 kb fragment in the 14rHA lines. Lane L: DIG labelled marker weight III (Roche). Lane WT: Wild type tobacco DNA. Lanes 1-4: 14rHA-1, 14rHA-5, 14rHA-6 and 14rHA-8.

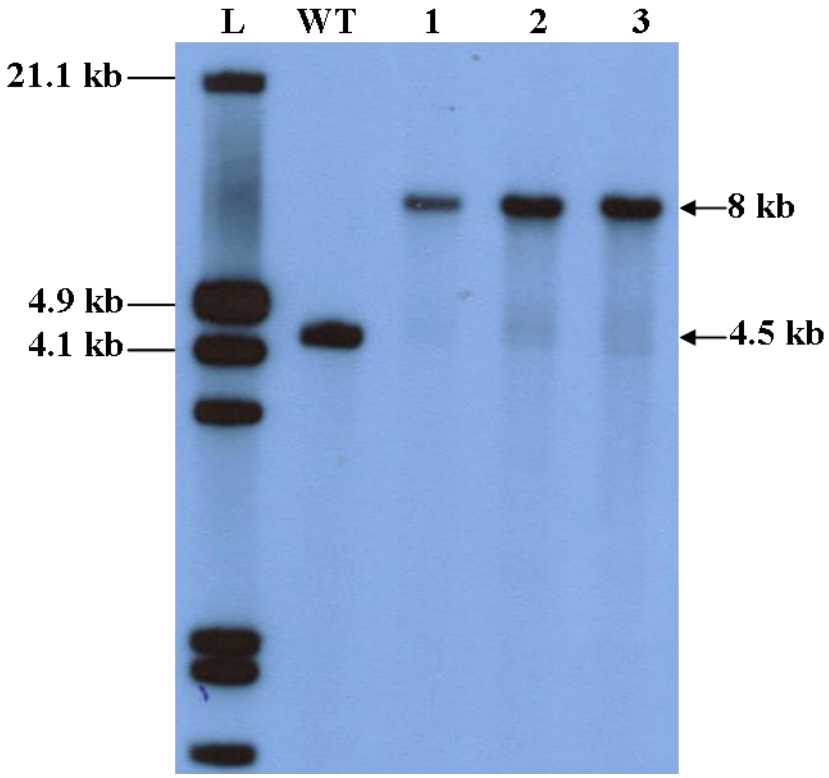

Figure 3.29: Southern blot analysis of T_0 generation of 14gHA transformed plants. Total DNA from 14gHA transformed plants was digested with *BamHI*. Digests were separated on a 0.7% agarose gel, blotted onto a nylon membrane and hybridised with *psaB* probe. Hybridisation of the *psaB* probe with the WT Petit Havana produces a 4.5 kb fragment and an 8 kb fragment in the 14gHA lines. Lane L: DIG labelled marker weight III (Roche). Lane WT: Wild type tobacco DNA. Lanes 1-3: 14gHA-3, 14gHA-7 and 14gHA-8.

(A)

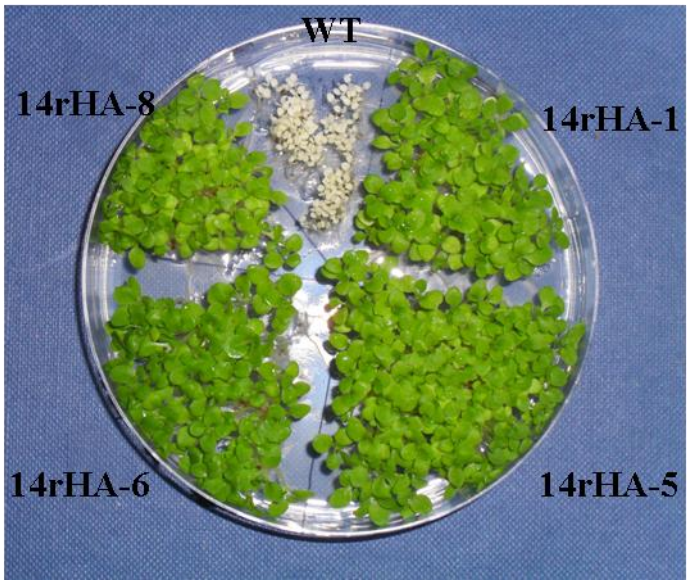

(B)

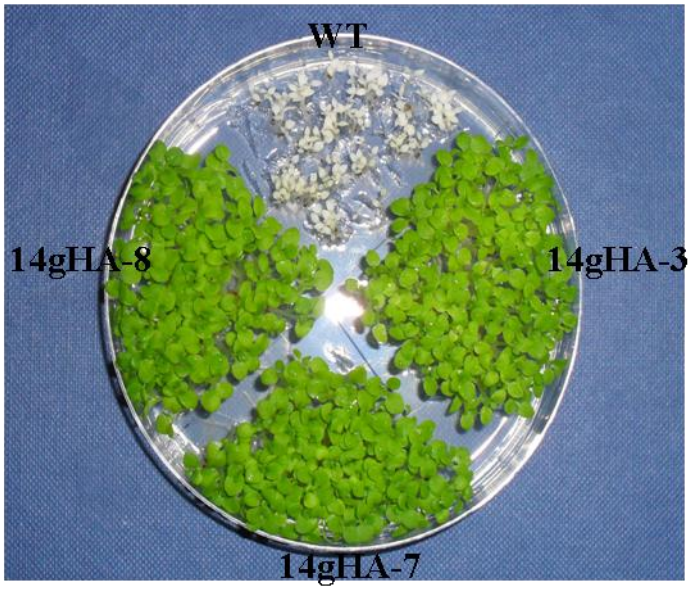

Figure 3.30: Seeds resulting from the self pollination of WT and transgenic lines. Seeds were germinated on germinating medium containing 500 mg/L spectinomycin. Inheritance test on 14rHA (A) and 14gHA (B) transplastomic lines. 100% of 14rHA and 14gHA seedlings germinated green and showed no phenotypic effects while wild type (WT) seedlings bleached white.

was detected using the anti-HA307-319 antibody in the ISF but not the SF samples prepared from two transgenic lines, 14rHA-6 and 14rHA-8 (Figure **3.31** A, lanes 1 and 3). However, this is significantly smaller than the expected size of the fusion protein which is estimated to be 58 kDa.

A similar sized fusion protein was detected in the ISF fraction isolated from two of the 14gHA lines, (14gHA-7 and 14gHA-8; Figure **3.31** B, lanes 1 and 3). Equal amounts of protein were loaded onto both gels, however considerably less protein accumulation was observed in the 14gHA lines when compared to the 14rHA lines. No protein was detected in either of the plant lines using the anti-HA antibody (data not shown).

3.2.13.2 DNA sequence analysis of the plastome integrated 14rHA and 14gHA gene expression cassettes

A possible explanation for the smaller than expected fusion proteins in the 14rHA and 14gHA recombinant lines is the presence of a pre-mature stop codon in the plastid integrated *HA* gene construct. The 14rHA and 14gHA expression cassettes were PCR amplified using the primer pair Prrn-Fw and TrbcL-Rv and the PCR products were sequenced. One line was tested for each construct and three independent PCR reactions were set up for each line. No pre-mature stop codon was detected in any of the integrated gene sequences. This suggests that the smaller protein detected by western blot analysis is probably not due to pre-mature termination of protein translation.

(A)

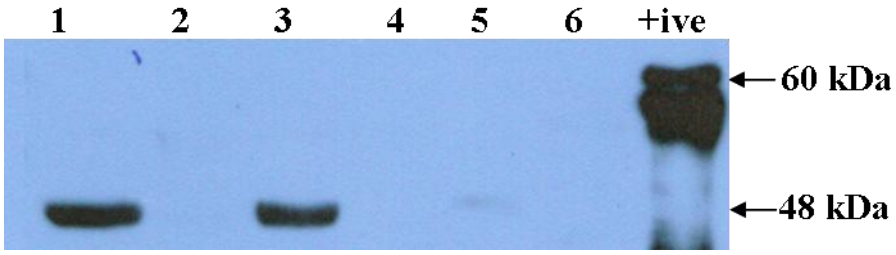

(B)

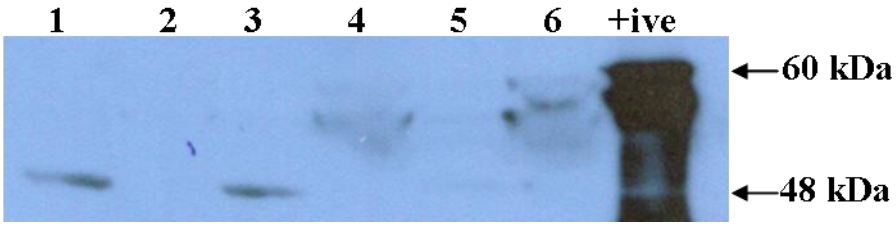

Figure 3.31: Expression analysis of pMO14rHA and pMO14gHA in transplastomic lines. 20μg of protein extracted from leaves from wild type and two representative pMO14rHA and pMO14gHA lines using a two step extraction procedure were subjected to SDS-PAGE on a 10% gel, transferred to a nitrocellulose membrane and probed with anti-HA307-319 antibody. Western blot analysis detected a protein of approximately 48 kDa in all four representative lines tested. (A) Lanes 1-2: 14rHA-6 ISF and SF, lanes 3-4: 14rHA-8 ISF and SF, lanes 5-6: Wild type ISF and SF and lane +ive: pProExHA in *E. coli* (positive control). (B) Lanes 1-2: 14gHA-7 ISF and SF, lanes 3-4: 14gHA-8 ISF and SF, lanes 5-6: Wild type ISF and SF and lane +ive: pProExHA in *E. coli* (positive control).

3.3 Discussion

Previous studies in the lab have generated transplastomic lettuce and tobacco plants using flu virus *HA* gene constructs (Lelivelt *et al.*, 2005; Dr. Karen Shiel, unpublished data). However, although the HA transgenes were expressed at the mRNA level, no HA protein could be detected in any of the transplastomic lines generated. This suggested that the HA protein might be unstable when expressed in the plant plastid. The aim of this work was to generate a range of HA fusion gene constructs (pMO14rHA, pMO14gHA, pMOGFP/HA and pMOGFP/HA1) to assess if a protein fusion strategy might achieve stable HA or HA1 protein accumulation in tobacco plastids.

A high frequency of spectinomycin-resistant shoots were recovered for both of the 14aa N-terminal HA fusion constructs (pMO14rHA and pMO14gHA). Stably transformed transplastomic lines were also confirmed for both HA fusion constructs. However, a relatively low number of the putatively transformed shoots were eventually confirmed as true primary plastid transformants - four 14rHA and three 14gHA transplastomic shoots. PCR analysis confirmed that the *aadA* transgene had correctly integrated into the plastome in the majority of shoots tested (seven out of ten 14rHA and seven out of nine 14gHA). However, less that half of these putative transformed shoots contained the 14rHA / 14gHA transgenes. Neither of the full length GFP/HA or GFP/HA1 constructs generated any transplastomic lines containing the HA or HA1 transgenes. In the case of the pMOGFP/HA1 construct, only two of the seven plastid-transformed plant lines that were analysed contained the *aadA* gene but not the GFP/HA1

fusion gene at the plastid integration site suggesting that these lines may be the result of a secondary recombination event. No true plastid transformants were recovered using the pMOGFP/HA construct. Taken together, this data suggests that accumulation of HA or HA1 in plastids, even as fusion proteins, may be detrimental to plants and may be strongly selected against during the plant regeneration process. Influenza HA (H3 subtype) requires a form of lipid modification, palmitoylation, for viral assembly (Chen *et al.*, 2005) and studies have shown that lipid modifications can occur inside chloroplasts (Glenz *et al.*, 2006). HA palmitoylation is known to target the HA protein to membranes enriched with lipids (Melkonian *et al.*, 1999). The chloroplast envelope and the thylakoid membranes are composed primarily of glycolipids and galactolipids (Siegenthaler, 1998), so it is possible that the HA or HA1 protein could associate with these plastid membranes. Association of HA or HA1 with the thylakoid membranes could inhibit photosynthesis and be detrimental to regenerating plants. Lipidated proteins have been shown to insert into thylakoid membranes and the effects of such insertions have previously been observed in transgenic tobacco plants transformed with an outer surface protein A from *Borrelia burgdorferi* (OspA) (Henning *et al.*, 2007). Transplastomic plants were unable to grow autotrophically and required a supply of exogenous sugars due to the localisation of a high level of OspA protein to the thylakoid membranes which not only impaired photosynthetic electron transport but also the integrity of photosystem II (Henning *et al.*, 2007).

In both the 14rHA and 14gHA transplastomic lines a 48 kDa protein was detected using the anti-HA307-319 antibody but not the anti-HA91-108 antibody. These proteins are smaller than expected for the fusion protein (58 kDa). The 14rHA and 14gHA plastid-integrated expression cassettes were sequenced in selected lines, however no pre-mature stop codons were detected that could account for the smaller size of the fusion proteins detected. This suggests that the fusion proteins may be proteolytically cleaved during, or after, translation in the plastid and perhaps in this processed state the proteins are less harmful to plastid function. Proteolytic cleavage of the HIV-1 fusion inhibitor / cyanovirin-N (CV-N) fusion protein was reported in transgenic tobacco plants although the full length protein was also detected in this instance (Elghabi *et al.*, 2011).

However, we cannot completely rule out the possibility that these truncated proteins are the result of translational termination at a premature stop codon introduced at the RNA level. Some premature codons are introduced during transcription as a result of "polymerase stuttering" (Jacques & Kolakofsky, 1991). Plastid ribosomes are known to stutter at runs of U residues, switching to a different reading frame and then encountering stop codons, where they terminate. Polymerase stuttering involves the repeated copying of the same template base and is thought to be due to polymerase pausing, backtracking and realignment of the mRNA relative to the template within the polymerase active site (Hausmann *et al.*, 1999). The product is then a protein with the correct N-terminal sequence, but an incorrect C-terminus that depends on the reading

frame that was translated after the U-rich region. Since both fusion gene constructs are generating a protein of the same size, stuttering within the *HA* gene at a precise site would account for the detection of a truncated protein of the same molecular weight in all transgenic plant lines. We looked at the *HA* gene sequence and discovered a run of five U's starting at position 265 on the HA RNA transcript. It is therefore plausible that stuttering at this position could result in a frameshift leading to the introduction of a premature stop codon resulting in a protein of a smaller molecular weight than expected.

Both the truncated 14rHA and 14gHA fusion proteins accumulate in the insoluble protein fraction of total plant proteins and are not detected in the soluble protein fraction at all. This suggests that the proteins may be accumulating as insoluble protein aggregates. Such aggregates might be less likely to interfere with overall plastid function and might explain why these transgenic lines came through the selection process. Accumulation of the truncated fusion proteins as insoluble protein aggregates could also contribute to fusion protein stability within the plastid. The formation of protein aggregates has previously been observed in transgenic tobacco plants transformed with the cholera toxin of *Vibrio cholerae* (CTB) where it was suggested that the conformation of the aggregated chloroplast synthesised CTB allowed for a more stable accumulation of the protein in the plastid (Daniell *et al.,* 2001).

The14rHA transplastomic lines accumulate significantly more fusion protein in the insoluble fraction than the 14gHA lines. Significant differences in protein accumulation levels have been reported for the *Thermobifida fusca* endoglucanase CEL6A protein depending on the N-terminal fusion tag used Cel6A recombinant protein N-terminally fused to the first 14 amino acids of RBCL accumulated to a level of 4% TSP in tobacco plastids (Yu *et al.,* 2007). . In contrast, Cel6A recombinant protein N-terminally fused to the first 14 amino acids of GFP accumulated to significantly lower levels in tobacco plastids (0.3% TSP) (Gray *et al.,* 2009). Although the 14aaGFP fusion tag was used to increase EPSPS production in chloroplasts by 50-fold (>10% TSP; Ye *et al.,* 2001), other studies have reported relatively low accumulation levels of recombinant protein using this tag. The effect of fusion tags on recombinant protein accumulation levels in tobacco plants were compared using gene constructs coding for the first 14 amino acids of GFP, TetC and NPTII N-terminally fused to *T. fusca β*-glucosidase (BglC) (Gray *et al.,* 2011). In this study the GFP fusion tag resulted in the lowest level of BglC accumulation observed in transgenic lines, approximately 0.05% TSP compared to 1.6 – 2.6% TSP for the TetC and 8 – 12% TSP for the NPTII tags. Taken together, these results suggest that the choice of fusion tag can greatly affect recombinant protein accumulation in transplastomic plants. It is well known that N-terminal amino acids have a significant impact on levels of protein accumulation in the plastid (Ye *et al.,* 2001; Lenzi *et al.,* 2008). In the case of the HA fusion constructs used in this study the RBCL 14aa tag achieved a greater level of fusion-protein accumulation than the GFP 14aa tag.

The work presented here suggests that plastid-based expression of full length HA or HA1 is not feasible even in the context of a fusion protein. The most likely explanation for this is that these viral proteins inhibit plastid function – possibly by associating with the plastid membranes. However, the bottom line is that the tobacco plastid is not a useful system for producing full-length flu virus HA and HA1 proteins suitable for vaccine development. Transplastomic lines generated with the pMO14rHA and pMO14gHA constructs produced a protein smaller than expected that was detected with the anti-HA307-319 antibody but not the anti-HA91-108 antibody. Our working hypothesis is that this is a truncated HA fusion-protein that is accumulating in the plastid as protein aggregates. Mass spectroscopy / N-terminal sequencing analysis of these proteins is still required to confirm that the proteins are indeed truncated HA proteins. However, if this turns out to be the case, the fact that the protein can adopt a conformational structure that allows it to be recognised by at least one of the HA antibodies suggests that these plastid-based proteins, although not full length, might have some vaccine potential against flu virus.

Chapter 4
Transformation of tobacco with GFP/HA epitope fusion constructs

4 Transformation of tobacco with gfp/HA epitope fusion constructs

4.1 Introduction

Current approved vaccines fail to induce a broad level of protection to the different influenza strains mainly due to the frequent and unpredictable changes of the two surface glycoproteins: hemagglutinin and neuraminidase. One strategy which can overcome this problem is the use of epitope-based vaccines using conserved influenza epitope(s) responsible for protection against the virus (Ben-Yedidia *et al.*, 1998). Epitope based vaccines allow vaccination with a minimal structure, consisting of well defined antigens in order to stimulate an effective specific immune response while simultaneously avoiding potential hazardous effects (Ben-Yedidia, 1998). The use of synthetic epitopes in influenza based vaccines also offers practical advantages such as the ease of production of the vaccine (Adar *et al.*, 2009) as well as eliminating the need for yearly re-administration of the vaccine following the emergence of a new viral strain. A recent study has demonstrated that a peptide-based vaccine expressing six highly conserved influenza epitopes induced both humoral and cellular responses in mice and conferred some protection against a lethal challenge with the avian influenza strain H5N1 (Adar *et al.*, 2009) further illustrating the potential for use of epitopes in influenza vaccines.

Ideally, peptide-based vaccines should contain epitopes that are important for the induction of neutralizing antibodies (B-cell epitopes) and epitopes that will induce a protective T helper (Th) and CTL response (T-cell epitopes). B-cells play a huge role in the humoral immune response as their main function is in the production of antibodies against antigens and eventually developing into

memory B-cells after activation by antigen interaction. The influenza HA91-108 epitope has been identified as a dominant B-cell epitope. Mice immunised with this epitope expressed in a chimeric flagellin protein, have previously been shown to elicit anti-influenza neutralising antibodies. These antibodies reacted with the intact influenza virus of several H3 influenza strains to a comparable level (Arnon & Ben-Yedidia, 2003) as this epitope is known to be conserved among the different H3 strains of influenza (Laver *et al.*, 1980). Immunisation of mice with recombinant flagellin expressing three epitopes including the HA91-108 epitope as a single recombinant product has also demonstrated significant protection against sub-lethal viral challenge (Jeon *et al.*, 2002).

T-helper cells are essential for the activation of cytotoxic T cells which kill infected cells. The influenza HA307-319 epitope is a universal T helper epitope. HA307-319 is known to bind to an assortment of human leukocyte antigen-D related (HLA-DR) molecules which are found in antigen presenting cells and hence are readily presented to the immune system, eliciting an immune response. Previous work has shown the potential of a vaccine comprising the HA307-319 epitope in addition to three other conserved epitopes (NP 335-350, NP 380-393 and HA91-108) in protecting a human / mouse radiation chimera against the H3N2, H2H2, and H1N1 influenza strains (Ben-Yedidia *et al.*, 1998; Levi & Arnon, 1996) making it an obvious target for vaccine development.

Several viral epitopes have already been expressed in plant plastids. These include the 2L21 epitope of the VP2 protein from the canine parvovirus (CPV) (Molina *et al.*, 2004), a 25 amino acid epitope of the VP1 protein from the foot

and mouth disease virus (Lentz *et al.*, 2010), the hemagglutinin-neuraminidase-neutralizing epitope from the Newcastle disease virus (Sim *et al.*, 2009) and a multi-epitope diphtheria, pertussis and tetanus (DPT) fusion protein (Soria-Guerra *et al.*, 2009), all of which were expressed in the tobacco plastid. The expression of small molecules, such as epitopes, as independent products in transgenic plants, or in any transgenic system, can be problematic due to low stability and immunogenicity of the epitope alone.

To improve the yield of viral antigen proteins in the plastid, it is important to maximise the efficiency of gene expression and protein stability (Ortigosa *et al.*, 2010). Thus, the effectiveness of a peptide-based vaccine depends on stable expression and adequate presentation of the epitope to the immune system (Ben-Yedidia *et al.*, 1999). Previous studies have shown that fusion of epitopes to a number of different carrier proteins can stabilise the target peptide (Ortigosa *et al.*, 2010). To increase the accumulation levels of a highly immunogenic epitope from the structural protein VP1 of the foot and mouth disease virus, the epitope was expressed as a fusion protein with the β-glucuronidase reporter gene (*uidA*). This fusion resulted in recombinant protein expression levels of 51% TSP (Lentz *et al.*, 2010). Both the cholera toxin B subunit (CTB) and GFP have also been used as carrier proteins to express the 2L21 epitope from the VP2 capsid protein of the canine parvovirus in tobacco plastids with expression levels equivalent to 31.1% TSP and 22.6% TSP achieved respectively (Molina *et al.*, 2004). In addition, the 2L21 peptide has also been expressed in tobacco plants as a translational fusion to the 42 amino acid tetramerisation domain (TD) from the human transcription factor p53 (Ortigosa *et al.*, 2010). The B subunit of the

Escherichia coli heat labile enterotoxin was used as a fusion protein partner for a hemagglutinin-neuraminidase neutralizing epitope (Sim *et al.*, 2009) and resulted in recombinant LTB-HNE protein accumulation levels of approximately 0.5% TSP. In addition, *Salmonella* flagellin has also been used as a carrier partner for influenza epitopes (Ben-Yedidia *et al.*, 1998).

The aim of this work was to achieve stable accumulation of HA epitope fusion proteins in tobacco chloroplasts. A series of *gfp* gene and epitope constructs were designed. This series included four single epitope/gene constructs coding for the HA91-108 or the HA307-319 epitope N-terminally or C-terminally fused to GFP (HA91-108/GFP, GFP/HA91-108, HA307-319/GFP and GFP/HA307-319) and two double epitope gene constructs HA91-108/GFP/HA307-319 and HA307-319/GFP/HA91-108. These gene constructs were introduced into tobacco chloroplasts by biolistics-mediated transformation and transplastomic plant lines were assessed for HA epitope fusion protein accumulation and stability.

4.2 Results

A series of six gene constructs coding for two influenza hemagglutinin epitopes fused to GFP were designed and these constructs are illustrated in Figure 4.1. All six gene constructs were cloned into the transformation vector pMO16 (Oey *et al.,* 2009a) for insertion between the *trnG* and *trnfM* genes in the tobacco plastome.

4.2.1 HA epitopes

4.2.1.1 Cloning HA91-108/GFP into pCR2.1-TOPO

The HA91-108 epitope was N-terminally fused to the modified *gfp* gene (Section 3.2.5.1) using primer overlap extension in two steps (Figure 4.2). The first reaction used the primer pair HA91-108-F1 and GFP-XbaIR. HA91-108-F1 and was designed to fuse the first 33 nucleotides of the HA91-108 coding region to the 5' end of the *gfp* gene. A 756 bp PCR product was generated, cleaned using a Qiagen PCR clean-up kit and used as template DNA for second round PCR. The second PCR reaction used the primer pair HA91-108-F2 and GFP-XbaIR. The HA91-108-F2 primer fused the final 21 nucleotides of the HA91-108 epitope to the 5' end of the *gfp* gene while simultaneously adding an *NdeI* restriction site immediately upstream of the start codon. This reaction produced a 783 bp PCR product (Figure 4.3 A). The HA91-108/GFP fusion-gene was gel extracted, ligated into pCR2.1-TOPO and transformed into *E. coli* cells. Plasmid DNA was isolated from 10 colonies, digested with *NdeI* and *XbaI* and analysed by agarose gel electrophoresis on a 0.7% gel. All 10 plasmids generated the 3.9

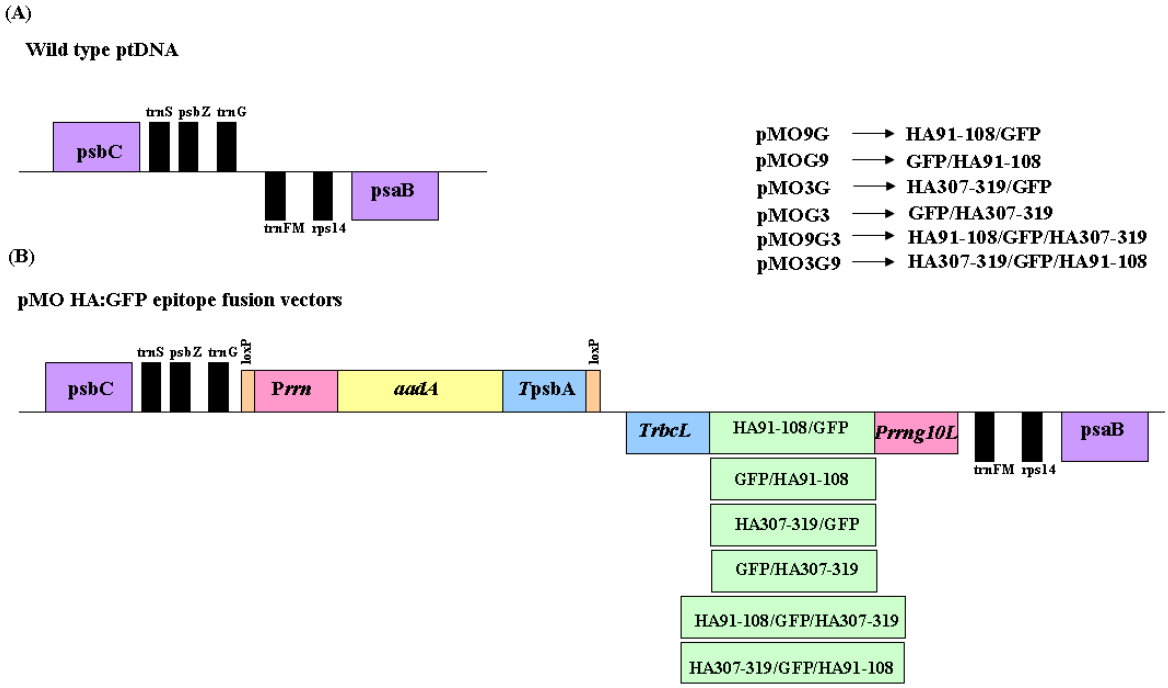

Figure 4.1: (A) Physical map (not to scale) of the targeted region on the tobacco plastid genome. (B) The targeted region showing the expected transgene insertions following plastid transformation with the various GFP/HA epitope fusion gene constructs and the selectable marker gene *aad*A. The transgenes are targeted to the intergenic region between *trnG* and *trnfM*.

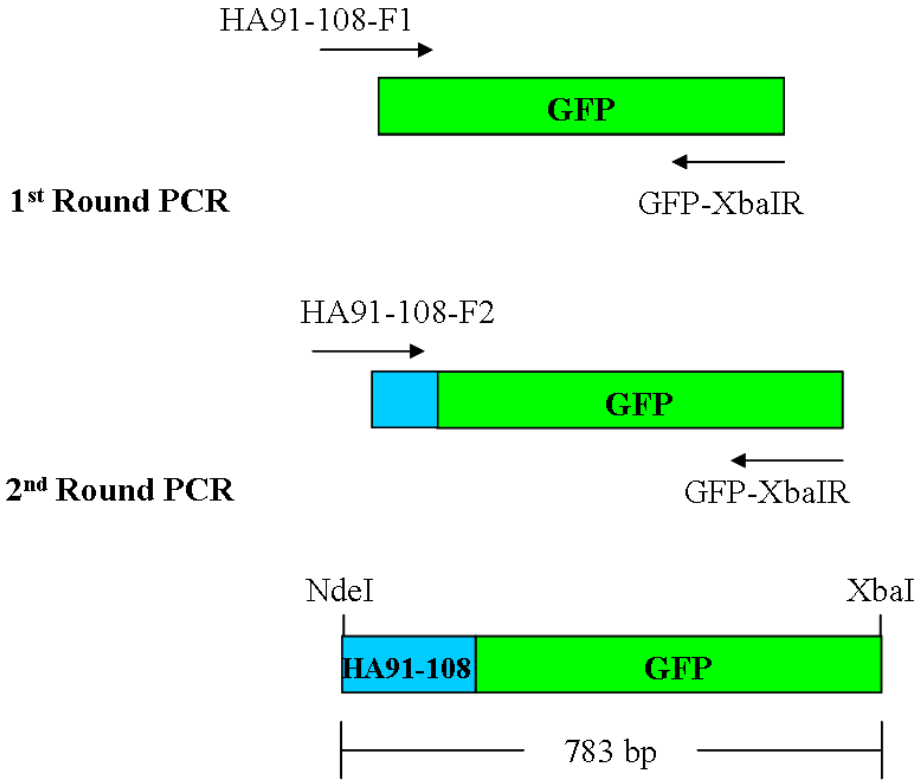

Figure 4.2: Schematic representation of the strategy used to generate the fusion gene coding for the HA91-108 epitope N-terminally fused to GFP by PCR overlap extension. First round PCR generated a PCR product using primer pair HA91-108-F1 and GFP-XbaIR. The first round PCR product was used as template and the primer pair HA91-108-F2 and GFP-XbaI generated the full length HA91-108/GFP fusion gene incorporating an *NdeI* and an *XbaI* site at the 5' and 3' ends respectively.

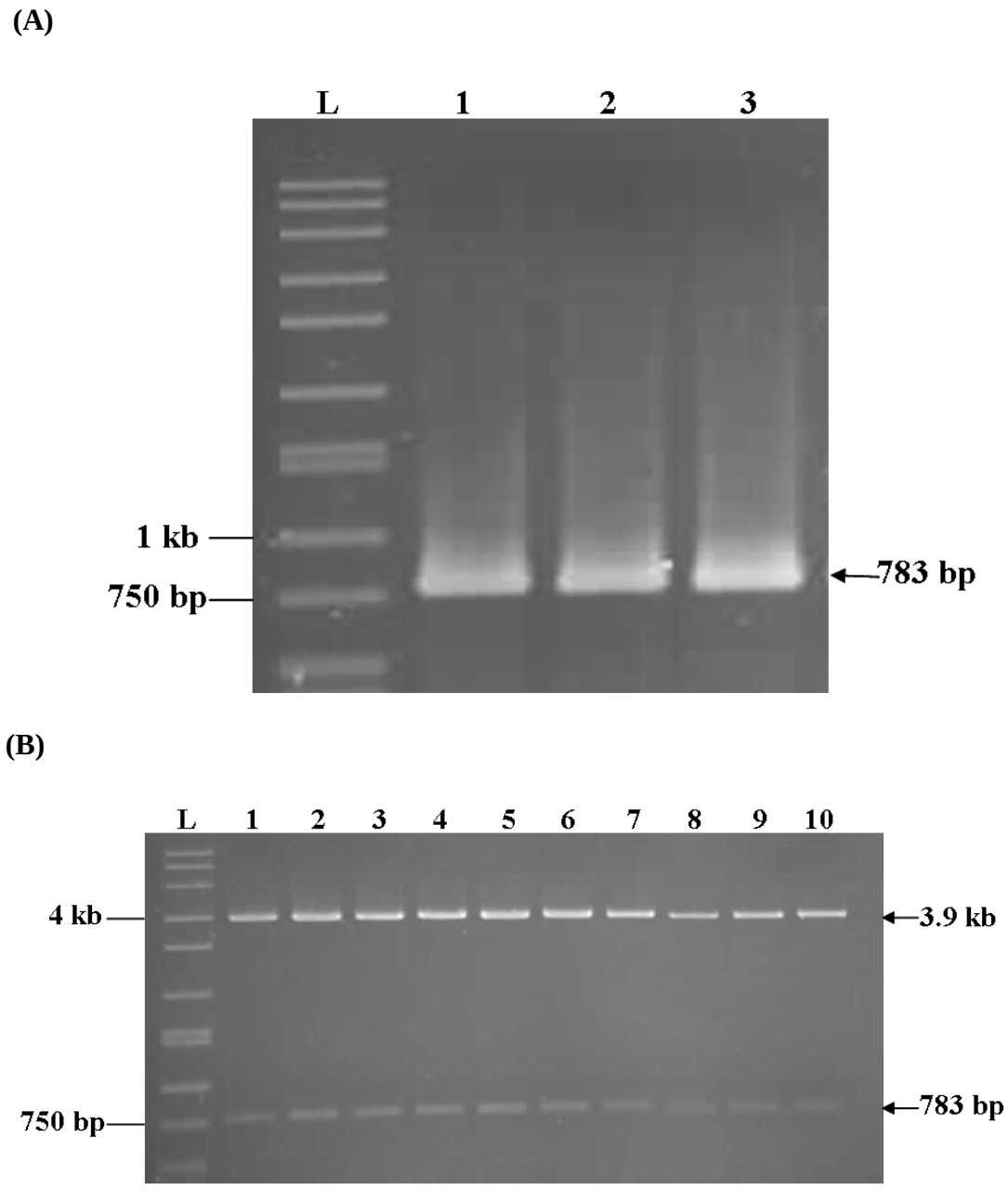

Figure 4.3 Analysis of the full length HA91-108/GFP fusion genes. (A) PCR products following second round PCR using the primers HA91-108-F2 and GFP-XbaIR. Lane L: 10 kb Ladder (Sigma). Lanes 1-3: products from three independent PCR reactions to generate a full length HA91-108/GFP fusion gene (783 bp). (B) Recombinant plasmids containing HA91-108/GFP in the vector pCR2.1-TOPO were digested with *NdeI* and *XbaI*. Restriction digests produced the 3.9 kb pCR2.1-TOPO vector backbone and the excised HA91-108/GFP insert at 783 bp. Lane L: 10 kb ladder (Sigma). Lanes 1-10: pCR-HA91-108/GFP plasmids.

kb vector backbone and the 783 bp HA91-108/GFP fragment (Figure **4.3** B). pCRHA91-108/GFP plasmids1, 2 and 3 were sequenced completely. All three plasmid inserts sequenced correctly and demonstrated that no errors had been introduced into the fusion-gene coding sequence during PCR amplification.

All five remaining GFP/HA epitope fusion genes, GFP/HA91-108, HA307-319/GFP, GFP/HA307-319, HA91-108/GFP/HA307-319 and HA307-319/GFP/HA91-108, were generated using the same overlap extension method described above using the primer combinations illustrated in Figure 4.4. All five fusion-genes contained an *NdeI* and *XbaI* restriction site at the 5' and 3' ends of the genes respectively to allow for further cloning. Gel images illustrating the various steps involved in generating these five fusion-genes can be found in Appendix A.

4.2.2 Generation of pMO-GFP/HA epitope gene constructs

The plastid transformation vector pMO16 was kindly provided by Prof. Ralph Bock. The GFP/HA epitope fusion genes could not be cloned directly into the *NdeI* and *XbaI* restriction sites in the pMO16 vector as the two sites were not unique. To get around this, the entire *plyGBS* expression cassette from pMO16 was sub-cloned into a pBluescript SK (+) vector. This allowed for replacement cloning of the GFP / HA epitope fusion genes into the expression cassette using *NdeI* and *XbaI* restriction sites before cloning them back into the pMO16 vector backbone to give the final plastid transformation vectors (Figure 4.5).

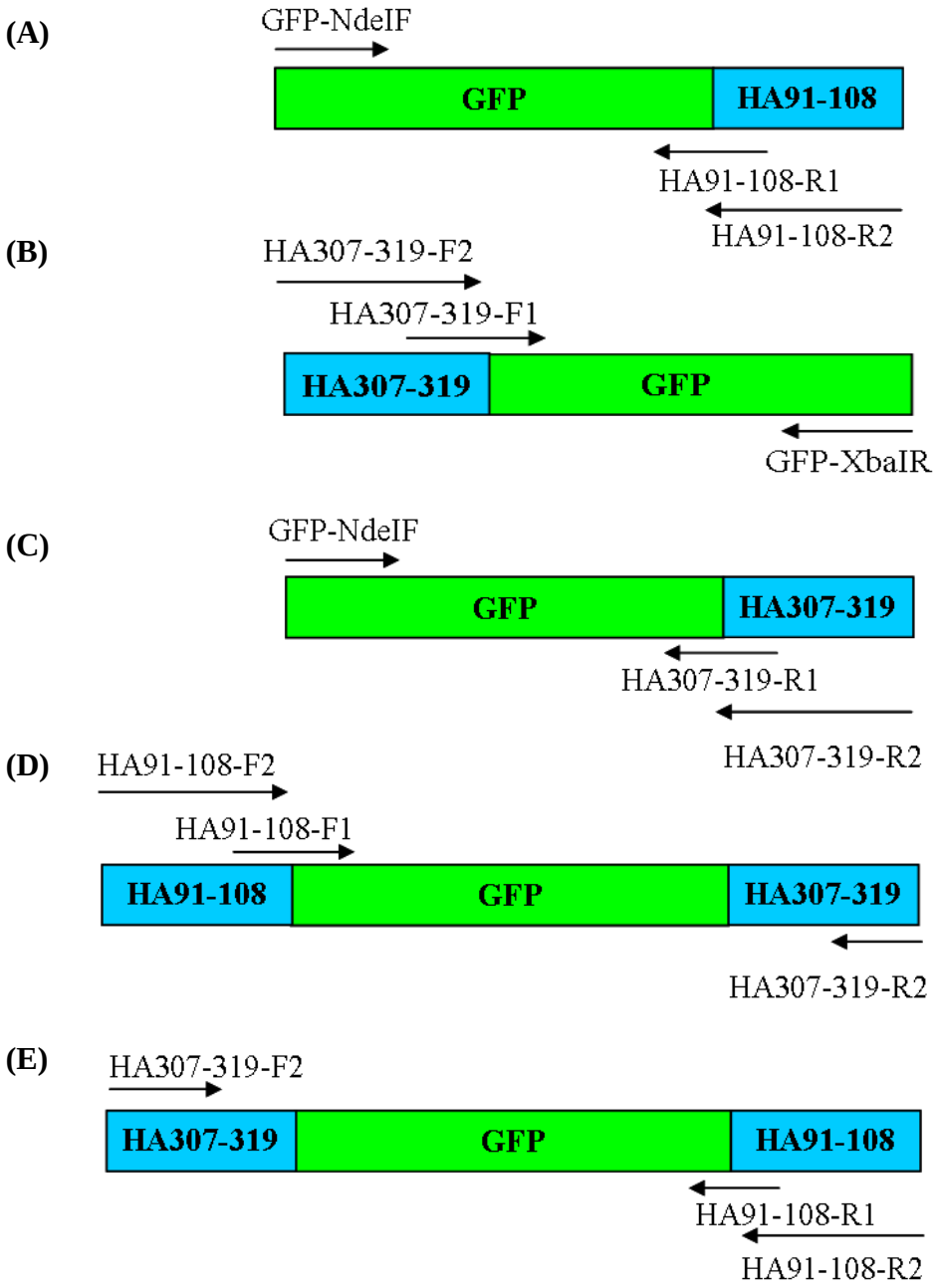

Figure 4.4: Schematic representation of primers using to generate the remaining five epitope fusion genes using primer overlap extension. (A) GFP/HA91-108, (B) HA307-319/GFP, (C) GFP/HA307-319, (D) HA91-108/GFP/HA307-319 and (E) HA307-319/GFP/HA91-108.

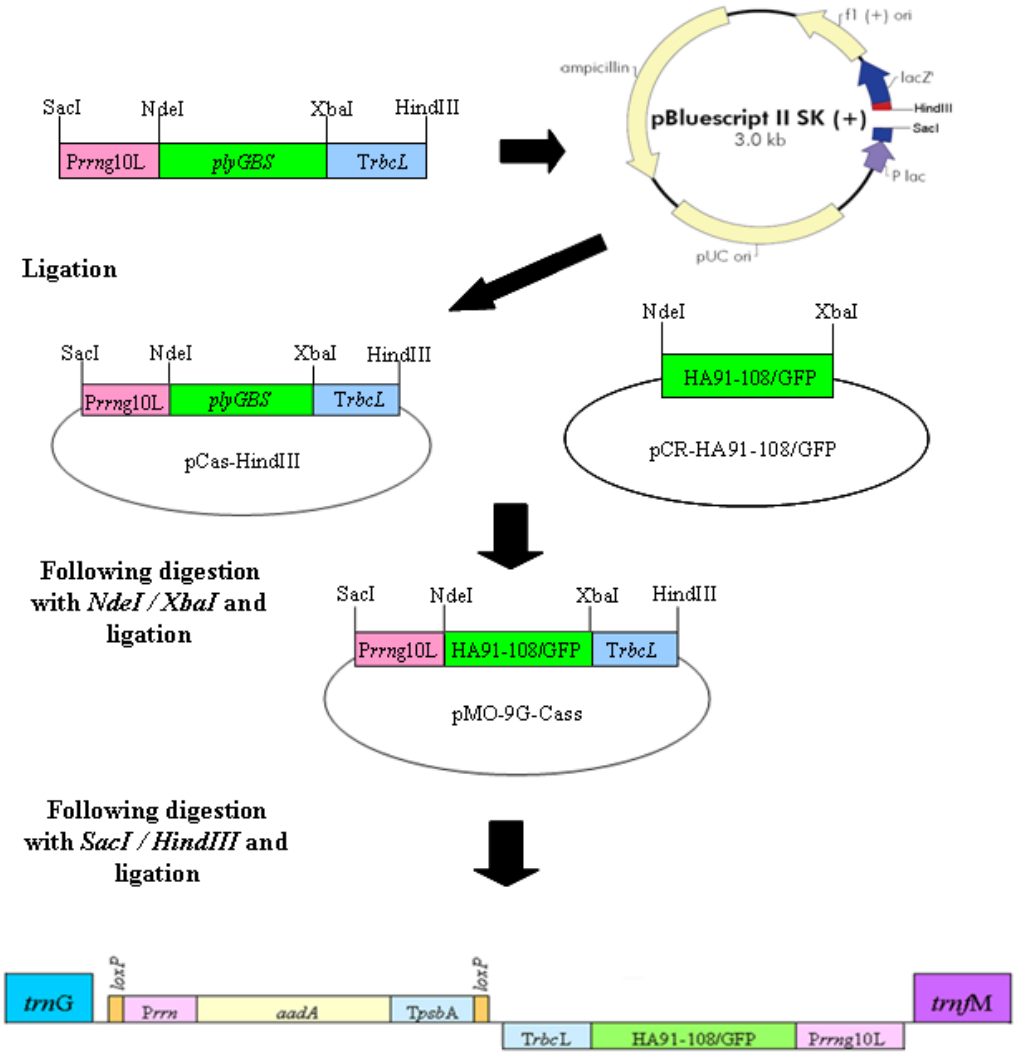

Figure 4.5: Schematic representation of the strategy used for cloning the HA91-108/GFP fusion gene into the pMO16 transformation vector. The *plyGBS* gene expression cassette was removed from the pMO16 transformation vector using *SacI* and *HindIII* digestion and was ligated into pBluescript SK (+) to produce pCas-HindIII. The *plyGBS* gene was replaced with the HA91-108/GFP fusion gene following restriction digestion of pCas-HindIII and pCR-HA91-108/GFP with *NdeI* and *XbaI*. The transgene cassette was ligated back into the pMO16 vector to give the pMO9G transformation vector.

All six epitope fusion genes, HA91-108/GFP, GFP/HA91-108, HA307-319/GFP, GFP/HA307-319, HA91-108/GFP/HA307-319 and HA307-319/GFP/HA91-108, were cloned into the pMO16 vector using this method to produce the pMO9G, pMOG9, pMO3G, pMOG3, pMO9G3 and pMO3G9 plastid transformation vectors respectively.

4.2.3 Assessing the functional integrity of the pMO GFP/HA epitope fusion constructs.

4.2.3.1 GFP/HA epitope expression in *E.coli*

All six recombinant GFP/HA epitope fusion-gene constructs were tested for expression in *E. coli* by western blot and GFP functional analyses. Total protein extracts from recombinant bacterial cultures were separated by SDS-PAGE on a 12% gel, transferred to nitrocellulose membrane and incubated with either a HA91-108 or a HA307-319 specific antibody (kindly supplied by Tamar Ben-Yedidia, The Weizmann Institute of Science, Israel). A protein of the expected size of 29 kDa was detected in the pMO9G, pMOG9, pMO3G and pMOG3 single epitope recombinants. A protein at the expected size of 31 kDa was also detected in the pMO9G3 and pMO3G9 double epitope recombinants. This confirmed that both the HA91-108 and HA307-319 epitopes were being expressed and that the antibodies were capable of detecting the epitopes. A representational western blot is shown in Figure 4.6 A.

E. coli cells containing the various pMO GFP/HA epitope transformation vectors were streaked onto plates containing spectinomycin (500 mg/L) and

(A)

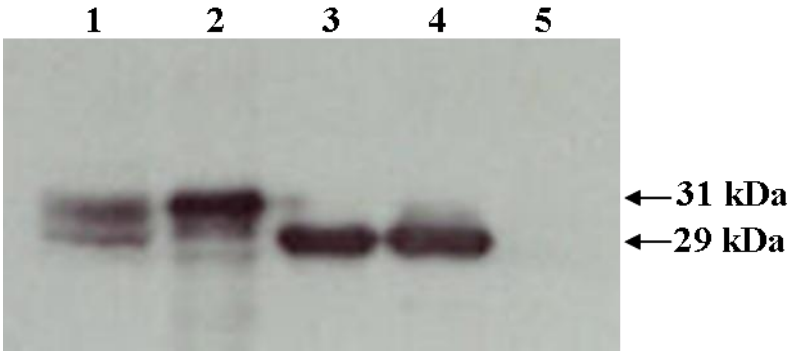

(B)

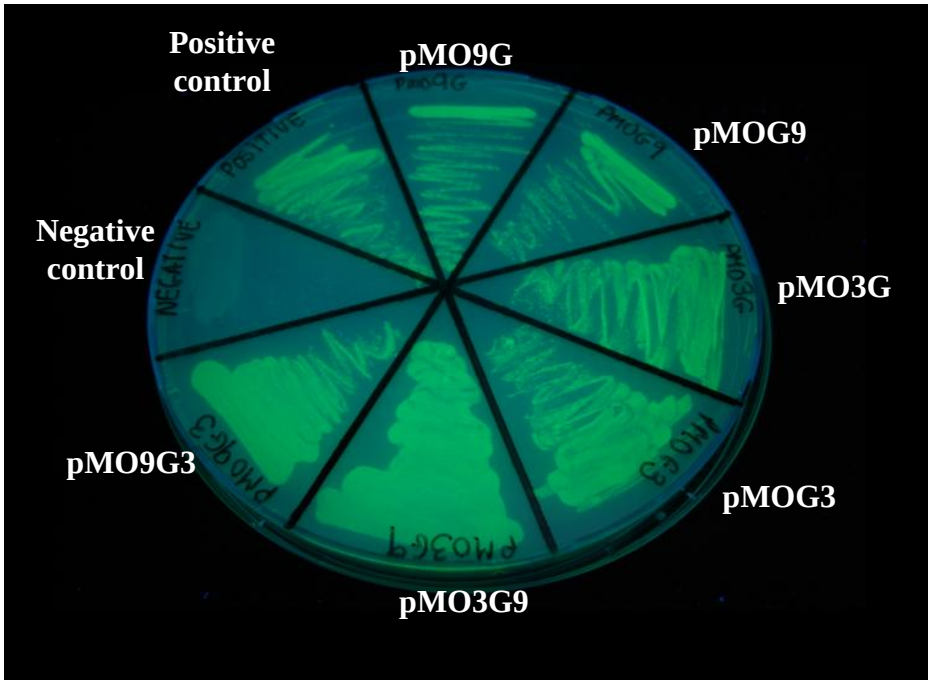

Figure 4.6: Western blot analysis of pMO GFP/HA epitope fusion gene constructs in *E. coli* and functional analysis (A) Western blot analysis of total protein isolated from *E. coli* cells transformed with four transformation constructs containing the HA307-319 epitope. The HA307-319 antibody detected the pMO9G3 and pMO3G9 protein at 31 kDa and the pMO3G and pMOG3 protein at 29 kDa as expected. Lane 1: pMO9G3, lane 2: pMO3G9, lane 3: pMO3G, lane 4: pMOG3 and lane 5: pZS-UreB (Negative Control) (B) All six pMO GFP/HA epitope fusion constructs were streaked onto a LB agar plate containing 500 mg/L spectinomycin. MSK18 and pZSUreB were streaked as positive and negative controls respectively. The plate was placed under UV light to check expression of genes. Bacteria from all six constructs grew in the presence of spectinomycin and fluoresced indicating that both the *aadA* gene and the GFP/HA epitope fusion genes were expressed.

grown overnight at 37^0C. The bacteria grew in the presence of the antibiotic indicating that the *aadA* gene was being expressed. The plates were placed under UV light to assess GFP expression. Recombinant bacteria containing all six GFP/ HA epitope constructs fluoresced confirming that the GFP/HA epitope fusion protein was accumulating in these cells (Figure 4.6 B).

4.2.4 Tobacco chloroplast transformation with the GFP/HA epitope fusion constructs

Large scale DNA preparations of the pMO9G, pMOG9, pMO3G, pMOG3, pMO9G3 and pMO3G9 plasmids were prepared for plastid transformation. Transforming DNA was introduced into tobacco leaf chloroplasts on the surface of gold particles using the Bio-Rad PDS-1000/ He gun (outlined in Section 2.9.5). Following bombardment, leaves were cut into 10 mm^2 pieces and placed on RMOP medium containing 500 mg/L spectinomycin. The first spectinomycin resistant shoots were visible after three to four weeks. Spectinomycin resistant shoots were subsequently transferred to MS medium containing 500 mg/L spectinomycin for root formation.

4.2.5 Molecular characterisation of primary transformants

Total DNA was extracted from regenerated shoots and was subjected to PCR analysis using a combination of both gene specific internal primers (aadA-Rev, GFP-XbaIR, HA91-108-F2 and HA307-319-R2) and external primers (Ext-For and Ext-Rev) that flanked the vector integration site. These primer combinations allowed for the identification of chloroplast transformants only.

4.2.5.1 Characterisation of GFP/HA epitope regenerated lines

DNA was isolated from ten spectinomycin resistant shoots and analysed by PCR to determine if the 9G gene construct had integrated into the plastome at the expected vector integration site. The first PCR used the primer pair Ext-For / aadA-Rev which anneal upstream of the vector integration site and within the *aadA* gene respectively. This PCR amplified a 1.7 kb PCR product of the expected size in nine out of ten primary regenerated shoots (Figure 4.7 A and data not shown). The second PCR used the primers GFP-XbaIR / Ext-Rev which anneal to the 9G gene and downstream of the vector integration site respectively. This reaction produced a 2.9 kb PCR product of the expected size in seven of the nine primary regenerated shoots tested indicating that targeted integration had been achieved (Figure 4.7 B). No PCR product was amplified from WT DNA.

The same combination of primers (Ext-For / aadA-Rev; Ext-Rev / a gene specific primer) as described above, were used to test for the targeted integration of the remaining five GFP HA gene constructs. Four out of six G9 putative transformants, six out of eight 3G putative transformants, eight out of ten G3 putative transformants and five out of nine 3G9 putative transformants generated products of the expected size with both primer sets. No transplastomic lines were generated using the 9G3 gene construct (data not shown). Five of the seven plastid transformed plant lines that were analysed contained the *aadA* gene but not the HA91-108/GFP/HA307-319 fusion gene at the plastid integration site. The remaining six plant lines (9G3-3, 9G3-8, 9G3-9, 9G3-10, 9G3-12 and 9G3-13) that were recovered displayed a severe stunted growth

(A)

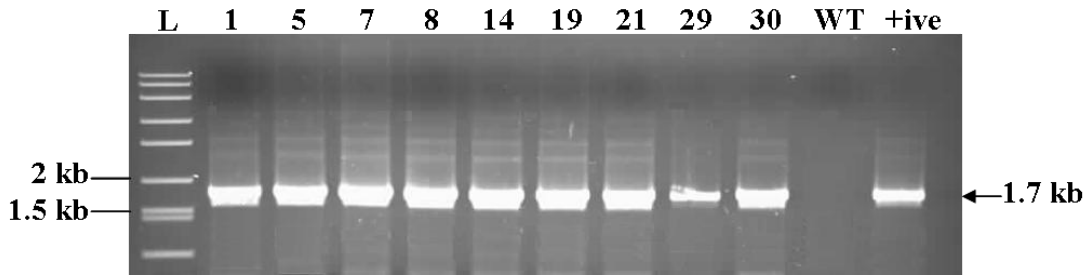

(B)

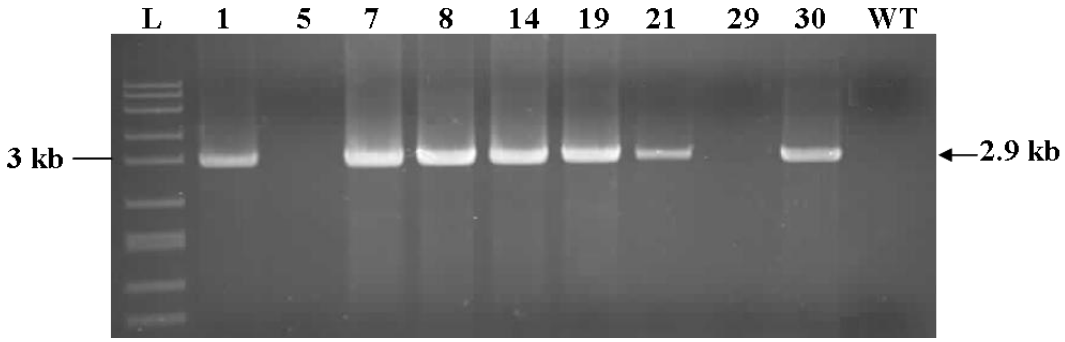

Figure 4.7: PCR analysis of putative pMO9G plants. (A) Primers Ext-For, specific to the chloroplast genome and aadA-Rev, specific to the *aadA* gene were used to confirm the integration of HA91-108/GFP into the tobacco chloroplast genome. The expected product size of 1.7 kb was amplified in all 9 plants. Lane L: 10 kb ladder (Sigma). Lanes 1-9: 9G-1, 9G-5, 9G-7, 9G-8, 9G-14, 9G-19, 9G-21, 9G-29, 9G-30. Lane WT: Wild type Petite Havana (negative control). Lane Pos: 3G-2 (positive control) (B) Primers GFP-NdeIF, specific to the *GFP* gene and Ext-Rev, specific to the chloroplast genome were used to confirm the integration of HA91-108/GFP into the tobacco chloroplast genome. The expected product size of 2.9 kb was amplified in all 9 plants. Lane L: 10 kb ladder (Sigma). Lanes 1-9: 9G-1, 9G-5, 9G-7, 9G-8, 9G-14, 9G-19, 9G-21, 9G-29, 9G-30. Lane WT: Wild type Petite Havana (negative control).

phenotype and could not be analysed. All confirmatory PCR gels can be found in Appendix A

Following PCR, leaves from confirmed transformants were subjected to three rounds of regeneration on RMOP medium containing 500 mg/L spectinomycin to achieve homoplasmy. Table 4.1 provides the transplastomic line numbers generated with the five GFP/HA epitope gene constructs.

4.2.6 Summary of biolistic transformation results

Table 4.2 provides a summary of biolistic experiments carried out and the resulting transformed lines obtained using the six GFP HA epitope gene constructs.

4.2.7 Southern blot analysis of transplastomic plants

Lines transformed with the pMO9G, pMOG9, pMO3G, pMOG3 and pMO3G9 constructs were assessed for homoplasmy by Southern blot hybridisation. Total DNA was isolated from wild type tobacco and PCR confirmed T_0 transformed lines, digested with *BamHI*, Southern blotted and probed with a DIG labelled *psaB* probe. This probe is expected to hybridise to a 4.5 kb *BamHI* fragment in wild type tobacco DNA and to a 7.1 kb *BamHI* fragment in pMO9G, pMOG9, pMO3G and pMOG3 transformed plants and to a 7.3 kb *BamHI* fragment in pMO3G9 transformed lines (Figure 4.8).

Table 4.1: Transplastomic plant line names

Transformation Vector	Gene of Interest	Transplastomic Plant Line Numbers
pMO9G	HA91-108/GFP	9G-1, 9G-7, 9G-8, 9G-14, 9G-19, 9G-21, 9G-30
pMOG9	GFP/HA91-108	G9-1, G9-2, G9-3, G9-4
pMO3G	HA307-319/GFP	3G-1, 3G-2, 3G-7, 3G-14, 3G-25, 3G-28
pMOG3	GFP/HA307-318	G3-1, G3-3, G3-11, G3-14, G3-15, G3-17, G3-30, G3-32
pMO3G9	HA307-319/GFP/HA91-108	3G9-5, 3G9-9, 3G9-12, 3G9-14, 3G9-15

Table 4.2: Summary of biolistic results and transplastomic plants obtained

Constructs	Number of shots	Number of shoots recovered	Number of shoots analysed by PCR	PCR confirmed *aadA* presence	PCR confirmed left border region[A]	PCR confirmed right border region[B]	Confirmed primary transformation events
pMO9G	20	25	10	9	9	7	7
pMOG9	20	18	6	4	4	4	4
pMO3G	20	35	8	8	7	6	6
pMOG3	20	20	10	9	9	8	8
pMO3G9	20	24	10	9	8	5	5
pMO9G3	20	13	7	5	4	0	0

[A] Primers Ext-For and aadA-Rev were designed to amplify *aadA, trnG* and part of the *psbZ* gene

[B] A gene specific primer and Ext-Rev were designed to amplify the GOI, *trnfM, rps14* and part of the *psaB* gene

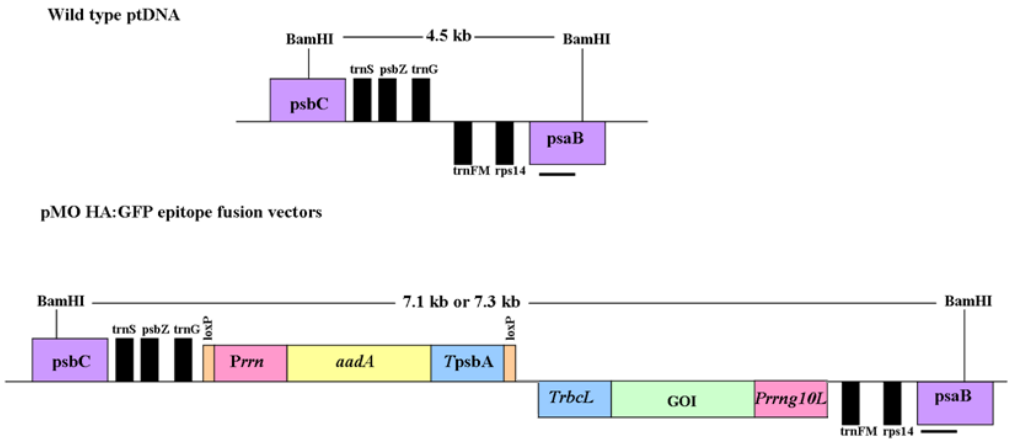

Figure 4.8: Map of the targeted region in the WT plastid genome and the expected region in transplastomic GFP/HA epitope lines generated (not drawn to scale). Relevant restriction sites used for Southern blot analysis of transplastomic lines are marked. The location of the *psaB* probe is shown as a black bar. This probe hybridises to a 4.5 kb fragment in wild type plants and is expected to hybridise to a 7.1 kb fragment in pMO9G, pMOG9, pMO3G, pMOG3 and a 7.3 kb fragment in pMO3G9 transplastomic lines.

The Southern blots confirmed that all eight lines transformed with pMOG3 had achieved homoplasmy (Figure 4.10 B). Although many of the transgenic plant lines transformed with the pMO9G, pMOG9, pMO3G and pMO3G9 gene constructs had achieved homoplasmy (Figure 4.9 A: lanes 1-5 & 7; Figure 4.9 B: lanes 1-3; Figure 4.10 A: lanes 1-3, 5 & 6; Figure 4.11: lanes 1, 3 & 5), a number of lines (for all four constructs) showed the *psa*B probe hybridizing to a smaller than expected *BamHI* restriction fragment (4.5 kb) (Figure 4.9 A: lane 6; Figure 4.9 B: lane 4; Figure 4.10 A: lane 4; Figure 4.11: lanes 2 & 5). This suggested that a recombination event secondary to the intended primary event may have occurred in these lines. These secondary recombination events are explored further in Chapter 5.

4.2.8 Analysis of T1 generation plants

4.2.8.1 Seedling analysis

All homoplasmic pMO9G, pMOG9, pMO3G, pMOG3 and pMO3G9 transformants were transferred to growth chambers and grown to flowering in soil. Plants were allowed to self pollinate and the seeds were collected. Seeds from wild type tobacco and transgenic lines were germinated on media containing 500 mg/L spectinomycin. 100% of seedlings from all five transformed lines displayed the same spectinomycin-resistant phenotype. Representative samples of wild type and transgenic seedlings on media containing 500 mg/L spectinomycin are shown in Figure 4.12. Reciprocal genetic crosses were carried out between wild type and T_1 transformed plants. 100% of the seedlings obtained following pollination of transplastomic flowers

(A)

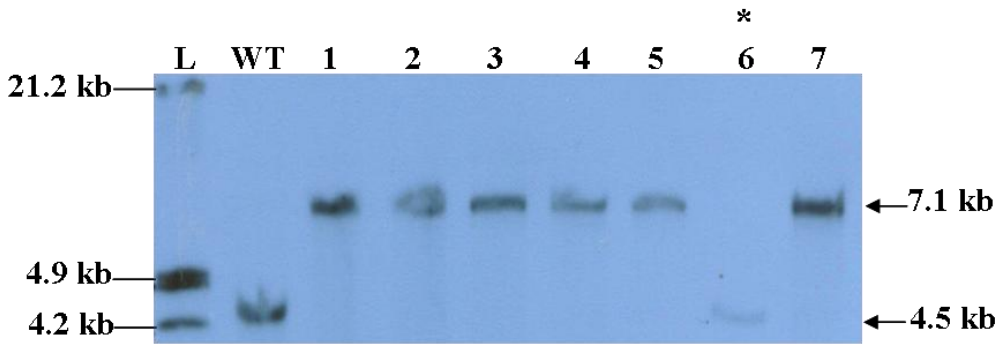

(B)

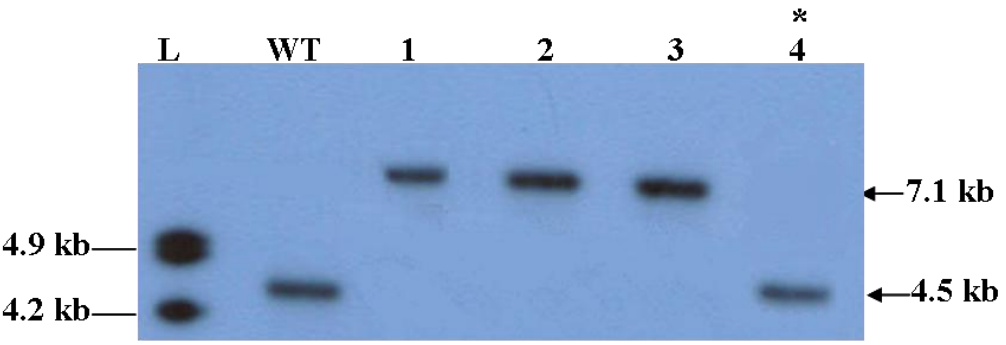

Figure 4.9: Southern blot analysis of T_0 generation pMO9G and pMOG9 transformed plant lines. Total DNA from pMO9G and pMOG9 transformed plants was digested with *BamHI* southern blotted and hybridised with a DIG-labelled *psaB* probe. (A) The probe hybridized to a fragment of the expected size (7.1 kb) in most of the pMO3G lines (Lanes 1-5 and lane 7) except for line 9G-21 which gave a wild-type hybridisation pattern (4.5 kb band, lane 6 indicated by asterix). Lane L: DIG labelled Marker weight III (Roche). Lane WT: Wild type tobacco DNA. Lanes 1-7: 9G-1, 9G-7, 9G-8, 9G-14, 9G-19, 9G-21, 9G-30 (B) Three of the pMOG9 transgenic lines gave the expected hybridisation pattern (7.1 kb band, lanes 1-3). One line gave a wild-type hybridisation pattern (4.5 kb band, lane 4 indicated by an asterix). Lane L: DIG labelled Marker weight III (Roche). Lane WT: Wild type tobacco DNA. Lanes 1-4: G9-1, G9-2, G9-3, G9-4.

(A)

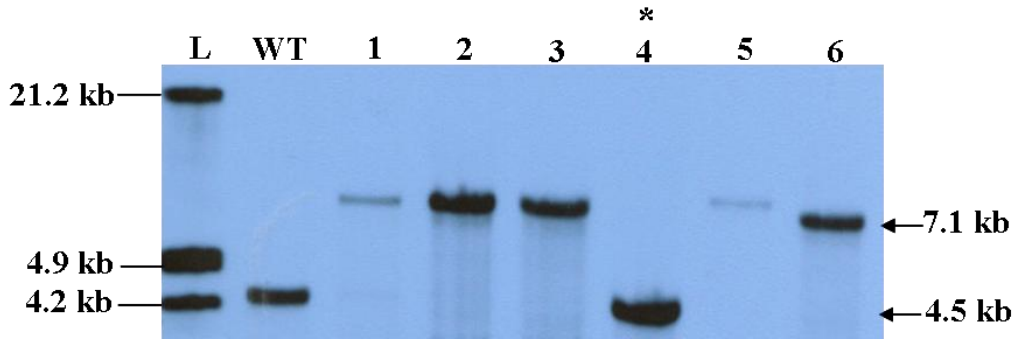

(B)

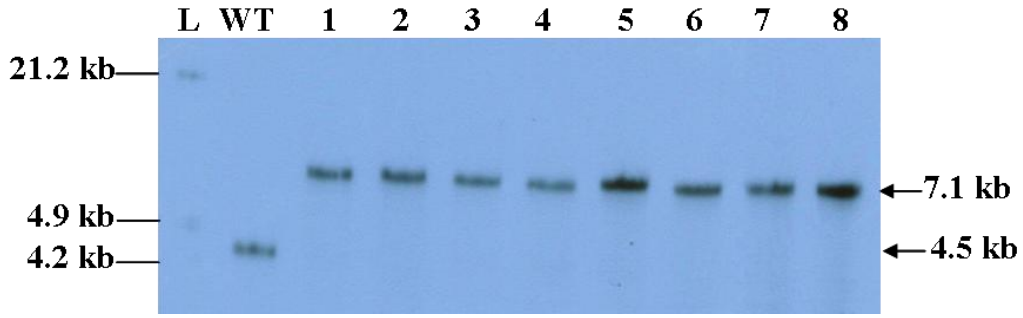

Figure 4.10: Southern blot analysis of T_0 generation pMO3G and pMOG3 transformed plant lines. Total DNA from pMO3G and pMOG3 transformed plants was digested with *BamHI* southern blotted and hybridised with a DIG-labelled *psaB* PROBE. (A) Five of the six pMO3G transformed lines hybridized to a fragment of the expected size (7.1 kb, lanes 1-3, 5 and 6). One line gave a wild-type hybridisation pattern (4.5 kb band, Lane 4 indicated by an asterix) Lane L: DIG labelled Marker weight III (Roche). Lane WT: Wild type tobacco DNA. Lanes 1-6: 3G-1, 3G-2, 3G-7, 3G-14, 3G-25 and 3G-28 (B) All eight of the pMOG3 transgenic lines gave the expected hybridisation pattern (7.1 kb band, lanes 1-8). Lane L: DIG labelled Marker weight III (Roche). Lane WT: Wild type tobacco DNA. Lanes 1-8: G3-1, G3-3, G3-11, G3-14, G3-15, G3-17, G3-30, G3-32.

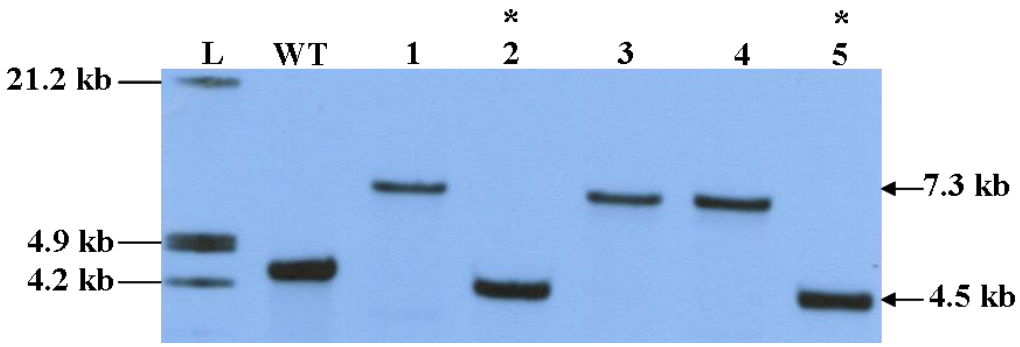

Figure 4.11: Southern blot analysis of T_0 generation pMO3G9 transformed plants. Total DNA from pMO3G9 transformed plants was digested with *BamHI* southern blotted and hybridised with a DIG-labelled *psaB* probe. Three pMO3G9 lines hybridized to a fragment of the expected size (7.1 kb, lanes 1, 3, and 4). Two lines gave a wild-type hybridisation pattern (4.5 kb band, lanes 2 and 5) indicated by an asterix). Lane L: DIG labelled marker weight III (Roche). Lane WT: Wild type tobacco DNA. Lanes 1-5: 3G9-5, 3G9-9, 3G9-12, 3G9-14 and 3G9-15.

(A)

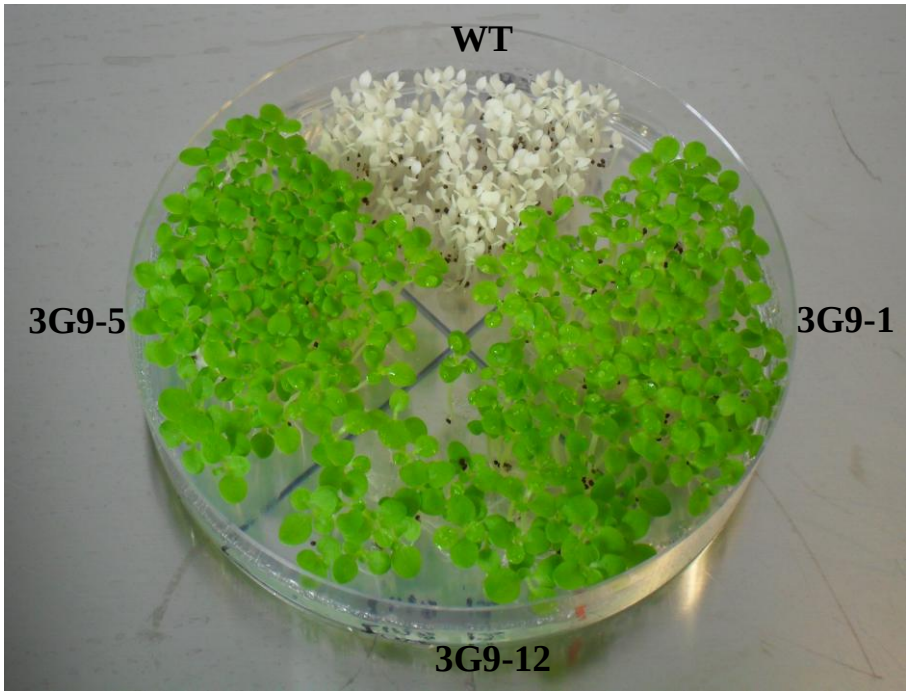

(B)

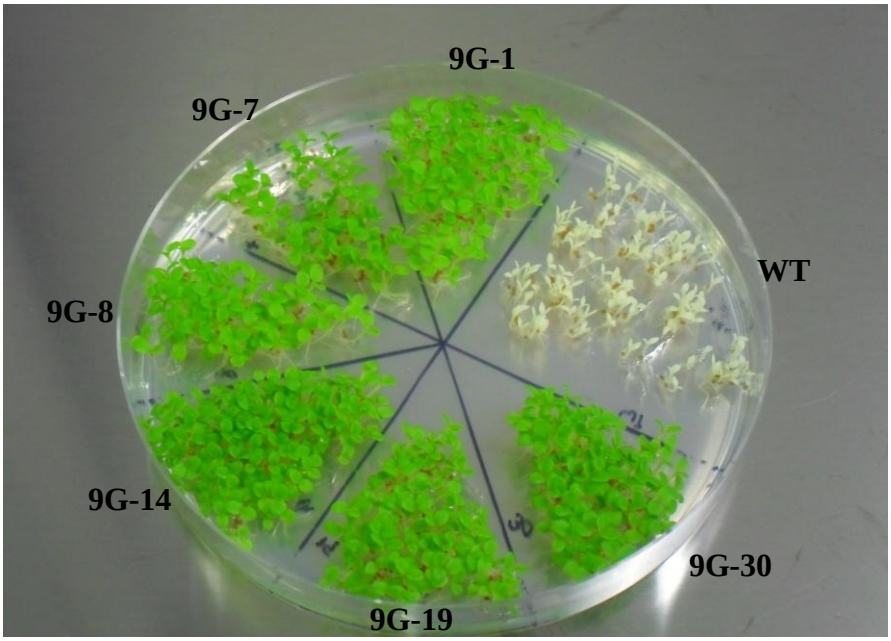

Figure 4.12: Spectinomycin resistance in T_0 seedlings. Seeds resulting from self pollination of transgenic T_0 lines were germinated on medium containing 500 mg/L spectinomycin. 100% of seedlings from the transformed lines produced green cotyledons under selection while wild-type control seedlings bleached white. Uniform resistance to spectinomycin in the self pollinated progeny confirms that the homoplasmy has been achieved in these lines.

with wild type pollen were uniformly resistant to spectinomycin. In contrast, the seedlings obtained from crosses between wild type flowers and transgenic pollen were sensitive to spectinomycin and bleached white. These crosses confirmed maternal inheritance of the transgenes. Figure 4.13 shows seedlings derived from crosses between wild type and pMO9G plants and wild type and pMOG3 plants grown under selection.

4.2.8.2 Analysis of GFP expression by confocal microscopy

Since GFP functions as a visible marker, this allowed all transgenic lines to be visually screened for GFP expression using confocal microscopy. Leaves from T_0 round 1 (R1) plant lines were cut into 4 cm X 4 cm sections and screened for GFP fluorescence using the GFP excitation filter. GFP expression was initially observed in all PCR-confirmed plastid transformed plant lines obtained with each of the five constructs (pMO9G, pMOG9, pMO3G, pMOG3 and pMO3G9). An example of GFP expression in plants transformed with pMOG3 is shown in Figure 4.14.

4.2.9 GFP/HA epitope expression analysis

Western blot analysis was performed on all PCR- and fluorescence-confirmed transgenic plant lines with either an anti-HA91-108 or anti-HA307-319 antibody. Western blot analysis showed GFP-epitope protein in all transgenic plant lines transformed with the pMO9G and pMOG3 gene constructs (Section 4.2.9.1).

(A)

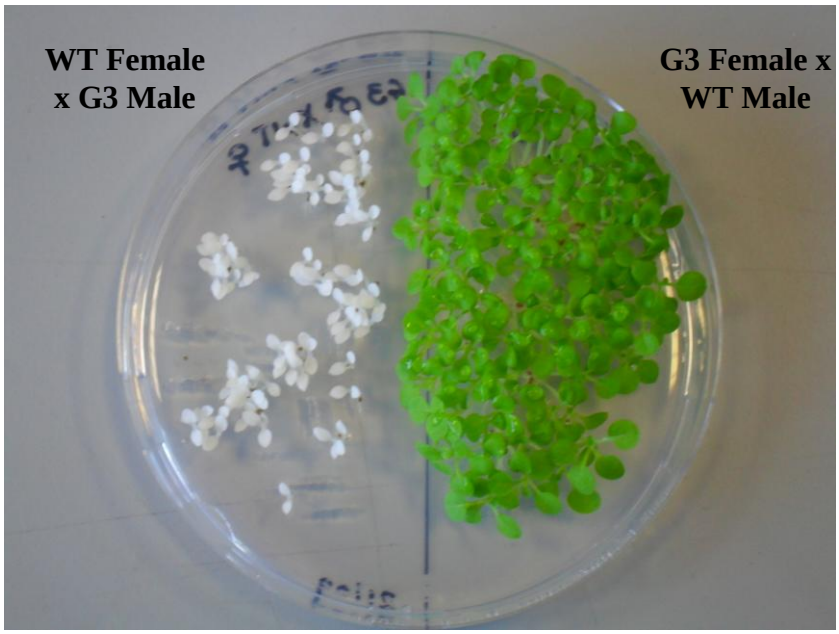

(B)

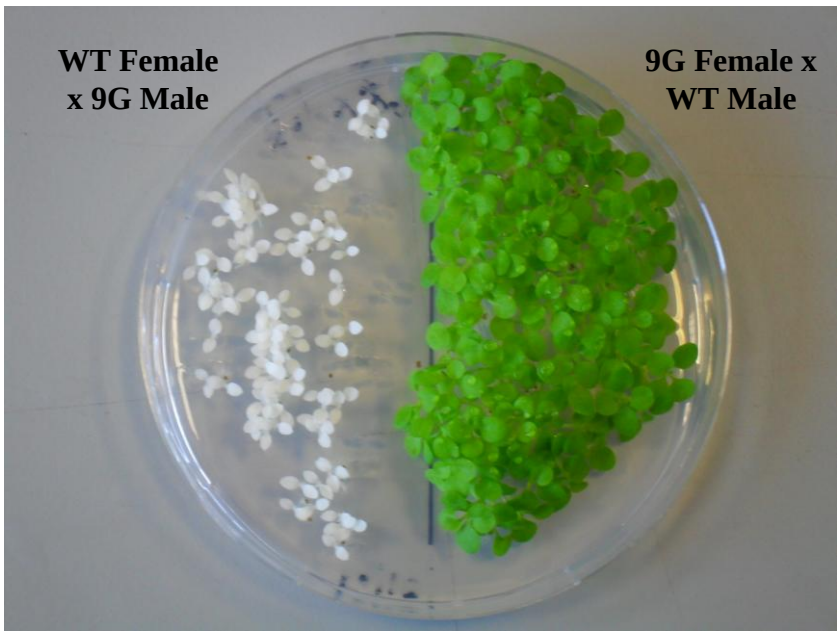

Figure 4.13: Maternal inheritance of spectinomycin resistance in transgenic plant lines. Seeds were germinated on medium containing 500 mg/L spectinomycin. (A) Seedlings resulting from reciprocal crosses between wild type and pMOG3 line. Left hand side of the plate: WT female x G3 male. Right hand side of the plate: G3 female x WT male (B) Seedlings resulting from reciprocal crosses between wild type and pMO9G line. Left hand side of the plate: WT female x 9G male. Right hand side of the plate: 9G female x WT male. Only seedlings that derived their plastids from a female transformed plant produce green cotyledons under selection**.**

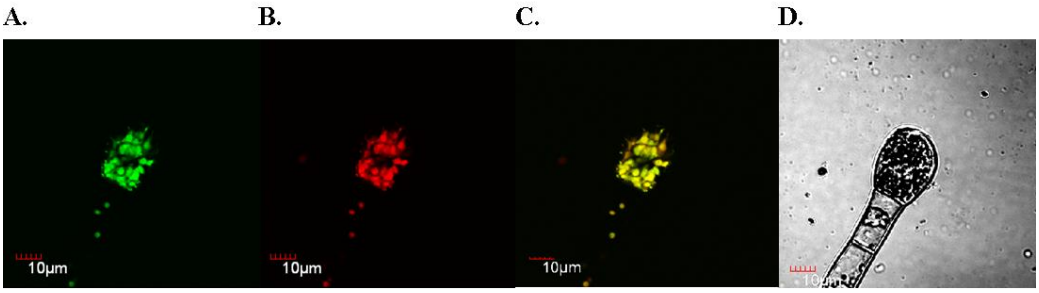

Figure 4.14: Confocal microscope image of plastid-localized GFP in tricome cells of transgenic tobacco line G3-32 transformed with construct GFP/HA307-319 (G3). (A) Chloroplast localized GFP fluorescence (B) Autofluorescence of chloroplasts (C) Chloroplast localized GFP fluorescence superimposed on chloroplast autofluorescence (D) Tricome cells photographed under bright field.

However, no GFP expression was detected in any of the pMOG9, pMO3G and pMO3G9 transformed plant lines (discussed in section 4.2.10).

4.2.9.1 Analysis of GFP-HA epitope protein localisation in pMO9G and pMOG3 transformed plants

Total soluble protein was extracted from one 9G (9G-4) and one G3 (G3-2) T_1 plant line using a mild protein extraction buffer. The proteins was separated on a 12% SDS gel and transferred to nitrocellulose membrane. Blots incubated with an anti-GFP antibody detected protein at the expected size of 29 kDa in the 9G line. However, only minute amounts of protein were detected in the G3 line even though confocal microscopy indicated significant GFP expression. This suggested that the GFP/HA epitope protein may not be localized in the soluble protein fraction in this line. Protein extractions were repeated for the same plant lines using a two-step extraction method. As before, a mild triton based extraction buffer was initially used to extract total soluble protein (SF). This was followed by a more stringent SDS-based extraction procedure to extract insoluble protein (ISF) from the pellet. Protein was also extracted from a plant line expressing GFP alone using the same extraction methods. 5 μg of protein was run on a 12% SDS-PAGE gel, transferred to nitrocellulose and incubated with an anti-GFP antibody.

Following detection, a protein of the expected size (29 kDa) was seen in the SF of the GFP expressing line (Figure 4.15 lane 1). Although a considerable amount of GFP-HA epitope protein was detected in the SF of the 9G transgenic

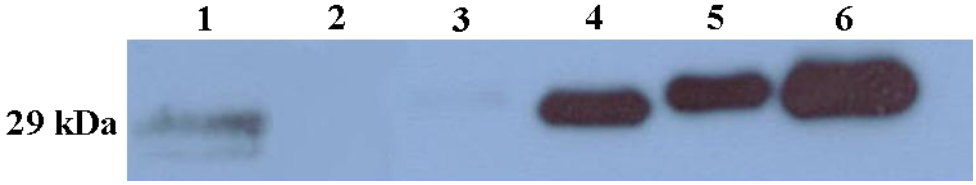

Figure 4.15: GFP-HA epitope protein localisation in pMO9G and pMOG3 transformed plants. Total soluble (SF) and insoluble protein (ISF) was extracted from one 9G (9G-4) and one G3 (G3-2) T_1 plant lines. Proteins were separated by SDS-PAGE, western blotted and probed with an anti-GFP antibody. Lane 1 - GFP-SF, lane 2 -GFP-ISF; lane 3- G3-SF, lane 4 - G3-ISF; lane 5 - 9G-SF and lane 6 - 9G-ISF.

line (lane 5) considerably more GFP/HA epitope protein was detected in the ISF (lane 6). In the G3 line practically all of the GFP/HA epitope protein was found in the ISF (lane 4). These data indicate that both of the HA epitopes affect GFP solubility in the plastid. However, whether it is the nature of the individual epitopes or the relative positions of the epitopes (N-terminal or C- terminal end of GFP), or both which is having the greatest effect on GFP solubility has not been determined.

4.2.9.2 Analysis of GFP-HA epitope protein stability in pMO9G and pMOG3 transformed plants

HA91-108/GFP and GFP/HA307-319 protein stability was assessed in leaves of different ages in one pMO9G and pMOG3 plant lines (9G-1 and G3-3). Soluble and insoluble protein was extracted using the SDS-based extraction procedure from leaves 1-8 (leaf 1, oldest, leaf 8, youngest) from approximately 8-week old plants grown in soil and maintained in a 25^0C growth chamber (16 hour light / 8 hour dark photoperiod). 5 μg of protein was separated by SDS-PAGE, transferred to nitrocellulose and incubated with an anti-HA91-108 or an anti-HA307-319 antibody. The western blots show that both HA-epitope proteins are stable in leaves of all ages (Figure **4.16** A and B). Accumulation of both proteins is highest in leaf 4 (Figure **4.16** A and B) but considerable amounts of both proteins are seen in leaves of all ages. To assess the accuracy of the protein quantifications 20 μg of protein from each leaf from each line was separated by SDS-PAGE and stained with coomassie blue. The stained gels indicated equal

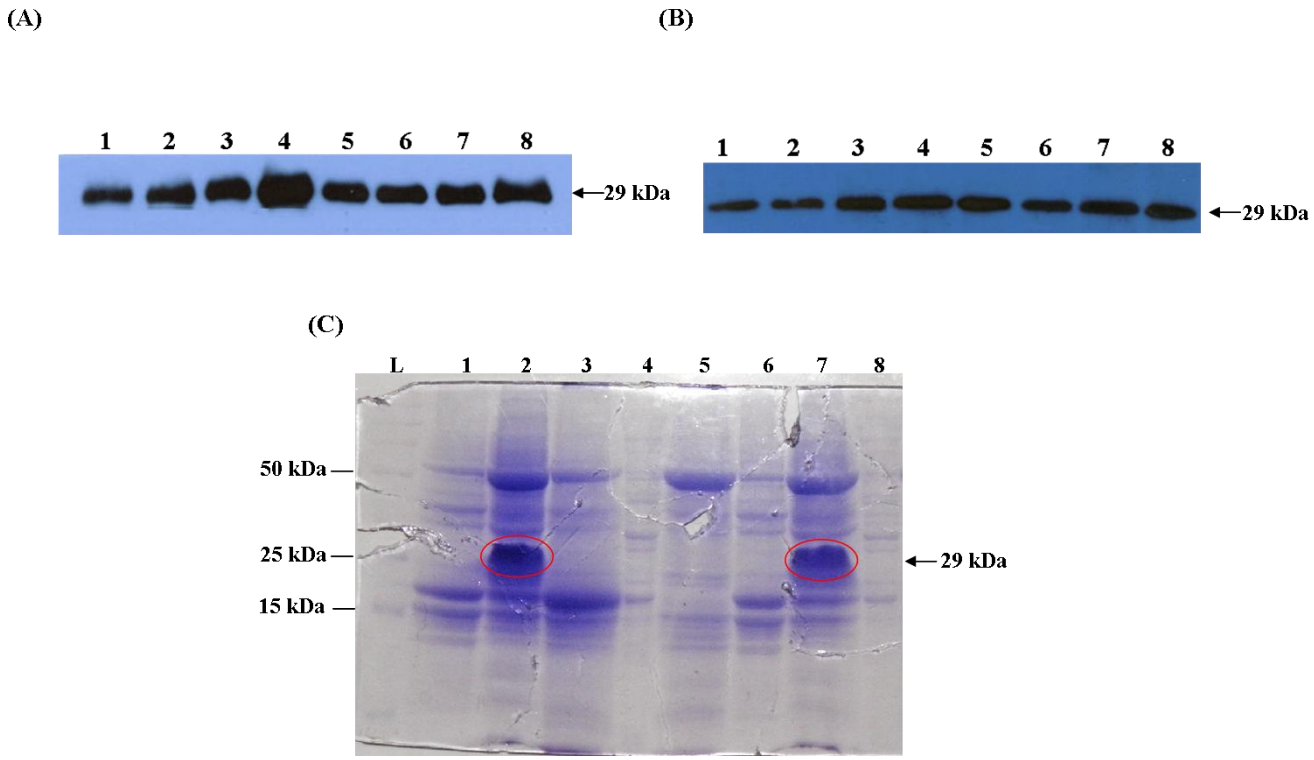

Figure 4.16: Analysis of GFP-HA epitope protein stability in leaves of different ages in pMO9G and pMOG3 transformed plants (A) Protein was extracted from leaves 1-8 of plant line 9G-1. 5 µg of protein was separated by SDS-PAGE, blotted onto nitrocellulose and incubated with an anti-HA91-108 antibody. (B) Protein was extracted from leaves 1-8 of plant line G3-3. 5 µg of protein was separated by SDS-PAGE, blotted onto nitrocellulose and incubated with an anti-HA307-319 antibody. (C) Approximately 20 µg of protein extracted from plant line G3-3 separated by SDS PAGE and stained with coomassie blue. Lane L: Broad range molecular marker (Fermentas). Lane 1: WT SF, lane 2: G3-1 ISF, lane 3: G3-1 SF, lane 4: pMOG3 in *E. coli*, positive control, lane 5: WT SF, lane 6: G3-3 SF, lane 7: G3-3 ISF, lane 8: pMOG3 in *E. coli*, positive control. Protein sizes are indicated in kilo Daltons (kDa).

amounts of proteins loaded across all lanes. A representative SDS gel showing the detection of GFP/HA307-319 by coomassie blue staining (Figure 4.16 C).

4.2.9.3 Estimation of HA-epitope accumulation in pMO9G and pMOG3 lines

HA91-108/GFP and GFP/HA307-319 accumulation in the pMO9G and pMOG3 lines was assessed by western blot analysis. Protein was extracted from leaves of the T_1 generation pMO9G transformed lines (9G-1 and 9G-7) and pMOG3 transformed lines G3-1 and G3-3 using 1% SDS protein extraction buffer. 5 μg of the total soluble protein samples were run on 12% SDS-PAGE gels along with known amounts of purified GFP (50 ng, 150 ng, 250 ng, 350 ng and 450 ng of GFP protein from Millipore) to allow for quantification of plant-based GFP-HA epitope protein accumulation. The GFP standard contains an N-terminal His-tag and the protein has a molecular weight to 29 kDa the same size as the GFP/HA epitope fusion proteins. Protein gels were blotted onto nitrocellulose membrane and detected using an anti-GFP antibody (Figure 4.17 A and B). Following detection, the intensity of the protein bands was quantified by densitometry using Image J (National Institutes of Health). Using this program, density profiles were generated which compared the number of pixels for each band against background (Figure 4.17 C and D). The numerical data obtained was used to compare the intensity if the bands obtained from the plant samples to the GFP standards. The accumulation of the recombinant 9G protein in lines 9G-1 and 9G-7 was estimated at 0.278 μg and 0.1755 μg per 120 mg of plant tissue, approximately 5.6% and 3.5% of TSP respectively. The accumulation of G3 protein in lines G3-1 and G3-3 was estimated as 0.0865 μg and 0.1515 μg

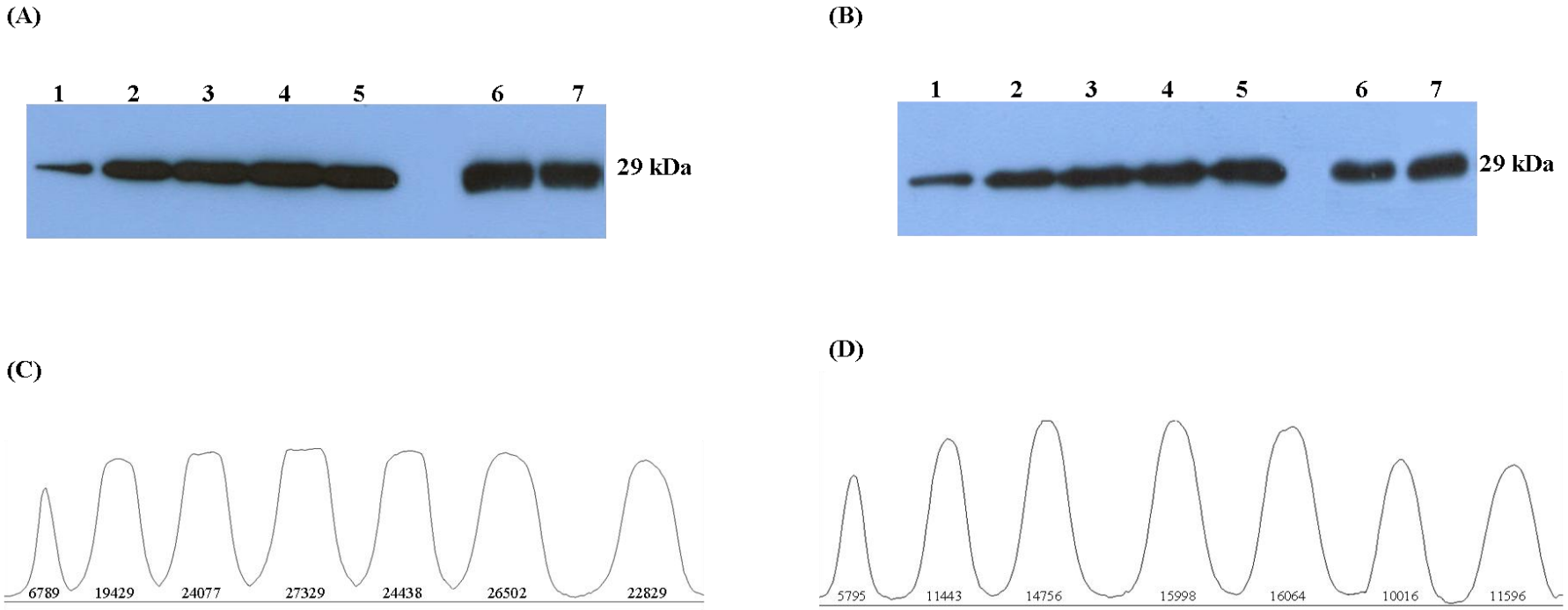

Figure 4.17: Estimation of HA91-108/GFP and GFP/HA307-319 accumulation in T_1 generation transgenic lines pMO9G and pMOG3. (A) 5 µg of protein extracted from leaves of 9G-1 and 9G-7 transformed plants were run on an SDS-PAGE gel with known amounts of purified GFP. Western blots were probed with an anti-GFP antibody. Lanes 1-5: 50 ng, 150 ng, 250 ng, 350 ng and 450 ng of purified GFP protein. Lane 6-7: protein extracted from lines 9G-1 and 9G-7 respectively. (B) 5 µg of protein extracted from leaves of G3-1 and G3-3 transformed plants were run on an SDS-PAGE gel with known amounts of purified GFP. Western blots were probed with an anti-GFP antibody. Lanes 1-5: 50 ng, 150 ng, 250 ng, 350 ng and 450 ng of purified GFP protein. Lane 6-7: protein extracted from lines 9G-1 and 9G-7 respectively. (C) Signal intensities for each of the 9G bands determined using the Image J program. (D) Signal intensities for each of the G3 bands determined using the Image J program.

per 120 mg of plant tissue, approximately 1.73% and 3.03% of TSP respectively.

4.2.10 Characterisation of pMOG9, pMO3G and pMO3G9 transformed lines

Plant lines transformed with the pMOG9, pMO3G and pMO3G9 constructs were confirmed as plastid transformants by PCR and by GFP fluorescence in first-round regenerated primary transformants. However, no GFP expression was detected in any of the pMOG9, pMO3G and pMO3G9 transformed lines in approximately eight to ten week old first round primary transformants (data not shown). This could be due to a number of reasons: transgene loss, lack of transcription or recombinant protein instability.

4.2.10.1 Northern blot analysis of GFP / HA-epitope transgenic lines

Transcription of the *aadA* and *gfp* genes was assessed in pMOG9, pMO9G, pMOG3, pMO3G and pMO3G9 plant lines by northern blot analysis. Total RNA (5 μg) from one representative plant line generated for each construct (G9-1, 9G-19, G3-3, 3G-2 and 3G9-5) and from a wild type plant were separated by electrophoresis on 1% agarose / formaldehyde gels and blotted onto nylon membranes. The blots were probed with *aadA* and *gfp* gene specific probes. The *aadA* probe hybridised to a single transcript of the expected size (840 bp) in all of the transgenic lines (Figure 4.18 A, lanes 1-5). The *gfp* probe hybridised to a single transcript of the expected size only in the 9G-19 and G3-3 lines (lanes 2 and 3) however, no *gfp* transcript was detected for the G9-1, 3G-2 or 3G9-5

(A)

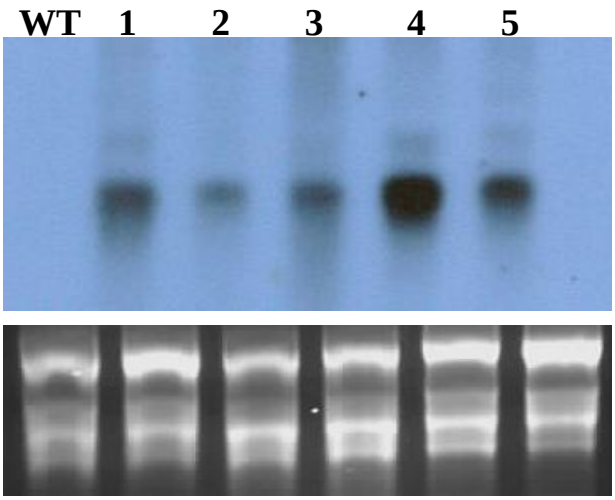

(B)

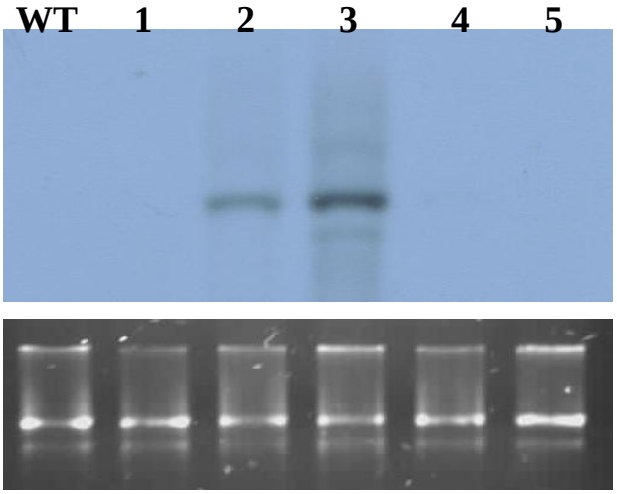

Figure 4.18: Northern Blot analysis of transplastomic tobacco plants. Total RNA from wild type (WT) and transplastomic T1 lines G9-1, 9G-19, G3-3, 3G-2 and 3G9-5 was separated by electrophoresis and blotted onto nylon membranes. To confirm equal loading, the ethidium bromide-stained agarose gels are also shown. (A) The blot was hybridized with an *aadA* gene specific probe. Lane WT: wild type tobacco RNA. Lanes 1-5: G9-1, 9G-19, G3-3, 3G-2 and 3G9-5. (B) Blot hybridised with a *gfp* gene specific probe. Lane WT: wild type tobacco RNA. Lanes 1-5: G9-1, 9G-19, G3-3, 3G-2 and 3G9-5.

lines (Figure 4.18 B, lanes 1, 4 and 5). Neither of the probes hybridised to wild type RNA (Figure 4.18). The lack of *gfp* transcripts in G9-1, 3G-2 or 3G9-5 lines could be due to a number of factors: loss of functional promoters in the genome-integrated G9, 3G and 3G9 gene cassettes; gene silencing caused by DNA methylation; or transcript instability.

4.2.10.2 DNA sequence analysis of the plastome integrated G9, 3G and 3G9 gene expression cassettes

The integrity of the plastid-integrated G9, 3G and 3G9 gene expression cassettes was assessed by DNA sequence analysis. For each of the three lines the cassettes were amplified by PCR using the pair aadA-3'-For and rps14-Rev and the amplicons were sequenced. The transgene expression cassette was also amplified from the 9G expressing plant line. PCRs were performed in triplicate to eliminate any Taq related or sequencing errors. Sequences were aligned using the Multalin program (multalin.toulouse.inra.fr/multalin/). The sequence data revealed no errors / changes in the promoter regions of any of the integrated expression cassettes that could explain the lack of transcription.

4.2.11 Analysis of DNA methylation in pMOG9, pMO3G and pMO3G9 transformed lines

To test if methylation might account for the lack of G9, 3G and 3G9 transcription, locus-specific adenosine and cytosine methylation was assessed in non-expressing T_1 transplastomic lines G9-1 and 3G-2 and in expressing T_1

transplastomic lines 9G-19 and G3-3. Total DNA was isolated from each of the lines, digested with methylation-sensitive/insensitive restriction enzymes, Southern blotted and probed with a DIG-labelled HA307-319/GFP/HA91-108 gene probe. To test for adenine methylation the two isoschizomeric restriction enzymes *MboI* (methylation-sensitive enzyme) and *DpnI* (methylation-dependent enzyme) were used. The probe hybridized to *MboI* fragments of the expected size in all four transplastomic plant lines (Figure 4.19 A). The probe hybridized to unresolved high molecular weight DNA in all four transplastomic plant lines digested with *DpnI* (Figure 4.19 B). This indicates lack of adenosine methylation at the transgene locus in these lines (Figure 4.19 B). To test for cytosine methylation the methylation sensitive restriction enzyme *PvuI* was used. The HA307-319/GFP/HA307-319 probe is expected to hybridise to a 2.9 kb fragment if the transgene locus is not methylated. However, a 2.9 kb fragment was not detected in any of the plant lines – not even the expressing lines (Figure 4.19 C). Since the hybridization profile was pretty much the same in all of the transplastomic lines it was concluded that the *PvuI* recognition sequences in the plastid DNA of these selected transplastomic lines was probably not modified by cytosine methylation.

Due to the lack of time and lack of funding for any additional experimental work it was not possible to examine the half-life or stability of transgene transcripts in these lines.

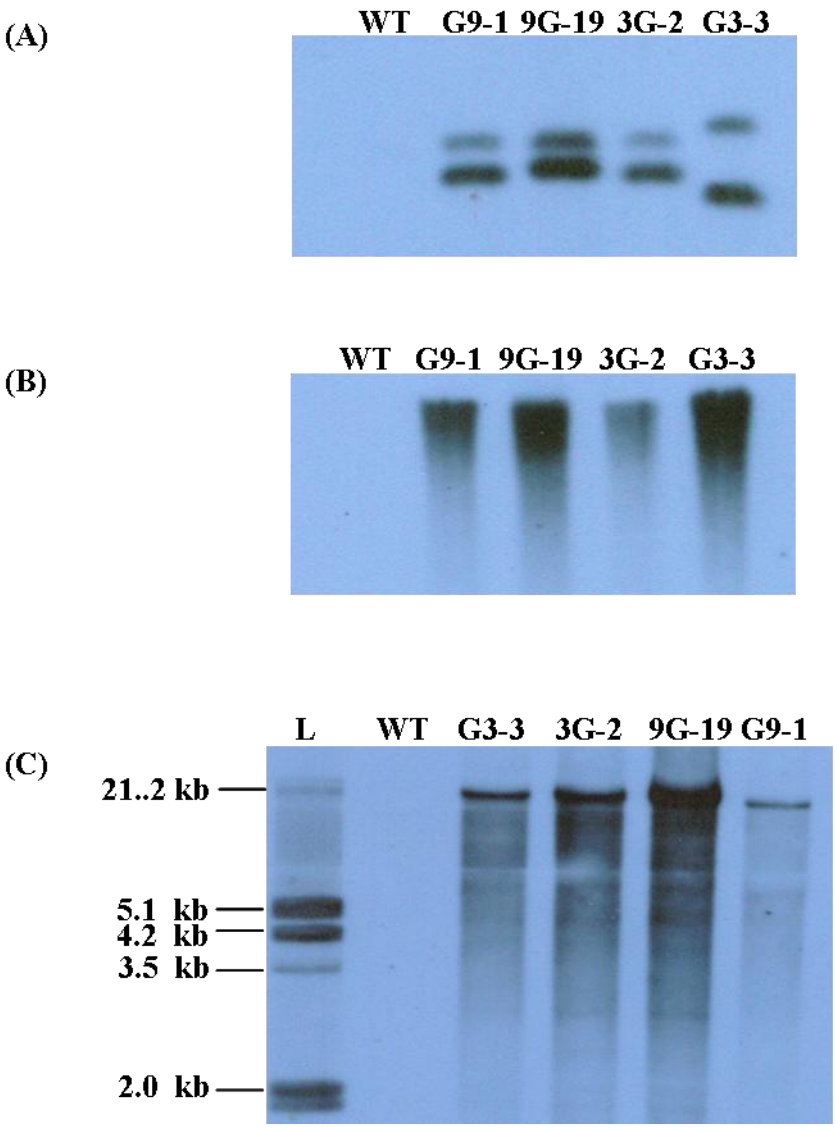

Figure 4.19: Analysis of DNA methylation in the plastid genome of G9, 9G, 3G and G3 plants. The same plant lines, G9-1, 9G-19, 3G-2 and G3-3, that were subject to northern blot analysis were analysed for methylation. (A) Test for adenine methylation with the *MboI*, methylation sensitive, restriction enzyme. Complete digestion of the plastid DNA indicates the absence of adenine methylation. (B) Test for adenine methylation with the *DpnI*, methylation dependent, restriction enzyme. Lack of cleavage of the plastid DNA also indicates the absence of adenine methylation. (C) Test for cytosine methylation using the *PvuI*, methylation sensitive, restriction enzyme. Lane L: DIG labelled Marker weight III (Roche).

4.3 Discussion

Hemagglutinin (HA) is a major influenza antigen. Current seasonal influenza vaccines act mainly by eliciting neutralizing antibodies against the HA antigen (Wang *et al.*, 2010). However, these vaccines need to be reformulated and re-administered annually due to antigenic drift. A vaccine that could provide protective immunity against multiple influenza subtypes would be of great benefit in combating the virus. The use of vaccines based on conserved influenza epitopes is one approach which has the potential to replace seasonal influenza vaccines. The aim of this work was to generate transplastomic tobacco plants expressing a range of HA epitope GFP fusion gene constructs (HA91-108/GFP, GFP/HA91-108, HA307-319/GFP, GFP/HA307-319, HA91-108/GFP/HA307-319 and HA307-319/GFP/HA91-108) and to analyse the stability and level of expression for the different fusion proteins.

Stably transformed transplastomic lines were generated with five of the six HA epitope fusion constructs [HA91-108/GFP (9G), GFP/HA91-108 (G9), HA307-319/GFP (3G), GFP/HA307-319 (G3) and HA307-319/GFP/HA91-108 (3G9)]. The HA91-108/GFP/HA307-319 (9G3) gene construct did not generate any transplastomic lines containing the HA91-108/GFP/HA307-319 transgene. Five of the seven plastid transformed plant lines that were analysed contained the *aadA* gene but not the HA91-108/GFP/HA307-319 fusion gene at the plastid integration site suggesting that these lines are the result of a secondary recombination event that led to transgene excision during or after integration. The remaining six plant lines (9G3-3, 9G3-8, 9G3-9, 9G3-10, 9G3-12 and 9G3-

13) that were recovered displayed a severe stunted growth phenotype and could not be analysed.

Southern blot analysis of the T_0 transgenic lines confirmed that after three rounds of regeneration, homoplasmic lines had been obtained for all five constructs. All of the third-round G3 regenerated plants analysed were homoplasmic. However, a number of the lines generated with the other four constructs (9G, G9, 3G and 3G9), displayed an unexpected banding pattern when hybridised with a *psaB* probe. Six of the seven transplastomic plant lines generated with the 9G gene construct were homoplasmic for the transgene insertion. However, one line (9G-21) gave a pattern of hybridization that was similar to wild-type with the *psaB* probe and the HA91-108/GFP transgene construct could not be detected in this line. The same anomalous hybridization pattern was also observed among the G9, 3G and 3G9 transplastomic lines. The apparent loss of the GFP-HA epitope transgene in these transplastomic lines was subsequently found to be due to secondary recombination events that had occurred between plastid gene regulatory elements on the transformation vector and native tobacco plastid gene regulatory elements. These secondary recombination events are discussed in more detail in Chapter 5.

The homoplasmic nature of the transplastomic plant lines was confirmed by analysis of the T_1 progeny germinated on spectinomycin-containing media. All transplastomic seedlings demonstrated spectinomycin resistance in the T_1 generation. Reciprocal genetic crosses carried out between WT and transgenic

plants demonstrated maternal inheritance of the transgenes as expected for a plastid-encoded trait (Ruf *et al.*, 2007).

As all of the HA epitope fusion gene constructs contained GFP, all transplastomic plant lines were first screened for GFP expression using fluorescent microscopy. GFP expression was readily detected in all lines transformed with the five epitope gene constructs in first round T_0 regenerants. Western blot analysis of third round T_0 confirmed HA-epitope accumulation in all 9G and G3 plant lines. A difference in solubility of the HA91-108/GFP and GFP/HA307-319 proteins was also observed. GFP was found to accumulate in the soluble fraction only. The HA91-108/GFP protein accumulated in both the soluble and insoluble fractions however, a strong preference for protein accumulation in the insoluble protein fraction was observed. The GFP/HA307-319 protein accumulated predominantly in the insoluble protein fraction. .This suggests that the HA peptides, or perhaps the peptide position on GFP (N-terminal or C-terminal) is affecting the solubility of the fusion protein in plastids. The HA epitopes may be causing the fusion protein to either self-associate into aggregates or to associate with other structures (such as membrane systems) within the plastid.

Accumulation levels for HA91-108/GFP and GFP/HA307-319 in transformed tobacco lines was estimated at 3.5-5.6% TSP for HA91-108/GFP and 1.73-3.03% TSP for GFP/HA307-319. This is very low compared to the levels of protein accumulation achieved for other viral epitopes in plant plastids. The VP1 epitope protein from the foot and mouth virus accumulated to 51% TSP in

transgenic tobacco lines (Lentz *et al.*, 2010). High levels of protein accumulation were also achieved for the 2L21 epitope protein from the canine parvovirus which accumulated to 22.6% TSP when fused to GFP and 31.1% TSP when fused to CTB (Molina *et al.*, 2004). However, there are reports of relatively low levels of epitope accumulation also being achieved in the plastid system. When the 2L21 epitope protein was fused to the p53 tetramerisation domain, protein accumulation was estimated at 6% (Ortigosa *et al.*, 2010). A fusion DPT protein containing immunoprotective exotoxin epitopes of *Corynebacterium diphtheriae, Bordetella pertussis* and *Clostridium tetani* accumulated to 0.8% TSP in transplastomic tobacco lines (Soria-Guerra *et al.*, 2009). In addition, when compared to the expression of other hemagglutinin epitopes in tobacco the levels of protein accumulation achieved in this study are quite high. The hemagglutinin-neuraminidase neutralising epitope from the Newcastle disease virus only resulted in recombinant protein accumulation levels of 0.5% of TSP in the leaves of transplastomic tobacco plants following fusion to LTB (Sim *et al.*, 2009).

It seems likely that both the carrier protein and the nature of the epitopes themselves can impact on the protein accumulation levels that can be achieved within the plastid system. There is a strong possibility that the accumulation estimates made in this study are actually underestimations of GFP-epitope accumulation. The solubility of the two GFP-epitopes is quite different in plastid-transformed lines. The GFP/HA307-319 protein was detected only in the insoluble protein fraction and accumulation levels were estimated at 1.73 - 3.03% TSP. The HA91-108/GFP protein was detected in both the SF and ISF

and accumulation levels were estimated to be higher at 3.5 - 5.6% TSP. It is possible that the higher protein accumulation levels estimated for HA91-108/GFP compared to GFP/HA307-319 is due to differences in protein solubility. Protein solubility has been discussed in other studies and the formation of protein aggregates is thought to lead to an underestimation of protein accumulation levels and to hinder accurate quantification of plastid expressed protein (Arlen *et al.,* 2008; Ruhlman *et al.,* 2007; Daniell *et al.,* 2001). Daniell *et al.* (2001) reported that aggregation of the cholera toxin of *Vibrio cholerae* (CTB) resulted in an underestimation of the levels of protein accumulation (4.1% of TSP) in tobacco chloroplasts due to the formation of protein aggregates. Ruhlman *et al.,* (2007) reported that the aggregation of oligomers of a fusion protein containing CTB and human proinsulin protein also resulted in an underestimation of the levels of protein accumulation (16% of TSP in tobacco chloroplasts and 2.5% of TSP in lettuce chloroplasts) due to the formation of protein aggregates.

Taking into account that both the HA91-108/GFP and GFP/HA307-319 protein can clearly be visualised on Coomassie stained polyacrylamide gels and that the potential for protein aggregation to occur in plant extracts increases with the concentration of protein in question (Ruhlman *et al.,* 2007), there is a strong possibility that the quantity estimations made in this study are underestimations.

As chloroplast protein biosynthesis is highly active in young leaves but declines with leaf age, the age-dependent decrease in foreign protein accumulation provides a good indicator of protein stability (Oey *et al.,* 2009a). Although high

levels of protein expression were achieved for both the 2L21/GFP and 2L21/CTB epitope fusions, the accumulation of protein was found to be highly dependent on leaf age (Molina *et al.*, 2004). In addition, the accumulation of VP6 protein was also highly dependent on leaf age with maximum accumulation observed in cotyledons and young leaves and declining as the leaves aged (Birch-Machin *et al.*, 2004). However, no age-dependant decline in HA91-108/GFP or GFP/HA307-319 protein accumulation was detected in transplastomic plants suggesting that the HA91-108/GFP and GFP/HA307-319 proteins are extremely stable in tobacco chloroplasts. Similar epitope/carrier protein stability was also reported for the 2L21 peptide fused to the p53 tetramerisation domain (Ortigosa *et al.*, 2010) and for the A27L protein of vaccinia virus in young and mature tobacco leaves (Rigano *et al.*, 2009).

Western blot analysis of first round transplastomic plant lines generated with the other three gene constructs (G9, 3G and 3G9) revealed no HA-epitope protein accumulation in any of the plant lines. This was very surprising since initial screening of the first round regenerants, using fluorescent confocal microscopy, had indicated GFP fluorescence. Several possible explanations for the lack of HA epitope fusion protein accumulation in the G9, 3G and 3G9 plants were hypothesised: (a) the plastid encoded HA epitope fusion genes were not being transcribed, (b) the mRNAs were not stable, or (c) the proteins were not translated or were unstable in the plastid. Northern blot analysis confirmed that the *aadA* gene was transcribed in all of the transplastomic lines analysed. However, analysis using a *gfp* specific probe showed that the HA-epitope fusion genes were only being transcribed in the 9G and G3 lines and not in the G9, 3G

or 3G9 lines. To exclude the possibility that nucleotide changes within the transgene promoter regions might account for lack of transcription the entire plastid-integrated-transgene expression cassette was sequenced for one representative from each of the 9G, G9, 3G and 3G9 plant lines. All three integrated epitope fusion transgenes sequenced correctly, in particular the promoter regions, indicating that a possible pre-or post-transcriptional effect was the reason for the lack of epitope fusion protein accumulation in these transplastomic plants.

One possible pre-transcriptional effect that could explain the lack of transgene transcription in the G9, 3G and 3G9 lines is gene silencing due to plastid DNA methylation. We looked examined patterns of adenine and cytosine methylation at the transgene locus in expressing and non-expressing lines using methylation-sensitive and methylation dependent restriction enzymes. No evidence of adenine or cytosine methylation at the transgene locus was observed in the G9, 3G or 3G9 transplastomic plant lines. These results are consistent with the findings of Ahlert *et al.,* (2009) who reported that methylation is unlikely to be involved in the transcriptional regulation of plastid gene expression. Another possibility that could explain the lack of detectable transgene transcription in G9, 3G and 3G9 lines is extreme transgene mRNA instability in these lines. However, due to time constraints and funding limitations it was not possible to examine transcript half-life/stability in these lines and to compare the results to transgene transcript half-life/stability in the 9G and G3 expressing plant lines

The work presented here demonstrates that conserved influenza virus HA epitopes can be expressed in plant chloroplasts. However, the orientation of the HA epitope coding-region with respect to the GFP coding region appears to play a major role in affecting transgene expression possibly by affecting transcript stability. No transgene transcripts were detected in G9, 3G and 3G9 lines however transgene transcripts and GFP-epitope protein were readily detected in 9G and G3 transformed lines. Recognition of the HA91-108 and HA307-319 epitopes by their respective antibodies in Western blots indicates that these epitopes are correctly presented when fused to GFP. Although the protein accumulation levels calculated for the two HA epitope fusions is quite low in comparison to other plastid expressed recombinant proteins, in reality, the insoluble nature of the majority of the GFP/HA epitope proteins suggest that these percentages may be a significant underestimation of actual protein accumulation levels within the tobacco plastid system.

Chapter 5
Analyses of secondary recombination events in transgenic tobacco plants

5 Analyses of secondary recombination events in transgenic tobacco plants

5.1 Introduction

The chloroplast genome is highly conserved within most land plants and is generally mapped and represented as a single circular chromosome containing two inverted repeat (IR) regions, a small single copy (SSC) region and a large single copy (LSC) region (Gray *et al.*, 2009b). However, the situation *in vivo* may not be so simple since up to 45% of plastid DNA molecules have been reported to occur as linear molecules, circular multimers and/or irregular molecules containing uneven numbers of IR regions (Lilly *et al.*, 2001).

Transformation of the plastid genome relies on homologous recombination between the plastid genome and homologous DNA sequences on the transformation vector. To ensure efficient recombination and integration of transgenes into the chloroplast genome, transgenes are usually flanked by between 0.5 – 1.5 kb stretches of plastid DNA (Gray *et al.*, 2009b). In addition, transgenes are typically engineered to contain additional short plastid DNA regulatory elements e.g. promoters, 5' untranslated regions (5' UTRs) and 3'UTRs. However, the shorter plastid DNA regulatory elements can also participate in unintended recombination events with native plastid sequences and these secondary unintended recombinant DNA species can account for up to 10-60% of the integrated transgenic sequence in T_0 plants (Gray *et al.*, 2009b).

An unintended recombination event was reported between the 400 bp *psbA* 3' UTR used to regulate the *aadA* selectable marker gene in the transforming DNA and the native *psbA* terminator in transgenic tobacco lines (Svab & Maliga, 1993). This recombination event resulted in a large deletion of the plastid genome which caused the plastid genome to remain heteroplasmic when plants were regenerated under selection (Svab & Maliga, 1993). Staub and Maliga (1994) also reported an 868 bp *Nicotiana* plastid extrachromosomal element, (NICE1), in tobacco plastids that was generated during transformation as an unexpected product of homologous recombination. NICE1, which contained plastid DNA sequence from the *trnI* gene, was thought to have resulted from intermolecular recombination between two imperfect 16 bp repeats in direct orientation (Staub & Maliga, 1994). Recombination between direct 649 bp repeats of the native and an introduced *atpB* gene promoter region were reported by Kode *et al.*, (2006). This recombination event resulted in the excision of a 6.1 kb fragment in transformed chloroplast DNA and resulted in mutant plants which were heterotrophic, pale-green and that contained round plastids with reduced amounts of thylakoids (Kode *et al.*, 2006). A similar, unintended, recombination event was also observed in transgenic tobacco lines engineered to express the HIV antigen p24 (McCabe *et al.*, 2008). Recombination between the native and an introduced *rbcL* terminator region (T*rbcL*), in direct orientation, resulted in a large deletion of the plastid genome and the formation of a circular sub-genomic 21 kb molecule (McCabe *et al.*, 2008). Zhou *et al.*, (2008) also observed recombination between the T*rbcL*, used to regulate the HIV antigen p24 transgene, and the native terminator of the plastid *rbcL* gene. However, these recombination products did not dominate to the same extent as reported by

McCabe *et al.,* (2008). Unintended recombination was observed at "recombination hot-spots" when plastid-targeted CRE recombinase was stably expressed in transplastomic tobacco plants containing *loxP* sites. CRE-mediated deletions involving *loxP* sites and plastid DNA sequences in the *3'rps12* gene leader (lox-rps12) or in the *psbA* promoter core (lox-psbA) were observed in these lines (Corneille *et al.,* 2003). Deletion of sequences between two directly orientated *lox-psbA* sites was also observed but not between the *lox-rps12* sites. Recombination events were thought to be mediated by Cre recombinase and imperfect endogenous CRE binding sites in the P*psbA* and the *rps12* 5'UTR. In addition, deletion *via* duplicated *Prrn* sequences was also frequently observed in CRE-active plants. However in this case CRE-mediated recombination is unlikely be involved, as no recombination junction between *loxP* and *Prrn* was observed (Corneille *et al.*, 2003).

The tendency for homologous recombination to occur between repeated DNA elements in the plastid genome has been exploited for marker gene excision. Two copies of the *rrn* promoter in direct orientation on either side of the marker gene *aadA* were used to create "loop-out" homologous recombination events and marker gene removal from transformed tobacco chloroplast genomes (Iamtham & Day, 2000). Kode *et al.,* (2006) used a homology based marker excision method that could be detected visually. Recombination between 649 bp direct repeats resulted in the excision of the *aadA, gusA* and native plastid *rbcL* genes. Loss of the photosynthetic *rbcL* gene resulted in arrested chloroplast development and the production of yellow cells that were easily visualised as pigment deficient sectors on leaves (Kode *et al.*, 2006).

Homologous recombination between repeated DNA elements in the plastid genome has also been exploited to generate plastid gene knockout mutations. Heteroplasmic transgenic tobacco lines containing knockouts of the *psbA* gene were generated using the *psbA* 5' UTR and the *psbA* 3' UTR (Khan *et al.*, 2007). The selectable marker gene *aadA* and the *psbA* 5' UTR and *psbA* 3' UTR gene deletion cassette was introduced into the *trnI / trnA* intergenic region within the IR on the plastid genome. Subsequent *psbA* gene deletion was achieved by gene replacement mediated by homologous copy correction using the native *psbA* 5' and 3' UTR sequences and the integrated gene deletion cassette within the IR (Khan *et al.*, 2007). Rogalski *et al.,* (2008a) generated homoplasmic transplastomic tobacco lines containing knockouts of the *rpl*20, *rpl*33, *rps*2, and *rps*4 genes. This was achieved by replacing, or disrupting, each of the genes with a chimeric selectable marker gene *aad*A by homologous recombination. A similar method was also used to obtain homoplasmic transplastomic tobacco lines containing knockouts of the *ycf9* gene (Ruf *et al.*, 2000).

Recombination events between native and introduced plastid DNA in reverse orientation have also been observed. These so called 'flip-flop' recombination events between native and introduced plastid DNA in reverse orientation result in the intervening DNA being inverted within, but not lost from, the plastid genome following the recombination event. Rogalski *et al.,* (2006) observed a "flip-flop" recombination event between the native *psbA* terminator sequence and an introduced T*psbA* sequence in reverse orientation following transgene integration. This recombination event resulted in approximately 70 kb of the

large single copy region becoming flipped within some of the transformed plastid genomes (Rogalski *et al.,* 2006). This 'flip-flop' recombination event, involving the native *psbA* terminator sequences and an introduced T*psbA* sequence, has been observed at several genome integration sites following transformation including at the *trnG/trnfM, trnG/trnR* and *trnS/trnT* intergenic regions (Rogalski *et al.,* 2008b). A "flip-flop" recombination event was also observed in transgenic tobacco plants transformed with the HIV p24 and Nef antigen genes (McCabe *et al.*, 2008; Zhou *et al.,* 2008). In both of these cases, an unintended recombination event occurred between two imperfect *Prrn* copies introduced in opposite orientation on transforming DNA and resulted in the inversion of the two *Prrn* promoters (McCabe *et al.*, 2008; Zhou *et al.*, 2008).

Gray *et al.,* (2009b) identified and quantified multiple recombinant DNA species in transplastomic tobacco plants arising as a result of recombination between regulatory plastid DNA elements in transgenic plants and their native counterparts. They estimated that at least two unintended recombination species can occur for each regulatory plastid DNA element included on the transformation vector. In two of the transgenic plant lines tested, 9-11 DNA species were identified as a result of unintended secondary recombination events. The level of novel recombinant DNA species was found to be higher in T_0 than in T_1 plant lines, suggesting that these unintended recombination events occur during the selection and regeneration of transformants (Gray *et al.*, 2009b).

Southern blot analyses carried out on transgenic plants transformed with the five *gfp*/HA epitope gene constructs, discussed in Chapter 4, revealed an unexpected hybridisation pattern when probed with a DIG-labelled *psaB* probe. Along with the expected *psaB*-hybridising fragments observed in WT and transformed plastid DNA, an additional smaller than expected fragment (4.5 kb) hybridised to the probe in some of the lines transformed with the G9, 3G9, 3G and 9G constructs. In addition, a decoupling of the selectable marker gene *aadA* and the transgene cassette was observed in plant lines transformed with the 9G3 and GFP/HA1 gene constructs resulting in the failure to recover any primary transformed plant lines containing the transgenes. All *gfp*/HA epitope and GFP/HA1 transgenic plant lines were analysed using a series of Southern blot hybridisations and PCRs to determine if the smaller than expected hybridising fragments and the decoupling of the *aadA* gene from the 9G3 and GFP/HA1 transgene cassettes might be the result of some secondary recombination event.

5.2 Results

The transgenic plant lines G9-4, 3G9-9, 3G9-15, 3G-14 and 9G-21 that generated an unexpected hybridisation pattern with the *psaB* probe (see Chapter 4) were analysed in detail using a series of Southern blot hybridisations and PCRs. The DIG-labelled probes used for this series of hybridisations are illustrated in Figure 5.1. The transgenic plant lines generated with pMO9G3 and pMOGFP/HA1 gene constructs were also analysed by Southern blot hybridisation and/or PCR to determine the reason behind the de-coupling of the *aadA* and the transgene cassettes in these lines.

5.2.1 Characterisation of G9, 3G9, 3G and 9G regenerating lines (R1-R3) using a psaB gene-specific probe.

Firstly, we examined how the *gfp*/HA-epitope gene constructs were being retained in the plastid genome during the three rounds of regeneration used to generate expected homoplasmic T_0 lines. DNA was extracted from WT tobacco and from round 1 (R1), 2 (R2) and 3 (R3), regenerated T_0 tobacco lines 3G9-9, 3G9-15 and 3G-14. The DNA was digested with *BamHI*, Southern blotted and hybridised with a DIG-labelled *psa*B probe. The *psa*B probe hybridised to a 4.5 kb fragment of the expected size in wild type DNA (Figure 5.2) and to a 7.1 kb and 7.3 kb restriction fragment in 3G-14 and 3G9-15 R1 and R2 DNAs respectively indicating transgene integration in these regenerated lines (Figure 5.1 and Figure 5.2). However, the probe also hybridised to an additional fragment of approximately 4.5 kb in size in R2 DNAs and only to this 4.5 kb fragment in R3 DNAs (Figure 5.2). The probe only hybridized to the 4.5 kb

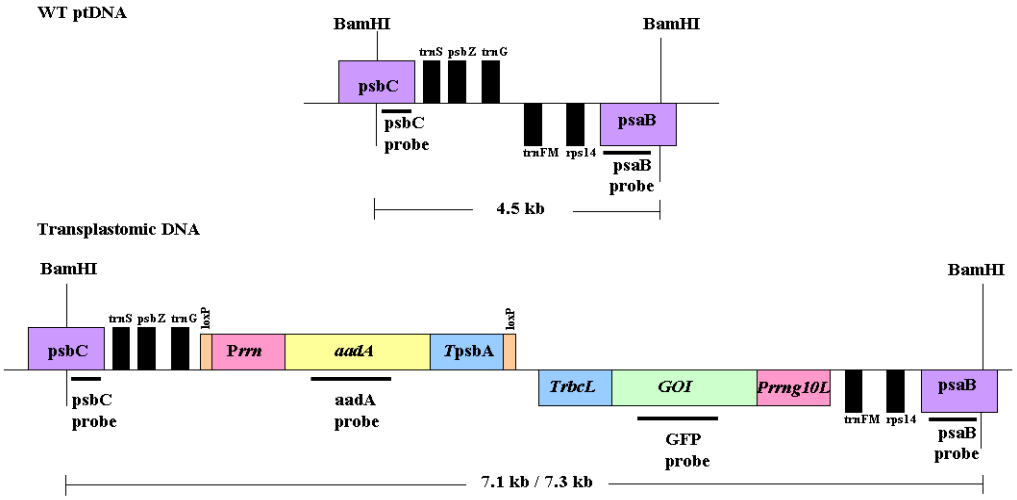

Figure 5.1: Map of the targeted region in the WT plastid genome and the region expected in transplastomic GFP/HA epitope lines (not drawn to scale). *Bam*HI restriction sites are indicated. The location of the various probes used for the detection of recombinant DNA species is shown underneath each line drawing with a black bar. The size of the *BamHI* fragment indicated in WT ptDNA is 4.5 kb; the size of the *BamHI* fragment indicated in transplastomic DNA is 7.1 or 7.3 kb (depending on the size of the integrated gene of interest – GOI).

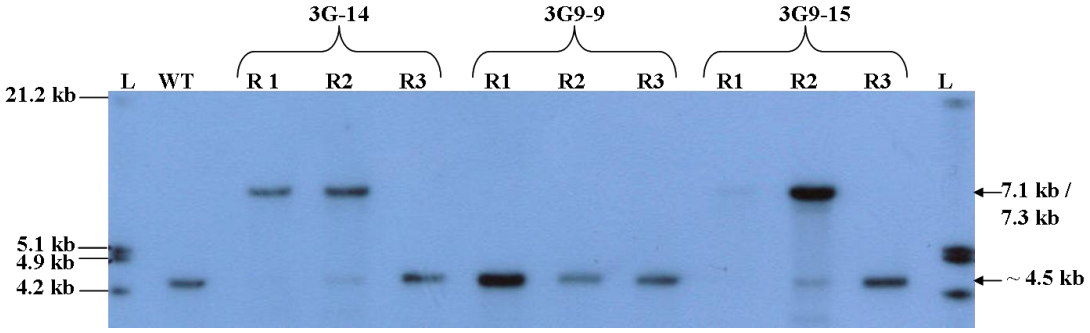

Figure 5.2: Southern blot analysis of R1, R2 and R3 regenerated plants lines (3G-14, 3G9-9 and 3G9-15). The Southern blot was probed with a DIG-labelled *psaB* probe. The probe hybridised to a 4.5 kb fragment of the expected size in wild-type DNA (Lane WT) and to an unexpected 4.5 kb fragment in R2 and R3 3G-14 and 3G9-15 regenerated lines and in all three regenerated 3G9-9 lines. Lane L: DIG-labelled marker weight III (Roche).

fragment in DNA isolated from 3G9-9 R1, R2 and R3 plants (Figure 5.2). This latter hybridization pattern was also observed in DNA isolated from R1-3 9G-21 and G9-4 plant lines (data not shown).

5.2.2 Characterisation of regenerating lines (R1-R3) using aadA and gfp gene-specific PCR

To determine if this unexpected hybridisation pattern indicated transgene loss, from transformed genomes and reversion to wild type DNA during plant regeneration we used PCR to assay for the presence of *aad*A and *gfp* in all of the regenerating lines.

PCR carried out using *aad*A gene-specific primers (aadA-For and aadA-Rev) amplified a product of the expected size (792 bp) in all three regenerating rounds for all five of the transformed plant lines (G9, 3G9, 3G and 9G) (Figure 5.3 A and data not shown). No PCR product was amplified from WT DNA (Figure 5.3 A). PCR carried out using *gfp*-specific primers (GFP-NdeIF and GFP-XbaIR) amplified a product of the expected size (746 bp) in most of the R1 plants (except 9G-21). However, by R3 and in some cases by R2, this product is either absent or only present in very small amounts in all of the lines (Figure 5.3 B and data not shown).

(A)

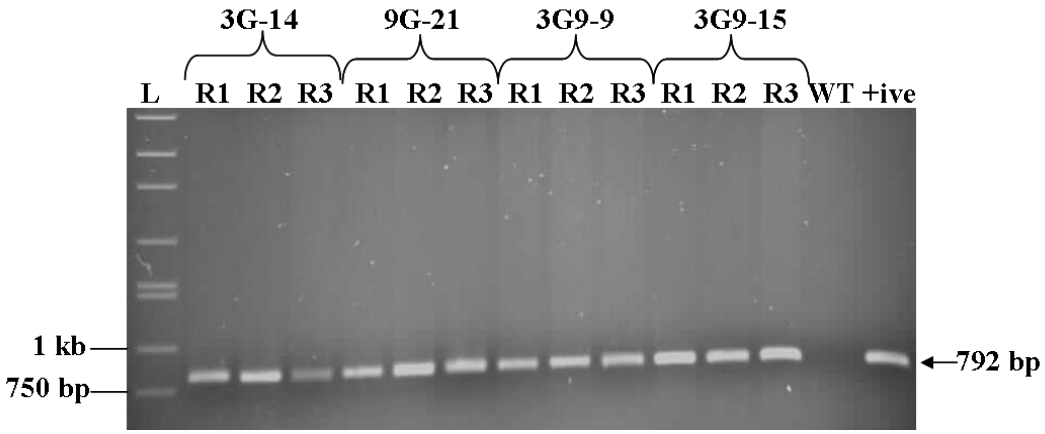

(B)

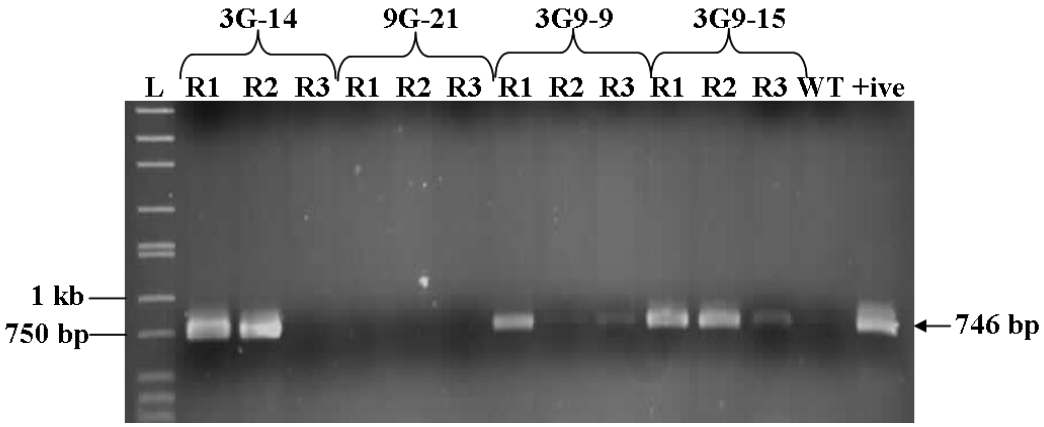

Figure 5.3: PCR analysis of R1, R2 and R3 regenerants for transgenic plant lines 3G-14, 9G-21, 3G9-9 and 3G9-15. (A) PCR products generated using *aadA* gene-specific primers. A product of the expected size (792 bp) was generated in all transgenic plant lines. Lane L: 10 kb ladder (Sigma). Lane WT: Wild type. Lane +ive: pMO9G in *E. coli.* (B) PCR products generated using *gfp* gene-specific primers. A product at the expect size (749 bp) was generated in R1 and R2 3G-14 regenerated transgenic plant lines and in all three rounds of regenerated plant lines for 3G9-9 and 3G9-15. No product was amplified in any of the 9G-21 regenerated plant lines. Lane L: 10 kb ladder (Sigma), Lane WT: Wild type. Lane +ive: pMO9G in *E. coli.*

5.2.3 Southern blot characterisation of regenerating lines (R1-R3) using *aadA*, *gfp* and *psb*C gene-specific probes.

Southern blot analyses using DIG-labelled gene-specific probes confirmed the presence of *aad*A in all of the regenerating plants. However, in addition to the expected hybridization fragments (7.3 kb in 3G9-15, 3G9-14 and 7.1 kb in 3G-14, 9G-21 and G9-4 lines) two unexpected *aadA*-hybridizing fragments were also observed (5.3 kb and 4.5 kb). The 5.3 kb fragment was observed in DNA from all three rounds of regenerated 3G9-15, 3G9-9, 3G-14, 9G-21 and G9-4 plant lines. The 4.5 kb fragment was also detected in these lines however the intensity of this hybridizing fragment is less than that of the 5.3 kb fragment. A representative blot is shown in Figure 5.4 A.

Southern blot analysis using a DIG-labelled *gfp* gene-specific probe indicates loss of *gfp* during the plant regeneration process (Figure 5.4 B). Although no fragment hybridised to the *gfp* probe in 3G9-15 R3 and the 3G9-9 transgenic plants some *gfp* product was amplified by PCR from these lines (Figure 5.3 B) indicating that there are still some *gfp*-containing DNA molecules in these lines – although only detectable with the more sensitive PCR detection method.

The *gfp*-probed blot was stripped and re-probed with a *psbC* gene-specific probe. The *psbC* probe hybridized to the expected 7.1 kb / 7.3 kb fragment in R1 and R2 3G-14 and 3G9-15 plant lines respectively. The probe also hybridized to a 5.3 kb and a 4.5 kb fragment in most of the regenerated plant

(A)

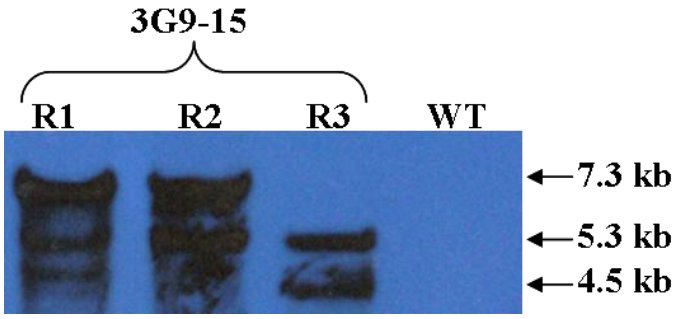

(B)

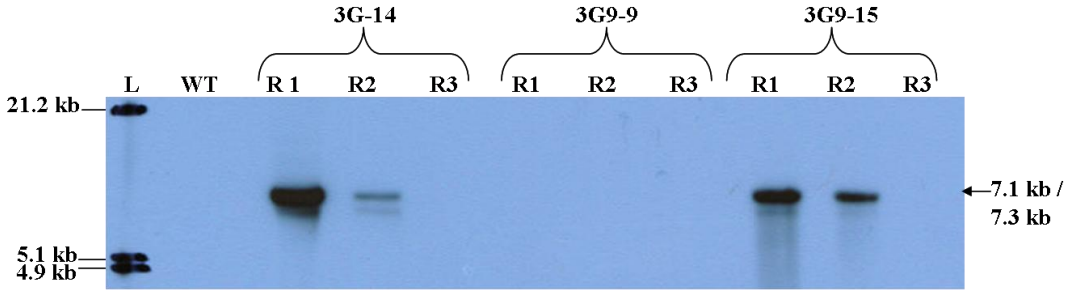

Figure 5.4: Southern blot analysis of R1, R2 and R3 plants for lines 3G-14, 3G9-9 and 3G9-15. (A) Southern blot probed with an *aadA* gene-specific probe. A representative blot (3G9-15) showing the probe hybridizing to the expected 7.3 kb transgenic band in R1 and R2 plant lines. Additional, unexpected fragments (5.3 kb and 4.5 kb) also hybridise to the probe in R1, R2 and R3 regenerated plants. Lane WT: Wild type. Lane L: DIG labelled marker weight III (Roche). (B) Southern blot probed with a *gfp*-specific probe. The *gfp* probe hybridised to fragments of the expected size in 3G-14 R1 and R2 transgenic plants and 3G9-15 R1 and R2 regenerated plants. No hybridisation fragment was detected in the 3G9-9 regenerated plants. Lane WT: Wild type. Lane L: DIG labelled marker weight III (Roche).

lines (Figure 5.5). These fragments are similar in size to those that hybridized to the *aadA* gene-specific probe (Figure 5.4 A).

The combined Southern blot data indicate that the G9, 3G9, 3G and 9G lines are true plastid transformants that contain the *aad*A gene linked to the plastid *psbC* gene and that these lines did not revert to wild-type at any stage during regeneration. The data also indicate that the *gfp*-HA epitope transgene is being lost from several lines during plant regeneration – possibly by some secondary recombination event.

5.2.4 Characterisation of 2^0 recombinant DNA species in the *gfp*/HA epitope transplastomic plants.

The novel hybridization patterns discussed above suggested that the *gfp*/HA epitope transgene may be lost from some plastid transformed lines by secondary recombination events, possibly mediated by plastid gene regulatory elements included on the transformation vector. To address this possibility we identified all possible 2^0 recombination events that could occur across all the plastid gene regulatory elements on the transforming DNA (14 in total). Within these 14 possible 2^0 recombination events we identified four that could result in *aad*A gene retention and *gfp*/HA epitope transgene loss (Figure 5.6). PCR primers were designed to test for the presence of all four possible recombinant plastid DNA populations (Table 5.1) in DNA isolated from 3G9-9 plant lines. PCR analysis of 3G9-9 plant lines with the primer combination psbC-probe-Fw / trnH-Rv amplified a 3.3 kb product indicating that a secondary recombination event had indeed occurred between the TpsbA in the transformation construct

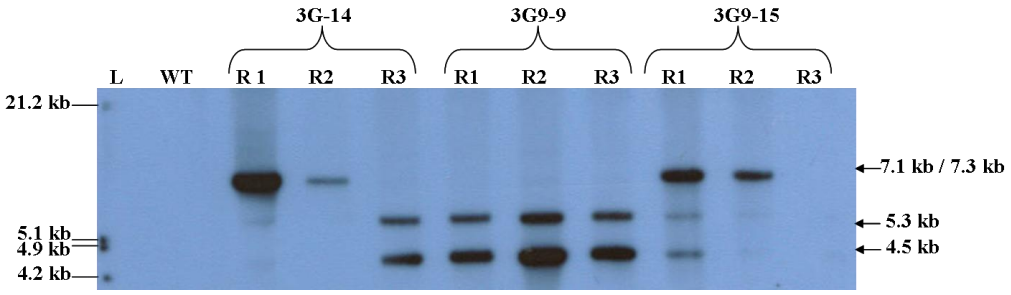

Figure 5.5: R1, R2 and R3 regenerated 3G-14, 3G9-9 and 3G9-15 plant lines hybridised with a *psbC* gene-specific probe. The probe hybridised to fragments of the expected size (7.1 and 7.3 kb) in R1 and R2 3G-14 and R1 and R2 3G9-15 plant lines respectively. Additional hybridisation fragments were also detected at 5.3 kb and 4.5 kb in R3 3G-14, R1, R2 and R3 3G9-9 and in R1 and R2 3G9-15 regenerated plant lines. Lane WT: Wild type. Lane L: DIG labelled marker weight III (Roche).

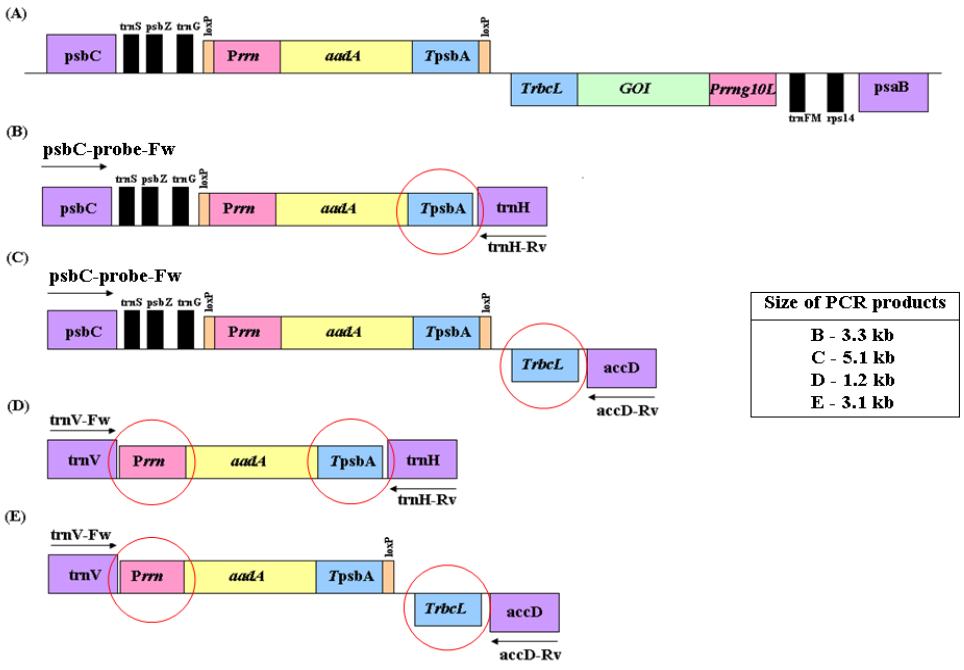

Figure 5.6: Schematic representation (not to scale) of the expected 1^0 recombination event achieved using the transformation vectors described in Chapter 4 (A). Four possible 2^0 recombination events that could achieve *aad*A gene retention and *gfp*-HA epitope gene loss mediated by plastid gene regulatory elements contained within the transforming DNA (B-E). DNA elements circled in red indicate the elements involved in the 2^0 recombination events. The primers used to amplify the fragments resulting from the 2^0 recombination events and the expected PCR product sizes are also indicated.

Table 5.1: PCR primer combinations used to detect the four possible 2^0 recombination events.

Primer Combinations	Corresponding Recombinant Population
psbC-probe-Fw / trnH-Rv	B
psbC-probe-Fw / accD-Rv	C
trnV-Fw / trnH-Rv	D
trnV-Fw / accD-Rv	E

and the native *psb*A gene terminator generating recombinant molecule B (Figure 5.6 and 5.7A). No product was amplified from WT tobacco DNA using this primer pair. PCR using the primer combination trnV-Fw / trnH-Rv amplified a 1.2 kb product indicating that two secondary recombination events had occurred involving the *Prrn* in the transforming DNA and the native *rrn16* promoter and involving the *TpsbA* in the transforming DNA and the native *psb*A gene terminator sequence generating recombinant molecule D (Figure 5.6 and 5.7A). No product was amplified from WT tobacco DNA using this primer combination. PCR analysis of the 3G-14, 3G9-15, G9-4, GFP/HA1-7, GFP/HA1-8 and all 9G3 transgenic plant lines with the primer combinations psbC-probe-Fw / trnH-Rv and trnV-Fw / trnH-Rv also amplified both the 3.3 kb and 1.2 kb products (data not shown). No PCR products were amplified using the primer pairs psbC-probe-Fw/accD-Rv and trnV-Fw / accD-Rv (data not shown).

5.2.4.1 Confirmation of 2^0 recombinant molecules

2^0 recombinant molecules were also assessed for in transgenic 3G-14, 3G9-9, 3G9-15, GFP/HA1-7 and GFP/HA1-8 lines by Southern blot hybridization. Both of the GFP/HA1 transgenic plant lines were included on this blot since it was thought that secondary recombination events could be hindering the recovery of primary transformed shoots with these constructs.

Both of the 2^0 recombinant DNA populations (B and D) identified by PCR involved recombination across TpsbA and were, therefore, predicted to have the

(A)

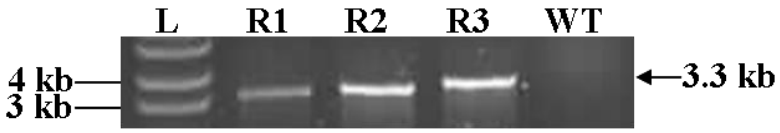

(B)

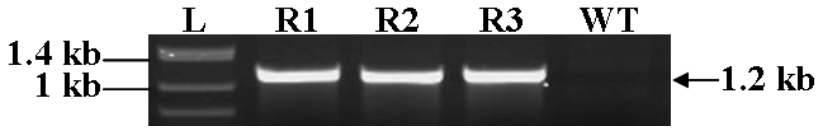

Figure 5.7: Screening 3G9-9 tobacco DNA for secondary recombinant DNA species by PCR (A) PCR product amplified of the expected size (3.3 kb) using the primer combination psbC-probe-Fw / trnH-Rv from 3G9-9 R3 DNA. This PCR product was the result of a recombination event involving the introduced and native copies of the T*psbA*. (B) PCR product at the expected size of 1.2 kb which was amplified using the primers trnV-Fw / trnH-Rv from 3G9-9 R3 DNA. This PCR product was the result of a recombination event between the native and introduced copies of the *Prrn* and the *TpsbA*.

trnH plastid gene flanking the 3' end of the selectable marker gene in these DNA molecules (Figure 5.6). To test for this a DIG-labelled *trnH/rpl2* probe was made. This probe was predicted to hybridize to four *Bam*HI fragments in heteroplasmic transformed plant lines - a 4.8 kb and 4.9 kb fragment in WT DNA (the probe spans one end of the inverted repeat), a 5.3 kb fragment in 2^0 recombinant B-class molecules and to a 4.5 kb fragment in 2^0 recombinant D-class molecules.

The *trnH/rpl2* probe hybridised to a 5.3 kb fragment in all five transgenic plant lines tested confirming a secondary recombination event between the introduced T*psbA* and the native terminator of the *psbA* gene in these lines (recombination event B, Figure 5.8). The probe also hybridised to the 4.8 kb and 4.9 kb WT fragments in all transgenic plant lines. No hybridizing 4.5 kb fragment, unique to the transgenic lines, was observed with the *trnH/rpl2* probe (Figure 5.8). Thus, we are unable to confirm the secondary recombination events between the Prrn in the transforming DNA and the native *rrn16* promoter and between the TpsbA in the transforming DNA and the native psbA gene terminator sequence (recombination event D, Figure 5.8) by Southern blot hybridization even though this was indicated by PCR. Perhaps longer exposure of this blot could have revealed this hybridizing fragment. In hindsight it would have been better to have used a restriction enzyme other than *Bam*HI that could generate fragments with more diversity in size across the predicted *trnH/rpl2* loci for this experiment.

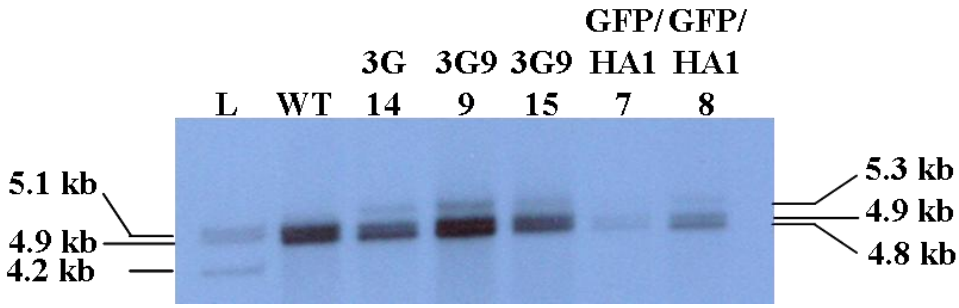

Figure 5.8: Southern blot analysis of transgenic plant lines to confirm secondary recombination events. Southern blot was probed with a *trnH / rps2l* probe. Hybridisation of the probe to a 5.3 kb fragment in all transgenic lines tested confirmed that a secondary recombination event had occurred between the introduced TpsbA and the native psbA gene. The probe also hybridised to a 4.8 kb and 4.9 kb WT fragment in all transgenic lines tested. Lane L: DIG labelled marker weight III (Roche). Lane WT: Wild type.

5.3 Discussion

Transgenes are typically introduced into leaf cell chloroplasts by particle bombardment where integration of the foreign DNA is directed by homologous recombination to a targeted location in the genome due to the presence of homologous flanking DNA sequences. Plastid DNA in the form of regulatory elements (e.g. plastid promoters, 5'UTRs and 3'UTRs) are also incorporated into the plastid transformation vectors for gene regulatory purposes. In 7 of the *gfp*/HA epitope and two GFP/HA1 transgenic plant lines tested here, the *psbA*-derived terminator (T*psbA*) on the transforming *aadA* expression cassette was involved in unintended secondary recombination events resulting in at least two unintended DNA species in transformed plastids. The first 2^0 recombination event was mediated by the introduced T*psbA* within the *aadA* expression cassette in the transforming DNA and the native *psbA* terminator region. The second 2^0 recombination event was mediated by the *Prrn* of the *aadA* cassette and the native *rrn* gene and the introduced and native T*psbA*.

Spectinomycin-resistant shoots that do not contain the transgene of interest can arise from ribosomal point mutations in the 16S rRNA and as shown here from unintended secondary recombination events that lead to deletion of the gene of interest and retention of the selectable marker gene (*aadA*). Typically, the selectable marker gene and the gene of interest are linked in plastid transformation vectors and following genome integration. However in some of the five *gfp/*HA epitope (3G-14, 3G9-9, 3G9-15, G9-4 and 9G-21), all 9G3 and GFP/HA1 transgenic plant lines analysed here, the selectable marker gene is retained while the gene of interest is lost as a result of two unintended secondary

recombination events. While selection pressure from the spectinomycin-containing regeneration medium retains the 2^0 molecules containing the *aadA* gene in addition to WT plastid DNA molecules, the 2^0 molecules that contain the gene of interest unlinked to the selectable marker gene are lost during the selection process. Svab & Maliga (1993) also observed unintended secondary recombination between an introduced T*psbA* and the native *psbA* gene following tobacco plastid transformation resulting in a population of plastids containing the *aadA* gene followed by the *trnH* and the inverted repeat which were maintained by antibiotic selection. In addition, Gray *et al.,* (2009b) also generated a transgenic tobacco plant line (UR-1) which contained an *aadA* gene decoupled from the gene of interest, maintained by antibiotic selection, as a result of an unintended recombination event. Recombination between the *rbcL* derived terminator of the p24 transgene and the native terminator of the plastid *rbcL* gene was also observed by McCabe *et al.*, (2008). However, in this case, the secondary recombination event resulted in the formation of a circularized extra-chromosomal 21 kb DNA molecule which was stably retained *in vivo* without the need for antibiotic selection (McCabe *et al.*, 2008).

Gray *et al.,* (2009b) estimated that each plastid gene regulatory element present on transforming DNA can mediate the formation of at least two DNA species by homologous recombination with native plastid DNA elements. This is only partially supported by this study. Of four 2^0 recombination events predicted to result in the formation of unintended populations of plastid DNAs containing the *aadA* cassette without a linked transgene, only two were confirmed within plastid transformed R3 lines (either by PCR or PCR and Southern blot

hybridisation). One of these events involved recombination between native and introduced T*psbA* elements and another involved recombination between native and introduced T*psbA* and native and introduced P*rrn* elements. However, no 2^0 recombination events involving native or introduced T*rbcL* sequences were detected in any transgenic lines analysed. This suggests that the propensity towards involvement in 2^0 recombination events is not directly related to the length of plastid gene regulatory elements present in transgene expression cassettes. While the T*psbA* is by far the largest element (407 nucleotides) on the transforming DNA used in these studies, T*rbcL* is the next largest element (219 nucleotides), followed by P*rrn* (174 nucleotides). Furthermore, secondary recombination events between sequences as short as 16 bp imperfect repeats have been reported to generate extrachromosomal elements in tobacco (Svab & Maliga, 1993) and regulatory elements as small as 174 bp have been used to intentionally remove selectable marker genes (Iamtham & Day, 2000). Repeated DNA sequences separated by quite large physical distances on the same chloroplast genome can be subject to 2^0 recombination events. Recombination between an introduced *psbA* 3'UTR at the *rbcL/accD* intergenic spacer and the native *psbA* 3'UTR in transformed chloroplast genomes resulted in a large inversion between the native and introduced regulatory elements despite their separation by nearly 60 kb of DNA sequence (Rogalski *et al.*, 2006). Thus, it is not clear to us why no secondary recombination across *TrbcL* was observed – perhaps it was titred out by high rates of recombination across the other homologous DNA elements on the transforming DNA.

It appears that the primary recombination event never occurred in plants transformed with the 9G3 and GFP/HA1 gene constructs as only the secondary recombination events were detected in regenerating lines by PCR. Transformation with the 3G, 3G9 and G9 gene constructs resulted in the intended primary transformation event. However, in some transgenic plant lines, secondary recombination events were detected in subsequent regenerated plant lines, this despite the fact that the transformed plastome remained stable in other transplastomic lines transformed with the same construct. GFP expression was initially observed in all regenerating transplastomic lines transformed with these three gene constructs, however, expression was subsequently lost in these lines. In contrast, only stably transformed transplastomic lines were generated with the G3, 14rHA and 14gHA gene constructs and no secondary recombination events were observed in these lines. Stably transformed transplastomic plants were also generated with the 9G construct with the exception of one plant line (9G-21) where the *aadA* gene was found to be uncoupled. However, the primary recombination event may never have taken place in this line since after the initial PCR analysis to confirm correct integration of the gene construct, the HA91-108/GFP gene could never be detected again suggesting that the initial PCR analysis may have given a false positive result. Gene transcription and recombinant protein accumulation was only detected in 9G, G3, 14rHA and 14gHA transgenic plant lines. Thus, there is a strange correlation between secondary recombination events and transgene transcription in plastid transformed lines. The only lines that generate recombinant protein accumulation (and the transgenes are both transcribed) are lines that exhibit

only the primary recombination event. It is not obvious to us why this correlation might exist or indeed if there is any real validity in this observation.

It has been proposed by Gray *et al*., (2009b) that a low level of unintended recombination events occur in all transplastomic plants and this is supported by the numerous observations of unintended DNA species in transplastomic tobacco lines transformed at multiple different loci and with multiple transgenes (McCabe *et al.*, 2008; Rogalski *et al.*, 2008a; Svab & Maliga, 1993). However, in this study, the level of unintended recombination events was so significant, that the 2^0 recombination events severely hindered efficient recovery of plastid transformed lines containing the desired transgenes and in some cases secondary recombination events resulted in the failure to recover any primary transformed plants as was the case with the 9G3 and GFP/HA1 gene constructs. Alternatively, there may have been severe selection against the primary recombination event because of the nature of the transgene in some lines. Unintended recombination events between native and introduced gene regulatory elements were observed regardless of the transgene used. One way to obviate this problem might be to use non-plastid gene regulatory elements in plastid transformation vectors where possible e.g. the bacterial *trc* promoter (Newell *et al.*, 2003), the mitochondrial *atpA* promoter (Bohne *et al.*, 2007), a T7 promoter in conjunction with a plastid-targeted, nuclear-encoded T7 RNA polymerase (McBride *et al.*, 1994), the *E. coli rrnB* terminator (Newell *et al.*, 2003) and thus facilitate a higher efficiency of selection and regeneration of primary transformants.

Chapter 6
Optimisation of conditions required for biolistic-mediated transformation of lettuce and trial bombardments

6 Optimisation of conditions required for biolistic-mediated transformation of lettuce and trial bombardments

6.1 Introduction

Lettuce (*Lactuca sativa* L.) is a crop plant belonging to the Asteraceae. Humans consume the leaves raw, and the time from seed to edible biomass is weeks compared to months for crops such as tomato, potato or carrot (Lelivelt *et al.*, 2005). In addition, lettuce is well suited for indoor cultivation by hydroculture systems limiting the possibility of horizontal transgene propagation (Kanamoto *et al.*, 2006).

Lettuce has previously been engineered to contain agronomically important transgenes via nuclear transformation. Resistance to bialaphos, a broad-spectrum herbicide, was introduced into *Lactuca sativa* cv. Evola by *Agrobacterium tumefaciens*-mediated transformation using gene constructs containing the bialaphos resistance (*bar*) and neomycin phosphotransferase (*nptII*) genes (Mohapatra *et al.*, 1999). Stable expression of the BAR protein was observed and the presence of NPTII protein and PAT enzyme activity were demonstrated by ELISA and PAT enzyme assay respectively. Transgenic lettuce plants have also been engineered to accumulate the iron storage protein ferritin *via Agrobacterium tumefaciens*-mediated transformation using a gene construct containing the soybean ferritin cDNA (Goto *et al.*, 2000). Western-blot analysis showed that transgenic lettuce plants contained iron levels ranging from 1.2 to 1.7 times that of the control plants and that the growth of transgenic plants was enhanced at early developmental stages, resulting in plant fresh weights 27–

42% greater than those of control plants. These transgenic lettuce had photosynthesis rates superior to those of the controls, and grew larger and faster compared with the controls during the period of 3 months from germination. An *ipt* gene, which encodes isopentenyl phosphotransferase, under the control of the senescence-specific SAG12 promoter from *Arabidopsis* (PSAG12-IPT) was shown to significantly delay developmental and postharvest leaf senescence in mature heads of transgenic lettuce (*Lactuca sativa* L. cv Evola) which were homozygous for the transgene (McCabe *et al.*, 2001).

Lettuce has also been engineered to produce plant-based antigens *via* nuclear transformation including a hepatitis B virus subunit vaccine (Kapusta *et al.*, 1999). Lettuce nuclear transformation with a transgene coding for a synthetic cholera toxin B subunit (CTB) protein resulted in accumulation levels of 0.24% TSP in transgenic plants (Kim *et al.*, 2006). The measles virus hemagglutinin (MV-H) protein was also successfully expressed in transgenic lettuce *via* nuclear transformation and was found to be immunogenic in mice (Webster *et al.*, 2006). Lettuce extracts containing the MV-H protein induced measles virus neutralising antibodies following intraperitoneal injection and intranasal inoculation of mice. More recently, an immunogenic fusion protein (F1-V) from *Y. pesti* was introduced into lettuce *via Agrobacterium*-mediated transformation (Rosales-Mendoza *et al.*, 2010). Although the F1-V protein accumulation levels in lettuce was only 0.08% TSP, mice immunized subcutaneously lettuce TSP developed systemic humoral responses indicating the potential of using lettuce as a production platform for recombinant antigens (Rosales-Mendoza *et al.*, 2010). However, plant nuclear transformation has its disadvantages. As seen

with the F1-V protein, recombinant protein accumulation levels are typically quite low (usually <1% TSP; Daniell *et al.,* 2009). Other disadvantages include minimal transgene containment, positional effects and potential gene silencing (Ruhlman *et al.*, 2007).

Chloroplast transformation can overcome these disadvantages, however despite this, plastid transformation is only routinely used in tobacco (*Nicotiana tabacum*). Although the efficiency of plastid transformation in tobacco is high (1-14 transformants per bombardment), the development of efficient chloroplast transformation procedures for other plant and crop species is severely limited by low transformation efficiencies (Daniell *et al.*, 2001b; Maliga, 2003). For example, tomato plastid transformation efficiency is about 1 transformant per 10 bombardments (Ruf *et al.*, 2001). The efficiency of plastid transformation in eggplant (*Solanum melongena* L.) is similar to tomato - one transformant per 10.5 bombardments (Singh *et al.*, 2010). The efficiency of sugarbeet plastid transformation is even lower still – estimated at one transformant per 36 bombarded plates (De Marchis *et al.*, 2009). The low recovery of transplastomic shoots can be attributed to several factors including the efficiency of the regeneration protocol. The plastid transformation efficiency in potato was initially reported as one transgenic event per 15 - 30 bombarded plates (Sidorov *et al.*, 1999). This efficiency was increased to one transgenic event per bombardment by improving the regeneration procedure for potato and by using a potato-specific transformation vector (Valkov *et al.*, 2011).

Chloroplast transformation of lettuce was first achieved using the polyethylene glycol (PEG)-mediated transformation system (Lelivelt *et al.*, 2005). This method involves the enzymatic removal of the cell wall to obtain protoplasts and the exposure of these protoplasts to transforming DNA in the presence of PEG. The PEG-mediated transformation system generated fertile, homoplasmic chloroplast transformed lines containing the influenza *HA* gene (Lelivelt *et al.*, 2005). Although PEG-mediated lettuce plastid transformation is possible, the system is not without its drawbacks. Producing sufficient amounts of high quality protoplasts is laborious and technically demanding. PEG treatment can result in protoplast fusion events that generate polyploid cells at a very high frequency. It is relatively difficult to regenerate shoots from polyploid cells and when they do regenerate the plants are usually infertile. Transplastomic lettuce callus was obtained by PEG-mediated transformation using a *gfp* gene construct and GFP accumulated to 1% TSP in the callus tissue. However, all of the transformed callus material was polyploid and transformed plants were not regenerated (Lelivelt *et al.*, 2005).

In contrast to PEG-mediated transformation the biolistics system is technically less demanding, the problems of polyploidy do not arise and the time from transformation to regenerated plastid-transformed shoots is only weeks rather than months (Nugent & Joyce, 2005). To establish a successful and reliable chloroplast transformation protocol for any species using biolistics, it is necessary to optimise both the physical parameters of the gene gun and the biological parameters associated with the target tissue. These include (1) the selection of target tissue which contains cells competent for plant regeneration

(2) the efficient introduction of the transforming DNA into the plastid by particle bombardment and (3) the optimisation of regeneration conditions for the selection of cells containing transformed plastids. Lettuce is extremely amenable to manipulation in tissue culture and plants can readily be regenerated from many types of explants including protoplasts (Lelivelt *et al.*, 2005), leaves (Kanamoto *et al.,* 2006; Ruhlman *et al.,* 2007; Ruhlman *et al.,* 2010) and cotyledons (Webster *et al.,* 2006). Achieving plastid-localization of transgenes requires optimization of bombardment parameters – including best choice of microcarrier, size of microcarrier, delivery of microcarrier etc. Tissue culture and plant regeneration are essential elements of plant transformation strategies, but can frequently prove to be one of the most challenging aspects of the plant transformation process. Plant growth regulators are essential elements in culture media and are critical for determining the eventual developmental pathway of plant cells. However, predicting the eventual effects of plant growth regulators can prove to be a difficult task due to the vast differences in hormone responses between species.

The aim of this work was to develop a biolistic-mediated plastid transformation system for lettuce. To this end we set out to assess the suitability (or otherwise) of cotyledons and cotyledon-derived callus as candidate regenerating explants for two lettuce cultivars Flora and Evola. A *GFP*-reporter gene construct was used to optimise biolistic conditions required for efficient delivery of the transgene to the plastid in lettuce cotyledons. Optimized plant regenerating conditions and biolistic parameters were subsequently used for trial biolistics-mediated lettuce chloroplast transformation experiments. During the course of

this work, successful biolistics-mediated lettuce chloroplast transformation was reported by two other research groups (Kanamoto *et al.*, 2006; Ruhlman *et al.*, 2007; Ruhlman *et al.*, 2010). At this stage the focus of the work switched to trying to achieve lettuce plastid transformation using the published methodologies. However, to date, this has not yet been achieved.

6.2 Results

As a preliminary to developing a chloroplast transformation system for lettuce, two different methods for plant regeneration were tested for two cultivars of lettuce. The suitability of cotyledon-derived callus and cotyledons for the cultivars Flora and Evola was assessed as candidate regenerating explants. Firstly, cotyledons for each cultivar were placed on MS media containing different combinations and concentrations of the plant growth regulators, 2,4-D, kinetin, zeatin and NAA to assess their ability to induce and maintain callus formation. Cotyledons were chosen as the explant of choice as they have been reported to be the most responsive seedling organ (Webb, 1992) resulting in readily regenerated shoots within a short space of time (Davey *et al.*, 2001). Subsequently, cotyledon-derived calli were then placed on MS media containing different combinations and concentrations of the plant growth regulators, kinetin, NAA and BAP in order to assess their ability to produce shoots. Secondly cotyledons were placed on MS media containing different combinations and concentration of the plant growth regulators NAA, kinetin and BAP to assess their ability to produce shoots and the frequency of shoot regeneration directly from cotyledons.

6.2.1 Shoot regeneration from cotyledon-derived callus (Method 1)

6.2.1.1 Callus formation from cotyledons

21 concentrations and combinations of plant growth regulators (Table **6.1**) were assessed for their ability to induce and maintain callus formation from cotyledon

.

Table 6.1: The concentrations and combinations of plant growth regulators, added to basic MS medium to induce and maintain callus formation.

Treatment Number	2,4-D (mg/L)	Kinetin (mg/L)	NAA (mg/L)	Zeatin (mg/L)
1	0.5	5	-	-
2	0.1	2	-	-
3	0.1	0.5	-	-
4	5	0.5	-	-
5	0.1	-	-	1
6	0.1	-	-	3
7	-	2	2	-
8	-	2	5	-
9	-	5	0.5	-
10	2	5	-	-
11	2	2	-	-
12	2	0.5	-	-
13	5	0.5	-	-
14	5	5	-	-
15	0.1	-	-	0.1
16	2	-	-	0.1
17	2	-	-	1
18	2	-	-	3
19	5	-	-	0.1
20	5	-	-	1
21	5	-	-	3

explants of the lettuce cultivars, Flora and Evola. Cotyledons from six-day old seedlings were excised at the petioles and scored laterally across the midrib with the blunt side of a scalpel blade. The cotyledons were placed, wounded side down, into 9 cm Petri dishes containing a basic MS medium supplemented with various combinations and concentrations of the plant growth regulators 2,4-D, kinetin, NAA and zeatin. Callus formation was generally initiated at the cut edges of the explants after seven days of culture and eventually extended all over the explants. The efficiency of callus formation under various hormone treatments was assessed by weighing the cotyledon + callus material after a four-week culturing period.

Distinct differences in the extent of callus formation were observed among the 21 treatments. Of the 21 hormonal treatments assessed, six induced and maintained callus formation for both cultivars. These were 0.5 mg/L 2,4-D & 5 mg/L kinetin (treatment 1); 0.1 mg/L 2,4-D & 2 mg/L kinetin (treatment 2); 0.1 mg/L 2,4-D & 0.5 mg/L kinetin (treatment 3); 5 mg/L NAA & 0.5 mg/L kinetin (treatment 4); 0.1 mg/L 2,4-D & 1 mg/L zeatin (treatment 5); and 0.1 mg/L 2,4-D & 3 mg/L zeatin (treatment 6). Of these six hormonal treatments, treatment 2 (0.1 mg/L 2,4-D & 2mg/L kinetin) and treatment 5 (0.1 mg/L 2,4-D & 1 mg/L zeatin) generated the greatest amount of callus per cotyledon explant for Flora and Evola respectively (Figure 6.1). Both combinations of plant growth regulators induced extensive callus formation in 100% of all explants after the four week culturing period. Evola cotyledons cultured on media containing treatment 6 (0.1 mg/L 2,4-D & 3 mg/L zeatin) also produced a lot of callus per cotyledon.

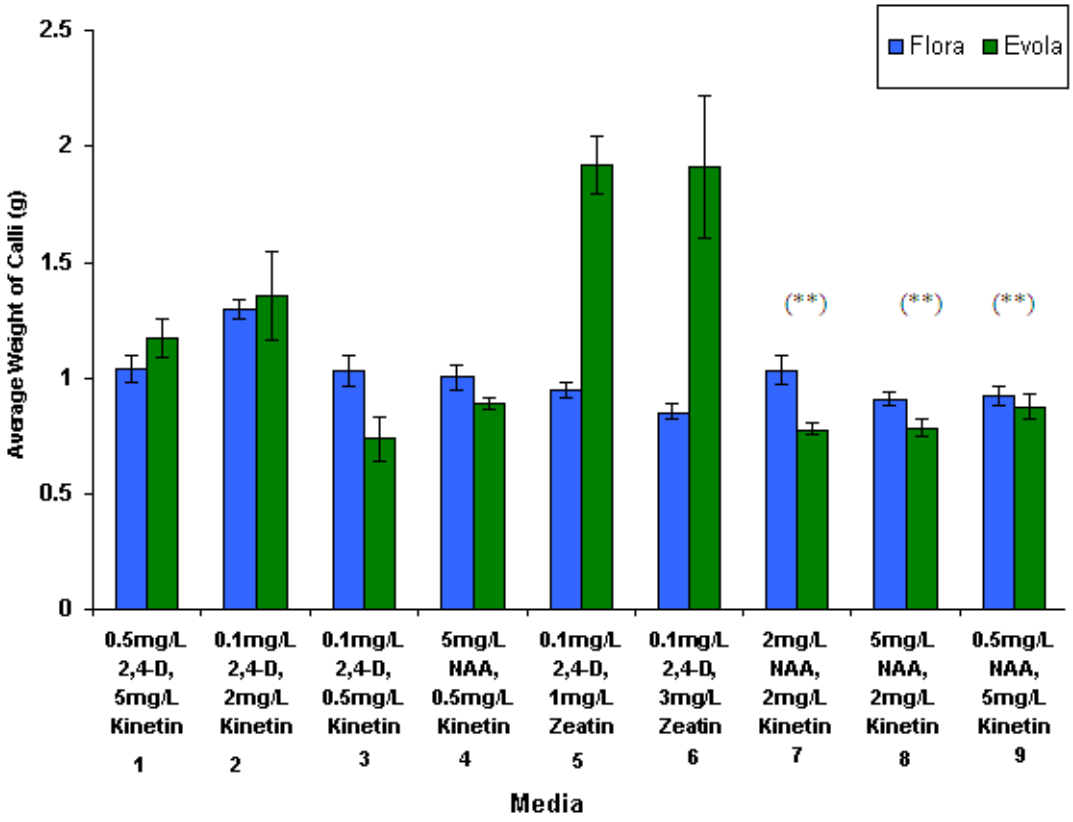

Figure 6.1: The average weight of cotyledon + callus produced per cotyledon after a four week period on media containing different combinations and concentrations of 2,4-D, kinetin, zeatin and NAA.
(**) indicates explants that only produced callus at wounding sites at the end of the four week incubation period.

Three other plant growth regulator treatments induced callus formation, 2 mg/L NAA & 2 mg/L kinetin (treatment 7); 5 mg/L NAA &2 mg/L kinetin (treatment 8) and 0.5 mg/L NAA & 5 mg/L kinetin (treatment 9). However, callus formation was observed only at the sites of wounding and at the site where the cotyledon had been excised. As extensive callus formation was not observed over the whole cotyledon surface by the end of the four-week culturing period, the calli produced by these three media were not studied any further. Cotyledon explants cultured on the other twelve hormonal treatments (10-21) formed almost no calli and turned yellow and necrotic after two-three weeks.

The consistency and appearance of callus material generated under each of the hormone treatments was also noted. The type of callus produced fell into two categories: (i) friable callus, yellow/brown in colour (Figure 6.2 A) and (ii) green, firm, compact callus (Figure 6.2 B). Treatments 1, 5 and 6 formed friable callus. Treatments 2, 3 and 4 produced green, compact callus bearing shoot primordia after the four week culturing period

6.2.1.2 Shoot regeneration from cotyledon-derived callus

Four-week old calli were transferred to 9 cm Petri dishes containing a basic MS medium supplemented with two combinations of the plant growth regulators kinetin, NAA and BAP to assess shoot regeneration (Table 6.2). The calli were sub-cultured every 14 days on these shooting media. Four weeks after the initial transfer to shooting media, the amount of shoot proliferation was recorded. The efficiency of shoot regeneration was assessed by comparing the mean number of shoots produced per callus over a four-week period. Cotyledon derived calli

(A)

(B)

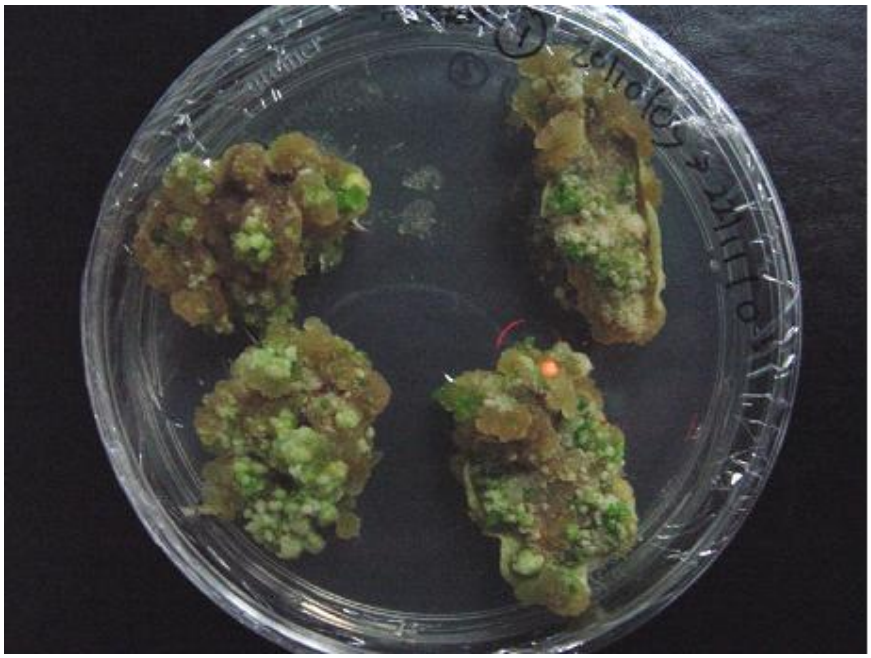

Figure 6.2: Callus formation from cotyledons cultured in a 9cm Petri dish. (A) Friable yellow/brown callus (cv. Flora) formation at the end of a four week culturing period on medium supplement with treatment 1 (B) Green nodular callus (cv Evola) bearing shoot primordia at the end of a four week culturing period on medium supplemented with treatment 4.

Table 6.2: The concentrations and combinations of plant growth regulators added to the basic MS medium to induce shoot formation from callus.

Treatment Number	Kinetin (mg/L)	NAA (mg/L)	BAP (mg/L)
SIM1	0.5	0.5	-
SIM2	-	0.04	0.5

from treatments 1, 2, 3, 4, 5 and 6 were transferred to shoot induction media SIM1 and SIM2**.** SIM2 gave the most shoot regeneration (Figure 6.3 B) from callus irrespective of the cultivar used when compared to SIM1 (Figure 6.3 A). SIM2 induced the most shoots per callus for Flora calli initiated under treatment 2 (an average of 43.8 shoots per callus) and Evola calli under treatment 3 (an average of 19.75 shoots per callus). Calli initiated for both cultivars on treatments 5 and 6 failed to produce any shoots over the four-week culturing period following transfer to SIM1 and SIM2.

6.2.2 Shoot regeneration directly from cotyledon explants (Method 2)

Cotyledons from six-day old seedlings were excised at the petioles and scored laterally across the midrib with the blunt side of a scalpel blade. The cotyledons were placed, wounded side down, onto MS medium with different combinations and concentrations of plant growth regulators kinetin and NAA (Table 6.3). The dishes were sealed with plastic wrap and placed in a growth room for four weeks at which time the amount of shoot regeneration per explant was recorded. The efficiency of shoot regeneration was analysed by comparing the mean number of shoots produced per cotyledon over a four week period.

Two combinations of plant growth regulators, 2 mg/L NAA & 0.5 mg/L kinetin (treatment 23) and 0.5 mg/L NAA & 2 mg/L kinetin (treatment 24) stimulated the formation of callus from cotyledons instead of shoots. Of the remaining four plant growth regulator combinations, treatment SIM1 (0.5 mg/L kinetin & 0.5 mg/L NAA) achieved the highest shoot regeneration efficiency – an average of 15.6 shoots per cotyledon for Flora, and 53 shoots per cotyledon for Evola at the

(**A)**

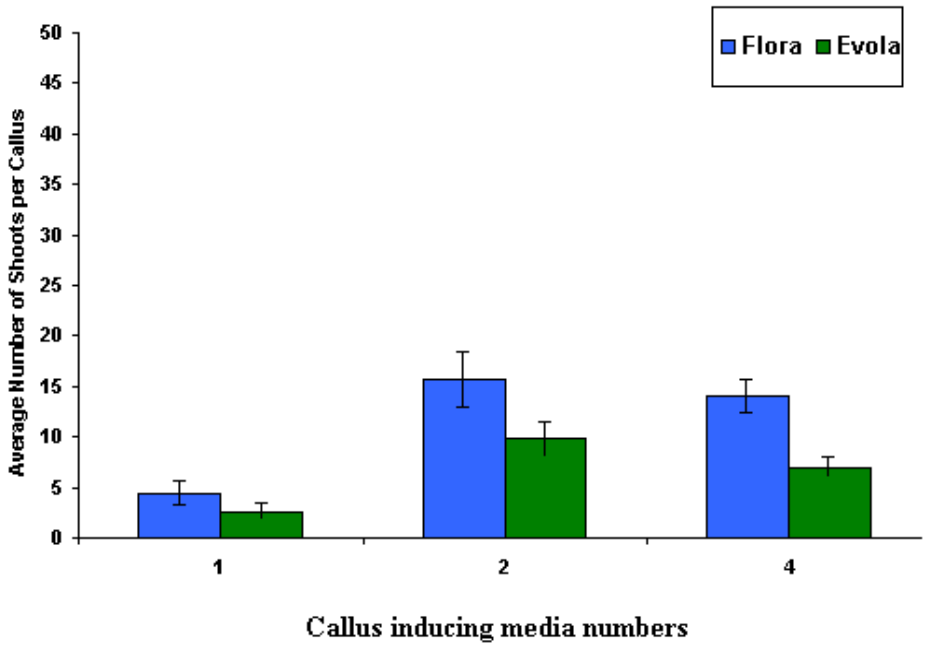

(B)

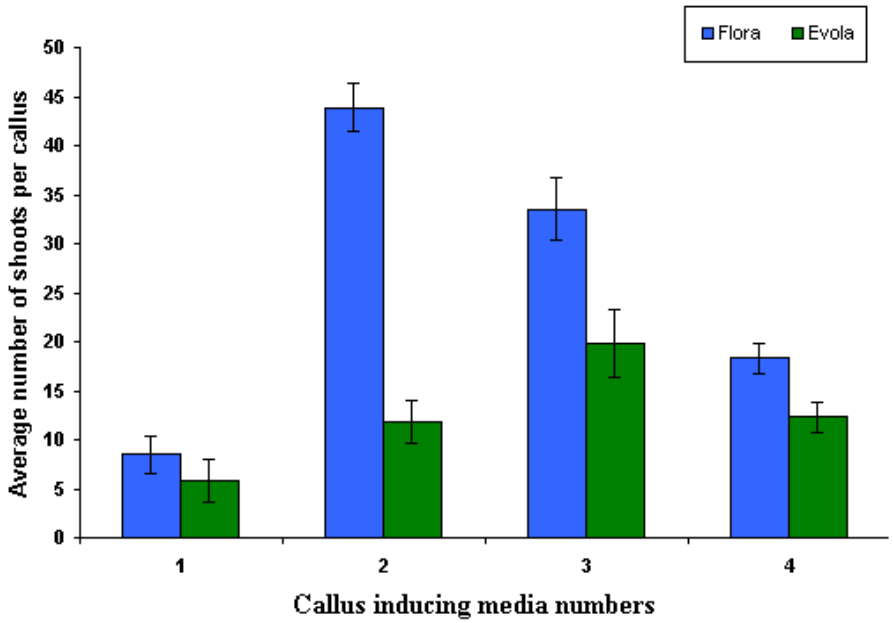

Figure 6.3: The average number of shoots produced per calli over a four week period. (A) The average number of shoots obtained per four-week old callus after transfer to shooting medium containing 0.5 mg/L kinetin and 0.5 mg/L BAP (SIM1). (B) The average number of shoots obtained per four-week old callus after transfer to shooting medium containing 0.04 mg/L NAA and 0.5 mg/L BAP (SIM2)

Table 6.3: The concentrations and combinations of plant growth regulators added to basic MS medium to induce shoot formation directly from cotyledon explants from both cultivars; Flora and Evola

Treatment Number	Kinetin (mg/L)	NAA (mg/L)
SIM1	0.5	0.5
23	0.5	2
24	2	0.5
25	0.5	5
26	5	2
27	5	5

end of the eight week culturing period (Figure 6.4 A). Treatments 25, 26 and 27 failed to produce enough shoots to analyse. To see if shoot regeneration could be obtained from callus initiated on treatments 23 and 24, the calli were placed on media containing SIM1 and SIM2. SIM1 produced the most shoots per callus (Evola) initiated on treatment 23 (Figure 6.4 A) and SIM2 produced the most shoots per callus for both Flora and Evola on treatment 24 (Figure 6.4 B). A representation of shoots produced can be seen in Figure 6.5.

6.2.2.1 Root formation of shoots regenerated from cotyledons and cotyledon-derived callus

A selection of shoots produced from both cotyledon, and cotyledon derived callus, were placed in tubs containing a basic MS medium to induce root formation. All shoots produced directly from cotyledons and from cotyledon derived callus for both cultivars formed roots and grew on the medium.

6.2.2.2 Regeneration results

Based on comparative analyses of the shoot regeneration methods, it was decided that the best strategy to employ for lettuce plastid transformation would be to bombard cotyledons and induce callus formation using callus inducing medium 2 (CIM2) prior to shoot induction on shoot inducing medium 2 (SIM2). The rational for this decision being that the longer the bombarded explants were maintained after chloroplast transformation, the greater the probability of accumulating homoplasmic chloroplasts-transformed lines after shoot regeneration.

(A)

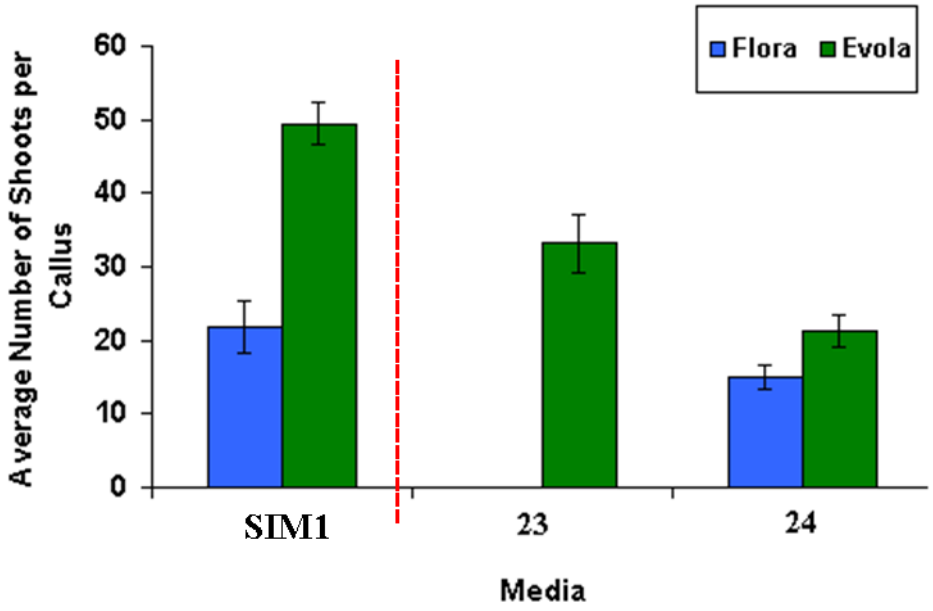

(B)

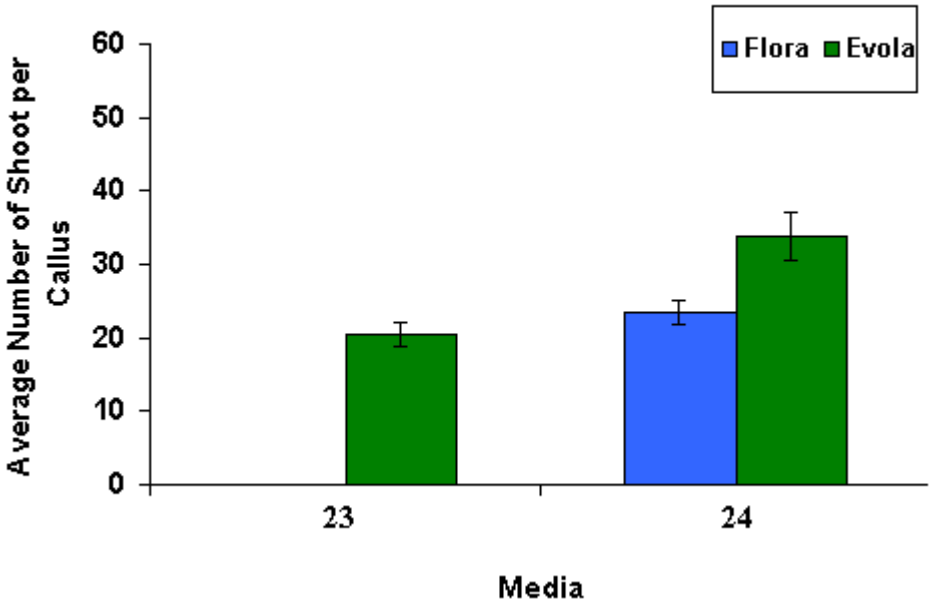

Figure 6.4: The average number of shoots produced following incubation on shoot inducing media SIM1 and SIM2 (A) The average number of shoots obtained directly from cotyledon explants (SIM1) and from calli produced by treatments 23 and 24 after transfer to shoot inducing medium containing 0.5 mg/L kinetin and 0.5 mg/L BAP (SIM1). (B) The average number of shoots obtained per four-week old callus after transfer to shoot inducing medium containing 0.04 mg/L NAA and 0.5 mg/L BAP (SIM2).

(A)

(B)

Figure 6.5: A representation of shoots produced following incubation on shoot inducing media. (A) Shoots regenerating directly from cotyledon (cv Flora). Photo taken approximately five weeks after culturing on shoot inducing medium. (B) Shoots regeneration from cotyledon derived callus (cv Evola) four weeks after transfer to shoot inducing medium supplemented with 0.04 mg/L NAA & 0.5 mg/L BAP (SIM2). Both photos were taken on a Siemens camera.

6.2.3 Optimisation of gene gun parameters

To choose optimal biolistics parameters, transient lettuce plastid transformation was carried out using a *gfp* gene construct (Lelivelt *et al.,* 2005). Lettuce cotyledons were bombarded with the pLCV2-GFP/aadA vector (Figure 6.6) using two different sizes of gold particles (0.6 μM & 1.0 μM) and three different gene-gun pressures (650 psi, 900 psi & 1100 psi). The efficiency of transformation was assessed by counting the number of plastids in the bombarded tissue showing GFP fluorescence 24 hours after bombardment.

6.2.3.1 Analysis of GFP plastid localisation

24 hours after bombardment, GFP was assessed for in plastids using a conventional fluorescence microscope. The efficiency of transformation was determined by counting the number of plastids expressing GFP / treatment. Table 6.4 summarises the results of these experiments.

Plastids expressing GFP were found in tissue bombarded under each set of parameters used. The highest number of transformation events (26 fluorescing plastids recorded) was observed after bombardment with 0.6 μM gold particles at 900 psi. The lowest number of transformation events (1 fluorescing plastid recorded) was observed following bombardment using 1 μM gold particles at 650 psi. A two-fold increase in the transformation frequency was observed after bombardment with 0.6 μM gold particles compared to 1 μM gold particles at 900 psi. In contrast, there was no significant difference observed after

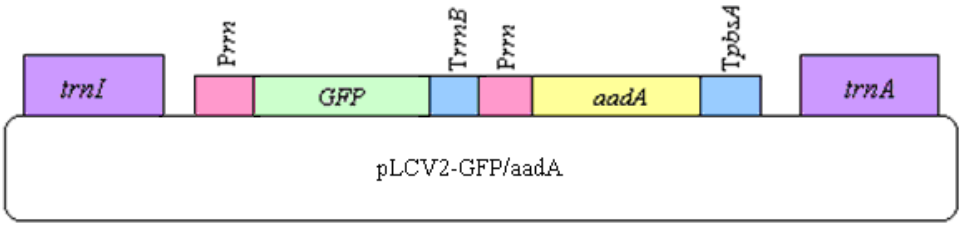

Figure 6.6: Schematic representation of the pLCV2-GFP/aadA lettuce chloroplast transformation vector. The vector contains two expression cassettes. The transgene cassette contains the tobacco *rrn* promoter (P*rrn*), the sm*GFP* gene and the *E.coli rrnB* terminator (T*rrnB*). The second cassette contains the *rrn* promoter (P*rrn*), the selectable marker gene *aadA* and the tobacco 3' UTR from the *pbsA* gene (T*pbsA*). The two expression cassettes are flanked by lettuce chloroplast DNA targeting sequences, the *trnI* and the *trnA* genes to facilitate homologous recombination.

Table 6.4: The number of transformation events obtained following bombardment with different combinations of gold particle size and gene-gun pressure.

Bombardment Pressure	**Bombardment Distance**	**Gold Particle Size (μM)**	**# Events per 50μl**
650 psi	6 cm	0.6 1.0	2 1
900 psi	6 cm	0.6 1.0	26 13
1100 psi	6 cm	0.6 1.0	11 16

bombardments at 650 psi and 1100 psi, regardless of the particle size used in either case. This experiment indicated the optimal conditions for delivering transforming DNA to lettuce chloroplasts to be 900 psi, 0.6 μM gold particles and a target distance of 6 cm. These conditions were used in all subsequent biolistics experiments.

6.2.4 Biolistics-mediated plastid transformation of lettuce tissue

Large-scale plasmid DNA preparations of the pLCV5-p24 transformation vector (kindly supplied by Dr. Bridget Hogg, NUI Maynooth) (Figure **6.7**) were prepared. This transforming DNA was bombarded at Flora and Evola lettuce cotyledon tissue on the surface of 0.6 μM gold particles using the Bio-Rad PDS-1000 He gun using 900 psi rupture discs and a target distance of 6 cm (as outlined in section 2.9.6). Following bombardment, the cotyledons were placed in the dark for two days. Cotyledons were then scored across the midrib and placed on callus inducing medium 2 (CIM2) containing 500 mg/L spectinomycin. The first spectinomycin resistant calli were visible after approximately eight - nine weeks. Spectinomycin resistant calli were subsequently transferred to shoot inducing medium 2 (SIM2) for shoot production. Shoots were then transferred to MS medium containing 500 mg/L spectinomycin for root production (Figure 6.8).

6.2.4.1 Molecular characterisation of spectinomycin resistant shoots

Total DNA was extracted from regenerated spectinomycin-resistant shoots and was subjected to PCR analysis using a combination of both gene specific

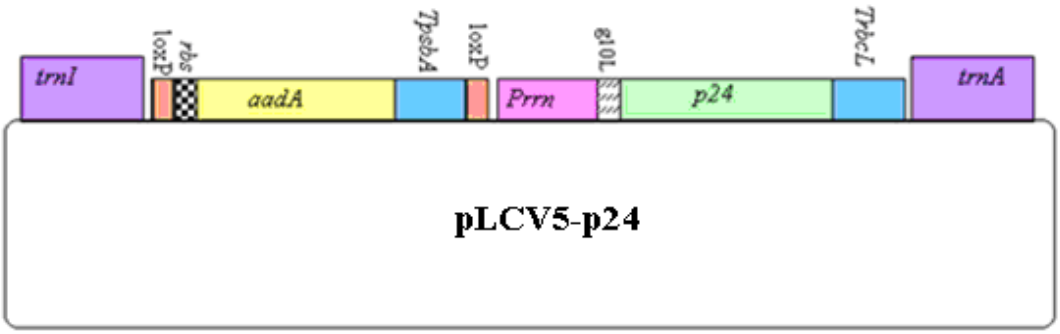

Figure 6.7: Schematic representation of the lettuce chloroplast vector pLCV5-P24. The pLCV5-P24 vector is targeted to the intergenic region between the *trnI* and *trnA* genes. The selectable marker gene *aadA* is driven by the strong constitutive 16s ribosomal RNA operon promoter *Prrn*, fused to the 3' UTR from the *psbA* gene (T*psbA*). The *aad*A expression cassette is flanked by two loxP sites to allow marker gene removal by Cre-mediated site-specific recombination. The transgene expression cassette consists of the ribosomal RNA operon promoter, *Prrn*, fused to the 5' leader from the gene 10 of phage T7 (g10L), the codon optimised HIV-1 p24 gene and the 3' UTR of the plastid rubisco large subunit gene (T*rbcL*).

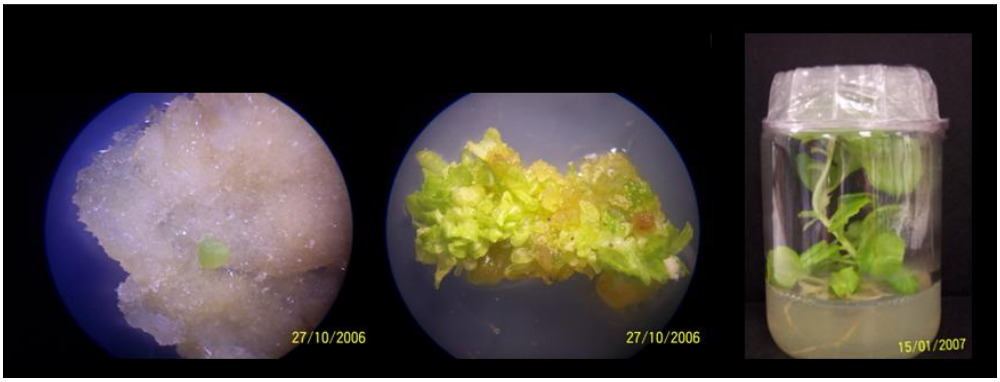

Figure 6.8: Images of a spectinomycin-resistant lettuce (cv. Flora) cell line (20X), regenerating spectinomycin resistant lettuce shoots (20X) and rooted spectinomycin resistant lettuce shoot (Picture taken with Siemens camera).

internal primers (aadA-For, and aadA-Rev, p24-For and p24-Rev) and external primers (Let-Ex-For and Let-Ex-Rev) that flank the vector integration site on the lettuce chloroplast genome.

6.2.4.2 Characterisation of pLCV5-p24 spectinomycin resistant shoots

DNA from three spectinomycin-resistant shoots was analysed by PCR to determine if the transgenes had integrated into the plastome and at the expected integration site. PCR using *aad*A gene specific primers generated a PCR product of the expected size (792 bp) in all three primary regenerated shoots (Figure 6.9 A). PCR using the primer pair p24-For and p24-Rev produced a product of the expected size (750 bp) in all three primary regenerated shoots tested (Figure 6.9 B). However, a third PCR performed using primers flanking the vector integration site (Let-Ex-For and Let-Ex-Rev), revealed that these shoots were not plastid transformants (data not shown).

6.2.4.3 Bombardment of lettuce using alternative explants and regeneration media.

During the course of this work, biolistics-mediated chloroplast transformation of lettuce was reported by two groups Kanamoto *et al.,* (2006) and Ruhlman *et al.*, (2007). In the method described by Kanamoto *et al.,* (2006) bombarded leaves were regenerated on basic MS medium supplemented with 0.1 mg/L BAP and 0.1 mg/L NAA (lettuce regeneration (LR) medium). The method of Ruhlman *et al.,* (2007) used a modified lettuce regeneration medium (LRM: MS supplemented with 0.1 mg/L NAA and 0.2 mg/L BAP) for shoot regeneration

(A)

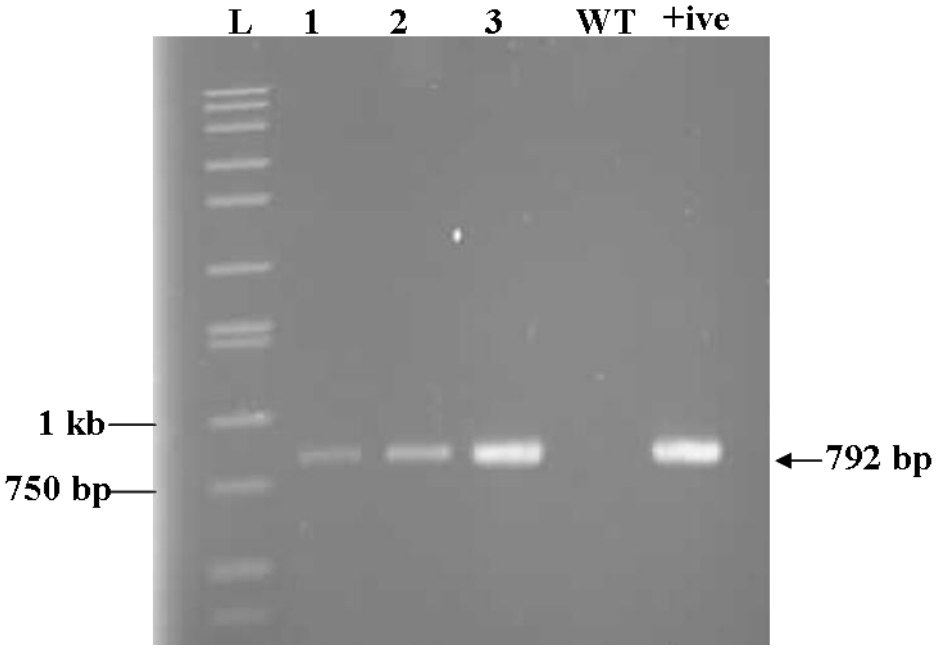

(B)

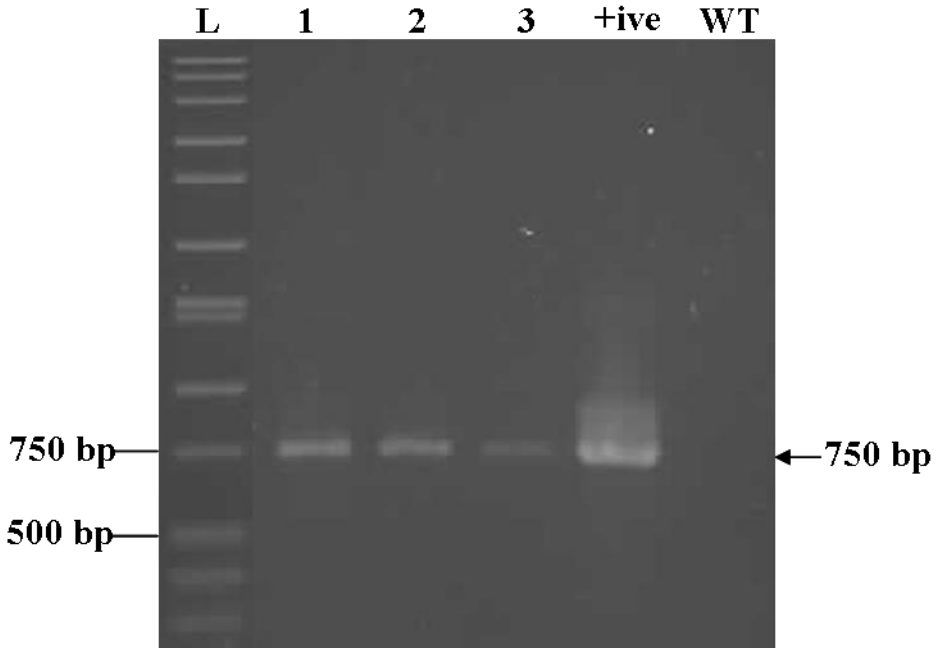

Figure 6.9: PCR analysis of putative pLCV5-p24 plants. (A) Primers aadA-For and aadA-Rev were used to confirm integration of the *aadA* gene. The expected fragment size of 792 bp was amplified in all three plants. (B) Primers p24-For and p24-Rev were used to confirm integration of the *p24* gene. The expected fragment size of 750 bp was amplified in all three plants. Lane L: 10 kb ladder (Sigma) Lanes 1-3: p24-1, p24-2 and p24-3. Lane WT: Wild type cv Flora (Negative control). Lane +ive: pLCV5-p24 in *E. coli*.

for the cultivar Simpson Elite. We used both these methods using a variety of lettuce transformation vectors and a range of lettuce cultivars to try and achieve biolistic-mediated lettuce plastid transformation (summarised in Table 6.5). However, no spectinomycin-resistant shoots were obtained following any of these bombardments.

6.3 Discussion

Tobacco plastid transformation is now an established technique used in many labs. Plastid transformation efficiency in tobacco is very high, approximately 1-14 events per bombardment (Daniell *et al.*, 2001b; Maliga, 2003). However, transformation efficiency in other plants and crops is generally low in comparison. As the efficiency of shoot regeneration (an important step in the transformation process) is known to be dependent on both the cultivar and the hormonal composition of the medium (Kanamoto *et al.*, 2006), one way to improve transformation efficiency is to ensure that an optimal and efficient regeneration protocol is in place. In order to develop a protocol for biolistics-mediated lettuce plastid transformation, the regeneration efficiency for two lettuce cultivars, Flora and Evola, was examined using different combinations of growth regulators.

Two regeneration methods were tested; (1) shoot regeneration from cotyledon-derived callus and (2) shoot regeneration directly from cotyledon explants. A total of 21 growth regulator treatments were analysed for their ability to induce and maintain callus on cotyledon explants. Six of the 21 treatments induced and maintain callus formation. 0.1 mg/L 2,4-D in combination with 2 mg/L kinetin

Table 6.5: Summary of lettuce cultivars, transformation vectors and bombardment numbers.

Cultivar used for bombardment	Explants used for bombardments	Construct used for bombardment	Total number of shots	Regeneration medium
Flora	Cotyledons	pLCV5-p24 (provided by Dr. Bridget Hogg, NUI Maynooth)	60 shots (approximately 40 cotyledons per shot)	CIM4 followed by SIM2
Flora	Cotyledons	pLCV6-p24NC (provided by Dr. Bridget Hogg, NUI Maynooth)	30 shots (approximately 40 cotyledons per shot)	CIM4 followed by SIM2
Flora	Leaves	pLCV6-p24NC (provided by Dr. Bridget Hogg, NUI Maynooth)	10 shots (1-2 leaves per shot)	CIM4 followed by SIM2
Flora	Leaves	pLCV7-p24Nef (provided by Dr. Bridget Hogg, NUI Maynooth)	35 shots (1-2 leaves per shot)	CIM4 followed by SIM2
Evola	Cotyledons	pLCV5-p24 (provided by Dr. Bridget Hogg, NUI Maynooth)	50 shots (approximately 40 cotyledons per shot)	CIM4 followed by SIM2
Cisco	Cotyledons	pLCV5-p24 (provided by Dr. Bridget Hogg, NUI Maynooth)	30 shots (approximately 40 cotyledons per shot)	LR
Cisco	Leaves	pLCV5-p24 (provided by Dr. Bridget Hogg, NUI Maynooth)	100 shots (1-2 leaves per shot)	LR
Simpson Elite	Cotyledons	pLCV6-p24NC (provided by Dr. Bridget Hogg, NUI Maynooth)	10 shots (approximately 40 cotyledons per shot)	LR
Simpson Elite	Leaves	pLCV6-p24NC (provided by Dr. Bridget Hogg, NUI Maynooth)	24 shots (1-2 leaves per shot)	LR
Simpson Elite	Leaves	pLCV2-LEC1 (Lelivelt *et al.*, 2005)	240 shots (1-2 leave per shot)	LRM
Simpson Elite	Leaves	pLCV2-GFP/aadA 231 (provided by Prof. John Gray, Cambridge)	240 shots (1-2 leave per shot)	LRM

(treatment 2) induced the greatest amount of callus formation (as determined by weight) from Flora cotyledons. High concentrations of zeatin (1 mg/L & 3 mg/L) in combination with 0.1 mg/L 2,4-D (treatments 5 and 6) induced the greatest amount of callus formation on Evola cotyledons. A range of concentrations of NAA, 0.5, 2 & 5 mg/L, in combination with high concentrations of kinetin, 2 & 5 mg/L, (treatments 7, 8 and 9) induced good callus formation for both cultivars but only at the sites of wounding.

Shoot formation was induced from Flora and Evola calli using two different shoot inducing media, SIM1 (0.5 mg/L kinetin & 0.5 mg/L NAA) and SIM2 (0.04 mg/L NAA & 0.5 mg/L BAP). SIM2 induced the most shoot regeneration from calli for both cultivars. The best overall shoot regeneration from callus was achieved for Flora calli initiated using hormone treatment 2 followed by transfer to SIM2 (43.8%). The best overall shoot regeneration from Evola calli was achieved with media containing hormone treatment 3 (0.1 mg/L 2,4-D & 0.5 mg/L kinetin) followed by transfer to SIM2 (19.75%).

The optimal medium for initiating shoots directly from cotyledon explants (method 2) was found to be MS supplemented with 0.5 mg/L kinetin & 0.5 mg/L NAA (SIM1). The shoot regeneration efficiency using this treatment was very high but also quite variable for the two cultivars (15.6 shoots / Flora cotyledon explant and 53 shoots / Evola cotyledon explant).

Based on the results obtained with the two regeneration methods, it was decided to attempt biolistic-mediated lettuce plastid transformation by bombarding

cotyledons, inducing callus formation using callus inducing medium 2 (CIM2) and then inducing shoot formation on medium 2 (SIM2). This method was chosen since periods of callus maintenance are thought to increase the probability of accumulating homoplasmic cells (Cheng *et al.*, 2010). Homoplastomic, plastid-transformed cauliflower was achieved following a prolonged period of callus maintenance (Nugent *et al.*, 2006). Indeed, a callus-induction and maintenance phase followed by shoot induction phase turned out to be the method used to generate the first transplastomic lettuce plants using particle bombardment (Kanamoto *et al.*, 2006).

To optimise the conditions required for biolistics-mediated plastid-delivery of transforming DNA a series of transient-expression experiments were carried out using a lettuce plastid transformation vector containing the *gfp* reporter gene (Lelivelt *et al*., 2005). Two sizes of gold particle (0.6 μM & 1.0 μM) and three different blast pressures were assessed (650 psi, 900 psi & 1100 psi). Gold particles were chosen instead of tungsten particles because some groups had reported tungsten toxicity to plants (Russell *et al.*, 1992). Also, the denser nature and more even surface of the gold particles is thought to allow for better control of penetration into plant tissue (Southgate *et al.*, 1995). After bombardment of the lettuce cotyledons, GFP fluorescence in the chloroplasts of bombarded cotyledon tissue indicated delivery of transforming DNA to the chloroplasts. The efficiency of DNA delivery was assessed by counting the number of plastids expressing GFP / bombardment. The best rate of DNA delivery to plastids was achieved with bombardments using 0.6 μM gold particles and a shooting pressure of 900 psi. Coincidentally, these conditions are the same ones

subsequently used by Kanamoto *et al.*, 2006 to achieve biolistic-mediated chloroplast transformed lettuce plants (cv Cisco). Ruhlman *et al.*, (2007) and Ruhlman *et al.*, (2010) also achieved biolistic-mediated lettuce chloroplast transformation using these same biolistic parameters.

The bombardment of lettuce cotyledons with the pLCV5-p24 transformation vector (using optimised plant regeneration conditions and transforming DNA delivery methods) resulted in the recovery of three spectinomycin-resistant lettuce shoots. PCR analyses of these shoots confirmed the presence of the *aadA* selectable marker gene and the gene of interest, p24. Although the gene construct was targeted to the plastid genome, PCR analyses with primers flanking the integration site revealed that these shoots were not plastid transformants. One possible explanation for this result is nuclear localisation of the transgenes, since particle bombardment is also an efficient means of plant nuclear transformation (Finer *et al.*, 1999).

The reason why plastid transformed lettuce shoots were not obtained may be due to the type of explant obtained. A similar regeneration protocol (inducing callus formation post bombardment followed by shoot induction) was successfully used to regenerate transplastomic lettuce plants expressing GFP using particle bombardment (Kanamoto *et al.*, 2006). In addition, the bombardment parameters optimised in this study were also used successfully to generate plastid transformed lettuce plants (Kanamoto *et al.*, 2006; Ruhlman *et al.*, 2007; Ruhlman *et al.*, 2010). However, in both these cases leaf rather than cotyledon explants were used as the target tissue. Although, cotyledon explants

have been used in the generation of nuclear transformed lettuce plants (Webster *et al.*, 2006) and more recently in the generation of chloroplast-transformed rapeseed (*Brassica napus*) plants (Cheng *et al.*, 2010), the presence of immature plastids (proplastids) in young cotyledons may lower the transformation efficiency. Chloroplasts in leaf cells are larger in size and their location along the periphery of the cell may make them an easier target for transformation. In addition, while mature chloroplasts contain around 100 copies of the plastid genome, immature proplastids contain only about 20 genome copies (Sugiura, 1992). Thus, although we may have achieved delivery of transforming DNA to proplastids in cotyledon tissue (as determined by the GFP fluorescing experiments) the likelihood of genome integration and stable transformation may be limited by the low genome copy number in this type of immature plastid.

Multiple bombardments of mature Cisco and Simpson Elite lettuce leaves (both used for successful biolistics-mediated lettuce plastid transformation – Kanamoto *et al.*, 2006; Ruhlman *et al.*, 2007; Ruhlman *et al.*, 2010) were also carried out in this study. To eliminate the possibility that the lack of shoot regeneration was due to the use of lettuce leaf tissue obtained from plants grown from seed *in vitro*, a problem noticed for tobacco (cv. Maryland Mammoth) plastid transformation (McCabe *et al.*, 2008), leaves from plants initiated from intermodal cuttings from both Cisco and Simpson Elite plants were also used for bombardment. However, no transformed shoots were recovered in any of these experiments.

Comparing the number of transplastomic lines recovered per bombardment in published lettuce transformation experiments (Kanamoto *et al.,* 2006, Ruhlman *et al.,* 2007, Ruhlman *et al.,* 2010) to the number of bombardments performed in this study, recovery of some plastid-transformed lettuce shoots should have been expected. Kanamoto *et al.,* (2006) reported a transformation efficiency of one transplastomic lettuce plant per bombardment using Cisco leaf explants. Ruhlman *et al.,* (2007) reported a lower transformation efficiency of one transplastomic plant per 30 lettuce leaves bombarded using Simpson Elite leaf explants. This transformation efficiency was later revised to five to six transplastomic shoots per ten bombardments (i.e. one transplastomic shoot per bombardment) following a change to the growth regulator concentration used in the shoot regeneration medium (Ruhlman *et al.,* 2010). We carried out 240 bombardments of Simpson Elite leaves using the pLCV2-LEC1 plasmid previously used to obtain PEG-mediated plastid transformed plant lines (Lelivelt *et al.,* 2005) and using the published bombardment and shoot regeneration conditions (Ruhlman *et al.,* 2010). However, no transformed shoots were recovered.

It is still not clear to us why we never recovered any plastid transformed lettuce plants using the particle bombardment method. Anecdotally we have heard that the transformation efficiency for the Cisco lettuce cultivar is much lower than has been reported in the literature. However, we have carried out so many bombardments we still should have expected to recover at least some transformed shoots even allowing for a much lower transformation efficiency. The closest we came to generating plastid-transformed lettuce lines was with the

two-stage regeneration method using cotyledon explants. We have not repeated this experiment using leaf explants, but perhaps this might be an approach to try in the future.

6.4 Final Conclusion

The work presented here demonstrates that conserved influenza virus HA epitopes can be expressed in plant chloroplasts. Although the protein accumulation levels calculated for the two HA epitope fusions (HA91-108/GFP & GFP/HA307-319) is quite low in comparison to other plastid expressed recombinant proteins (Lentz *et al.,* 2010; Molina *et al.,* 2004), in reality, the insoluble nature of the majority of the GFP/HA epitope proteins suggest that these percentages may be a significant underestimation of actual protein accumulation levels within the tobacco plastid system.

In contrast, the plastid-based expression of full length HA or HA1 may not be feasible even in the context of a fusion protein. Neither of the full length GFP/HA or GFP/ HA1 constructs generated any transplastomic lines containing the HA or HA1 transgenes. A possible reason for this may be that the viral protein is toxic to the plastid cells and is inhibiting plastid function possibly by associating with the plastid membranes. Removal of the transmembrane region within the HA coding sequence may reduce membrane association and increase selection of transformed plastids during the plant regeneration process.

Transplastomic lines generated with the 14aarbcL/HA and 14aaGFP/HA fusion constructs produced a truncated protein. The frequency of rare codons

encountered by the chloroplast translational machinery may explain why a truncated fusion protein and not the full length protein was detected in these transgenic lines. In tobacco, only 30 tRNAs are encoded by the chloroplast out of a possible 61 (Pfitzinge *et al.*,1987). A rare codon-rich segment may slow translation of HA as a consequence of ribosome pausing and stuttering causing unrecognised codons to act as stop codons causing premature termination of the protein (Green *et al.*, 1999).

Expression of recombinant proteins may also be restricted due to codon bias of the host cell (Gustafsson *et al.,* 2004). Analysis of the HA coding region using a software programme GeneArt (Invitrogen) suggested that approximately 45% of the native HA codons would rarely be encountered by the *Nicotiana tabacum* chloroplast tRNA population. Thus, altering the codon composition of HA to reflect frequent codons used by the tobacco chloroplast tRNA population without altering the coding capacity of the HA gene could be one solution that may result in HA protein accumulation in tobacco. Reports regarding changes in codon composition of foreign genes introduced into tobacco chloroplasts resulting in higher levels of protein accumulation are mixed. Ye *et al*., (2001), reported a one-fold increase in the accumulation of the codon optimised 5-enolpyruvylshikimate-3-phosphate synthase (EPSPS) protein compared to the native protein. More recently, Madesis *et al.,* (2010) reported that codon optimisation of the hepatitis C virus core protein only produced a modest five-fold increase in the core polypeptide accumulation compared to the native viral gene. However, there have also been reports of relatively high levels of protein accumulation in plastids following codon optimisation of the transgene.

Expression of recombinant human transforming growth factor-β3 increased by 75-fold when a synthetic sequence containing frequent chloroplast codons were used in comparison to the native coding region when expressed in tobacco chloroplasts (Gisby *et al*., 2011). Expression of recombinant HIV-1 p24 protein also increased following codon optimisation of the coding sequence (McCabe *et al.,* 2008; Zhou *et al.,* 2008) suggesting that the synthesis of a synthetic HA gene may be a more promising route to achieve HA protein accumulation.

Furthermore, caution should also be observed with regards to the choice of regulatory elements. In this study, the level of unintended recombination events was so significant that secondary recombination events severely hindered efficient recovery of plastid transformed lines containing the desired transgenes regardless of the transgene used. Where possible, the use of non-plastid gene regulatory elements [e.g. the bacterial *trc* promoter (Newell *et al.,* 2003), the mitochondrial *atpA* promoter (Bohne *et al.*, 2007), the T7 promoter in conjunction with a plastid-targeted, nuclear-encoded T7 RNA polymerase (McBride *et al.,* 1994) and the *E. coli rrnB* terminator (Newell *et al.,* 2003)] in plastid transformation vectors may be one way of reducing these unintended recombination events and thus facilitate a higher efficiency of selection and regeneration of primary transformants.

Chapter 7
Bibliography

7 Bibliography

Ada, G. L. & Jones, P. D. (1986). The immune response to influenza infection. *Current Topics in Microbiology and Immunology* **128,** 1-54.

Adar, Y., Singer, Y., Levi, R., Tzehoval, E., Perk, S., Banet-Noach, C., Nagar, S., Amon, R. & Ben-Yedidia, T. (2009). A universal epitope-based influenza vaccine and its efficacy against H5N1. *Vaccine* **27**, 2099-2107.

Ahlert, D., Stegemann, S., Kahlou, S., Ruf, S. &Bock, R. (2011). Insensitivity of chloroplast gene expression to DNA methylation. *Molecular Genetics and Genomics,* **282**, 17-24.

Apel, W., Schulze, W. X. & Bock, R. (2010). Identification of protein stability determinants in chloroplasts. *The Plant Journal* **63**, 636-650.

Apel, W. & Bock, R. (2009). Enhancement of carotenoid biosynthesis in transplastomic tomatoes by induced lycopene-to-provitamin A conversion. *Plant Physiology* **151**, 59-66.

Arlen, P. A., Singleton, M., Adamovicz, J. J., Ding, Y., Davoodi-Semiromi, A. & Daniell, H. (2008). Effective plague vaccination via oral delivery of plant cells expressing F1-V antigens in chloroplasts. *Infection and Immunity* **76**, 3640-3650.

Arnon, R. & Van Regenmortel, M. H. (1992). Structural basis of antigenic specificity and design of new vaccines. *Faseb Journal* **6**, 3265-3274.

Arnon, R., Tarrab-Hazdai, R. & Ben-Yedidia, T. (2001). Peptide-based synthetic recombinant vaccines with anti-viral efficacy. *Biologicals* **29**, 237-242.

Barone, P., Zhang, X. H. & Widholm, J. M. (2009). Tobacco plastid transformation using the feedback-insensitive anthranilate synthase alpha - subunit of tobacco (ASA2) as a new selectable marker. *Journal of Experimental Botany* **60**, 3195-3202.

Bathgate, B., Purton, M. E., Grierson, D. & Goodenough, P. W. (1985). Plastid changes during the conversion of chloroplasts to chromoplasts in ripening tomatoes. *Planta* **165**, 197-204.

Ben-Yedidia, T., Abel, L., Arnon, R. & Globerson, A. (1998). Efficacy of anti-influenza peptide vaccine in aged mice. *Mechanisms of ageing and development* **104**, 11-23.

Ben-Yedidia, T., Tarrab-Hazdai, R., Schechtman, D. & Arnon, R. (1999). Intranasal administration of synthetic recombinant peptide-based vaccine protects mice from infection by *Schistosoma mansoni*. *Infection and immunity* **67**, 4360-4366.

Ben-Yedidia, T. A., R (1998). Synthetic peptide-based vaccines against influenza. *Peptide Science* **5**, 341-344.

Bendich, A. J. (1987). Why do chloroplasts and mitochondria contain so many copies of their genome. *Bioessays* **6**, 279-282.

Benshaul, Y. & Klein, S. (1965). Development and structure of carotene bodies in carrot roots. *Botanical Gazette* **126**, 79-85.

Betakova, T., Ciampor, F. & Hay, A. J. (2005). Influence of residue 44 on the activity of the M2 proton channel of influenza A virus. *Journal of General Virology* **86,** 181-184.

Birch-Machin, I., Newell, C. A., Hibberd, J. M. & Gray, J. C. (2004). Accumulation of rotavirus VP6 protein in chloroplasts of transplastomic tobacco is limited by protein stability. *Plant Biotechnology Journal* **2**, 261-270.

Bock, R. (2001). Transgenic plastids in basic research and plant biotechnology. *Journal of Molecular Biology* **312**, 425-438.

Bock, R. & Warzecha, H. (2010). Solar-powered factories for new vaccines and antibiotics. *Trends in Biotechnology* **28**, 246-252.

Bogorad, L. (2000). Engineering chloroplasts: an alternative site for foreign genes, proteins, reactions and products. *Trends in Biotechnology* **18**, 257-263.

Bohlmann, J., Lins, T., Martin, W. & Eilert, U. (1996). Anthranilate synthase from Ruta graveolens - Duplicated AS alpha genes encode tryptophan-sensitive and tryptophan-insensitive isoenzymes specific to amino acid and alkaloid biosynthesis. *Plant Physiology* **111**, 507-514.

Bohne, A.-V., Ruf, S., Börner, T. & Bock, R. (2007). Faithful transcription initiation from a mitochondrial promoter in transgenic plastids. *Nucleic Acids Research* **35**, 7256-7266.

Boltz, D., Aldridge, J. J., Webster, R. & Govorkov, E. (2010). Drugs in development for influenza. *Drugs* **70**, 1349-1362.

Boynton, J. E., Gillham, N. W., Harris, E. H., Hosler, J. P., Johnson, A. M., Jones, A. R., Randolph-Anderson, B. L., Robertson, D., Klein, T. M., Shark, K. B. (1988). Chloroplast transformation in *Chlamydomonas* with high-velocity microprojectiles. *Science* **240**, 1534-1538.

Calder, L. J., Wasilewski, S., Berriman, J. A. & Rosenthal, P. B. (2010). Structural organization of a filamentous influenza A virus. *Proceedings of the National Academy of Sciences USA* **107**, 10685-10690.

Cardi, T., Lenzi, P. & Maliga, P. (2010). Chloroplasts as expression platforms for plant-produced vaccines. *Expert Review of Vaccines* **9**, 893-911.

Carrer, H., Hockenberry, T. N., Svab, Z. & Maliga, P. (1993). Kanamycin resistance as a selectable marker for plastid transformation in tobacco. *Molecular & General Genetics* **241**, 49-56.

Cerutti, H., Osman, M., Grandoni, P. & Jagendorf, A. T. (1992). A homolog of *Escherichia coli* RecA protein in plastids of higher plants. *Proceedings of the National Acedemy of Sciences U S A* **89**, 8068-8072.

Chakrabarti, S. K., Lutz, K. A., Lertwiriyawong, B., Svab, Z. & Maliga, P. (2006). Expression of the cry9Aa2 *B.t.* gene in tobacco chloroplasts confers resistance to potato tuber moth. *Transgenic Research* **15**, 481-488.

Chen, B. J., Takeda, M. & Lamb, R. A. (2005). Influenza virus hemagglutinin (H3 subtype) requires palmitoylation of it cytoplasmic tail for assembly: M1 proteins of two subtyoes differ in their abilty to support assembly. *The Journal of Virology* **79**, 13673-13684.

Chen, J. & Deng, Y. M. (2009). Influenza virus antigenic variation, host antibody production and new approach to control epidemics. *Virology Journal* **6**, 1-3.

Cheng, L., Li, H.-P., Qu, B., Huang, T., Tu, J.-X., Fu, T.-D. & Liao, Y.-C. (2010). Chloroplast transformation of rapeseed (*Brassica napus*) by particle bombardment of cotyledons. *Plant Cell Reports* **29,** 371-381.

Cheng, Q., Nelson, D., Zhu, S. W. & Fischetti, V. A. (2005). Removal of group B streptococci colonizing the vagina and oropharynx of mice with a bacteriophage, lytic enzyme. *Antimicrobial Agents and Chemotherapy* **49**, 111-117.

Clarke, J. L. & Daniell, H. (2011). Plastid biotechnology for crop production: present status and future perspectives. *Plant Molecular Biol*ogy **76**, 211-220.

Coloma, R., Valpuesta, J. M., Arranz, R., Carrascosa, J. L., Ortin, J. & Martin-Benito, J. (2009). The structure of a biologically active influenza virus ribonucleoprotein complex. *Plos Pathogens* **5**, E1000491, 1-10.

Corneille, S., Lutz, K., Svab, Z. & Maliga, P. (2001). Efficient elimination of selectable marker genes from the plastid genome by the CRE-lox site-specific recombination system. *Plant Journal* **27**, 171-178.

Corneille, S., Lutz, K. A., Azhagiri, A. K. & Maliga, P. (2003). Identification of functional lox sites in the plastid genome. *Plant Journal* **35**, 753-762.

Couch, R. B. & Kasel, J. A. (1983). Immunity to influenza in man. *Annual Review of Microbiology* **37,** 529-549.

Cox, M. M. J. & Hollister, J. R. (2009). FluBlok, a next generation influenza vaccine manufactured in insect cells. *Biologicals* **37**, 182-189.

Cox, N. J., Neumann, G., Donis, R. O. & Kawaoka, Y. (2007). *Orthomyxoviruses: Influenza*, 10 edn: Topley and Wilson.

Cox, R. J., Brokstad, K. A. & Ogra, P. (2004). Influenza virus: immunity and vaccination strategies. Comparison of the immune response to inactivated and live, attenuated influenza vaccines. *Scandinavian Journal of Immunology* **59**, 1-15.

Craig, W., Lenzi, P., Scotti, N. & other authors (2008). Transplastomic tobacco plants expressing a fatty acid desaturase gene exhibit altered fatty acid profiles and improved cold tolerance. *Transgenic Research* **17**, 769-782.

Daniell, H., Lee, S. B., Panchal, T. & Wiebe, P. O. (2001a). Expression of the native cholera toxin B subunit gene and assembly as functional oligomers in transgenic tobacco chloroplasts. *Journal of Molecular Biology* **311**, 1001-1009.

Daniell, H., Streatfield, S. J. & Wycoff, K. (2001b). Medical molecular farming: production of antibodies, biopharmaceuticals and edible vaccines in plants. *Trends in Plant Science* **6**, 219-226.

Daniell, H., Wiebe, P. O. & Millan, A. F. S. (2001c). Antibiotic-free chloroplast genetic engineering - an environmentally friendly approach. *Trends in Plant Science* **6**, 237-239.

Daniell, H., Khan, M. S. & Allison, L. (2002). Milestones in chloroplast genetic engineering: an environmentally friendly era in biotechnology. *Trends in Plant Science* **7**, 84-91.

Daniell, H., Singh, N. D., Mason, H. & Streatfield, S. J. (2009). Plant-made vaccine antigens and biopharmaceuticals. *Trends in Plant Science* **14**, 669-679.

Davarpanah, S., Jung, S., Kim, Y., Park, Y.-I., Min, S., Liu, J. & Jeong, W. (2009). Stable plastid transformation in *Nicotiana benthamiana*. *Journal of Plant Biology* **52,** 244-250.

Davoodi-Semiromi, A., Schreiber, M., Nalapalli, S., Verma, D., Singh, N. D., Banks, R. K., Chakrabarti, D. & Daniell, H. (2010). Chloroplast-derived vaccine antigens confer dual immunity against cholera and malaria by oral or injectable delivery. *Plant Biotechnology Journal* **8**, 223-242.

De Cosa, B., Moar, W., Lee, S. B., Miller, M. & Daniell, H. (2001). Overexpression of the Bt cry2Aa2 operon in chloroplasts leads to formation of insecticidal crystals. *Nature Biotechnology* **19**, 71-74.

De Marchis, F., Wang, Y., Stevanato, P., Arcioni, S. & Bellucci, M. (2009). Genetic transformation of the sugar beet plastome. *Transgenic Research* 18, 17-30.

Disis, M. L., Gralow, J. R., Bernhard, H., Hand, S. L., Rubin, W. D. & Cheever, M. A. (1996). Peptide-based, but not whole protein, vaccines elicit immunity to HER-2/neu, oncogenic self-protein. *Journal of Immunology* **156**, 3151-3158.

Doroshenko, A. & Halperin, S. A. (2009). Trivalent MDCK cell culture-derived influenza vaccine Optaflu (Novartis Vaccines). *Expert Review of Vaccines* **8**, 679-688.

Dufourmantel, N., Pelissier, B., Garcon, F., Peltier, G., Ferullo, J. M. & Tissot, G. (2004). Generation of fertile transplastomic soybean. *Plant Molecular Biology* **55**, 479-489.

Dufourmantel, N., Dubald, M., Matringe, M., Canard, H., Garcon, F., Job, C., Kay, E., Wisniewski, JP., Ferullo, JM., Pelissier, B., Sailland, A., Tissot, G. (2007). Generation and characterization of soybean and marker-free tobacco plastid transformants over-expressing a bacterial 4-hydroxyphenylpyruvate dioxygenase which provides strong herbicide tolerance. *Plant Biotechnology Journal* **5,** 118-133.

D'Aoust, M.-A., Couture, M. M. J., Charland, N., Trépanier, S., Landry, N., Ors, F. & Vézina, L.-P. (2010). The production of hemagglutinin-based virus-like particles in plants: a rapid, efficient and safe response to pandemic influenza. *Plant Biotechnology Journal* **8**, 607-619.

Egea, I., Barsan, C., Bian, W., Purgatto, E., Latché, A., Chervin, C., Bouzayen, M. & Pech, J.-C. (2010). Chromoplast differentiation: Current status and perspectives. *Plant and Cell Physiology* **51**, 1601-1611.

Elghabi, Z., Karcher, D., Zhou, F., Ruf, S. & Bock, R. (2011). Optimisation of the expression of the HIV fusion inhibitor cyanovirin-N from the tobacco plastid genome. *Plant Biotechnology Journal* **9,** 599-608.

Engler, O. B., Dai, W. J., Sette, A., Hunziker, I. P., Reichen, J., Pichler, W. J. & Cerny, A. (2001). Peptide vaccines against hepatitis B virus: from animal model to human studies. *Molecular Immunology* **38**, 457-465.

Fernandez-San Millan, A., Mingo-Castel, A., Miller, M. & Daniell, H. (2003). A chloroplast transgenic approach to hyper-express and purify Human Serum Albumin, a protein highly susceptible to proteolytic degradation. *Plant Biotechnology Journal* **1**, 71-79.

Fernandez-San Millan, A., Ortigosa, S. M., Hervas-Stubbs, S., Corral-Martinez, P., Segui-Simarro, J. M., Gaetan, J., Coursaget, P. & Veramendi, J. (2008). Human papillomavirus L1 protein expressed in tobacco chloroplasts self-assembles into virus-like particles that are highly immunogenic. *Plant Biotechnology Journal* **6**, 427-441.

Finer, J. J., Finer, K. R. & Ponappa, T. (1999). Particle bombardment mediated transformation. in *Plant Biotechnology- Current Topics in*

Microbiology and Immunology, "Plant Biotechnology: New Products and Applications. Eds. J Hammond, PB McGarvey, V Yusibov, Berlin: Springer-Verlag Berlin. **240**, 59-80.

Fischer, N., Stampacchia, O., Redding, K. & Rochaix, J. D. (1996). Selectable marker recycling in the chloroplast. *Molecular & General Genetics* **251**, 373-380.

Fischetti, V. A., Nelson, D. & Schuch, R. (2006). Reinventing phage therapy: are the parts greater than the sum? *Nature Biotechology* **24**, 1508-1511.

Fouchier, R. A., Munster, V., Wallensten, A., Bestebroer, T. M., Herfst, S., Smith, D., Rimmelzwaan, G. F., Olsen, B. & Osterhaus, A. D. (2005). Characterization of a novel influenza A virus hemagglutinin subtype (H16) obtained from black-headed gulls. *Journal of Virology* **79**, 2814-2822.

Gahery, H., Daniel, N., Charmeteau, B., Ourth, L., Jackson, A., Andrieu, M., Choppin, J., Salmon, D., Pialoux, G. & Guillet, J. G. (2006). New CD4(+) and CD8(+)T cell responses induced in chronically HIV type-1-infected patients after immunizations with an HIV type 1 lipopeptide vaccine. *Aids Research and Human Retroviruses* **22**, 684-694.

Gerdil, C. (2003). The annual production cycle for influenza vaccine. *Vaccine* **21**, 1776-1779.

Gerhard, W., Mozdzanowska, K. & Zharikova, D. (2006). Prospects for universal influenza virus vaccine. *Emerging Infectious Diseases* **12**, 569-574.

Ghedin, E., Sengamalay, N. A., Shumway, M. & other authors (2005). Large-scale sequencing of human influenza reveals the dynamic nature of viral genome evolution. *Nature* **437**, 1162-1166.

Gisby, M., Mellors, P., Madesis, P., Ellin, M., Laverty, H., O'Kane, S., Ferguson, M. W. J. & Day, A. (2011). A synthetic gene increases TGFβ3 accumulation by 75-fold in tobacco chloroplasts enabling rapid purification and folding into a biologically active molecule. *Plant Biotechnology Journal* **9,** 618-628.

Glenz, K., Bouchon, B., Stehle, T., Wallich, R., Simon, M. M. & Warzecha, H. (2006). Production of a recombinant bacterial lipoprotein in higher plant chloroplasts. *Nature Biotechnology* **24,** 76-77.

Gocnik, M., Fislova, T., Mucha, V., Sladkova, T., Russ, G., Kostolansky, F. & Vareckova, E. (2008). Antibodies induced by the HA2 glycopolypeptide of influenza virus haemagglutinin improve recovery from influenza A virus infection. *Journal of General Virology* **89**, 958-967.

Golds, T., Maliga, P. & Koop, H. U. (1993). Stable Plastid Transformation in Peg-Treated Protoplasts of Nicotiana-Tabacum. *Bio-Technology* **11**, 95-97.

Goldschmidt-Clermont, M. (1991). Transgenic expression of aminoglycoside adenine transferase in the chloroplast: a selectable marker of site-directed transformation of C*hlamydomonas*. *Nucleic Acids Research* **19**, 4083-4089.

Gonzalez-Rabade, N., McGowan, E. G., Zhou, F., McCabe, M. S., Bock, R., Dix, P. J., Gray, J. C. & Ma, J. K. C. (2011). Immunogenicity of chloroplast-derived HIV-1 p24 and a p24-Nef fusion protein following subcutaneous and oral administration in mice. *Plant Biotechnology Journal* **9**, 629-638.

Goto, F., Yoshihara, T. & Saiki, H. (2000). Iron accumulation and enhanced growth in transgenic lettuce plants expressing the iron- binding protein ferritin. *TAG Theoretical and Applied Genetics* **100**, 658-664.

Grambas, S. & Hay, A. J. (1992). Maturation of influenza A virus hemagglutinin--estimates of the pH encountered during transport and its regulation by the M2 protein. in *Virology* **190,** 11-18.

Gray, B. N., Ahner, B. A. & Hanson, M. R. (2009a). High-level bacterial cellulase accumulation in chloroplast-transformed tobacco mediated by downstream box fusions. *Biotechnology and Bioengineering* **102**, 1045-1054.

Gray, B. N., Ahner, B. A. & Hanson, M. R. (2009b). Extensive homologous recombination between introduced and native regulatory plastid DNA elements in transplastomic plants. *Transgenic Research* **18**, 559-572.

Gray, B. N., Yang, H., Ahner, B. & Hanson, M. (2011). An efficient downstream box fusion allows high-level accumulation of active bacterial beta-glucosidase in tobacco chloroplasts. *Plant Molecular Biology* **76,** 345-355.

Guan, Y., Vijaykrishna, D., Bahl, J., Zhu, H., Wang, J. & Smith, G. (2010). The emergence of pandemic influenza viruses. *Protein & Cell* **1**, 9-13.

Gubareva, L. V., Kaiser, L. & Hayden, F. G. (2000). Influenza virus neuraminidase inhibitors. *Lancet* **335**, 827-835.

Gustafsoon, C., Govindarajan, S. & Minshull, J. (2004). Codon bias and heterologous protein expression. *Trends in Biotechnology* **22,** 346-353.

Hagemann, R. (1992). *Plastid Genetics in Higher Plants.* Wien, New York: Springer-Verla

Hahn, B.-S., Jeon, I.-S., Jung, Y.-J., Kim, J.-B., Park, J.-S., HA, S.-H., Kim, K.-H., Kim, H.-M., Yang, J.-S. & Ki, Y.-H. (2007). Expression of hemagglutinin-neuraminidase protein of Newcastle disease virus in transgenic tobacco. *Plant Biotechnology Reports* **1**, 85-92.

Harsanyi, A., Boddi, B., Boka, K. & Gaborjanyi, R. (2005). Pathogen affected greening process of barley seedlings infected with BSMV by seed transmission. *Cereal Research Communications* **33**, 209-212.

Hausmann, S., Garcin, D., Delenda, C. & Kolakofsky, D. (1999). The versitility of paramyxovirus RNA polymerase stuttering. *Journal of Virology* **73,** 5568-5576.

Heifetz, P. B. (2000). Genetic engineering of the chloroplast. *Biochimie* **82**, 655-666.

Hennig, A., Bonfig, K., Roitsch, T. & Warzecha, H. (2007). Expression of the recombinant batcerial outer surface protein A in tobacco chloroplasts leads to thylakoid localization and loss of photosynthesis. *FEBS Journal* **274,** 5749-5758.

Hernandez-Pinzon, I., Ross, J. H. E., Barnes, K. A., Damant, A. P. & Murphy, D. J. (1999). Composition and role of tapetal lipid bodies in the biogenesis of the pollen coat of *Brassica napus*. *Planta* **208**, 588-598.

Hibberd, J. M., Linley, P. J., Khan, M. S. & Gray, J. C. (1998). Transient expression of green fluorescent protein in various plastid types following microprojectile bombardment. *The Plant Journal* **16**, 627-632.

Hirose, T. & Sugiura, M. (1997). Both RNA editing and RNA cleavage are required for translation of tobacco chloroplast ndhD mRNA: a possible regulatory mechanism for the expression of a chloroplast operon consisting of functionally unrelated genes. *Embo Journal* **16**, 6804-6811.

Hobson, D., Curry, R.L., Beare, A.S., Ward-Gardner, A.(1972). The role of serum haemagglutination inhibiting antibody in protection against challenge infection with influenza A2 and B viruses. *Journal of Hygiene* **70**, 767–777.

Horner, H. T., Healy, R. A., Ren, G., Fritz, D., Klyne, A., Seames, C. & Thornburg, R. W. (2007). Amyloplast to chromoplast conversion in developing ornamental tobacco floral nectaries provides sugar for nectar and antioxidants for protection. *American Journal of Botany* **94**, 12-24.

Hou, B. K., Zhou, Y. H., Wan, L. H., Zhang, Z. L., Shen, G. F., Chen, Z. H. & Hu, Z. M. (2003). Chloroplast transformation in oilseed rape. *Transgenic Research* **12**, 111-114.

Huang, F. C., Klaus, S. M. J., Herz, S., Zou, Z., Koop, H. U. & Golds, T. J. (2002). Efficient plastid transformation in tobacco using the *aphA-6* gene and kanamycin selection. *Molecular Genetics and Genomics* **268**, 19-27.

Huang, Z., Dry, I., Webster, D., Strugnell, R. & Wesselingh, S. (2001). Plant-derived measles virus hemagglutinin protein induces neutralizing antibodies in mice. *Vaccine* **19**, 2163-2171.

Huber, V. C. & McCullers, J. A. (2008a). FluBlok, a recombinant influenza vaccine. *Current Opinion in Molecular Therapeutics* **10**, 75-85.

Huber, V. C. & McCullers, J. A. (2008b). Vaccines against pandemic influenza - What can be done before the next pandemic? *Pediatric Infectious Disease Journal* **27**, S113-S117.

Hurkman, W. J. & Kennedy, G. S. (1976). Fine-structure and development of proteoplasts in primary leaves of mung bean. *Protoplasma* **89**, 171-184.

Iamtham, S. & Day, A. (2000). Removal of antibiotic resistance genes from transgenic tobacco plastids. *Nature Biotechnology* **18**, 1172-1176.

Jacob, C. O., Leitner, M., Zamir, A., Salomon, D. & Arnon, R. (1985). Priming immunization against cholera-toxin and *Escherichia-coli* heat-labile toxin by a cholera-toxin short peptide-beta-galactosidase hybrid synthesized in *Escherichia-coli*. *Embo Journal* **4**, 3339-3343.

Jacques, J. P. & Kolakofsky, D. (1991). Pseudo templasted transcription in prokaryotic and eukaryotic organisms. *Genes & Development* **5,** 707-713.

Jefferson, R. A., Kavanagh, T. A. & Bevan, M. W. (1987). Beta-glucuronidase (Gus) as a sensitive and versatile gene fusion marker in plants. *The EMBO Journal* **6**, 3901-3907.

Jeon, S. H., Ben-Yedidia, T. & Arnon, R. (2002). Intranasal immunization with synthetic recombinant vaccine containing multiple epitopes of influenza virus. *Vaccine* **20,** 2772-2780.

Johnson, P. A., Conway, M. A., Daly, J., Nicolson, C., Robertson, J. & Mills, K. H. G. (2000). Plasmid DNA encoding influenza virus haemagglutinin induces Th1 cells and protection against respiratory infection despite its limited ability to generate antibody responses. *Journal of General Virology* **81**, 1737-1745.

Juneau, P., Le Lay, P., Böddi, B., Samson, G. & Popovic, R. (2002). Relationship between the structural and functional changes of the photosynthetic apparatus during chloroplast–chromoplast transition in flower bud of Lilium longiflorum. *Photochemistry and Photobiology* **75**, 377-381.

Kalthoff, D., Giritch, A., Geisler, K., Bettmann, U., Klimyuk, V., Hehnen, H.-R., Gleba, Y. & Beer, M. (2010). Immunization with plant-expressed hemagglutinin protects chickens from lethal highly pathogenic avian influenza virus H5N1 challenge infection. *The Journal of Virology* **84**, 12002-12010.

Kanamoto, H., Yamashita, A., Asao, H., Okumura, S., Takase, H., Hattori, M., Yokota, A. & Tomizawa, K. (2006). Efficient and stable transformation of *Lactuca sativa* L. cv. Cisco (lettuce) plastids. *Transgenic Research* **15**, 205-217.

Kang, T.-J., Loc, N.-H., Jang, M.-O., Jang, Y.-S., Kim, Y.-S., Seo, J.-E. & Yang, M.-S. (2003). Expression of the B subunit of *E. coli* heat-labile enterotoxin in the chloroplasts of plants and its characterisation. *Transgenic Research* **12,** 683-691.

Kapusta, J., Modelska, A., Figlerowicz, M., Pniewski, T., Letellier, M., Lisowa, O., Yusibov, V., Koprowski, H., Plucienniczak, A. & Legocki, A. B. (1999). A plant-derived edible vaccine against hepatitis B virus. *Faseb Journal* **13**, 1796-1799.

Kashala, O., Amador, R., Valero, M. V., Moreno, A., Barbosa, A., Nickel, B., Daubenberger, C. A., Guzman, F., Pluschke, G. & Patarroyo, M. E. (2002). Safety, tolerability and immunogenicity of new formulations of the Plasmodium falciparum malaria peptide vaccine SPf66 combined with the immunological adjuvant QS-21. *Vaccine* **20**, 2263-2277.

Katagiri, S., Ohizumi, A. & Homma, M. (1983). An outbreak of type-C influenza in a childrens home. *Journal of Infectious Diseases* **148**, 51-56.

Khan, M. S., Hameed, W., Nozoe, M. & Shiina, T. (2007). Disruption of the psbA gene by the copy correction mechanism reveals that the expression of plastid-encoded genes is regulated by photosynthesis activity. *Journal of Plant Research* **120**, 421-430.

Khandelwal, A., Vally, K. J. M., Geetha, N., Venkatachalam, P., Shaila, M. S. & Lakshmi Sita, G. (2003). Engineering hemagglutinin (H) protein of rinderpest virus into peanut (*Arachis hypogaea* L.) as a possible source of vaccine. *Plant Science* **165**, 77-84.

Khandelwal, A., Renukaradhya, G. J., Rajasekhar, M., Sita, G. L. & Shaila, M. S. (2004). Systemic and oral immunogenicity of hemagglutinin protein of rinderpest virus expressed by transgenic peanut plants in a mouse model. *Virology* **323**, 284-291.

Kim, Y.-S., Kim, B.-G., Kim, T.-G., Kang, T.-J. & Yang, M.-S. (2006). Expression of a cholera toxin B subunit in transgenic lettuce (*Lactuca sativa* L.) using *Agrobacterium*-mediated transformation system. *Plant Cell, Tissue and Organ Culture* **87**, 203-210.

Kittiwongwattana, C., Lutz, K., Clark, M. & Maliga, P. (2007). Plastid marker gene excision by the phiC31 phage site-specific recombinase. *Plant Molecular Biology* **64**, 137-143.

Klaus, S. M. J., Huang, F. C., Golds, T. J. & Koop, H. U. (2004). Generation of marker-free plastid transformants using a transiently cointegrated selection gene. *Nature Biotechnology* **22**, 225-229.

Knoblauch, M., Hibberd, J. M., Gray, J. C. & van Bel, A. J. E. (1999). A galinstan expansion femtosyringe for microinjection of eukaryotic organelles and prokaryotes. *Nature Biotechnology* **17**, 906-909.

Kode, V., Mudd, E. A., Iamtham, S. & Day, A. (2006). Isolation of precise plastid deletion mutants by homology-based excision: a resource for site-

directed mutagenesis, multi-gene changes and high-throughput plastid transformation. *Plant Journal* **46**, 901-909.

Krichevsky, A., Meyers, B., Vainstein, A., Maliga, P. & Citovsky, V. (2010). Autoluminescent Plants. *PLoS ONE* **5**, e15461.

Kumar, S., Dhingra, A. & Daniell, H. (2004a). Plastid-expressed betaine aldehyde dehydrogenase gene in carrot cultured cells, roots, and leaves confers enhanced salt tolerance. *Plant Physiology* **136**, 2843-2854.

Kumar, S., Dhingra, A. & Daniell, H. (2004b). Stable transformation of the cotton plastid genome and maternal inheritance of transgenes. *Plant Molecular Biology* **56**, 203-216.

Kuroda, H. & Maliga, P. (2001). Sequences downstream of the translation initiation codon are important determinants of translation efficiency in chloroplasts. *Plant Physiology* **125**, 430-436.

Lal, P., Ramachandran, V. G., Goyal, R. & Sharma, R. (2007). Edible vaccines: current status and future. *Indian Journal of Medical Microbiology* **25**, 93-102.

Lalor, P. A., Webby, R. J., Morrow, J., Rusalov, D., Kaslow, D. C., Rolland, A. & Smith, L. R. (2008). Plasmid DNA-based vaccines protect mice and ferrets against lethal challenge with A/Vietnam/1203/04 (H5N1) influenza virus. *Journal of Infectious Diseases* **197**, 1643-1652.

Laver, W. G., Air, G. M., Dopheide, T. A. & Ward, C. W. (1980). Amino acids sequence changes in the Hemagglutinin of A/Hong Kong (H3N2) influenza virus during the period 1968–77. *Nature* **283**, 454-457.

Lee, M. Y. T., Zhou, Y. X., Lung, R. W. M., Chye, M. L., Yip, W. K., Zee, S. Y. & Lam, E. (2006a). Expression of viral capsid protein antigen against Epstein-Barr virus in plastids of *Nicotiana tabacum* cv. SR1. *Biotechnology and Bioengineering* **94**, 1129-1137.

Lee, S. B., Kwon, H. B., Kwon, S. J., Park, S. C., Jeong, M. J., Han, S. E., Byun, M. O. & Daniell, H. (2003). Accumulation of trehalose within transgenic chloroplasts confers drought tolerance. *Molecular Breeding* **11**, 1-13.

Lee, S. M., Kang, K. S., Chung, H., Yoo, S. H., Xu, X. M., Lee, S. B., Cheong, J. J., Daniell, H. & Kim, M. (2006b). Plastid transformation in the monocotyledonous cereal crop, rice (Oryza sativa) and transmission of transgenes to their progeny. *Molecules and Cells* **21**, 401-410.

Lelivelt, C. L. C., McCabe, M. S., Newell, C. A., deSnoo, C. B., van Dun, K. M. P., Birch-Machin, I., Gray, J. C., Mills, K. H. G. & Nugent, J. M. (2005). Stable plastid transformation in lettuce (*Lactuca sativa* L.). *Plant Molecular Biology* **58**, 763-774.

Lentz, E. M., Segretin, M. E., Morgenfeld, M. M., Wirth, S. A., Dus Santos, M. J., Mozgovoj, M. V., Wigdorovitz, A. & Bravo-Almonacid, F. F. (2010). High expression level of a foot and mouth disease virus epitope in tobacco transplastomic plants. *Planta* **231**, 387-395.

Lenzi, P., Scotti, N., Alagna, F., Tornesello, M. L., Pompa, A., Vitale, A., De Stradis, A., Monti, L., Grillo, S., Buonaguro, F. M., Maliga, P. & Cardi, T. (2008). Translational fusion of chloroplast-expressed human papillomavirus type 16 L1 capsid protein enhances antigen accumulation in transplastomic tobacco. *Transgenic Research* **17**, 1091-1102.

Lestrade, C., Pelissier, B., Rolans, A. & Dubald, M. (2009). Construct for obtaining transplastomic plant or plant cell comprises at least chimeric gene encoding selectable marker and chimeric color gene, or chimeric gene encoding luminescent protein, or chimeric gene encoding a negative marker. Edited by B. C. A. (Farb) Patent.

Levi, R. & Arnon, R. (1996). Synthetic recombinant influenza vaccine induces efficient long-term immunity and cross-strain protection. *Vaccine* **14**, 85-92.

Li, W., Ruf, S. & Bock, R. (2010). Chloramphenicol acetyltransferase as selectable marker for plastid transformation. *Plant Molecular Biology* **76,** 443-451.

Lilly, J. W., Havey, M. J., Jackson, S. A. & Jiang, J. M. (2001). Cytogenomic analyses reveal the structural plasticity of the chloroplast genome in higher plants. *The Plant Cell* **13**, 245-254.

Limaye, A., Koya, V., Samsam, M. & Daniell, H. (2006). Receptor-mediated oral delivery of a bioencapsulated green fluorescent protein expressed in transgenic chloroplasts into the mouse circulatory system. *Faseb Journal* **20**, 959-961.

Liu, C. W., Lin, C. C., Yiu, J. C., Chen, J. J. & Tseng, M. J. (2008). Expression of a Bacillus thuringiensis toxin (cry1Ab) gene in cabbage (*Brassica oleracea* L. var. capitata L.) chloroplasts confers high insecticidal efficacy against Plutella xylostella. *TAG Theoretical and Applied Genetics* **117**, 75-88.

Lopez-Juez, E. & Pyke, K. A. (2005). Plastids unleashed: their development and their integration in plant development. *The International Journal of Developmental Biology* **49**, 557-577.

Lossl, A. G. & Waheed, M. T. (2011). Chloroplast-derived vaccines against human diseases: achievements, challenges and scopes. *Plant Biotechnology Journal* **9**, 527-539.

Lutz, K. A., Knapp, J. E. & Maliga, P. (2001). Expression of bar in the plastid genome confers herbicide resistance. *Plant Physiology* **125**, 1585-1590.

Lutz, K. A., Azhagiri, A. K., Tungsuchat-Huang, T. & Maliga, P. (2007). A guide to choosing vectors for transformation of the plastid genome of higher plants. *Plant Physiology* **145**, 1201-1210.

Madesis, P., Osathanunkul, M., Georgopoulou, U., Gisby, M. F., Mudd, E. A., Nianiou, I., Tsitoura, P., Mavromara, P., Tsaftaris, A. & Day, A. (2010). A hepatitis C virus core polypeptide expressed in chloroplasts detects anti-core antibodies in infected human sera. *Journal of Biotechnology* **15**, 377-386.

Maliga, P. (2002). Engineering the plastid genome of higher plants. *Current Opinion in Plant Biology* **5**, 164-172.

Maliga, P. (2003). Progress towards commercialization of plastid transformation technology. *Trends in Biotechnology* **21**, 20-28.

Maliga, P. (2004). Plastid transformation in higher plants. *Annual Review of Plant Biology* **55**, 289-313.

Maliga, P. & Bock, R. (2011). Plastid biotechnology: food, fuel, and medicine for the 21st century. *Plant Physiology* **155,** 1501-1510.

Marquet-Blouin, E., Bouche, F. B., Steinmetz, A. & Muller, C. P. (2003). Neutralizing immunogenicity of transgenic carrot (*Daucus carota* L.)-derived measles virus hemagglutinin. *Plant Molecular Biology* **51**, 459-469.

Martin, V., Sims, L., Lubroth, J., Pfeiffer, D., Slingenbergh, J. & Domenech, J. (2006). Epidemiology and ecology of highly pathogenic avian influenza with particular emphasis on South East Asia. *Developmental Biology (Basel)* **124**, 23-36.

Matoba, N., Magerus, A., Geyer, B. C., Zhang, Y. F., Muralidharan, M., Alfsen, A., Arntzen, C. J., Bomsel, M. & Mor, T. S. (2004). A mucosally targeted subunit vaccine candidate eliciting HIV-1 transcytosis-blocking Abs. *Proceedings of the National Academy of Sciences USA* **101**, 13584-13589.

McBride, K. E., Schaaf, D. J., Daley, M. & Stalker, D. M. (1994). Controlled expression of plastid transgenes in plants based on a nuclear DNA-encoded and plastid-targeted T7 RNA polymerase. *Proceedings of the National Academy of Sciences USA* **91**, 7301-7305.

McBride, K. E., Svab, Z., Schaaf, D. J., Hogan, P. S., Stalker, D. M. & Maliga, P. (1995). Amplification of a chimeric Bacillus gene in chloroplasts leads to an extraordinary level of an insecticidal protein in tobacco. *Bio-Technology* **13**, 362-365.

McCabe, M. S., Garratt, L. C., Schepers, F., Jordi, W. J. R. M., Stoopen, G. M., Davelaar, E., van Rhijn, J. H. A., Power, J. B. & Davey, M. R. (2001). Effects of PSAG12-IPT gene expression on development and senescence in transgenic lettuce. *Plant Physiology* **127**, 505-516.

McCabe, M. S., Klaas, M., Gonzalez-Rabade, N., Poage, M., Badillo-Corona, J. A., Zhou, F., Karcher, D., Bock, R., Gray, J. C. & Dix, P. J. (2008). Plastid transformation of high-biomass tobacco variety Maryland Mammoth for production of human immunodeficiency virus type 1 (HIV-1) p24 antigen. *Plant Biotechnology Journal* **6**, 914-929.

Melkonian, K. A., Ostermeyer, A. G., Chen, J. Z., Roth, M. G. & Brown, D. A. (1999). Role of lipid modifications in targeting proteins to detergent-resistant membrane rafts. *Journal of Biological Chemistry* **274,** 3910-3917.

Mett, V., Musiychuk, K., Bi, H., Hong, B. I., Farrance, C. E., Horsey, A., Ugulava, N., Shoji, Y., De La Rosa, P., Palmer, G. A., Rabindran, S., Streatfield, S. J., Boyers, A., Russell, M., Mann, A., Lambkin, R., Oxford, J. S., Schild, G. C. & Yusibov, V. (2008). A plant-produced influenza subunit vaccine protects ferrets against virus challenge. *Influenza and Other Respiratory Viruses* **2**, 33-40.

Mohapatra, U., McCabe, M. S., Power, J. B., Schepers, F., Van Der Arend, A. & Davey, M. R. (1999). Expression of the *Bar* gene confers herbicide resistance in transgenic lettuce. *Transgenic Research* **8**, 33-44.

Molina, A., Hervas-Stubbs, S., Daniell, H., Mingo-Castel, A. M. & Veramendi, J. (2004). High-yield expression of a viral peptide animal vaccine in transgenic tobacco chloroplasts. *Plant Biotechnology Journal* **2**, 141-153.

Murashige, T. & Skoog, F. (1962). A revised medium for rapid growth and bio assays with tobacco tissue cultures. *Physiologia Plantarum* **15**, 473-497.

Nardin, E. H., Oliveira, G. A., Calvo-Calle, J. M., Castro, Z. R., Nussenzweig, R. S., Schmeckpeper, B., Hall, B. F., Diggs, C., Bodison, S., & Edelman, R. (2000). Synthetic malaria peptide vaccine elicits high levels of antibodies in vaccinees of defined HLA genotypes. *The Journal of Infectious Disease* **182**, 1486-1496.

Newcomb, E. H. (1967). Fine structure of protein-storing plastids in bean root tips. *Journal of Cell Biology* **33**, 143-163.

Newell, C. A., Birch-Machin, I., Hibberd, J. M. & Gray, J. C. (2003). Expression of green fluorescent protein from bacterial and plastid promoters in tobacco chloroplasts. *Transgenic Research* **12**, 631-634.

Nugent, G. D., Coyne, S., Nguyen, T. T., Kavanagh, T. A. & Dix, P. J. (2006). Nuclear and plastid transformation of *Brassica oleracea* var. botrytis (cauliflower) using PEG-mediated uptake of DNA into protoplasts. *Plant Science* **170**, 135-142.

Nugent, J. M. & Joyce, S. M. (2005). Producing human therapeutic proteins in plastids. *Current Pharmaceutical Design* **11**, 2459-2470.

Nwe, N., He, Q. G., Damrongwatanapokin, S., Du, Q. Y., Manopo, I., Limlamthong, Y., Fenner, B. J., Spencer, L. & Kwang, J. (2006). Expression of hemagglutinin protein from the avian influenza virus H5N1 in a baculovirus/insect cell system significantly enhanced by suspension culture. *Bmc Microbiology* **6**, 1-7.

Oey, M., Lohse, M., Kreikemeyer, B. & Bock, R. (2009a). Exhaustion of the chloroplast protein synthesis capacity by massive expression of a highly stable protein antibiotic. *Plant Journal* **57**, 436-445.

Oey, M., Lohse, M., Scharff, L. B., Kreikemeyer, B. & Bock, R. (2009b). Plastid production of protein antibiotics against pneumonia via a new strategy for high-level expression of antimicrobial proteins. *Proceedings of the National Academy of Sciences USA* **106**, 6579-6584.

Okumura, S., Sawada, M., Park, Y. W., Hayashi, T., Shimamura, M., Takase, H. & Tomizawa, K. I. (2006). Transformation of poplar (*Populus alba*) plastids and expression of foreign proteins in tree chloroplasts. *Transgenic Research* **15**, 637-646.

O' Neill, C., Horvath, G. V., Horvath, E., Dix, P. J. & Medgyesy, P. (1993). Chloroplast transformation in plants - Polyethylene-glycol (Peg) treatment of protoplasts is an alternative to biolistic delivery systems. *Plant Journal* **3**, 729-738.

Ortigosa, S. M., Fernandez-San Millan, A. & Veramendi, J. (2010). Stable production of peptide antigens in transgenic tobacco chloroplasts by fusion to the p53 tetramerisation domain. *Transgenic Research* **19**, 703-709.

Osterhaus, A. D., Rimmelzwaan, G. F., Martina, B. E., Bestebroer, T. M. & Fouchier, R. A. (2000). Influenza B virus in seals. *Science* **288**, 1051-1053.

Palmer, J. D. (1983). Chloroplast DNA exists in two orientations. *Nature* **301**, 92-93.

Peckham, G. D., Bugos, R. C. & Su, W. W. (2006). Purification of GFP fusion proteins from transgenic plant cell cultures. *Protein Expression and Purification* **49**, 183-189.

Pfitzinger, H., Guillemaut, P., Weil, J. H. & Pillay, D. T. N. (1987). Adjustment of the tRNA population to the codon usage in chloroplast. *Nucleic Acid Research* **15,** 1377-1386.

Ping, J., Li, C., Deng, G., Jiang, Y., Tian, G., Zhang, S., Bu, Z. & Chen, H. (2008). Single-amino-acid mutation in the HA alters the recognition of H9N2 influenza virus by a monoclonal antibody. *Biochemical and Biophysical Research Communications* **371**, 168-171.

Pinto, L. A., Berzofsky, J. A., Fowke, K. R. & other authors (1999). HIV-specific immunity following immunization with HIV synthetic envelope peptides in asymptomatic HIV-infected patients. *AIDS* **13**, 2003-2012.

Potter, C.W. (1982). Inactivated influenza virus vaccine. Beare, A.S. (ed.). Basic and applied influenza research. CRC Press, Boca Raton. 119–158.

Prasad, V., Satyavathi, V. V., Sanjaya, Valli, K. M., Khandelwal, A., Shaila, M. S. & Lakshmi Sita, G. (2004). Expression of biologically active Hemagglutinin-neuraminidase protein of Peste des petits ruminants virus in transgenic pigeonpea [Cajanus cajan (L) Millsp.]. *Plant Science* **166**, 199-205.

Raubeson, L. & Jansen, R. (2005). *Chloroplast Genomes of Plants*. Oxfordshire, United Kingdom: CABI Publishing.

Reed, M. L., Wilson, S. K., Sutton, C. A. & Hanson, M. R. (2001). High-level expression of a synthetic red-shifted GFP coding region incorporated into transgenic chloroplasts. *Plant Journal* **27**, 257-265.

Rigano, M. M., Manna, C., Giulini, A., Pedrazzini, E., Capobianchi, M., Castilletti, C., Di Caro, A., Ippolito, G., Beggio, P., De Giuli Morghen, C., Monti, L., Vitale, A. & Cardi, T. (2009). Transgenic chloroplasts are efficient sites for high-yield production of the vaccinia virus envelope protein A27L in plant cells. *Plant Biotechnology Journal* **7**, 577-591.

Rogalski, M., Ruf, S. & Bock, R. (2006). Tobacco plastid ribosomal protein S18 is essential for cell survival. *Nucleic Acids Research* **34**, 4537-4545.

Rogalski, M., Karcher, D. & Bock, R. (2008a). Superwobbling facilitates translation with reduced tRNA sets. *Nature Structural & Molecular Biology* **15**, 192-198.

Rogalski, M., Schottler, M. A., Thiele, W., Schulze, W. X. & Bock, R. (2008b). Rpl33, a nonessential plastid-encoded ribosomal protein in tobacco, is required under cold stress conditions. *Plant Cell* **20**, 2221-2237.

Rosales-Mendoza, S., Alpuche-Solis, A. G., Soria-Guerra, R. E., Moreno-Fierros, L., Martinez-Gonzalez, L., Herrera-Diaz, A. & Korban, S. S. (2009). Expression of an *Escherichia coli* antigenic fusion protein comprising the heat labile toxin B subunit and the heat stable toxin, and its assembly as a functional oligomer in transplastomic tobacco plants. *Plant Journal* **57**, 45-54.

Rosales-Mendoza, S., Soria-Guerra, R., Moreno-Fierros, L., Alpuche-Solís, Á., Martínez-González, L. & Korban, S. (2010). Expression of an immunogenic F1-V fusion protein in lettuce as a plant-based vaccine against plague. *Planta* **232**, 409-416.

Ruf, S., Biehler, K. & Bock, R. (2000). A small chloroplast-encoded protein as a novel architectural component of the light-harvesting antenna. *Journal of Cell Biology* **149**, 369-377.

Ruf, S., Hermann, M., Berger, I. J., Carrer, H. & Bock, R. (2001). Stable genetic transformation of tomato plastids and expression of a foreign protein in fruit. *Nature Biotechnology* **19**, 870-875.

Ruf, S., Karcher, D. & Bock, R. (2007). Determining the transgene containment level provided by chloroplast transformation. *Proceedings of the National Acedemy of Sciences USA* **104**, 6998-7002.

Ruhlman, T., Ahangari, R., Devine, A., Samsam, M. & Daniell, H. (2007). Expression of cholera toxin B-proinsulin fusion protein in lettuce and tobacco chloroplasts - oral administration protects against development of insulitis in non-obese diabetic mice. *Plant Biotechnology Journal* **5**, 495-510.

Ruhlman, T., Verma, D., Samson, N. & Daniell, H. (2010). The role of heterologous chloroplast sequence elements in transgene integration and expression. *Plant Physiology* **152**, 2088-2104.

Ruiz, O. N. & Daniell, H. (2005). Engineering cytoplasmic male sterility via the chloroplast genome. *Vitro Cellular & Developmental Biology-Animal* **41**, 1232-1246.

Russell, J. A., Roy, M. K. & Sanford, J. C. (1992). Physical trauma and tungsten toxicity reduce the efficiency of biolistic transformation. *Plant Physiology* **98**, 1050-1056.

Rybicki, E. P. (2009). Plant-produced vaccines: promise and reality. *Drug Discovery Today* **14**, 16-24.

Saelens, X., Vanlandschoot, P., Martinet, W., Maras, M., Neirynck, S., Contreras, R., Fiers, W. & Jou, W. M. (1999). Protection of mice against a lethal influenza virus challenge after immunization with yeast-derived secreted influenza virus hemagglutinin. *European Journal of Biochemistry* **260**, 166-175.

Saitoh, M., Kimura, H., Kozawa, K. & Shoji, A. (2008). Molecular evolution of HA1 in influenza A (H3N2) viruses isolated in Japan from 1989 to 2006. *Intervirology* **51**, 377-384.

Sambrook, J., Fritsch, E. F. & Maniatis, T. (1989). *Molecular Cloning: A Laboratory Manual*, 2nd edn. Cold Spring Harbour Laboratory,Cold Springs Harbour,NY, USA.

Sanford, J. C., Klein, T. M., Wolf, E. D. & Allen, N. (1987). Delivery of substances into cells and tissues using a particle bombardment process. *Particulate Science and Technology: An International Journal* **5**, 27-37.

Sanford, J. C. (1988). The biolistic process. *Trends in Biotechnology* **6**, 299-302.

Schwenkert, S., Soll, J. & Bolter, B. (2010). Protein import into chloroplasts-How chaperones feature into the game. *Biochimica et Biophysica Acta* **1808,** 901-911.

Scotti, N., Alagna, F., Ferraiolo, E., Formisano, G., Sannino, L., Buonaguro, L., De Stradis, A., Vitale, A., Monti, L., Grillo, S., Buonaguro, F. M. & Cardi, T. (2009). High-level expression of the HIV-1 Pr55(gag) polyprotein in transgenic tobacco chloroplasts. *Planta* **229**, 1109-1122.

Shiels, K., (2003). Developing the chloroplast as a potential vaccine production system. National University of Maynooth, Ireland. PhD Thesis.

Shih, A. C., Hsiao, T. C., Ho, M. S. & Li, W. H. (2007). Simulataneous amino acid substitutions at antigenic sites drive influenza A hemagglutinin evolution. *Proceedings of the National Acedemy of Sciences USA* **104,** 6283-6288.

Shimizu, M., Goto, M., Hanai, M., Shimizu, T., Izawa, N., Kanamoto, H., Tomizawa, K., Yokota, A. & Kobayashi, H. (2008). Selectable tolerance to herbicides by mutated acetolactate synthase genes integrated into the chloroplast genome of tobacco. *Plant Physiol*ogy **147**, 1976-1983.

Shoji, Y., Chichester, J. A., Bi, H., Musiychuk, K., De La Rosa, P., Goldschmidt, L., Horsey, A., Ugulava, N., Palmer, G. A., Mett, V. & Yusibov, V. (2008). Plant-expressed HA as a seasonal influenza vaccine candidate. *Vaccine* **26**, 2930-2934.

Shoji, Y., Farrance, C. E., Bi, H. Green, B., Manceva, S., Rhee, A., Ugulava, N., Roy, G., Musiychuk, K., Chichester, J. A., Mett, V. & Yusibov, V. (2009). Immunogenicity of hemagglutinin from A/Bar-headed Goose/Qinghai/1A/05 and A/Anhui/1/05 strains of H5N1 influenza viruses produced in *Nicotiana benthamiana* plants. *Vaccine* **27**, 3467-3470.

Sidorov, V. A., Kasten, D., Pang, S.-Z., Hajdukiewicz, P. T. J., Staub, J. M. & Nehra, Narender, Â. S. (1999). Stable chloroplast transformation in potato: use of green fluorescent protein as a plastid marker. *The Plant Journal* **19**, 209-216.

Siegenthaler P. A. (1998). Molecular organization of acyl lipids in photosynthetic membranes of higher plants. Lipids in photosynthesis: structure, function and genetics: Advances in photosynthesis, Siegenthaler, P. A., Murata, N. (eds: Kluwer Academic Publishers, Boston) **6**, 120–144.

Sikdar, S. R., Serino, G., Chaudhuri, S. & Maliga, P. (1998). Plastid transformation in *Arabidopsis thaliana*. *Plant Cell Reports* **18**, 20-24.

Sim, J.-S., Pak, H.-K., Kim, D.-S., Lee, S.-B., Kim, Y.-H. & Hahn, B.-S. (2009). Expression and characterization of synthetic heat-labile enterotoxin B subunit and hemagglutinin–neuraminidase-neutralizing epitope fusion protein in *Escherichia coli* and tobacco chloroplasts. *Plant Molecular Biology Reporter* **27**, 388-399.

Singh, A., Verma, S. & Bansal, K. (2010). Plastid transformation in eggplant (*Solanum melongena* L.). *Transgenic Research* **19,** 113-119.

Skarjinskaia, M., Svab, Z. & Maliga, P. (2003). Plastid transformation in *Lesquerella fendleri*, an oilseed Brassicacea. *Transgenic Research* **12**, 115-122.

Skehel, J. J. & Wiley, D. C. (2000). Receptor binding and membrane fusion in virus entry: The influenza hemagglutinin. *Annual Review of Biochemistry* **69**, 531-569.

Skehel, J. J. & Wiley, D. C. (2002). Influenza haemagglutinin. *Vaccine* **20**, S51-S54.

Smith, G. J., Bahl, J., Vijaykrishna, D., Zhang, J., Poon, L. L., Chen, H., Webster, R. G., Peiris, J. S. & Guan, Y. (2009). Dating the emergence of pandemic influenza viruses. *Proceedings of the National Academy of Sciences USA* **106**, 11709-11712.

Soria-Guerra, R. E., Alpuche-Solis, A. G., Rosales-Mendoza, S., Moreno-Fierros, L., Bendik, E. M., Martinez-Gonzalez, L. & Korban, S. S. (2009). Expression of a multi-epitope DPT fusion protein in transplastomic tobacco plants retains both antigenicity and immunogenicity of all three components of the functional oligomer. *Planta* **229**, 1293-1302.

Southgate, E. M., Davey, M. R., Power, J. B. & Marchant, R. (1995). Factors affecting the genetic engineering of plants by microprojectile bombardment. *Biotechnology Advances* **13**, 631-651.

Sporlein, B., Streubel, M., Dahlfeld, G., Westhoff, P. & Koop, H. U. (1991). Peg-mediated plastid transformation - A new system for transient gene-expression assays in chloroplasts. *Theoretical and Applied Genetics* **82**, 717-722.

Staehelin, L. A. (2003). Chloroplast structure: from chlorophyll granules to supra-molecular architecture of thylakoid membranes. *Photosynthesis Research* **76**, 185-196.

Staub, J. M. & Maliga, P. (1994). Extrachromosomal elements in tobacco plastids. *Proceedings of the National Academy of Sciences USA* **91**, 7468-7472.

Staub, J. M., Garcia, B., Graves, J., Hajdukiewicz, P. T. J., Hunter, P., Nehra, N., Paradkar, V., Schlittler, M., Carroll, J. A., Spatola, L., Ward, D., Ye, G. & Russell, D. A. (2000). High-yield production of a human therapeutic protein in tobacco chloroplasts. *Nature Biotechnology* **18**, 333-338.

Steinhauer, D. A. (2010). Influenza A virus hemagglutinin glycoproteins. Chapter 5, pp 69-108, in "Influenza: Molecular Virology" Q. Wang and Y. Tao (eds.) Horizon Scientific Press.

Stern, D. B., Higgs, D. C. & Yang, J. J. (1997). Transcription and translation in chloroplasts. *Trends in Plant Science* **2**, 308-315.

Sugiura, M. (1992). The Chloroplast Genome. *Plant Molecular Biology* **19**, 149-168.

Sun, M., Qian, K. X., Su, N., Chang, H. Y., Liu, J. X. & Chen, G. F. (2003). Foot-and-mouth disease virus VP1 protein fused with cholera toxin B subunit expressed in *Chlamydomonas reinhardtii* chloroplast. *Biotechnology Letters* **25**, 1087-1092.

Svab, Z., Hajdukiewicz, P. & Maliga, P. (1990). Stable transformation of plastids in higher-plants. *Proceedings of the National Academy of Sciences USA* **87**, 8526-8530.

Svab, Z. & Maliga, P. (1993). High-frequency plastid transformation in tobacco by selection for a chimeric *aada* gene. *Proceedings of the National Academy of Sciences USA* **90**, 913-917.

Tangphatsornruang, S., Birch-Machin, I., Newell, C. A. & Gray, J. C. (2010). The effect of different 3' untranslated regions on the accumulation and stability of transcripts of a gfp transgene in chloroplasts of transplastomic tobacco. *Plant Molecular Biol*ogy **76**, 385-396.

Taylor, N. J. & Fauquet, C. M. (2002). Microparticle bombardment as a tool in plant science and agricultural biotechnology. *DNA and Cell Biology* **21**, 963-977.

Toyoshima, Y., Onda, Y., Shiina, T. & Nakahira, Y. (2005). Plastid transcription in higher plants. *Critical Reviews in Plant Sciences* **24**, 59-81.

Treanor, J. J., Schiff, G. M., Hayden, F. G. & other authors (2007). Safety and Immunogenicity of a Baculovirus-Expressed Hemagglutinin Influenza Vaccine. *JAMA: The Journal of the American Medical Association* **297**, 1577-1582.

Tregoning, J. S., Nixon, P., Kuroda, H., Svab, Z., Clare, S., Bowe, F., Fairweather, N., Ytterberg, J., van Wiik, K. J., Dougan, G. & Maliga, P. (2003). Expression of tetanus toxin Fragment C in tobacco chloroplasts. *Nucleic Acids Research* **31**, 1174-1179.

Valkov, V. T., Gargano, D., Manna, C., Formisano, G., Dix, P. J., Gray, J. C., Scotti, N. & Cardi, T. (2011). High efficiency plastid transformation in potato and regulation of transgene expression in leaves and tubers by alternative 5 ' and 3 ' regulatory sequences. *Transgenic Research* **20**, 137-151.

Verma, D. & Daniell, H. (2007). Chloroplast vector systems for biotechnology applications. *Plant Physiology* **145**, 1129-1143.

Verma, D., Samson, N. P., Koya, V. & Daniell, H. (2008). A protocol for expression of foreign genes in chloroplasts. *Nature Protocols* **3**, 739-758.

Virelizier, J. L., Allison, A. C. & Schild, G. C. (1979). Immune responses to influenza virus in the mouse and their role in control of the infection. *British Medical Bulletin* **35,** 65-68.

Waheed, M. T., Thones, N., Muller, M., Hassan, S. W., Razavi, N. M., Lossl, E., Kaul, H. P. & Lossl, A. G. (2011). Transplastomic expression of a modified human papillomavirus L1 protein leading to the assembly of capsomeres in tobacco: a step towards cost-effective second-generation vaccines. *Transgenic Research* **20**, 271-282.

Wakasugi, T., Tsudzuki, T. & Sugiura, M. (2001). The genomics of land plant chloroplasts: Gene content and alteration of genomic information by RNA editing. *Photosynthesis Research* **70**, 107-118.

Wang, C., Takeuchi, K., Pinto, L. H. & Lamb, R. A. (1993). Ion channel activity of influenza A virus M2 protein: characterization of the amantadine block. *Journal of Virology* **67**, 5585-5594.

Wang, H. H., Yin, W. B. & Hu, Z. M. (2009). Advances in chloroplast engineering. *The Journal of Genetics and Genomics* **36**, 387-398.

Wang, T. T., Tan, G. S., Hai, R., Pica, N., Ngai, L., Ekiert, D. C., Wilson, I. A., Garcia-Sastre, A., Moran, T. M. & Palese, P. (2010). Vaccination with a synthetic peptide from the influenza virus hemagglutinin provides protection against distinct viral subtypes. in *Proceedings of the National Acedemy of Sciences USA* **107**, 18979-18984.

Warzecha, H., Mason, H. S., Lane, C., Tryggvesson, A., Rybicki, E., Williamson, A. L., Clements, J. D. & Rose, R. C. (2003). Oral immunogenicity of human papillomavirus-like particles expressed in potato. *Journal of Virology* **77**, 8702-8711.

Webb, D. T. (1992). Teaching concepts of plant development with lettuce seeds and seedlings. *Tested studies for laboratory teaching*, **6,** 27-49 (C.A. Goldman, S.E. Andrews, P.L. Hauta, and R. Ketchum, Eds)

Webster, D. E., Smith, S. D., Pickering, R. J., Strugnell, R. A., Dry, I. B. & Wesselingh, S. L. (2006). Measles virus hemagglutinin protein expressed in transgenic lettuce induces neutralising antibodies in mice following mucosal vaccination. *Vaccine* **24**, 3538-3544.

Whitney, S. M. & Sharwood, R. E. (2008). Construction of a tobacco master line to improve Rubisco engineering in chloroplasts. *Journal of Experimental Botany* **59**, 1909-1921.

Wiley, D. C., Wilson, I. A. & Skehel, J. J. (1981). Structural identification of the antibody-binding sites of Hong-Kong influenza hemagglutinin and their involvement in antigenic variation. *Nature* **289**, 373-378.

Wise, R. (2007). *The Diversity of Plastid Form and Function*. Advances in Photosynthesis and Respiration: Springer.

Yabuta, Y., Tamoi, M., Yamamoto, K., Tomizawa, K.-I., Yokota, A. & Shigeoka, S. (2008). Molecular design of photosynthesis-elevated chloroplasts for mass accumulation of foreign protein. *Plant and Cell Physiology* **49,** 375-385.

Ye, G. N., Hajdukiewicz, P. T. J., Broyles, D., Rodriguez, D., Xu, C. W., Nehra, N. & Staub, J. M. (2001). Plastid-expressed 5-enolpyruvylshikimate-3-phosphate synthase genes provide high level glyphosate tolerance in tobacco. *Plant Journal* **25**, 261-270.

Yu, L. X., Gray, B. N., Rutzke, C. J., Walker, L. P., Wilson, D. B. & Hanson, M. R. (2007). Expression of thermostable microbial cellulases in the chloroplasts of nicotine free tobacco. *Journal of Biotechnology* **131**, 362-369.

Zerges, W. (2000). Translation in chloroplasts. *Biochimie* **82**, 583-601.

Zhou, F., Badillo-Corona, J. A., Karcher, D., Gonzalez-Rabade, N., Piepenburg, K., Borchers, A. M., Maloney, A. P., Kavanagh, T. A., Gray, J. C. & Bock, R. (2008). High-level expression of human immunodeficiency virus antigens from the tobacco and tomato plastid genomes. *Plant Biotechnology Journal* **6**, 897-913.

Zhou, Y. X., Lee, M. Y. T., Ng, J. M. H., Chye, M. L., Yip, W. K., Zee, S. Y. & Lam, E. (2006). A truncated hepatitis E virus ORF2 protein expressed in tobacco plastids is immunogenic in mice. *World Journal of Gastroenterology* **12**, 306-312.

Zubkot, M. K., Zubkot, E. I., van Zuilen, K., Meyer, P. & Day, A. (2004). Stable transformation of petunia plastids. *Transgenic Research* **13**, 523-530.

Chapter 8
Appendix A

8 Appendix A

A.1 Cloning gfp/HA epitope constructs

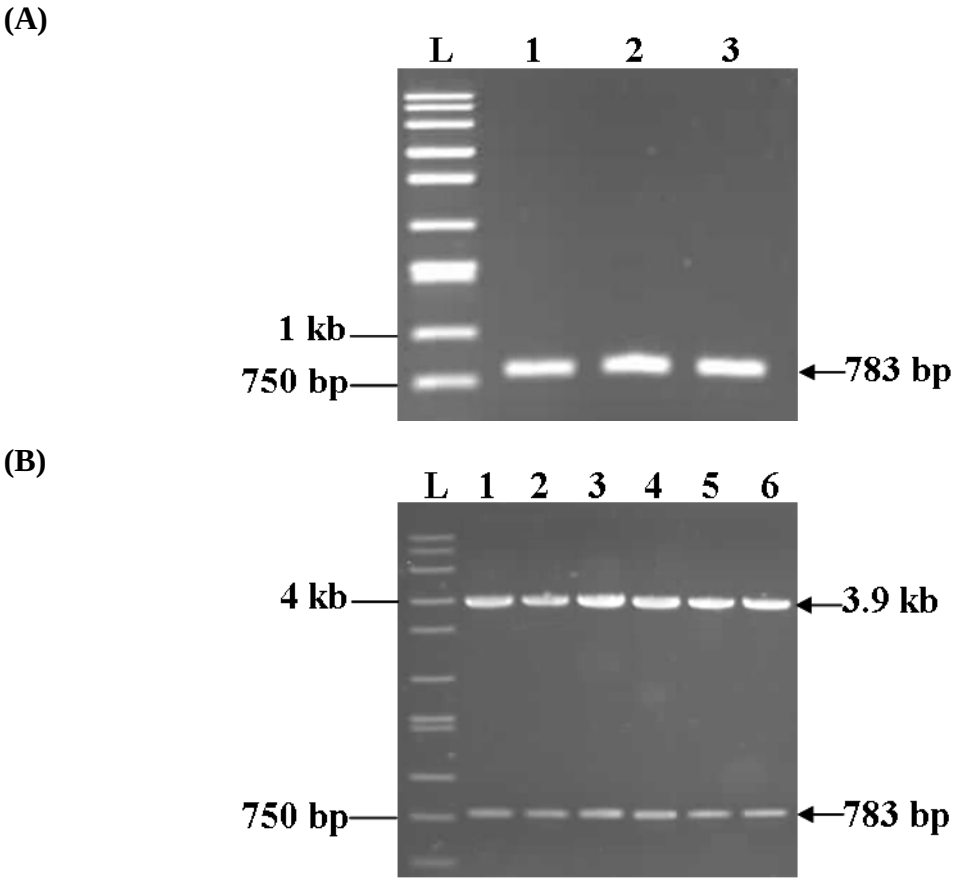

Figure 7.1: Analysis of the full length GFP/HA91-108 fusion genes. (A) PCR products following second round PCR using the primers GFP-NdeIF and HA91-108-R2. Lane L: 10 kb Ladder (Sigma). Lanes 1-3: products from three independent PCR reactions to generate a full length GFP/HA91-108 fusion gene (783 bp). (B) Recombinant plasmids containing GFP/HA91-108 in the vector pCR2.1-TOPO were digested with *NdeI* and *XbaI*. Restriction digests produced the 3.9 kb pCR2.1-TOPO vector backbone and the excised GFP/HA91-108 insert at 783 bp. Lane L: 10 kb ladder (Sigma). Lanes 1-6: pCR-GFP/HA91-108 plasmids.

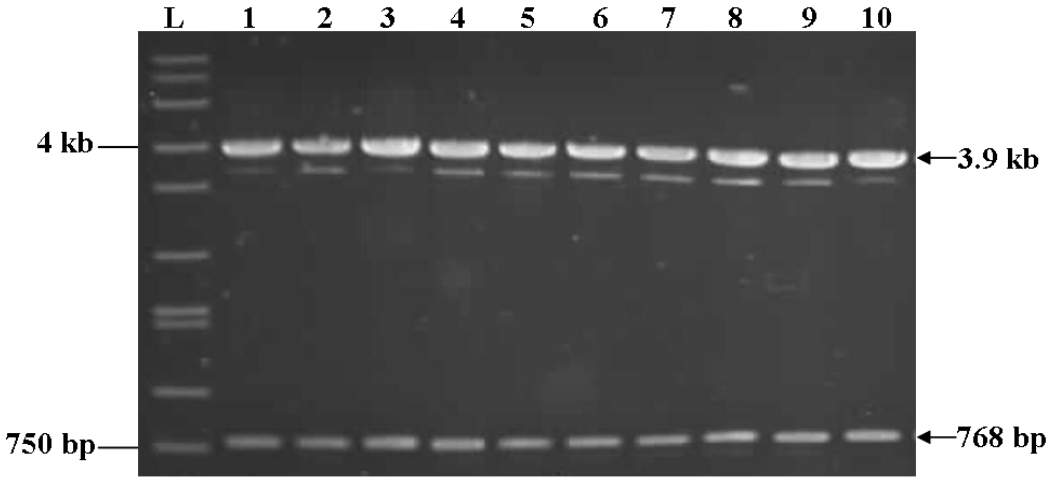

Figure 7.2: Analysis of the full length HA307-319/GFP fusion genes. Recombinant plasmids containing HA307-319/GFP in the vector pCR2.1-TOPO were digested with *NdeI* and *XbaI*. Restriction digests produced the 3.9 kb pCR2.1-TOPO vector backbone and the excised HA307-319 insert at 768 bp. Lane L: 10 kb ladder (Sigma). Lanes 1-10: pCR-HA307-319/GFP plasmids.

(A)

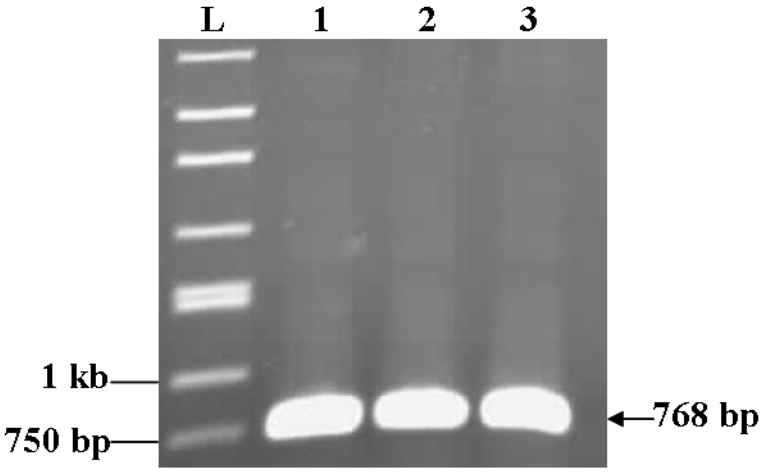

(B)

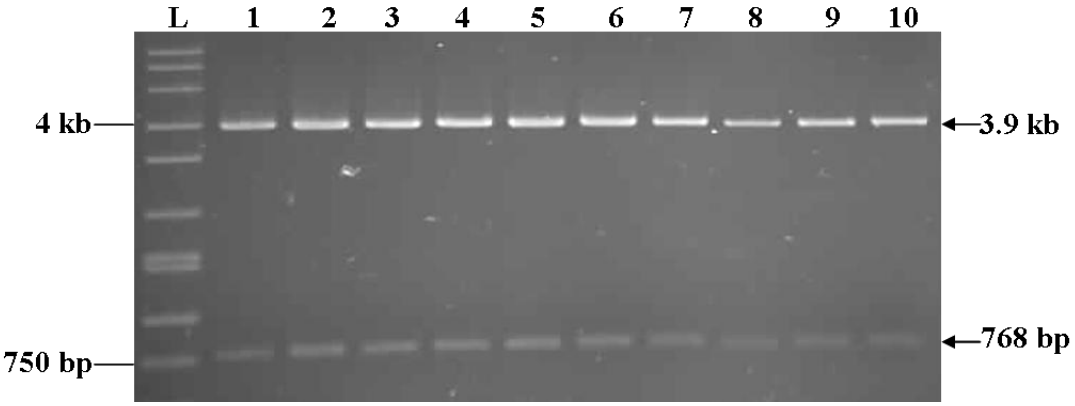

Figure 7.3: Analysis of the full length GFP/HA307-319 fusion genes. (A) PCR products following second round PCR using the primers GFP-NdeIF and HA307-319-R2. Lane L: 10 kb Ladder (Sigma). Lanes 1-3: products from three independent PCR reactions to generate a full length GFP/HA307-319 fusion gene (768 bp). (B) Recombinant plasmids containing GFP/HA307-319 in the vector pCR2.1-TOPO were digested with *NdeI* and *XbaI*. Restriction digests produced the 3.9 kb pCR2.1-TOPO vector backbone and the excised GFP/HA307-319 insert at 768 bp. Lane L: 10 kb ladder (Sigma). Lanes 1-10: pCR-GFP/HA307-319 plasmids.

(A)

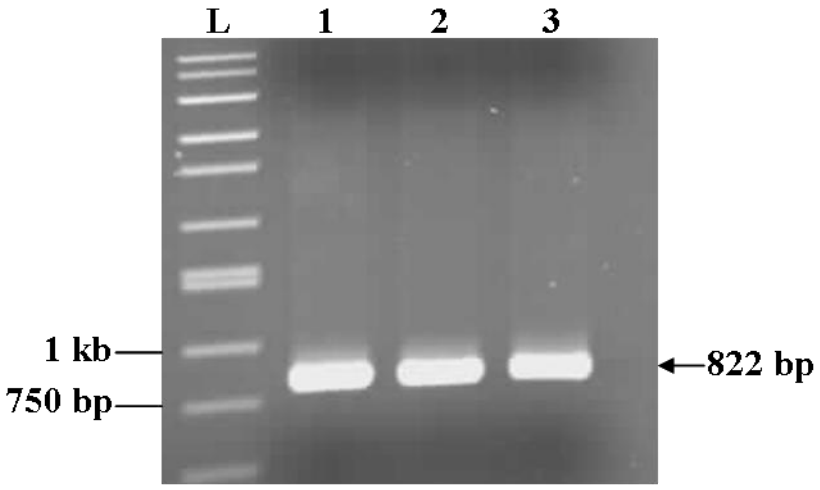

(B)

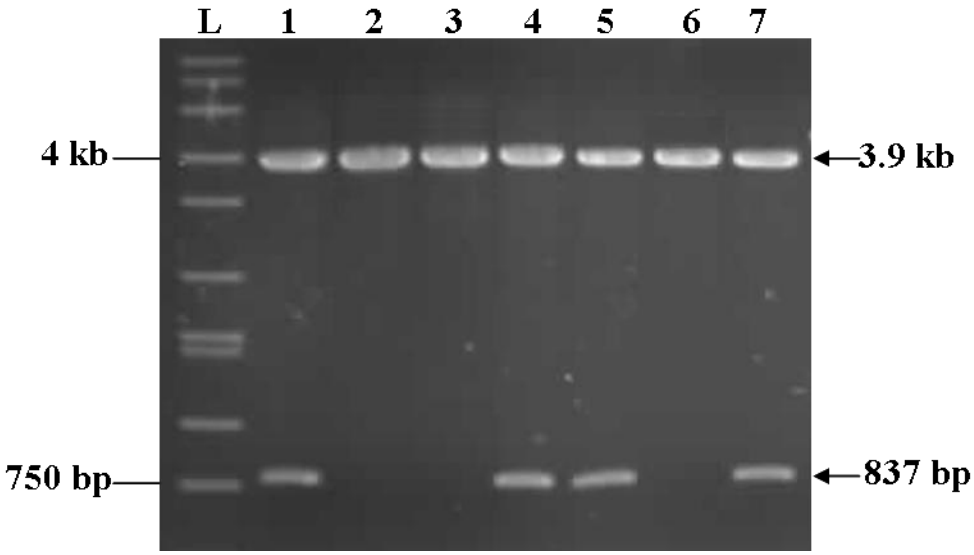

Figure 7.4: Analysis of the full length HA91-108/GFP/HA307-319 fusion genes. (A) PCR products following second round PCR using the primers HA91-108-F2 and HA307-319-R2. Lane L: 10 kb Ladder (Sigma). Lanes 1-3: products from three independent PCR reactions to generate a full length HA91-108/GFP/HA307-319 fusion gene (822 bp). (B) Recombinant plasmids containing HA91-108/GFP/HA307-319 in the vector pCR2.1-TOPO were digested with *EcoRI*. Restriction digests produced the 3.9 kb pCR2.1-TOPO vector backbone and the excised HA91-108/GFP/HA307-319 insert at 837 bp. Lane L: 10 kb ladder (Sigma). Lanes 1-7: pCR-HA91-108/GFP/HA307-319 plasmids.

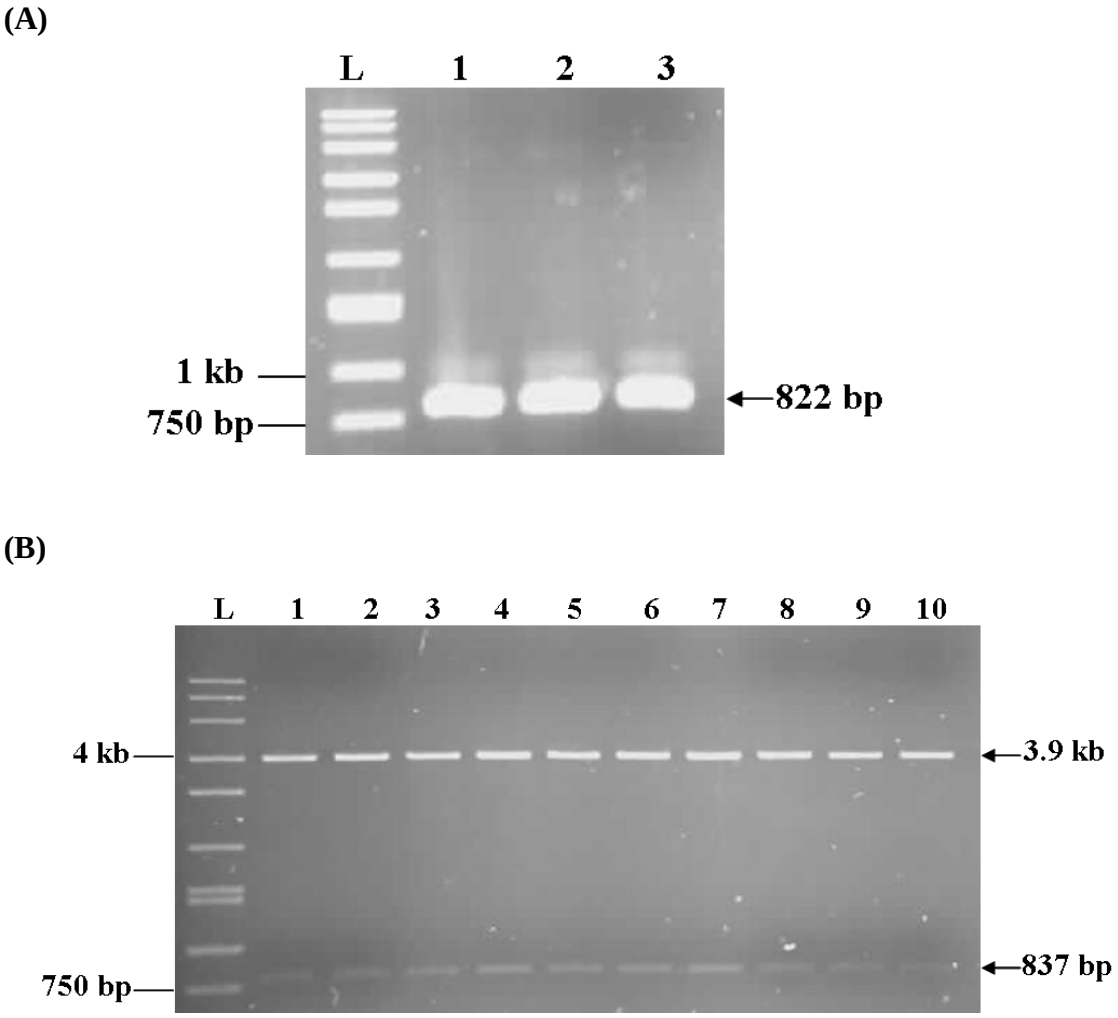

Figure 7.5: Analysis of the full length HA307-319/GFP/HA91-108 fusion genes. (A) PCR products following second round PCR using the primers HA307-319-F2 and HA91-108-R2. Lane L: 10 kb Ladder (Sigma). Lanes 1-3: products from three independent PCR reactions to generate a full length HA307-319/GFP/HA91-108 fusion gene (822 bp). (B) Recombinant plasmids containing HA307-319/GFP/HA91-108 in the vector pCR2.1-TOPO were digested with *EcoRI*. Restriction digests produced the 3.9 kb pCR2.1-TOPO vector backbone and the excised HA307-319/GFP/HA91-108 insert at 837 bp. Lane L: 10 kb ladder (Sigma). Lanes 1-10: pCR-HA307-319/GFP/HA91-108 plasmids.

A.2: PCR analysis of putative transformed gfp/HA epitope plant lines

(A)

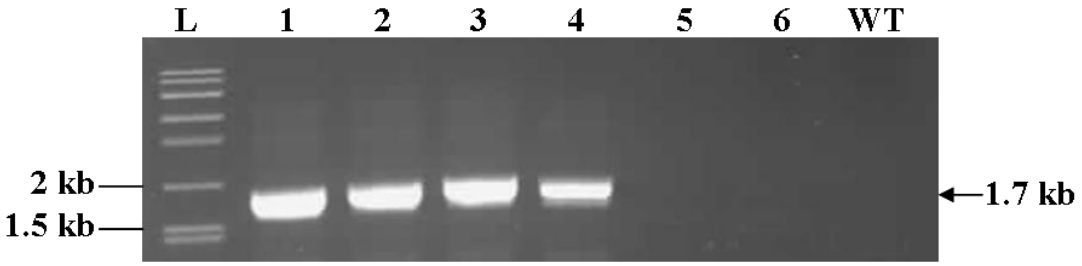

(B)

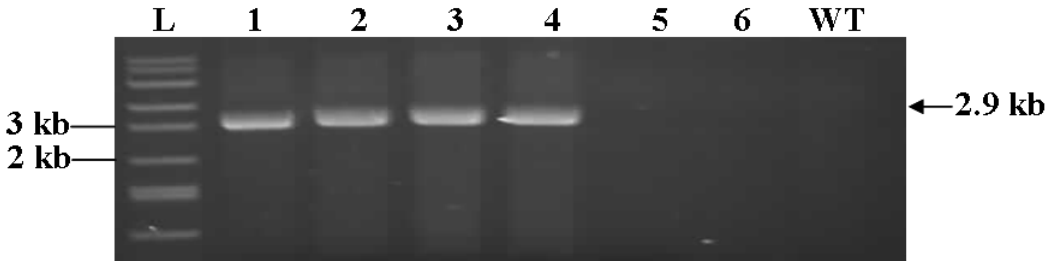

Figure 7.6: PCR analysis of putative pMOG9 plants. (A) Primers Ext-For, specific to the chloroplast genome and aadA-Rev, specific to the *aadA* gene were used to confirm the integration of GFP/HA91-108 into the tobacco chloroplast genome. The expected product size of 1.7 kb was amplified in four out of six plants. Lane L: 10 kb ladder (Sigma). Lanes 1-6: G9-1, G9-2, G9-3, G9-4, G9-5, G9-6. Lane WT: Wild type Petite Havana (negative control). (B) Primers GFP-NdeIF, specific to the GFP/HA91-108 gene and Ext-Rev, specific to the chloroplast genome were used to confirm the integration of GFP/HA91-108 into the tobacco chloroplast genome. The expected product size of 2.9 kb was amplified in four out of six plants. Lane L: 10 kb ladder (Sigma). Lanes 1-6: G9-1, G9-2, G9-3, G9-4, G9-5, G9-6. Lane WT: Wild type Petite Havana (negative control).

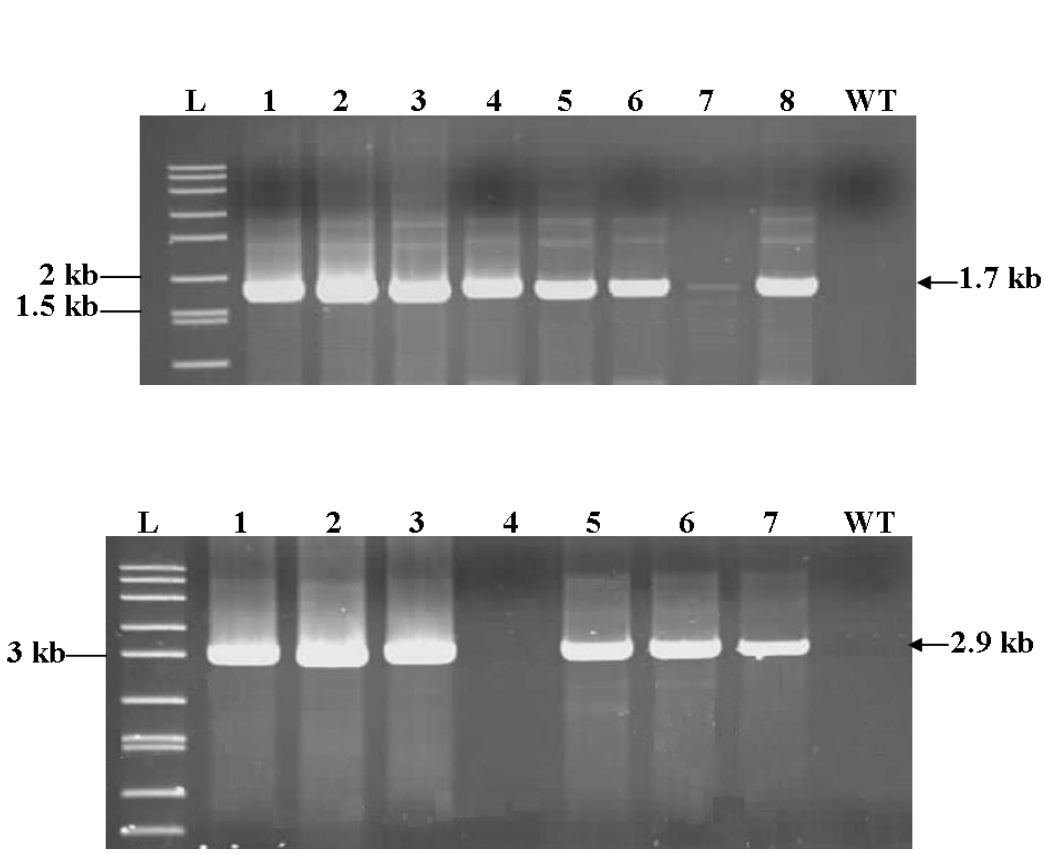

Figure 7.7: PCR analysis of putative pMO3G plants. (A) Primers Ext-For, specific to the chloroplast genome and aadA-Rev, specific to the *aadA* gene were used to confirm the integration of HA307-319/GFP into the tobacco chloroplast genome. The expected product size of 1.7 kb was amplified in seven out of eight plants. Lane L: 10 kb ladder (Sigma). Lanes 1-8: 3G-1, 3G-2, 3G-7, 3G-9, 3G-14, 3G-25, 3G-27, 3G-28 Lane WT: Wild type Petite Havana (negative control). (B) Primers HA307-319-F2, specific to the HA307-319/GFP gene and Ext-Rev, specific to the chloroplast genome were used to confirm the integration of HA307-319/GFP into the tobacco chloroplast genome. The expected product size of 2.9 kb was amplified in six out of seven plants. Lane L: 10 kb ladder (Sigma). Lanes 1-7: 3G-1, 3G-2, 3G-7, 3G-9, 3G-14, 3G-25, 3G-28. Lane WT: Wild type Petite Havana (negative control).

(A)

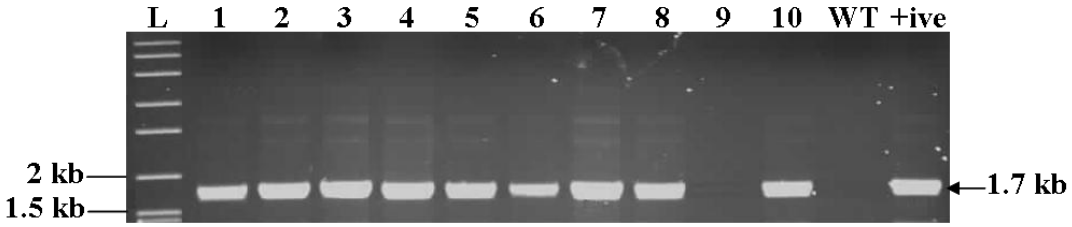

(B)

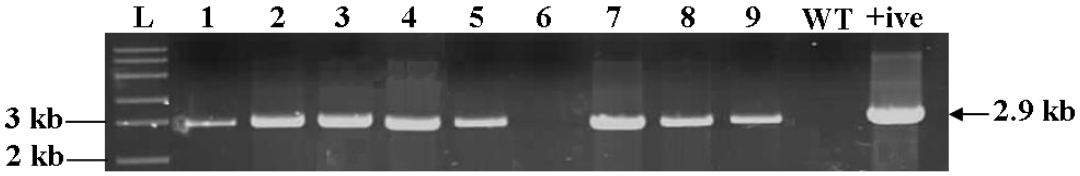

Figure 7.8: PCR analysis of putative pMOG3 plants. (A) Primers Ext-For, specific to the chloroplast genome and aadA-Rev, specific to the *aadA* gene were used to confirm the integration of GFP/HA307-319 into the tobacco chloroplast genome. The expected product size of 1.7 kb was amplified in nine out of ten plants. Lane L: 10 kb ladder (Sigma). Lanes 1-10: G3-1, G3-3, G3-11, G3-14, G3-15, G3-16, G3-17, G3-30, G3-31, G3-32. Lane WT: Wild type Petite Havana (negative control). Lane +ive: line G9-1 (positive control) (B) Primers GFP-NdeIF, specific to the GFP/HA307-319 gene and Ext-Rev, specific to the chloroplast genome were used to confirm the integration of GFP/HA307-319 into the tobacco chloroplast genome. The expected product size of 2.9 kb was amplified in eight out of nine plants. Lane L: 10 kb ladder (Sigma). Lanes 1-9: G3-1, G3-3, G3-11, G3-14, G3-15, G3-16, G3-17, G3-30 and G3-32. Lane WT: Wild type Petite Havana (negative control). Lane +ive: line G9-1 (positive control).

(A)

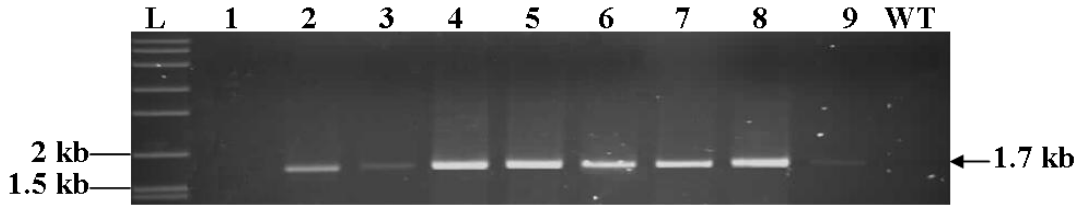

(B)

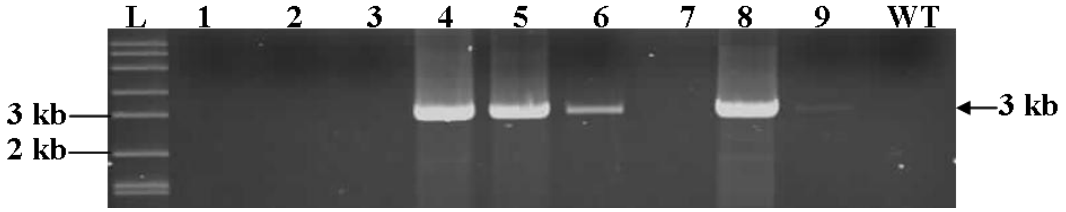

Figure 7.9: PCR analysis of putative pMO3G9 plants. (A) Primers Ext-For, specific to the chloroplast genome and aadA-Rev, specific to the *aadA* gene were used to confirm the integration of HA307-319/GFP/HA91-108 into the tobacco chloroplast genome. The expected product size of 1.7 kb was amplified in eight out of nine plants. Lane L: 10 kb ladder (Sigma). Lanes 1-9: 3G9-1, 3G9-3, 3G9-4, 3G9-5, 3G9-9, 3G9-12, 3G9-13, 3G9-14, 3G9-15. Lane WT: Wild type Petite Havana (negative control). (B) Primers HA307-319-F2, specific to the HA307-319/GFP/HA91-108 gene and Ext-Rev, specific to the chloroplast genome were used to confirm the integration of HA307-319/GFP/HA91-108 into the tobacco chloroplast genome. The expected product size of 3 kb was amplified in eight out of nine plants. Lane L: 10 kb ladder (Sigma). Lanes 1-9: 3G9-1, 3G9-3, 3G9-4, 3G9-5, 3G9-9, 3G9-12, 3G9-13, 3G9-14, 3G9-15. Lane WT: Wild type Petite Havana (negative control).

(A)

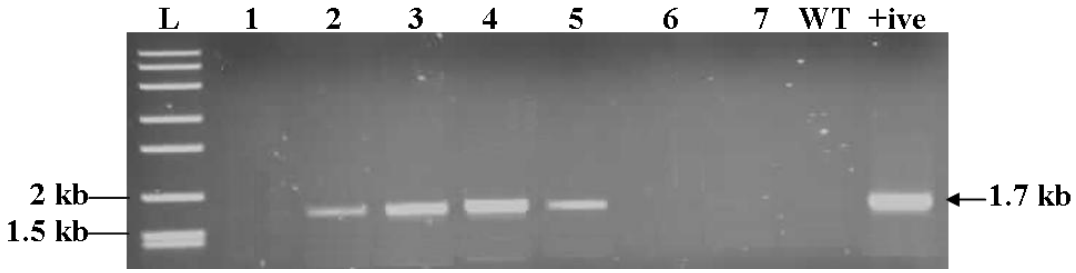

(B)

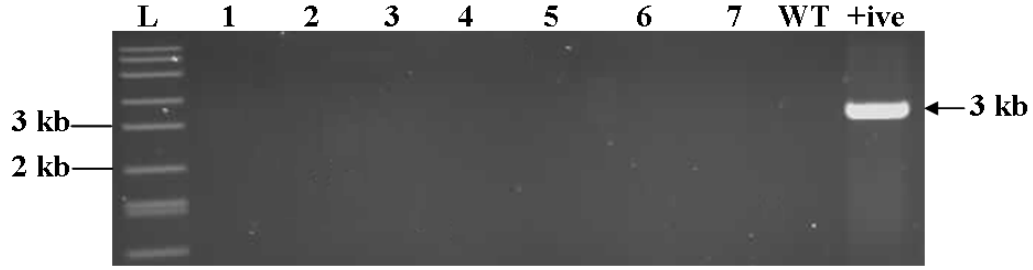

Figure 7.10: PCR analysis of putative pMO9G3 plants. (A) Primers Ext-For, specific to the chloroplast genome and aadA-Rev, specific to the *aadA* gene were used to confirm the integration of HA91-108/GFP/HA307-319 into the tobacco chloroplast genome. The expected product size of 1.7 kb was amplified in four out of seven plants. Lane L: 10 kb ladder (Sigma). Lanes 1-7: 9G3-1, 9G3-2, 9G3-4, 9G3-5, 9G3-6, 9G3-7, 9G3-11. Lane WT: Wild type Petite Havana (negative control), Lane +ive: 3G9-14 plant line. (B) Primers HA91-108-F2, specific to the HA91-108/GFP/HA307-319 gene and Ext-Rev, specific to the chloroplast genome were used to confirm the integration of HA91-108/GFP/HA307-319 into the tobacco chloroplast genome. The expected product size of 3 kb could not be amplified in any of the plant lines. Lane L: 10 kb ladder (Sigma). Lanes 1-7: 9G3-1, 9G3-2, 9G3-4, 9G3-5, 9G3-6, 9G3-7, 9G3-11. Lane WT: Wild type Petite Havana (negative control). Lane +ive: 9G-1 plant line.